Library, N.W. Bldg
MAY 1 1964
Reference book not to be
taken from the library.

Physical Aspects of Irradiation

Recommendations of the International Commission on Radiological Units and Measurements

Handbook 85

United States Department of Commerce
National Bureau of Standards

HANDBOOKS OF THE NATIONAL BUREAU OF STANDARDS

The following Handbooks issued by the Bureau are available by purchase from the Superintendent of Documents, Government Printing Office, Washington, D.C., 20402, at the prices indicated:

No.		Price
28	Screw-Thread Standards for Federal Services 1957, Part I (Amends in part H28, 1944 and in part its 1950 Supplement)	$1.25
28	Screw-Thread Standards for Federal Services 1957, Part II	.75
28	Screw-Thread Standards for Federal Services 1957, Part III	.60
28.	1963 Supplement Screw-Thread Standards for Federal Services (Parts I, II, and III)	.70
30	National Electrical Safety Code	2.25
44	Specifications, Tolerances, and Regulations for Commercial Weighing and Measuring Devices—2d Edition	1.25
48	Control and Removal of Radioactive Contamination in Laboratories	.20
49	Recommendations for Waste Disposal of Phosphorus-32 and Iodine-131 for Medical Users	.15
51	Radiological Monitoring Methods and Instruments	.20
53	Recommendations for the Disposal of Carbon-14 Wastes	.15
55	Protection Against Betatron-Synchrotron Radiations up to 100 Million Electron Volts	.25
57	Photographic Dosimetry of X- and Gamma Rays	.15
58	Radioactive-Waste Disposal in the Ocean	.20
59	Permissible Dose From External Sources of Ionizing Radiation	.35
63	Protection Against Neutron Radiation up to 30 Million Electron Volts	.40
64	Design of Free-Air Ionization Chambers	.20
65	Safe Handling of Bodies Containing Radioactive Isotopes	.15
66	Safe Design and Use of Industrial Beta-Ray Sources	.20
67	Checking Prepackaged Commodities	.35
69	Maximum Permissible Body Burdens and Maximum Permissible Concentrations of Radionuclides in Air and in Water for Occupational Exposure	.35
70	Tabulation of Data on Microwave Tubes	1.00
71	Specifications for Dry Cells and Batteries	.25
72	Measurement of Neutron Flux and Spectra for Physical and Biological Applications	.35
73	Protection Against Radiations from Sealed Gamma Sources	.30
74	Building Code Requirements for Reinforced Masonry	.15
75	Measurement of Absorbed Dose of Neutrons, and of Mixtures of Neutrons and Gamma Rays	.35
76	Medical X-ray Protection up to 3 Million Volts	.25
77	Precision Measurement and Calibration	
	Vol. I. Electricity and Electronics	6.00
	Vol. II. Heat and Mechanics	6.75
	Vol. III. Optics, Metrology, and Radiation	7.00
79	Stopping Powers for Use With Cavity Chambers	.35
80	A Manual of Radioactivity Procedures	.50
81	Safety Rules for the Installation and Maintenance of Electric Supply and Communication Lines	1.75
82	Weights and Measures Administration	1.75
83	Tabulation of Data on Receiving Tubes	1.25
84	Radiation Quantities and Units (ICRU Report 10a)	.20
85	Physical Aspects of Irradiation (ICRU Report 10b)	.70
86	Radioactivity (ICRU Report 10c)	.40
87	Clinical Dosimetry (ICRU Report 10d)	.40
88	Radiobiological Dosimetry (ICRU Report 10e)	.25
89	Methods of Evaluating Radiological Equipment and Materials (ICRU Report 10f)	.35
90	Handbook for CRPL Ionospheric Predictions Based on Numerical Methods of Mapping	.40
91	Experimental Statistics	4.25

UNITED STATES DEPARTMENT OF COMMERCE • Luther H. Hodges, *Secretary*

NATIONAL BUREAU OF STANDARDS • A. V. Astin, *Director*

Physical Aspects of Irradiation

Recommendations of the International Commission on Radiological Units and Measurements (ICRU) Report 10b 1962

National Bureau of Standards Handbook 85

Issued March 31, 1964

(This publication supersedes parts of H78. Handbooks 84 through 89 extend and largely replace H78. For an explanation, see the Foreword. Also, for a list of these titles, see page 3 of cover.)

For sale by the Superintendent of Documents, U.S. Government Printing Office, Washington, D.C., 20402.
Price 70 cents

Library of Congress Catalog Card Number: 63-6007

Foreword

The reports of The International Commission on Radiological Units and Measurements for a number of years have been published by the National Bureau of Standards in the Handbook series. In the past, each of the triennial reports of the ICRU represented a complete restatement of the recommendations of the Commission. Because of the increasing scope of its activities, however, the Commission in 1962 decided to modify the previous practice. It will issue a series of reports presenting the current recommendations of the Commission. Each report will cover a particular portion of the area of interest to the ICRU. This procedure will facilitate revision of ICRU recommendations and also spread out in time the workload of the Commission. This Handbook is one of the new series presenting the recommendations of the Commission on one aspect of the field with which the Commission is concerned. It presents recommendations agreed upon at the meeting of the Commission held in Montreux, Switzerland, in April 1962.

The National Bureau of Standards is pleased with its continuing opportunity of increasing the usefulness of these important reports by providing the publication outlet.

A. V. Astin, *Director.*

Contents

Preface

A. Scope

The International Commission on Radiological Units and Measurements (ICRU), since its inception in 1925, has had as its principal objective the development of internationally acceptable recommendations regarding:

(1) Quantities and units of radiation and radioactivity,

(2) Procedures suitable for the measurement and application of these quantities in clinical radiology and radiobiology,

(3) Physical data needed in the application of these procedures, the use of which tends to assure uniformity in reporting.

The Commission also considers and makes recommendations on radiation quantities, units and measurements in the field of radiation protection. In this connection, its work is carried out in close cooperation with the International Commission on Radiological Protection.

B. Policy

The ICRU endeavors to collect and evaluate the latest data and information pertinent to the problems of radiation measurement and dosimetry and to recommend the most acceptable values for current use.

Recognizing the confusion that exists in the evaluation of different radiological equipment and materials, the ICRU is studying standard methods of determination of characteristic data for the equipment and materials used in diagnostic and therapeutic radiology. This activity is confined to methods of measurement and does not include the standardization of radiological equipment or parts thereof.

The Commission's recommendations are kept under continual review in order to keep abreast of the rapidly expanding uses of radiation.

The ICRU feels it is the responsibility of national organizations to introduce their own detailed technical procedures for the development and maintenance of standards. However, it urges that all countries adhere as closely as possible to the internationally recommended basic concepts of radiation quantities and units.

The Commission feels its responsibility lies in developing a system of quantities and units having the widest possible range of applicability. Situations may arise from time to time when an expedient solution of a current problem may seem advisable. Generally speaking, however, the Commission feels that action based on expediency is inadvisable from a long-term viewpoint; it endeavors to base its decisions on the long-range advantages to be expected.

In 1955 the Commission entered into an official relationship with the World Health Organization (WHO). In this relationship, the ICRU will be looked to for primary guidance in matters of radiation units and measurements, and in turn the WHO will undertake the worldwide dissemination of the Commission's recommendations. In 1960 the ICRU entered into consultative status with the International Atomic Energy Agency (IAEA).

The above relations with other international bodies do not affect the basic affiliation of the Commission with the International Society of Radiology.

The ICRU invites and welcomes constructive comments and suggestions regarding its recommendations and reports. These may be transmitted to the Chairman.

C. Current Program

A two-week meeting of the ICRU was held in Montreux, Switzerland, April 2 to April 14, 1962. This meeting included the Main Commission and all the Committees that had reports prepared for final approval. Some 70 persons attended. An additional meeting of the Commission and Committee Officers was held in Ottawa from August 21 to August 23, 1962, for the principal purposes of the preparation of the status report for the Xth International Congress of Radiology and the outlining of program objectives for the next several years.

Several meetings of committees or committee task groups have been held during the past 3 years. There were meetings of various task groups of the Committee on Standards and Measurement of Radiological Exposure—Paris in January 1961 and London in April and September 1961. The Committee on Radiobiological Dosimetry also held a meeting in April 1961. The ICRU was also represented at a meeting of the Consultative Committee on Ionizing Radiation of the International Committee of Weights and Measures at Sevres in October 1961.

As noted in the last report, two joint Committees had been established between the ICRU and the ICRP. The Joint Committee on RBE has met twice with ICRU participation. The Committee on Methods and Instruments for Radiation Protection has not met.

Upon the request of the United Nations Scientific Committee on the Effects of Atomic

Radiations, the ICRU and the ICRP agreed to undertake a second study dealing with the Medical and Physical Parameters in Clinical Dosimetry. This committee met in New York for one week in September 1959 and for a week in Stockholm in June 1960. A report of this study entitled "Exposure of Man to Ionizing Radiation Arising from Medical Procedures with Special Reference to Radiation Induced Diseases, An Inquiry into Methods of Evaluation", was published in Physics in Medicine and Biology, **6**, No. 2, 199 (Taylor and Francis, Ltd., London, England, Oct. 1961).

Reports and recommendations of the ICRU originally designed for medical applications, have come into common use in other fields of science, particularly where "dosimetric" considerations are involved. For this reason the committees have included in their membership some scientists having competence outside of the medical radiology field. Material in the reports is designed to meet physical, biological, and medical requirements wherever possible.

This has introduced a small problem in terminology. The name of the Commission includes the term "radiological". In many European countries the term "radiological" is taken as inclusive of both the physical and biological sciences. In other countries, the United States, for example, "radiological" appears to carry the primary connotation of relationship to medicine. It therefore may be desirable to change the name of the Commission from "Radiological" to "Radiation". It is believed that this would be properly understood by all concerned. The question has been debated by the Commission, but final action is being delayed for future consideration.

D. The Current Series of Reports

Hitherto, the triennial reports of the ICRU have been published in single volumes. However the reports are now becoming too extensive, and in some cases too specialized, to make a single publication practicable. Beginning with this 1962 series, the ICRU reports will be issued in smaller entities, each dealing with a limited range of topics. The 1959 Report will not be reprinted. Revisions of the 1962 series will be undertaken individually as circumstances warrant. A full listing of ICRU recommendations, including the present series, is given on page iii of the cover of this report.

The current report series includes revisions of much of the material that appeared in the 1959 report in addition to a number of new topics. The following summary indicates some of the highlights of the current report series.

Radiation Quantities and Units (Report 10a)—One of the most important changes is the revision of the section on quantities and units. This revision resulted from the thorough study by the *Ad Hoc* Committee on Quantities and Units mentioned above. It includes new names for certain quantities and clarified definitions for others. It presents a system of concepts and a set of definitions which is internally consistent and yet of sufficient generality to cover present requirements and such future requirements as can be foreseen.

Radioactivity (Report 10c)—The portions of the report dealing with direct and relative measurements of radioactivity and the availability and requirements for radioactivity standards, and the parts dealing with the techniques and measurements of radioactivity in hospitals and biological laboratories are revisions of the 1959 report, embracing a review of the developments that have occurred since that report and bringing up to date the material included. In addition, a new section on low level radioactivity in materials as related to the problems of radiological measurements has been added. This topic is important because of the problems arising from the contamination, or possible contamination, in the last decade of a great many of the materials used in the construction of counting equipment, shields, and in the reagent chemicals employed in radioactivity measurements.

Clinical Dosimetry (Report 10d)—Much of the Commission's work on clinical dosimetry is brought together in this report. Included is an extensive discussion of practical calibration procedures and the determination of dose along the central ray. Depth dose data relative to stationary- and moving-field therapy have been extended as have the conversion data necessary to relate ionization measurements to absorbed dose.

The principal effort has been toward the definition of nomenclature and the indication of methods. While some examples are given and data are provided for these, in general the reader is referred to other published data. The report considers ways of increasing the accuracy and comparability in clinical dosimetry. The discussion includes not only the physical aspects of dose measurement but also the wider subject of planning treatment in such a way as to deliver the prescribed absorbed dose to a defined "target volume". It also includes comments upon the common sources of error in clinical dosimetry and discusses the information which should be recorded during treatment and that which should be reported about any new treatment technique. Appendices to this report include pertinent material taken from other reports in this series.

Radiobiological Dosimetry (Report 10e)—This report deals primarily with radiobiological dosime-

try, and considers methods of improving the accuracy and intercomparability of absorbed dose measurements in radiobiology. It is in effect a handbook for the experimental radiobiologist. It emphasizes the great importance of planning the experimental work in a way which makes the dosimetry easier and more accurate and it illustrates how this can be done.

Methods of Evaluating Radiological Equipment and Materials (Report 10f)—This is the first of a new group of ICRU reports dealing with methods of evaluating radiological equipment and materials. It includes a revised discussion on the measurement of focal spots and new sections on grids, image intensifiers and body section equipment.

E. Operating Funds

Throughout most of its existence, the ICRU has operated essentially on a voluntary basis, with the travel and operating costs being borne by the parent organizations of the participants. (Only token assistance was available from the ISR.) Recognizing the impracticability of continuing this mode of operation on an indefinite basis, operating funds were sought from various sources in addition to those supplied by the International Society of Radiology.

Prior to 1959, the principal financial assistance to the ICRU had been provided by the Rockefeller Foundation which supplied some $11,000 to make possible various meetings. In 1959 the International Society of Radiology increased its contribution to the Commission to $3,000 to cover the period until the Xth Congress. In 1960 the Rockefeller Foundation supplied an additional sum of some $4,000 making possible a meeting of the Quantity and Units Committee in 1960.

In 1960 and 1961 the World Health Organization contributed the sum of $3,000 each year to the Commission for carrying forward its work. This was increased to $4,000 in 1962. It is expected that this sum will be allocated annually, at least for the next several years. In addition the WHO has provided substantial assistance to the Commission in providing meeting space, secretarial services, etc., for the meetings held in Geneva and Montreux.

In connection with the Commission's Joint Study with the ICRP, the United Nations allocated the sum of $10,000 for the joint use of the two Commissions for the purpose of carrying out their second study. This fund has been administered by the ICRP.

The most substantial contribution to the work of the ICRU has come from the Ford Foundation through the particular efforts of Dr. Paul Pearson. Effective in December 1960, the Ford Foundation made available to the Commission the sum of $37,000 per year for a period of five years. This money is to be used for such items as travel expenses to meetings, for secretarial services and other operating expenses. To a large extent, it is because of this grant that the Commission has been able to hold the several meetings considered to be necessary to move forward actively with its program.

The International Atomic Energy Agency has allocated the sum of $6,000 per year for use by the ICRU. It is expected that this sum will be allocated annually at least for the next several years.

A valuable indirect contribution has been made by the U.S. National Bureau of Standards where the Secretariat has resided. The Bureau has provided substantial secretarial services, publication services and travel costs in the amount of several thousands of dollars.

The Commission wishes to express its deep appreciation to all of these and other organizations that have contributed so importantly to its work.

F. Composition of the ICRU

(a) It is of interest to note that the membership of the Commission and its committees for the period 1959–62 totals 139 persons drawn from 18 countries. This gives some indication of the extent to which the ICRU has achieved international breadth of membership within its basic selection requirement of high technical competence of individual members.

(b) The membership of the Main Commission during the preparation of this report was as follows:

Lauriston S. Taylor, Chairman	United States.
L. H. Gray, Vice-chairman	United Kingdom.
H. O. Wyckoff, Secretary	United States.
K. K. Aglintsev	U.S.S.R.
A. Allisy	France.
R. H. Chamberlain	United States.
F. Ellis	United Kingdom.
H. Fränz	Federal Republic of Germany.
H. E. Johns	Canada.
W. J. Oosterkamp	Netherlands.
B. Rajewsky	Federal Republic of Germany.
H. H. Rossi	United States.
M. Tubiana	France.

G. Composition of ICRU Committees Appointed To Draft This Report

ICRU Committee II, Standards and Measurement of Radiological Exposure Dose

A. Allisy, Chairman
A. Somerwil, Vice Chairman (x and γ rays)
R. S. Caswell, Vice Chairman (neutrons)

K. K. Aglintsev
G. H. Aston
E. J. Axton
C. B. Braestrup
M. Chiozzotto
G. von Droste
C. Garrett
W. Hübner
K. F. Larsson
J. S. Laughlin
K. Lidén
F. Netter
Z. Referowski
R. Thoraeus

Consultants

H. Berger
R. Bruce
D. V. Cormack
A. De Troyer
J. Dewire
R. D. Edge
K. W. Geiger
J. R. Greening
W. N. Hess
G. Hettinger
Y. Ibaraki
R. F. Farr
W. A. Jennings
D. E. A. Jones
W. Pohlit
J. Pruitt
K. Reinsma
S. W. Smith
J. Spaepen
E. Teranishi
E. D. Trout
G. N. Whyte
C. W. Wilson
S. J. Wright
H. O. Wyckoff

ICRU Committee III, Measurement of Absorbed Dose and Clinical Dosimetry—J. W. Boag, Chairman

Committee III–A, Measurement of Absorbed Dose—F. H. Attix, Chairman

K. K. Aglintsev
E. H. Belcher
E. J. Hart
G. S. Hurst
W. C. Roesch
G. N. Whyte
K. G. Zimmer
J. S. Laughlin (Consultant)

H. The Present Report

This report deals broadly with the physical aspects of irradiation with a considerable amount of new material added since the 1959 report. It includes an extensive discussion of the various techniques for the measurement of absorbed dose as well as exposure. Characteristics of radiation instrumentation are covered in some detail including the more sophisticated work on standards. The section on spectra has been up-dated and a new section added on neutron measurements and standards. Available data for stopping power ratios and the average energy (W) required to produce an ion pair in a gas have been reviewed. On the basis of this review it has been necessary to modify the previous ICRU tables for these factors. This modification amounts to about 1 or 2 percent change in stopping power ratios and up to 1 percent in W.

International Commission on Radiological Units and Measurements (ICRU) Report 10b (1962)

I. The Determination of Absorbed Dose

There are three methods of determining absorbed dose which can be used as reliable standards of comparison between different laboratories, or as reference methods within any one laboratory. These are, respectively, the ionization method, the calorimetric method, and the chemical method. The ionization method is still, for many purposes, the most accurate and convenient standard of reference. Calorimetry, as a method of absorbed dose measurement in x-ray or gamma-ray beams at conventional dose rates, is too difficult a technique to be recommended for routine work. The standard chemical methods are now well understood and their calibration constants (G values) are known with good accuracy. At least for hard radiation, they may be used as a standard of reference.

All the other methods described are secondary and many of them require frequent calibration if reasonable accuracy is to be maintained. It has been considered useful to present below a broad survey of possible methods, some of which have not yet been extensively employed and to discuss their special features such as small size, high sensitivity, or permanent storage of information which may make a particular method suitable in some special situation.

A. Theory of Ionization Methods

1. General Considerations

Although it is clearly recognized that the measurement of ionization is not the only approach by which the absorbed dose in rads can be determined, it nevertheless is the most common method now in use. This section is an attempt to summarize the usual techniques employed in such measurements, and to tabulate some of the data needed in carrying out the related calculations. These are selections from the current literature. It is anticipated that future experimental work will improve the accuracy with which some of these data are known. The ICRU plans to publish revised figures from time to time.

a. *The Bragg-Gray relation.* In general, absorbed dose may be estimated by application of the relation between the ionization produced in a gas-filled cavity at the place of interest in the material irradiated, and the energy imparted to unit mass of the material (Gray, 1936). When the cavity is sufficiently small the gas will be subjected to the same flow of ionizing particles as the material under consideration. Then the absorbed dose, D, in ergs imparted per gram of the material, is related to the number of ion pairs formed per gram of the gas, J_m, by the equation

$$D = J_m W s_m \qquad \text{(IA1)}$$

where

W = the average energy in ergs[1] expended by the ionizing particles crossing the cavity per ion pair formed, and

s_m = the effective value of the ratio of the mass stopping power of the medium to that of the cavity gas for these ionizing particles.[2]

To obtain the absorbed dose, D, in rad eq IA1 can be rewritten as

$$D = 0.01 \mathrm{J}_m \mathrm{W} \mathrm{s}_m \qquad \text{(IA2)}$$

The following paragraphs suggest convenient ways of applying the cavity relation to the measurement of absorbed dose. However, before proceeding further it will be worthwhile to define what is meant by the term "charged particle equilibrium" (CPE) as applied to x rays, γ rays and neutrons, and to describe the conditions necessary for its achievement.

b. *Charged-particle equilibrium (CPE) conditions for x rays, γ rays and neutrons.* Charged particle equilibrium would exist at a point within a medium under irradiation if (a) the intensity and energy spectrum of the primary radiation were constant throughout a region extending in all directions from the point, to a distance at least as great as the maximum range of the secondary charged particles generated by the primary radiation, and (b) the energy absorption coefficient for the primary radiation (see subsection IA1d) and the stopping power for the secondary charged particles were constant in the medium throughout the same region as in (a).

If these two conditions could be fulfilled, then on the average for every secondary charged particle leaving an infinitesimal volume surrounding the point, another secondary charged particle of practically the same energy would enter. Thus, the energy dissipated within the volume would be equal to that which would have been dissipated if all the secondary charged particles originating there had spent their entire energy within that volume. This is, therefore, an alternative definition of strict CPE. The presence of a small amount of foreign material at or near the point of interest (such as the air within a cavity ionization chamber) will not significantly upset CPE pro-

[1] W is often expressed in ev, where 1 ev = 1.602×10^{-12} erg. W is fully discussed in section 1A3. For air, W has a value of 33.7 ev per ion pair for electrons of energy greater than 20 kev.

[2] This factor is a function of the charged particle energy at the point of interest, the material and the gas, and to a smaller extent of the cavity dimensions. Values of s_m are discussed in subsection 1A2.

vided that the quantity of material is so small that a negligible part of the energy absorbed within it results from direct interaction of the primary radiation with the atoms of the foreign material. The only situation in which true CPE can exist in a rigorous sense is in an infinite medium containing a uniformly distributed radioactive material. When the primary photon or neutron source is external to the irradiated material, the secondary particle flux at a point of interest may differ appreciably from the true equilibrium value. However, for primary photon energies below a few Mev and for neutrons, the difference between the actual secondary particle flux and the true equilibrium value may not be important for many applications.

The energy spectrum of charged particles existing at a point under CPE conditions is called an *equilibrium spectrum*. If the charged particles involved are electrons, CPE is often referred to as "electronic equilibrium".

Some typical situations where CPE conditions do not exist are (i) near a source of radiation, where the intensity of the primary radiation is changing rapidly with distance; (ii) near boundaries between materials of differing composition, such as bone-tissue or air-tissue boundaries (see ICRU Report 10d); and (iii) at high energy where the primary radiation is appreciably attenuated in the absorbing medium over a distance equal to the mean range of the secondary particles produced. In this latter case we may speak of the attainment of "transient equilibrium" (by analogy with transient equilibrium in, e.g., Ra A decay) at a depth where the ratio of primaries to secondaries reaches a constant value.

c. *Absorbed dose in air exposed to x or gamma radiation.* The absorbed dose at a point in air or "air-equivalent" material that is surrounded on all sides by such material to a thickness at least equal to the range of the secondary electrons and uniformly exposed to 1 roentgen[3] of x or gamma radiation is equal to

$$\left(\frac{1\text{ esu}}{0.001293\text{ g air}}\right)\times\left(2.082\times10^{9}\frac{\text{electron}}{\text{esu}}\right)\times\left(33.7\frac{\text{ev}}{\text{electron}}\right)\times\left(1.602\times10^{-12}\frac{\text{erg}}{\text{ev}}\right)\times\left(\frac{1\text{ rad}}{100\text{ erg/g}}\right)=0.86_9\text{ rad} \quad \text{(IA3)}$$

(or ion pair)

for all x or gamma radiation with quantum energies greater than 20 kev, the energy range over which W is assumed constant.

D_{air} will be referred to as the absorbed dose at a point in an extended mass of air under CPE conditions.

It follows that if any ionization chamber or other measuring instrument that has been calibrated in roentgens (against a standard free-air chamber or by other suitable means) records under conditions of electronic equilibrium in the wall of the chamber an exposure of X roentgens in any situation, then D_{air} in rad is given by

$$D_{\text{air}}=0.86_9\,X \quad \text{(IA4)}$$

d. *Absorbed dose in tissue or other material exposed to x or gamma radiation.* The estimation of absorbed dose presents two somewhat different problems dependent upon whether or not electronic equilibrium may be assumed. These will be treated separately.

Case I. Electronic equilibrium.

(1) *Using an ionization chamber calibrated in roentgens.* The absorbed dose at some point within an irradiated medium can be measured indirectly by means of a roentgen-calibrated ionization chamber which can be positioned at the point within the medium. The calibration of the chamber should be correct for the spectrum of x rays present at the point in the medium, and the chamber walls thick enough to exclude electrons generated in the medium.

In position, the chamber measures a perturbed exposure X'. The exposure which would exist at the point in the absence of the chamber is

$$X=AX' \quad \text{(IA5)}$$

where A is a correction factor which accounts for all effects causing X and X' to differ, mainly (i) attenuation and scattering of x rays in that amount of medium which is displaced by insertion of the chamber, and (ii) x-ray scattering from the chamber connecting lead if one is used. (Modern ionization chambers can be made so small that A is very nearly equal to 1. See ICRU Report 10d, subsection IVB, for additional discussion.)

Having thus established X at the point in roentgens, the absorbed dose in the medium, D_{med} in rad is obtained from the following relation, assuming electronic equilibrium to exist,

$$D_{\text{med}}=0.86_9\left[\frac{(\mu_{\text{en}}/\rho)_{\text{med}}}{(\mu_{\text{en}}/\rho)_{\text{air}}}\right]X=fX \quad \text{(IA6)}$$

where (μ_{en}/ρ) is the mass energy-absorption coefficient[4] of the medium or of air, evaluated for the total spectrum of x or γ radiation arriving at the point of interest.

Table IA1 gives values of the mass energy absorption coefficient for a number of elements and for water, air, bone, muscle, and some plastics. Table IA1 also contains values of f in water,

[3] See appendix I for definitions.

[4] (τ_{en}/ρ), $(\sigma_{\text{en}}/\rho)$, and $(\kappa_{\text{en}}/\rho)$ are the mass energy-absorption coefficients for photoelectric effect, Compton effect, and pair production respectively. (μ_{en}/ρ) is the sum of these three terms. For present purposes these coefficients are appropriate, since they include corrections for energy losses through bremsstrahlung production by the electrons as they slow down, as well as losses in the form of fluorescence x rays and annihilation radiation. Such corrections are described by Fano (1953) and in ICRU Report 10a (1962). Their total effect is small for the energy range considered here. The data in table IA1 (Berger, 1961), include these corrections.

TABLE IA1. *Values of the mass energy-absorption coefficients* [a] *and of the factor f*

Photon energy	Mass energy-absorption coefficient, (μ_{en}/ρ), cm²/g																			$f=0.86_9 \frac{(\mu_{en}/\rho)_{med}}{(\mu_{en}/\rho)_{air}}$		
	H	C	N	O	Na	Mg	Al	P	S	A	K	Ca	Polystyrene $(C_8H_8)_n$	Perspex, plexiglass, lucite $(C_5H_8O_2)$	Polyethylene $(CH_2)_n$	Bakelite $(C_{43}H_{38}O_7)$	Water	Air	Compact bone [b]	Muscle [b]	Water / Air	Compact bone [b] / Air	Muscle [b] / Air
Mev																						
0.010	0.0099	1.94	3.42	5.50	15.4	20.9	26.5	40.1	49.7	62.0	77.0	89.8	1.79	2.92	1.66	2.43	4.89	4.66	19.0	4.96	0.912	3.54	0.925
.015	.0110	0.517	0.916	1.49	4.43	6.09	7.65	11.9	15.2	19.4	24.6	28.9	0.478	0.788	0.444	0.651	1.32	1.29	5.89	1.36	.889	3.97	.916
.020	.0133	.203	.360	0.587	1.77	2.47	3.16	5.00	6.41	8.31	10.5	12.5	.188	.311	.176	.257	0.523	0.516	2.51	0.544	.881	4.23	.916
.030	.0186	.0592	.102	.163	0.482	0.684	0.880	1.45	1.85	2.46	3.12	3.75	.0561	.0892	.0534	.0743	.147	.147	0.743	.154	.869	4.39	.910
.040	.0230	.0306	.0465	.0700	.194	.274	.351	0.570	0.731	0.974	1.25	1.52	.0300	.0426	.0295	.0368	.0647	.0640	.305	.0677	.878	4.14	.919
.050	.0270	.0226	.0299	.0410	.0996	.140	.176	.282	.361	.484	0.626	0.764	.0229	.0288	.0232	.0259	.0394	.0384	.158	.0409	.892	3.58	.926
.060	.0305	.0203	.0244	.0304	.0637	.0845	.104	.166	.214	.284	.367	.443	.0211	.0243	.0218	.0226	.0304	.0292	.0979	.0312	.905	2.91	.929
.080	.0362	.0201	.0218	.0239	.0369	.0456	.0536	.0780	.0971	.124	.158	.191	.0213	.0226	.0224	.0217	.0253	.0236	.0520	.0255	.932	1.91	.939
.10	.0406	.0213	.0222	.0232	.0288	.0334	.0372	.0500	.0599	.0725	.0909	.111	.0228	.0235	.0241	.0227	.0252	.0231	.0386	.0252	.948	1.45	.948
.15	.0485	.0246	.0249	.0252	.0258	.0275	.0282	.0315	.0351	.0368	.0433	.0488	.0264	.0267	.0280	.0261	.0278	.0251	.0304	.0276	.962	1.05	.956
.20	.0530	.0267	.0267	.0271	.0265	.0277	.0275	.0292	.0310	.0302	.0339	.0367	.0287	.0289	.0305	.0283	.0300	.0268	.0302	.0297	.973	0.979	.963
.30	.0573	.0288	.0289	.0289	.0278	.0290	.0283	.0290	.0301	.0278	.0304	.0319	.0310	.0311	.0329	.0305	.0320	.0288	.0311	.0317	.966	.938	.957
.40	.0587	.0295	.0296	.0296	.0283	.0295	.0287	.0290	.0301	.0274	.0299	.0308	.0317	.0319	.0337	.0312	.0329	.0296	.0316	.0325	.966	.928	.954
.50	.0589	.0297	.0297	.0297	.0284	.0293	.0287	.0288	.0300	.0271	.0294	.0304	.0319	.0320	.0339	.0314	.0330	.0297	.0316	.0327	.966	.925	.957
.60	.0588	.0296	.0296	.0296	.0283	.0292	.0286	.0287	.0297	.0270	.0291	.0301	.0318	.0319	.0338	.0313	.0329	.0296	.0315	.0326	.966	.925	.957
.80	.0573	.0288	.0289	.0289	.0276	.0285	.0278	.0280	.0287	.0261	.0282	.0290	.0310	.0311	.0329	.0305	.0321	.0289	.0306	.0318	.965	.920	.956
1.0	.0555	.0279	.0280	.0280	.0267	.0275	.0269	.0270	.0280	.0252	.0272	.0279	.0300	.0301	.0319	.0295	.0311	.0280	.0297	.0308	.965	.922	.956
1.5	.0507	.0255	.0255	.0255	.0243	.0250	.0246	.0245	.0254	.0228	.0247	.0253	.0274	.0275	.0291	.0270	.0283	.0255	.0270	.0281	.964	.920	.958
2.0	.0464	.0234	.0234	.0234	.0225	.0232	.0227	.0228	.0235	.0212	.0228	.0234	.0252	.0252	.0267	.0247	.0260	.0234	.0248	.0257	.966	.921	.954
3.0	.0398	.0204	.0205	.0206	.0199	.0206	.0201	.0204	.0210	.0193	.0208	.0213	.0219	.0220	.0232	.0216	.0227	.0205	.0219	.0225	.962	.928	.954
4.0	.0351	.0184	.0186	.0187	.0184	.0191	.0188	.0192	.0199	.0182	.0199	.0204	.0197	.0198	.0208	.0194	.0205	.0186	.0199	.0203	.958	.930	.948
5.0	.0316	.0170	.0172	.0174	.0173	.0181	.0180	.0184	.0192	.0176	.0193	.0200	.0181	.0183	.0191	.0179	.0190	.0173	.0186	.0188	.954	.934	.944
6.0	.0288	.0160	.0162	.0166	.0166	.0175	.0174	.0179	.0187	.0175	.0190	.0198	.0170	.0172	.0178	.0168	.0180	.0163	.0178	.0178	.960	.949	.949
8.0	.0249	.0145	.0148	.0154	.0158	.0167	.0169	.0175	.0184	.0172	.0190	.0197	.0153	.0156	.0160	.0153	.0165	.0150	.0165	.0163	.956	.956	.944
10.0	.0222	.0137	.0142	.0147	.0154	.0163	.0167	.0174	.0183	.0173	.0191	.0201	.0144	.0147	.0149	.0144	.0155	.0144	.0159	.0154	.935	.960	.929

[a] See footnote 4.
[b] See footnote 5.

muscle, and bone for monoenergetic photons.[5] Mean values, $\bar{f}$, of f integrated over several typical primary x-ray spectra (some measured and some calculated by Kramers' rule, 1923), or directly measured are given in table IA2. For practical use, variations in $\bar{f}$ in terms of HVL

[5] For the purposes of calculation throughout this report the following percentage compositions by weight were assumed for muscle and bone (from data of Joyet *et al.*, (1953), except for the omission of the small amount of Cl):

Element	Muscle (striated)	Compact bone (femur)
H	10.2	6.4
C	12.3	27.8
N	3.5	2.7
O	72.9	41.0
Na	0.08	
Mg	.02	0.2
P	.2	7.0
S	.5	0.2
K	.3	
Ca	.007	14.7

Air was taken to be 75.5 percent N_2, 23.2 percent O_2, and 1.3 percent A, by weight.

The values given in the literature for the calcium content of various bones vary greatly. For example, D'Ans and Lax (1949) give 20.2 percent Ca for the skull, 14.5 percent for femur, and 15.2 percent for ribs. Geyger (1955) gives 11 percent Ca for long bones and ribs. The data of Joyet *et al.*, (1953) were arbitrarily chosen as roughly representative of bones in general. The errors resulting from this assumption are probably no greater than those resulting from (a) neglecting the scattered radiation in calculating f_{bone} (see table IA2) and (b) ignoring the nonhomogeneous structure of bone.

TABLE IA2. *Mean conversion factor $\bar{f}$ in compact bone and muscle for various x-ray spectra*

HVL mm Al	HVL mm Cu	Tube potential kv	$\bar{f}$ Compact bone* rad/R	$\bar{f}$ Muscle* rad/R	Method (see footnotes below)	References
------	------	50	4.04	0.92_3	(a)	Ehrlich (1956).
------	------	50	4.06	0.92_5	(a)	Do.
------	------	50	4.08	0.92_7	(a)	Do.
0.25e	------	50	4.15	0.92_7	(a)	Do.
.35e	0.01e	50	3.99	0.92_3	(a)	Wang, et al., (1957a).
.9e	.03e	45	4.22	0.92_3	(a)	Hettinger, Starfelt (1958a).
1.0e	------	30	4.26	0.92_2	(a)	Aitken, Dixon (1958).
1.2e	.03e	50	4.22	0.92_3	(a)	Ehrlich (1956).
1.2e	.06e	75	4.11	0.92_3	(a)	Hettinger, Starfelt (1958a).
1.2e	------	40	4.26	0.92_4	(a)	Aitken, Dixon (1958).
1.6e	------	50	4.22	0.92_7	(a)	Do.
1.8e	------	60	4.19	0.92_7	(a)	Do.
1.8e	------	70	4.12	0.92_8	(a)	Do.
1.8e	------	80	4.00	0.92_4	(a)	Do.
2.5	.08	60	4.13	0.91_7	(b)	Allisy, Astier (1958).
------	------	------	4.16	0.91_8	(a)	Helle (1958).
3.2	.12	80	3.90	0.92_9	(b)	Allisy, Astier (1958).
------	------	------	3.87	0.91_9	(a)	Helle (1958).
4.2	.18	100	3.63	0.92_3	(b)	Allisy, Astier (1958).
------	------	------	3.47	0.92_4	(a)	Helle (1958).
------	.18	100	3.47	0.93_0	(a)	Hettinger, Starfelt (1958a).
4.5d	.19d	140	2.79	0.93_4	(a)	Cormack et al., (1958a).
------	.2	150	2.67	0.93_2	(a, c)	ICRU Report (1956).
------	.22	80	3.54	0.92_6	(a)	Kolb and Heitzmann (private communication).
------	.25	100	3.07	0.93_2	(a, c)	ICRU Report (1956).
------	.30	140	3.12	0.93_1	(a)	Hettinger, Starfelt (1958a).
------	.39	170	2.80	0.93_3	(a)	Do.
------	.50	200	2.63	0.94_2	(a, c)	ICRU Report (1956).
------	.55	220	2.44	0.93_7	(a)	Hettinger, Starfelt (1958a).
------	.59	100	2.51	0.93_2	(a)	Do.
------	.50	150	2.53	0.93_7	(b)	Allisy, Astier (1958).
------	------	------	2.48	0.93_7	(a)	Helle (1958).
------	.60	120	2.49	0.93_5	(a)	Kolb and Heitzmann (private communication).

TABLE IA2. *Mean conversion factor $\bar{f}$ in compact bone and muscle for various x-ray spectra*—Continued

HVL mm Al	HVL mm Cu	Tube potential kv	$\bar{f}$ Compact bone* rad/R	$\bar{f}$ Muscle* rad/R	Method (see footnotes below)	References
------	.65d	250	2.56	0.93_8	(a)	Hettinger, Starfelt (1958a).
------	.86d	280	2.21	------	(a)	Cormack et al., (1958b).
------	1.0	160	1.84	0.94_2	(a)	Kolb and Heitzmann (private communication).
------	1.0d	250	1.74	0.93_7	(a)	ICRU Report (1956).
------	1.07d	250	2.11	0.94_2	(a)	Hettinger, Lidén (1960).
------	1.07d	280	2.05	------	(a)	Cormack et al., (1958b).
------	1.17d	280	2.00	------	(a)	Do.
------	1.2	200	1.87	0.94_5	(b)	Allisy, Astier (1958).
------	------	------	1.88	0.94_5	(a)	Helle (1958).
------	1.24	140	1.74	0.94_0	(a)	Hettinger, Starfelt (1958a).
------	1.25d	250	1.94	0.94_2	(a)	Hettinger, Lidén (1960)
------	1.42d	250	1.81	0.94_2	(a)	Do.
------	1.53	200	1.55	0.94_1	(a)	Kolb and Heitzmann (private communication).
------	1.54d	280	1.74	------	(a)	Cormack et al., (1958b).
------	1.55d	250	1.79	0.94_2	(a)	Hettinger, Lidén (1960).
------	1.63d	250	1.71	0.95_5	(a)	Do.
------	1.68d	250	1.65	0.95_3	(a)	Do.
------	1.7	280	1.43	0.95_7	(a)	ICRU Report (1956).
------	1.71d	280	1.65	------	(a)	Cormack et al., (1958b).
------	1.77e	280	1.64	------	(a)	Do.
------	2.0d	250	1.41	0.95_2	(a, c)	ICRU Report (1956).
------	2.07d	280	1.52	------	(a)	Cormack et al., (1958b).
------	2.1e	220	1.35	0.95_4	(a)	Greening (1947).
------	2.17d	280	1.45	------	(a)	Cormack et al., (1958b).
------	2.24	170	1.31	0.94_5	(a)	Hettinger, Starfelt (1958a).
------	2.50	280	1.21	0.95_2	(a)	ICRU Report (1956).
------	2.63e	280	1.33	------	(a)	Cormack et al., (1958b).
------	3.1	280	1.12	0.95_7	(a)	ICRU Report (1956).
------	3.14e	280	1.17	------	(a)	Cormack et al., (1958b).
------	3.9	220	1.08	0.95_8	(a)	Hettinger, Starfelt (1958a).
------	4.0	400	1.07	0.95_7	(a)	Johns et al., (1952b).
------	4.16	400	1.11	0.96_1	(a)	ICRU Report (1956).
------	4.8d	250	1.00	0.96_3	(a)	Hettinger, Starfelt (1958a).

*See footnote 5.

[a] Ratios calculated from spectral distribution.

[b] Ratios measured by method of gas equivalents (Astier and Allisy, 1959).

[c] HVL calculated from the spectral distribution of the primary beam.

[d] HVL calculated from the spectral distribution of the beam in a water phantom.

[e] Ratio calculated from theoretical spectral distribution of Kramers (1923).

of some radiations have been plotted in figure IA1a and IA1b. Table IA2 gives information about kv and HVL for the plotted points.

(2) *Using an absolute ionization chamber.* In the event that no roentgen-calibrated ionization chamber is available, an air-filled cavity ionization chamber with nearly air-equivalent walls (e.g., carbon) can be employed as an absolute device.[6]

[6] It will be assumed throughout this report, unless otherwise stated, that the cavity walls are thick enough to exclude any externally produced electrons and that the cavity is small in comparison with the ranges of most of the electrons present. In the low-energy x-ray region, this latter requirement is difficult to fulfill, and the calibrated chamber method is preferable to the use of the cavity as an absolute device.

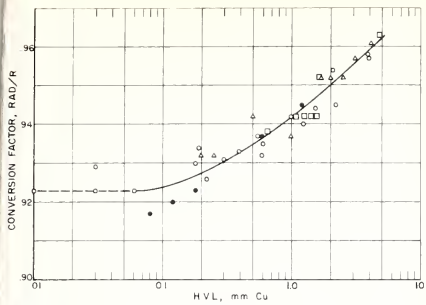

FIGURE IA1a. *Conversion factor $\bar{f}$ in muscle from data of table IA2.*

Δ ICRU 1956
○ Calculated from primary spectra
● Measured by means of gas equivalents
□ Calculated from spectrum in phantom.

When such a chamber is centered at the point of interest in the medium and the ionization is measured, it gives the absorbed dose in a thin inner layer of its own wall material, through application of the Bragg-Gray relation eq (IA1). Thus, in rad,

$$D_{\text{wall}}=0.86_9 Q s_m \tag{IA7}$$

where Q is the charge in esu carried by the ions of either sign produced per 0.001293g of air in the cavity and s_m is the effective ratio of the mass stopping power in the wall material to that in air.

If the measurement had been made by means of a small air-filled cavity in the medium itself, D_{med} would have been obtained instead. D_{wall} differs from D_{med} for two reasons: (i) The energy absorption coefficient in the actual chamber wall differs from that in the medium for the x-ray spectrum at the point, and (ii) the x-ray intensity at the point is altered by the introduction of the chamber. The main cause of intensity change is usually the difference in x-ray attenuation in the chamber wall and in the layer of medium it displaces. Scattering of x rays by the chamber and its connections may also contribute slightly to the change.

D_{med} and D_{wall} (in rad) are related as follows:

$$D_{\text{med}}=B\frac{(\mu_{\text{en}}/\rho)_{\text{med}}}{(\mu_{\text{en}}/\rho)_{\text{wall}}}D_{\text{wall}}=0.86_9 Q s_m B\frac{(\mu_{\text{en}}/\rho)_{\text{med}}}{(\mu_{\text{en}}/\rho)_{\text{wall}}} \tag{IA8}$$

where B is a correction factor for the effects noted in (ii) above, which for a small chamber of small wall thickness will have a value close to unity. Note that B will be closer to 1.00 than will A (see subsection IA1d) for identical cavity chambers. The evaluation of the stopping power factor will be treated in section IA2.

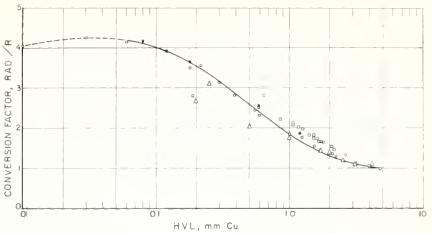

FIGURE IA1b. *Conversion factor $\bar{f}$ in bone from data of table IA2.*

Δ ICRU 1956
○ Calculated from primary spectra
● Measured by means of gas equivalents
□ Calculated from spectrum in phantom.

Case II. Electronic equilibrium conditions not satisfied (e.g., near tissue-air or bone-tissue boundaries).[7]

The ionization in this case is measured at the place of interest in an air-filled ionization chamber having walls that are very thin compared with the range of the secondary electrons at the place of interest. If the walls are so thin that they make a negligible contribution to the total secondary electron emission that ionizes the air in the chamber, the material of which the walls are composed is not important. But because this condition is difficult to fulfill, it may be found to be advantageous to make the walls of a material that match fairly close in composition the immediately surrounding medium. The depth of the ionization chamber should be small in the direction of the gradient of the absorbed dose (see ICRU Report 10d (1962).

If a charge Q esu is carried by the ions of either sign generated per 0.001293 g of air, then applying the general cavity relation, D_{med}, (in rad) is given by

$$D_{\text{med}}=0.86_9 Q s_m \tag{IA9}$$

where s_m is evaluated for the electron spectrum at the point of interest.

e. *Absorbed dose in tissue or other material exposed to fast electrons.* For electrons, as for x rays, the condition of electronic equilibrium may or may not be satisfied. These cases will again be discussed separately.

Case I. Electronic equilibrium. If a β-ray emitter is homogeneously distributed throughout a medium in which the absorbed dose is to be measured, the conditions for electronic equilibrium will be almost ideally satisfied except near the boundaries of the medium. However, contrary to the above procedures for x rays, a thin-walled ionization chamber should be used,

[7] It should be pointed out that in such a region the spectral distribution of the electrons is not in equilibrium, and hence is not given by the reciprocal of the stopping power in the medium (neglecting δ rays), as is usually assumed (Spencer and Attix, 1955). However, because s_m for near-air-equivalent materials does not vary rapidly with energy, it can be evaluated approximately by assuming that the equilibrium conditions apply (see subsection IA1b).

as in the nonequilibrium x-ray case. The chamber walls merely act as electron absorbers, and should be minimized in thickness. However, the thickness should be varied in order to extrapolate the ionization current to zero wall thickness.

It is sometimes possible to eliminate the inserted cavity wall entirely, enclosing the air within walls of the medium itself. The inner surface of these walls must be made electrically conducting (if not already so) by a thin coating of a conducting material (e.g., graphite). Equation (IA9) is used in calculating the absorbed dose.

Case II. Electronic nonequilibrium. If a medium is exposed to an externally applied beam of electrons, the electron flux and spectrum will certainly vary from point to point within the medium, particularly in depth. Thus, the electronic-equilibrium conditions are not satisfied.

Here, again, a very thin- (or zero-) walled chamber should be employed. However, one cannot assume that the spectral distribution is the same as that for equilibrium, so values of the stopping power ratio for equilibrium may not be applicable (see subsection IA2c).

f. *Absorbed dose in tissue exposed to fast neutron radiation.* The theory of cavity ionization given above, and already discussed in some detail for gamma radiation, applies equally well to the dosimetry of neutron radiation. In nearly all practical devices the walls and gas have nearly identical atomic composition, hence, the question of stopping power is not a critical one in neutron dosimetry. Consideration is given in subsection IA3 to the question of the appropriate W for neutron dosimetry. In section IG practical methods of neutron dosimetry are discussed in detail.

g. *Distribution of the absorbed energy (concept of LET).* The absorbed dose specifies the total energy imparted by ionizing particles per unit mass of the irradiated material. The detailed spatial distribution of this dose depends primarily on the velocity and charge of the particles traversing the medium. Rather similar distribution patterns may be produced by electrons and protons of appropriate energies. Hence the "quality" of the radiation is best specified in terms of the type of tracks produced, rather than in terms of the nature of the primary radiation (x rays, neutrons, etc.), or of the secondary ionizing particles (electrons, protons, etc.).

A full description of the type of track would require a knowledge of the number and spatial distribution of all the collision processes which occur and this is clearly impossible. A single parameter which has been found useful for characterizing the track is the LET, and this parameter has been found in general to correlate well with the biological effectiveness of the radiation.

Even for a homogeneous primary radiation there will usually be a wide variation of LET along the tracks of individual secondary particles and between tracks of differing initial energy. The situation can, therefore, best be represented by giving the distribution of LET throughout the irradiated object. This can be done in two ways—in relation to dose, or to track length. For all chemical and many biological effects, the chief interest lies in the proportion of the total dose which is deposited in different LET intervals. This is the "distribution-in-LET" of the absorbed dose, and a typical spectrum of this kind is presented in figure IA2. An experimentally de-

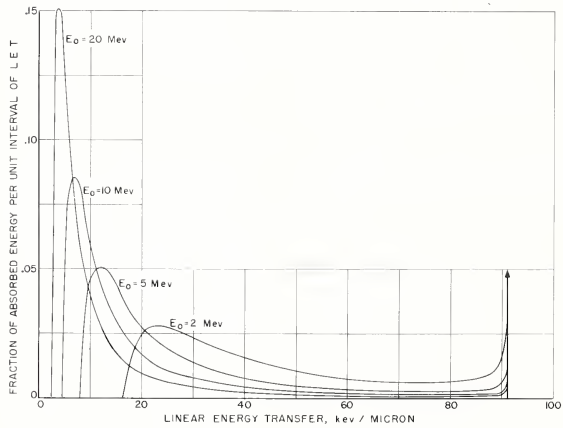

FIGURE IA2. LET *distribution for recoil protons produced in water by monoenergetic neutrons, when first collisions only are considered; i.e., when the irradiated object is thin compared with the mean free path of the neutrons in it.*

The ordinate gives the fraction of the total dose deposited per unit interval of LET. Additional LET distribution curves for mixed energy neutron beams and for total absorption of the neutrons in multiple collisions are given by Boag (1954).

termined distribution is given for comparison in figure IA3. The experimental curves differ from the theoretical ones in part, because they include recoiling heavier nuclei that are not included in the theoretical treatment; however, the main source of disagreement is due to the fact that an actual energy-loss distribution, no matter how obtained, must include fluctuations in energy deposition by particles of given nature and energy. Such fluctuations are ignored in the theoretical treatment.

It is important to note that figure IA2 represents a distribution with respect to dE/dx measured along the track of the recoil protons; and that the energy loss dE is obtained by including all energy transfers between the moving particle and the molecules encountered within a path length dx. Some of these energy transfers will be large enough to give rise to independent delta-ray tracks, and the energy communicated in such a transfer is not dissipated locally along dx, but along the delta ray. If delta rays above an arbitrary initial energy are considered as independent tracks, a different LET distribution will be obtained.

For certain biological effects depending upon the transit of secondary particles across small biological structures, the interest lies in the proportion of the total track length which falls into different LET intervals, i.e., the "distribution-in-LET", of the track length. When a mean value of LET is quoted, instead of a distribution, it is necessary to specify exactly how this mean has been taken, i.e., whether it refers to the LET of a particle of the mean energy of the secondaries,

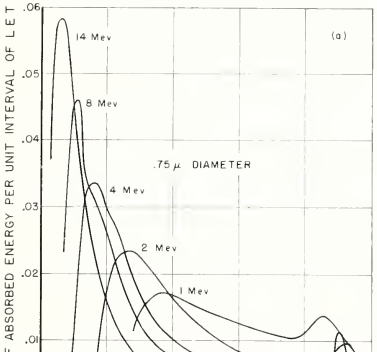

FIGURE IA3. *Experimentally determined* LET *distributions.*

These were determined for nearly monoenergetic neutrons of the indicated energies and for a test sphere corresponding to a diameter of 0.75 μ in soft tissue (Rosenzweig and Rossi, 1959).

or to a mean value of LET with respect to dose, or with respect to path length. The fuller information conveyed by a distribution curve, however approximate, is much more valuable than a single mean value. For a fuller discussion of LET distribution, see the original papers (Burch, 1957; Cormack, 1956; Cormack et al., 1957; Howard-Flanders, 1958, and Schneider and Cormack, 1959).

2. Stopping Powers of Electrons for Use with Cavity Chambers

a. *Electronic equilibrium in media exposed to x or gamma radiation.* The value of the stopping power ratio, s_m, is usually obtained from calculations based on the Bethe stopping power formula. This formula contains a constant I, the mean excitation potential, which is adjusted to fit the equation to experimental data. The values of s_m given below were calculated using values of I which were selected by a Study Group of the U.S. National Committee on Radiation Protection (NCRP, 1961) as best representing the experimental situation in the field of stopping power measurements. These values are listed in table IA3. There is some experimental disagreement between I values for heavy elements determined with low energy and with high energy protons. It has been suggested (Brandt, 1958) that the low energy data need a further correction arising from the binding of the electrons in the atoms of the irradiated medium. This led the NCRP Study Group to accept as correct the I values obtained with high energy protons. Work appearing since the completion of the NCRP report (Bichsel, 1961; Burlin, 1961, 1962) supports this choice. These I values differ from those used in the 1959 Report of the ICRU; the latter were obtained from the relation $I=13\ Z$. The resulting changes in s_m for the light elements are in the range of one to two percent.

TABLE IA3. *Selected values of the mean excitation potential*

Element	Mean excitation potential (ev)	Notes
1 H	20.7	Liquid.
	17.6	Saturated.
	14.8	Unsaturated.
3 Li	38	
4 Be	67	
6 C	78.4	Graphite.
	77.3	Saturated.
	75.1	Unsaturated.
	64.8	Highly chlorinated.
7 N	99.5	Amines, nitrates.
	85.1	Liquid.
	76.8	Ring.
Air	85	Gas.
8 O	98.5	–O–.
	98.3	Liquid.
	88.9	O=
13 Al	164	
17 Cl	170	
26 Fe	264	
29 Cu	306	
47 Ag	462	
50 Sn	517	
74 W	750	
82 Pb	812	
92 U	945	

In the Bragg-Gray theory the charged particles were assumed to lose energy continuously along their tracks and the ratio of the stopping powers in two media was assumed to be independent of particle energy. Laurence (1937) took into account the energy-dependence of the ratio. Spencer and Attix (1955) and Burch (1955) allowed both for the energy dependence of the ratio and for the fact that charged particles do not lose energy continuously but in discrete amounts, i.e., that delta rays are produced. The latter theories show that to obtain s_m it is necessary to calculate the integral of the ratio of the mass stopping power of the cavity gas to that of the wall material over the energy of each particle, and over the spectrum of starting energies of all the particles and that s_m is the reciprocal of this mean value. If s_m is calculated in this way for each element present, then the effective value for the given compound or mixture of elements comprising the wall material is obtained from Bragg's law: that is by multiplying s_m for each element by the proportion by weight of the element in the wall material, and summing over all constituents. Thompson (1952) has shown that Bragg's law holds with great accuracy if the stopping power of hydrogen is assumed to be different in saturated and unsaturated compounds and a few similar changes are made in the values for other light elements. Thompson's rules are reflected in the series of values quoted in tables IA3 to IA6. A more detailed theory of s_m is given in the NCRP report (1961).

Tables IA4 and IA5 give the values of s_m relative to air obtained for electrons in a region where electronic equilibrium exists and where all the electrons are emitted with the same energy T_o. These values were calculated by the Laurence method. Tables IA6 and IA7 give values of s_m that have, in addition, been averaged over the spectrum of Compton recoil electrons. For many practical purposes this value of s_m may be used for the light elements with adequate accuracy; if a significant number of photoelectrons or pair-electrons are produced, however, s_m has to be found by taking a weighted mean of the values for Compton, photo- and pair electrons using as weighting factors σ_{en}/μ_{en}, τ_{en}/μ_{en}, and κ_{en}/μ_{en}, respectively. Photoelectrons are practically monoenergetic and electron pair energies are fairly symmetrically distributed about their mean, so in both cases one may take values from tables IA4 and IA5 for these contributions. For compounds, a weighted average of the values in tables IA4 and IA5 or IA6 and IA7, or the value corrected for photo and pair electrons is used; the

TABLE IA4. *Mean mass stopping power ratios, s_m, relative to air and corrected for the polarization effect, for electronic equilibrium spectra generated by monoenergetic initial electrons*

Initial energy Mev	Element and state of molecular binding								
	Hydrogen, saturated	Hydrogen, unsaturated	Carbon, saturated	Carbon, unsaturated	Carbon, highly chlorinated	Nitrogen, amines, nitrates	Nitrogen, ring	Oxygen, –O–	Oxygen, O=
0.1	2.52	2.59	1.016	1.021	1.047	0.976	1.018	0.978	0.994
.2	2.52	2.59	1.015	1.019	1.043	.978	1.016	.979	.995
.3	2.48	2.55	1.014	1.018	1.040	.979	1.016	.981	.995
.327	2.48	2.54	1.014	1.018	1.040	.979	1.015	.981	.995
.4	2.46	2.53	1.014	1.018	1.038	.980	1.015	.981	.996
.5	2.44	2.51	1.013	1.017	1.037	.980	1.015	.982	.996
.6	2.44	2.50	1.012	1.016	1.035	.980	1.013	.981	.995
.654	2.43	2.49	1.011	1.014	1.034	.979	1.012	.981	.994
.7	2.42	2.48	1.010	1.013	1.033	.978	1.011	.980	.993
.8	2.40	2.46	1.009	1.012	1.031	.978	1.010	.979	.992
1.0	2.39	2.44	1.004	1.008	1.026	.975	1.005	.977	.988
1.2	2.37	2.42	1.001	1.004	1.022	.973	1.002	.974	.985
1.308	2.36	2.42	0.999	1.002	1.019	.971	1.000	.972	.983
1.5	2.35	2.39	.995	0.998	1.015	.967	0.996	.969	.980

TABLE IA5. *Mean mass stopping power ratios, s_m, relative to air and corrected for polarization effect, for electronic equilibrium spectra generated by monoenergetic initial electrons*

Initial energy Mev	Graphite	Al	P	Ca	Cu	Sn	Pb
0.1	1.014	0.859	0.875	0.852	0.711	0.555	0.468
.2	1.013	.870	.886	.869	.734	.595	.508
.3	1.011	.876	.891	.876	.745	.614	.526
.327	1.010	.877	.892	.878	.747	.617	.530
.4	1.009	.879	.894	.882	.752	.625	.539
.5	1.007	.881	.896	.885	.757	.633	.548
.6	1.005	.882	.898	.887	.761	.639	.555
.654	1.004	.883	.899	.889	.762	.642	.557
.7	1.003	.883	.899	.890	.764	.645	.560
.8	1.001	.884	.901	.892	.767	.649	.565
1.0	0.998	.885	.902	.895	.771	.655	.572
1.2	0.995	.885	.904	.898	.775	.660	.578
1.308	0.993	.885	.905	.899	.775	.663	.581
1.5	----------	-------	.907	.902	-------	.666	.584

TABLE IA6. *Mean mass stopping power ratios, s_m, relative to air and corrected for the polarization effect, for electronic equilibrium spectra generated by Compton recoil electrons*

Gamma ray energy Mev	Element and state of molecular binding								
	Hydrogen, saturated	Hydrogen, unsaturated	Carbon, saturated	Carbon, unsaturated	Carbon, highly chlorinated	Nitrogen, amines, nitrates	Nitrogen, ring	Oxygen, –O–	Oxygen, O=
0.15	2.73	2.85	1.020	1.027	1.058	0.970	1.022	0.972	0.992
.25	2.62	2.72	1.017	1.022	1.050	.974	1.019	.976	.994
.4	2.55	2.63	1.016	1.020	1.045	.977	1.017	.978	.995
.6	2.50	2.57	1.014	1.018	1.040	.979	1.016	.980	.995
1.0	2.44	2.50	1.008	1.012	1.032	.977	1.009	.978	.991
1.5	2.39	2.45	1.001	1.005	1.023	.972	1.003	.973	.985
2.0	2.36	2.42	0.994	0.997	1.014	.966	0.995	.967	.978
2.5	2.32	2.37	.987	.990	1.007	.960	0.988	.962	.973

TABLE IA7. *Mean mass stopping power ratios, s_m, relative to air and corrected for the polarization effect, for electronic equilibrium spectra generated by Compton recoil electrons*

Gamma ray energy Mev	Graphite	Al	P	Ca	Cu	Sn	Pb
0.15	1.017	0.835	0.823	0.776	0.657	0.458	0.380
.25	1.015	.853	.850	.816	.696	.538	.443
.4	1.013	.866	.867	.842	.723	.575	.487
.6	1.011	.874	.879	.857	.740	.605	.518
1.0	1.005	.881	.888	.873	.758	.634	.548
1.5	0.999	.883	.894	.883	.768	.650	.567

weighting factors are the parts by weight of the elements in the compounds (Bragg's law). In table IA8 values of s_m are presented for a few compounds and a few particular gamma-ray-emitting isotopes.

The s_m values in tables IA4 to IA7 include corrections for the polarization effect (also called the density effect) (Whyte, 1954). Sternheimer (1952, 1956) and Nelms (1958) calculated polarization corrections to certain stopping powers. Unfortunately, many of those data were inappropriate for use in calculating tables IA4 to IA7 because they were based on other I values than those given in table IA3. In view of this and because the polarization corrections for water and the other organic compounds considered are very similar, an average correction for s_m was calculated and applied in tables IA4 and IA6. The error in s_m expected from using this average correction is less than about one-quarter percent. These average corrections are given in table IA9. In tables IA5 and IA7, only graphite and aluminium have been corrected for the polarization effect; the correction is negligible for the heavier elements.

TABLE IA8. *Mean mass stopping power ratios,* s_m, *relative to air and corrected for the polarization effect, and absorbed dose per esu/0.001293* g *air for selected materials and gamma rays (for electronic equilibrium spectra)*

Gamma ray emitter	Gamma ray energy Mev	Polyethylene	Water	Tissue*	Polystyrene	Lucite	Graphite
		s_m					
Au-198	0.41	1.233	1.149	1.149	1.139	1.124	1.013
Cs-137	.67	1.225	1.145	1.145	1.133	1.120	1.010
Co-60	1.25	1.209	1.135	1.133	1.120	1.109	1.002
		Rads per esu/0.001293 *g* air**					
Au-198	0.41	1.071	0.998	0.998	0.990	0.977	0.880
Cs-137	.67	1.064	.995	.995	.985	.973	.878
Co-60	1.25	1.051	.986	.985	.973	.964	.871

*Assuming the composition given in footnote 5 for muscle and air and that 10 percent of the bonds are unsaturated or O=.

**Assuming W = 33.7 ev, so that an exposure of 1 R will produce an absorbed dose in air of 0.869 rad under conditions of charged particle equilibrium.

TABLE IA9. *Average polarization correction to* s_m *for water and organic materials*

Monoenergetic electrons		Compton recoil electrons	
Initial energy Mev	Correction	Photon energy Mev	Correction
0.6	0.001	1.0	0.005
.654	.002	1.5	.011
.7	.003	2.0	.018
.8	.004	2.5	.025
1.0	.008	----------	----------
1.2	.011	----------	----------
1.308	.013	----------	----------
1.5	.017	----------	----------

Some calculations of stopping power ratios are available which use the Spencer-Attix theory and these have been compared with results of the Laurence theory. It is characteristic of the theories that allow for delta ray effects that s_m is a function of cavity size. The NCRP report gives (in their fig. 3.a—3.e) the ratio of the s_m values calculated according to the Laurence and the Spencer-Attix theories as a function of chamber size. The difference is less than 20 percent in the very worst case considered, that of a small lead-wall chamber filled with air. Such a wide difference in atomic number of the wall and gas is hardly ever needed in practical applications of cavity chambers. The review made by the NCRP Study Group (1961) showed that most of the experimental data for walls of low atomic number agree with the Laurence theory to within the experimental uncertainties. These uncertainties are generally about 1 to 2 percent, although under special conditions they may be as low as 0.5 percent.

If it becomes necessary to use chamber walls of high atomic number, the information in the figures in the NCRP report together with the information in the present tables can be useful in interpreting results. In such cases, however, it frequently happens that still another correction is needed. All the theories for s_m published so far assume that the cavity is small enough not to perturb appreciably the flux of secondary electrons in the vicinity of the cavity. When the wall and gas of the chamber differ considerably in atomic number, this is likely to be incorrect. No theories have yet been published that deal with such cavity perturbations. The NCRP Study Group found an empirical method of extrapolating to zero chamber size and thus removing the perturbation; this method can be studied in their report (NCRP, 1961).

b. *Electronic equilibrium in media exposed to beta rays.* If a beta-ray emitter is uniformly distributed throughout a medium in which the absorbed dose is to be measured, the conditions for electronic equilibrium will be almost ideally satisfied except near the boundaries of the medium. s_m should be obtained by averaging over the electron spectrum existing in the medium. It has been found, however, that for electronic equilibrium conditions, s_m will be practically the same as for Compton recoil electrons whose average energy on emission is the same as the average energy of the emitted beta rays (NCRP, 1961). For the Compton electrons this average energy is $(\sigma_a/\sigma)h\nu$, see figure IA4. For the beta rays, the average energy is about one-third the maximum beta-ray energy.

c. *Electronic non-equilibrium conditions.* s_m should always be obtained by averaging over the electron spectrum existing in the medium at the point of interest. There is seldom much information about this electron spectrum for non-equilibrium. In such cases, the best that can be done may be to use the s_m appropriate to electronic equilibrium conditions.

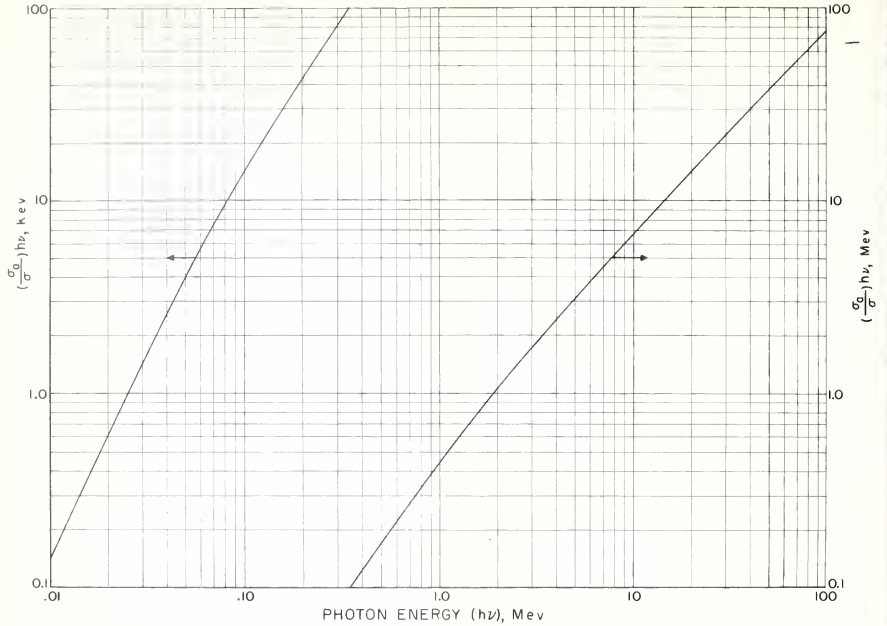

FIGURE IA4. *Graph of $(\sigma_a/\sigma)\ h\nu$, the mean initial energy of the Compton recoil electrons produced by monochromatic γ rays of quantum energy $h\nu$.*

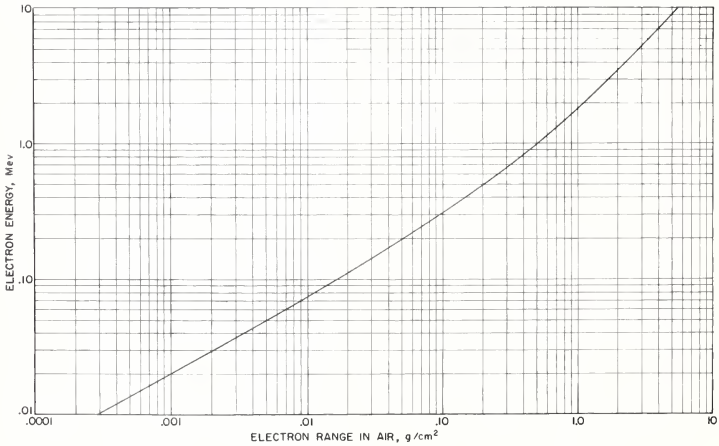

FIGURE IA5. *Approximate maximum range-versus-energy curve for electrons in air, calculated by Nelms (1956).*

In the case of an externally applied beam of monoenergetic electrons penetrating a thin foil, all the electrons will have very nearly their incident energy and the ratio of the mass stopping powers at that energy may be used for s_m. The same will be true near the surface of thicker absorbers. At greater depths in a thick absorber the average energy of the electrons can be estimated from the range-energy relation (see fig. IA5) and s_m for an equilibrium spectrum of that same average energy used.

3. Average Energy per Ion Pair, W

The average energy expended by a charged particle in a gas per ion pair produced will be designated by W. It is usually expressed in electron volts (ev). It varies from gas to gas and, to a small extent, for different kinds of particle. The dependence on energy is negligible for electrons in all gases (at least above 20 kev) and for α particles in the noble gases; there is a small dependence for the low-energy α particles in air (see below).

Absolute measurements of W for electrons are difficult to make accurately, but a number of recent measurements for air, based on a variety of techniques, are reasonably consistent. The results are listed in table IA10, along with a mean value derived from them. (It should be noted that all of these values are derived, directly or indirectly, from calorimetric determinations of energy.) In sets of measurements on different gases made with the same apparatus, the relative values obtained are probably more reliable than the absolute values. Table IA11 presents a number of such sets. Where possible, they have been normalized to the mean value of 33.73 ev derived from the absolute measurements in air. Values depending on stopping-power ratios have been recalculated on the basis of data in a report by the National Committee on Radiation Protection and Measurements (1961). With one or two exceptions, the different figures for a given gas show a satisfactory consistency. The final column of the table lists weighted mean values for each gas, based on the standard deviations quoted by the authors. (For the purposes of this calculation, the standard deviation in the results of Jesse and Sadauskis (1955) was assumed to be 0.5 ev.) The standard deviations recorded for the mean values are derived from the individual standard deviations. In most cases they are consistent with the spread in values among different experiments.

Table IA12 lists W values for α particles with initial energies between 5 and 6 Mev, based on the total ionization collected when the full energy is expended in the gas. No results for experiments based on fast collection of electrons have been included, since these appear to give higher values than experiments based on ion collection (Herwig and Miller, 1954). (In dosimetric problems the collection time is usually long and the ions are collected.) Since absolute measurements with α particles present fewer difficulties than those with electrons, no attempt has been made to renormalize the results. The last column again presents weighted mean values, with standard

Table IA10. W *values for electrons in air*

Reference	Radiation	W (ev)
(a)	2 Mv x ray	33.9±0.8
(b)	$S^{35}\beta$ rays	33.6±0.3
(c)	$S^{35}\beta$ rays	33.7±0.3
(d)	$Cs^{137}\gamma$ rays	33.9±0.5
(e)	Cs^{137} & $Co^{60}\gamma$ rays	33.8±0.4
(f)	$Co^{60}\gamma$ rays	33.84±0.34
	Weighted Mean=33.73±0.15 ev	

[a] Weiss and Bernstein (1956).
[b] Gross et al., (1957).
[c] Bay et al., (1957).
[d] Goodwin (1959).
[e] Reid and Johns (1961).
[f] Myers et al., (1961).

Table IA11. W *values for electrons (ev.)*

Reference Radiation	a*† 2 Mev x rays	g* A^{37}, $H\beta$ rays	h*† 2 Mev x rays	i* Ni^{63}, $H\beta$ rays	j $S^{35}\beta$ rays	k† 1–34 Mev electrons	Weighted mean
Gas							
H_2		36.6±0.7	36.3±0.7	35.9		38.1±0.7	36.6±0.3
He		31.3±0.6	39.6±0.8	41.9		42.8±0.9	41.5±0.4**
N_2	34.7±0.5	34.5±0.7	34.5±0.7	34.4	34.9±0.5	34.5±0.8	34.6±0.3
O_2	30.7±0.5	31.1±0.6	31.0±0.6	30.6			30.8±0.3
Ne			36.1±0.7	36.2			36.2±0.4
A	26.1±0.3	26.1±0.5	26.4±0.5	26.1			26.2±0.2
Kr			24.6±0.5	23.9			24.3±0.4
Xe			21.9±0.4	21.8			21.9±0.3
Air	(33.73)	(33.73)	(33.73)	(33.73)			33.73±0.15
CO_2	33.1±0.4			32.7			32.9±0.3
CH_4	26.8±0.4	29.1±0.6		27.0	27.3±0.5		27.3±0.3
C_2H_2				25.8	25.6±0.5		25.7±0.4
C_2H_4	26.5±0.4		26.6±0.5	25.9			26.3±0.3
C_2H_6				24.6	24.5±0.5		24.6±0.4

*Normalized to W=33.73 for air.
†Stopping-power factor revised.
**The low value of reference g is not included. Values for helium are very sensitive to impurities.
[a] Weiss and Bernstein (1955).
[e] Valentine and Curran (1952).
[h] Weiss and Bernstein (1956).
[i] Jesse and Sadauskis (1955).
[j] Jesse (1958).
[k] Barber (1955).

TABLE IA12. W *values for α particles (ev)*

Reference	(g)	(l)	(m)	(n)	(o)	(p)	(q)	(r)	(s)	(t)	Weighted mean
Gas											
H_2	37.0±0.7	36.3			35.96±0.15	37.0±0.13					36.2±0.2
He*	31.7±0.6	42.7		29.6±0.3		46.0±0.5					
N_2	36.0±0.7	36.6	36.4±0.4	36.30±0.15	36.50±0.15	36.3±0.4	36.39±0.07	36.38±0.07		36.6±0.5	36.39±0.04
O_2	32.2±0.6	32.5	32.9±0.3	32.17±0.15		32.2±0.3					32.3±0.1
Ne		36.8									36.8
A	25.9±0.5	26.4	26.3±0.3	26.25±0.12		26.4±0.3				26.5±0.3	26.3±0.1
Kr		24.1									24.1
Xe		21.9									21.9
Air	35.2±0.7	35.5	35.6±0.4		34.95±0.18	35.0±0.3	34.96±0.07	34.97±0.07		35.5±0.5	34.98±0.05
CO_2		34.5	34.2±0.3	33.5±0.3	34.3±0.3	34.3±0.3		34.04±0.1	34.0±0.3		34.1±0.1
CH_4	29.0±0.6	29.2	29.1±0.4		29.00±0.15	29.4±0.3					29.1±0.1
C_2H_2		27.5									27.5
C_2H_4		28.0				28.0±0.3	28.03±0.05				28.03±0.05
C_6H_6		26.6									26.6
BF_3					35.3±0.4	36.0±0.4					35.6±0.3

*Values for helium are very sensitive to impurities. That of Bortner and Hurst (1954) probably corresponds most closely to pure helium.

[g] Valentine and Curran (1952).
[l] Jesse and Sadauskis (1953).
[m] Sharpe (1952).
[n] Haeberli et al., (1953).
[o] Biber et al., (1955).
[p] Bortner and Hurst (1954).
[q] Jesse (1960).
[r] Bay et al., (1961).
[s] Widder and Huber (1958).
[t] Genin (1956).

deviations derived from the stated errors of the authors.

The results for the noble gases except helium appear consistent with the assumption that the W values are the same for α particles and electrons. Note that this is not true for air and a number of other gases.

For neutron dosimetry, W values for protons with energies up to several Mev are of interest. For the noble gases these should be the same as for α particles and electrons. The variation with energy for low-energy α particles in air (e.g., Ishiwari et al., 1956) and the difference between the values for α particles and electrons in many gases suggest that in these gases W increases slightly with increasing specific ionization. The values for protons would therefore be expected to lie between those for electrons and those for α particles. The few measurements that have been made in the energy range of interest (e.g., Jentschke, 1940; Larson, 1958) tend to give values slightly *higher* than those for α particles. Using the same values for protons as for α particles should not involve errors of more than a few percent in the worst case.

The W value for a mixture of gases must be determined experimentally; it is not in general equal to the weighted mean of the values for the components of the mixture. Information for a number of mixtures is provided by Bortner and Hurst (1954); Moe, et al., (1957); and Valentine and Curran (1958).

In the previous report it was recommended that a W value of 34 ev be used for calculations concerning x and gamma radiation of quantum energy greater than 20 kev. It was realized at that time that the value might actually be somewhat lower, but the evidence was incomplete. In view of the more extensive evidence now available (table IA10), a value of 33.7 ev has been used throughout this report in calculating quantities depending upon it.

4. Saturation in Ionization Measurements

Failure to collect all the ions produced in an ionization chamber may be due to either initial or general recombination. The amount of initial recombination depends upon the LET of the ionizing particle and upon the strength of the collecting field and its direction in relation to the particle track. The best treatment of initial recombination is that by Jaffe (1929) with modifications by Zanstra (1935), and that by Kara-Michailova and Lea (1940). Initial recombination does not depend upon dose rate and is usually only troublesome for slow particles or high gas pressures.

General recombination can be treated theoretically in simple cases but it must be stressed that difficulty in achieving saturation is often due principally to inappropriate design of the ionization chamber. If there are regions in the chamber where the field strength is much lower than the maximum, it will be difficult to achieve saturation in these regions without exceeding, in other parts of the chamber, the field strength at which multiplication of ions by collision can begin.

For plane parallel ionization chambers uniformly irradiated at constant dose rate, a saturation curve can be drawn (Boag, 1956) as a function of the dimensionless variable $\xi = m(d^2\sqrt{q}/V)$ where d is the spacing (cm), V the collecting voltage (volts), q the charge density production rate (esu/cm^3-sec) and m is a constant depending upon the type and density of the gas. This curve is illustrated in figure IA6, where $F(\xi)$=collection efficiency, and it can be represented with adequate accuracy by the formula $F(\xi) = 2/(1+\sqrt{1+\xi^2})$. For air at 760 mm and 20° C, the constant m has the value 30.

For cylindrical or spherical geometry in the ionization chamber the foregoing saturation curve still applies, but instead of d, one must insert $K(a-b)$, where $(a-b)$ is the radial spacing of the

electrodes, and K is a shape factor whose values are given in figure IA7.

The foregoing curve and formula for $F(\xi)$ apply to continuous radiation. In the case of instantaneous pulses of radiation (Boag, 1956) whose duration is short compared with the time required to collect the ions, the appropriate dimensionless variable is $u=\mu(d^2r/V)$, where r is the charge density per pulse (esu/cm^3). In this case the collection efficiency, $F(u)=(1/u)\ \log\ (1+u)$. For air at 760 mm and 20° C, $\mu=1000$. $F(u)$ is given graphically in figure IA8 for plane geometry. The extension to cylindrical and spherical geometry again involves the shape factors K_{cyl} and K_{sph} from figure IA7.

When an x-ray tube is run on a pulsating potential supply, the x-ray output occurs in pulses whose duration may be long compared with the collection time of the ions in the ionization chamber. In this case, the collection efficiency depends upon the average dose rate during the pulse, and, as in the case of instantaneous pulses, it is independent of the pulse repetition frequency. Saturation curves taken with a pulsating x-ray output agree well with those taken with continuous output when the average intensity *during the pulse* is the parameter used.

Chambers that include regions of plane, cylindrical, and spherical geometry can be dealt with by considering the collection efficiency in each of the regions separately and adding together the currents from all regions. These formulas and curves should be regarded as a guide to the variables which determine saturation but not as a substitute for accurate experimental checks on saturation conditions in a particular chamber.

B. Calorimetric Methods

For most absorbing materials all but a few percent of the energy absorbed from a radiation field ultimately appears as heat. Therefore, a calorimetric measurement of this energy is, in principle, a very direct approach although one that requires considerable experimental refinement. Calorimetric systems have been devised which measure intensity and others which measure absorbed-dose rate. These systems operate by absorbing energy from the radiation field, retaining this energy until it is degraded to thermal energy, and evaluating this heat by measuring the rise in temperature of the system. The heat capacity of the system can be determined very accurately by introducing known electrical power. The loss of absorbed radiation energy to forms other than heat is a fundamental difficulty in calorimetric measurements. Intensity measurements will be in error if energy is carried away by bremsstrahlung or by neutrons; in absorbed-dose measurements on the other hand such escape should be permitted. Conversion of energy into a chemical form will produce an error, however. At the present time it seems that the uncertainty due to lack of knowledge about these losses to chemical energy in many substances is at least as large as the uncertainty in

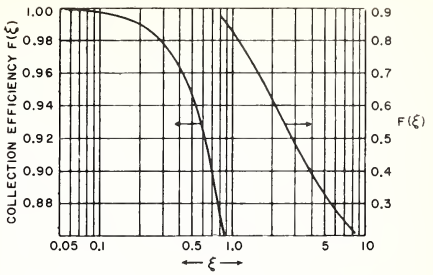

FIGURE IA6. *Collection efficiency in an ionization chamber exposed to continuous radiation.*

The curve is broken into two parts for greater accuracy in reading. The left-hand ordinate scale applies to the left-hand portion of the curve, and the right-hand ordinate scale to the remainder of the curve (Boag, 1956).

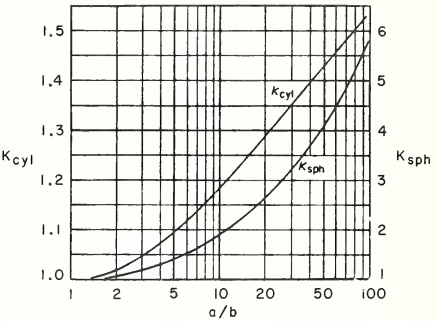

FIGURE IA7. *Factors for calculating the equivalent gap length in cylindrical and spherical ionization chambers.*

The a and b are external and internal radii of the chamber, respectively. Equivalent gap length $=K_{cyl}(a-b)$ for cylindrical geometry. Equivalent gap length $=K_{sph}(a-b)$ for spherical geometry (Boag, 1956).

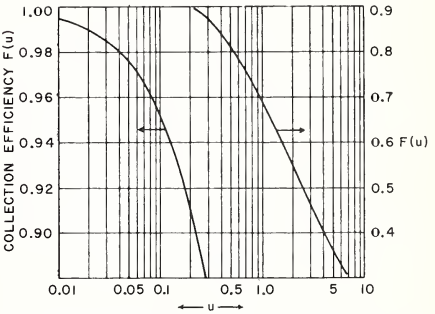

FIGURE IA8. *Collection efficiency of an ionization chamber exposed to pulsed radiation.*

The curve has been broken into two parts for accuracy in reading. Examples: For $u=0.2$, $F(u)=0.91$; for $u=2$, $F(u)=0.55$ (Boag, 1956).

ionization measurements due to lack of accuracy in W.

The calorimetric measurement of absorbed dose at any point within an extended medium under irradiation involves measurement of the temperature rise in a small thermally-insulated mass of material centered at that point. Such thermal insulation must not significantly perturb the absorption or the spectral distribution of the radiation field. The temperature sensors and heaters must constitute only a relatively small fraction of the mass of the thermally-insulated material. Successful measurements of this type for both copper and polystyrene media have been described by Genna and Laughlin (1956) for Cobalt-60 gamma rays.

Measurements of the energy absorbed from Co^{60} gamma radiation in small pieces of Dural and of graphite suspended in an evacuated glass tube have been carried out (Bernier et al., 1956; Reid and Johns, 1961) and the ionization in chambers of similar materials and geometry measured under identical conditions for comparison. Similar experiments were done with graphite irradiated by Co^{60} gamma rays (Hart et al., 1958), and by x rays of 22 Mvp (Skarsgard et al., 1957). All of these experiments involve measurements of absorbed dose in a small isolated mass, not in a segment of an extended medium as would be necessary in plotting fields within a phantom.

Endothermic radiation-induced chemical reactions may occur in many materials. Measurements made with the Fricke ferrous sulphate dosimeter and with an absorbed dose calorimeter under identical geometrical conditions indicated that in polyethylene irradiated by Co^{60} gamma rays, 3 percent of the energy went into chemical change (Milvy et al., 1958). In later work endothermic chemical reactions were avoided by using pure carbon as the absorber in the calorimeter, (Milvy et al., 1960). In pure water also, under steady irradiation conditions, there is no net loss to chemical reactions (Brynjolfsson, 1960). The standard deviation of measurements made with these calorimeters at a rate of 50 rad/min was one percent. The accompanying table, IB1, gives a synopsis of work done with calorimetric dosimeters.

Comparisons of calorimetric measurements with corresponding measurements by ionization or chemical methods have provided values of W_{air} (ev expended in air per ion pair formed), and of G (molecules reacting per 100 ev absorbed) for certain reactions. These results are reported in some of the references included in the table.

C. Chemical Dosimetry

Chemical dosimetry is based on the principle that certain quantitative oxidation and reduction reactions take place upon irradiation, to an extent directly proportional to the absorbed dose. Of all the chemical systems available for dosimetry, only ferrous sulfate is reliable enough for routine use but other systems are readily calibrated by reference to it. Ceric sulfate is next in usefulness and reliability and it is followed by a group of systems included in this report primarily because of their utility in extending the range of the ferrous sulfate dosimeter. The ferrous sulfate and ceric sulfate systems are capable of measuring absorbed dose with standard analytical techniques to within one percent. Absolute calibration of the ferrous sulfate dosimeter to absorbed dose has been made by calorimetry.

1. Ferrous Sulfate Dosimeter (Fricke Dosimeter)

The chemical reaction which has been most extensively used as a standard of reference for dose is the oxidation of ferrous sulfate in 0.1 to 0.8 *N* sulfuric acid solution. This reaction was first studied by Fricke and Morse (1929). The reproducibility and ease of measurement are good

TABLE IB1. *Experiments in calorimetric dosimetry*

Reference	Calorimeter type	Type of radiation	Minimum practical rate described	Precision under Column 4 conditions (±%)	Comments
Laughlin and Beattie (1951).	Total beam	130 kvp x rays			
Laughlin et al., (1953).		200 kvp x rays			
Laughlin and Genna (1956).		250 kvp x rays	50R/min	1	
		400 kvp x rays			
		Cobalt-60 γ rays			
		22.5 Mvp x rays	0.5 milliwatts/cm²	1	
Edwards and Kerst (1953).	do	150 Mvp x rays			
		200 Mvp x rays	10 milliwatts/cm²	2	
		250 Mvp x rays			
		300 Mvp x rays			
McElhinney et al., (1957).	do	1.4 Mvp x rays	~20R/min	1.8	
Dolphin and Innes (1956).	do	1500 kvp x rays	50R/min	1	
		1 mvp x rays	40R/min	1.5	
Goodwin (1959)	do	Cesium-137 γ rays	14R/min	1	
Genna and Laughlin (1955, 1956).	Absorbed dose	Cobalt-60 γ rays	50 rads/min	0.7	In segment located in extended medium: (copper, polystyrene) endothermic chemical reaction in polystyrene.
Milvy et al., (1958).					
Milvy et al., (1960)	do	do	do	1	Carbon, no chemical energy loss.
Bernier et al., (1956).	do	do	30 rads/min	0.6	Small isolated mass (dural, graphite).
Skarsgard et al., (1957)	do	22 Mvp γ rays	30 rads/min		
Reid and Johns (1961)	do	Cobalt-60 γ rays	50 rads/min	0.4	Small isolated mass (aluminum, graphite).
		Cesium-137 γ rays	20 rads/min	0.5	
Petree (1958)	do	Cobalt-60 γ rays	$8x10^3$ rads/min	0.15	Small isolated mass (carbon).
			120 rads/min	0.5	
Brynjolfsson (1960)	do	do	$2x10^3$ rads/min	<0.1	Ice-water system.

Disadvantages lie in the variation of the yield with the LET of the incident radiation, and in the requirement that the concentration of dissolved oxygen in the solution be kept above a certain limit throughout the exposure. The mechanism of the reaction is now well understood, even in detail (Allen and Rothschild, 1957; Allen et al., 1957). In the light of present knowledge of its behavior the following standard procedure can be recommended.

A solution is prepared, which is about 1 mM in ferrous sulfate or ferrous ammonium sulfate, 1 mM in sodium chloride (to counteract the effect of possible organic impurities originally present in the water or introduced by the irradiation cell), and 0.8 N in sulfuric acid (Dewhurst, 1952; Wiess et al., 1956). The water is distilled beforehand from alkaline permanganate solution in an all-glass system; further purification is unnecessary. Pyrex or silica irradiation cells are preferred, although cells constructed from polystyrene or polyethylene have been successfully used. Irradiation cells made from plasticized polymers are to be avoided (Hall and Oliver, 1961). Chemicals of analytical grade may be used without further purification. Using a solution initially in equilibrium with the atmosphere, a dose of between 5,000 and 50,000 rads of x, gamma or fast-electron radiation may be measured, but to avoid depletion of the oxygen content of the solution the upper limit should not be exceeded. Higher doses of x, gamma or fast-electron radiation up to 200,000 rads may be measured if the solution is saturated beforehand with oxygen, if care is taken not to introduce additional impurities during equilibration with this gas, and if higher initial ferrous ion concentration ($4mM$) is used. With radiations of higher LET, the consumption of oxygen is less rapid and somewhat higher doses may be given without oxygen depletion if the solution is well stirred during irradiation to maintain the oxygen concentration in the irradiated zone.

The temperature coefficient of the gamma-ray induced oxidation is low (0.04 ± 0.03 percent °C between 0 and 70 °C, Schwarz, 1954), and the yield is independent of dose rate between 6 rad/min and 10^{10} rad/min (Schuler and Allen, 1956; Glazunov and Pikayev, 1960; Anderson, 1962). With radiations of high LET, a slight dependence of yield on ferrous ion concentration is observed. For example, with the recoiling radiations from the $B^{10}(n, \alpha)Li^6$ process, the ferric yield in 10 mM ferrous solutions is about 4 percent higher than in 1 mM (Schuler and Barr, 1956); with deuterons, about 1.5 percent (Schuler and Allen, 1957); but with gamma rays, the difference is negligible.

In the absence of radiation, aerated ferrous sulfate solutions are slowly oxidized in a thermal reaction with dissolved oxygen. The rate of this oxidation is proportional to the square of the ferrous ion concentration and the first power of the oxygen concentration (Huffman and Davidson, 1956). In 10 mM ferrous solutions this spontaneous oxidation proceeds to the extent of about 2 μM/liter day at 25 °C, and sets a lower limit of dose rate at which the system can be used with accuracy.

Standard procedure for taking this thermal reaction into account is to measure the difference in ferric ion concentration between the irradiated solution and the unirradiated solution which has been stored in an identical vessel for the same length of time.

The analysis of the ferric ion is most readily undertaken by direct spectrophotometry on the dosimeter solution at 304–5 mμ. The extinction coefficient varies somewhat with temperature (0.69 percent per degree in the range 20–30 °C, at 304 mμ (Scharf and Lee, 1961)), so that for high precision a constant temperature cell holder is advisable. Recent determinations of the molar extinction coefficient are in agreement when corrected to 25 °C by the above temperature coefficient. The values are: 2193 ± 6 (Schuler and Allen, 1956), 2197 ± 10 (Lazo, et al., 1954), 2187 ± 5 (Holm et al., 1961) and 2196 ± 5 (Scharf and Lee, 1961), all in 0.8 N sulfuric acid. The sensitivity of this method can be doubled by measuring the absorbance at the 224 mμ ferric ion peak instead of at 304 mμ. Two advantages accrue. At the shorter wavelength the molar extinction coefficient is 4565 liter $mole^{-1}cm^{-1}$ compared with 2196 and the temperature coefficient of the extinction coefficient in the range 20–30 °C is only 0.13 percent per degree (Scharf and Lee, 1961). If a spectrophotometer is not available, an alternative colorimetric method of determining ferrous ion as the complex with o-phenanthroline is simple and reliable (Miller, 1956; Bouzigues et al., 1961).

The ferrous sulfate system is less useful with electromagnetic radiation of such quality that photoelectric absorption or pair formation processes take place to an appreciable extent in aqueous solutions. With Co^{60} gamma rays, the ratio of the doses absorbed in 0.8 N sulfuric acid and in water exposed to the same quantity of radiation can usually be taken as equal to the ratio of the electron densities of the two media, that is 1.024, but at lower photon energy this is, of course, no longer the case, and a detailed calculation requires a knowledge of the spectral distribution. The sulfuric acid concentration can be lowered to a minimum of 0.1 N with only a 2 percent fall in the ferric yield observed with Co^{60} gamma rays (Allen et al., 1957), but at lower concentrations of acid the gamma ray yield falls, and the mechanism of the reaction ceases to be simple. It can be taken, therefore, that a concentration of 0.1 N sulfuric acid is the lowest that can be used for reproducible dosimetry. From the analytical point of view the use of other acidities in this range introduces no complication since the extinction coefficient of the ferric ion shows little variation with acidity in the region 0.1 to 0.8 N (Haybittle et al., 1956). Adjustment of low-acidity ferrous sulfate solutions to 0.8 N sulfuric acid is, however, recommended before the spectrophotometric measurement is made.

Even in 0.1 N acid, however, it may in some

conditions be difficult to correct for photoelectric absorption precisely; moreover the ferric yield at constant acidity falls with increasing LET (Back and Miller, 1957). Accurate dosimetry of radiations of 200 kev and lower is thus difficult to attain. Similar complications exist with very hard radiation on account of pair production, but few studies of the system with such radiation have been made (Laughlin et al., 1957; Minder, 1961).

Curve A of figure IC1 is a plot of $G(Fe^{3+})$ as a function of the initial LET of the particles concerned. The yields are integrated over the whole particle tracks, i.e., they are values of the ratio $\Delta M/E_i$, where ΔM is the total number of ferric ions formed by each ionizing particle, and E_i the mean initial energy of the particles in units of 100 ev. Curve A illustrates the trend and the consistency of the results which are detailed in table IC1. An interpolation in this curve will provide $G(Fe^{3+})$ for radiations not listed. Where more recent work may be considered to have superseded earlier measurements the latter are omitted. It will be noted that a consistent picture of the behavior of the system has emerged, though some anomalies remain, such as between the sets of results 6 and 7 (fig. IC1), both obtained with deuterons from a cyclotron.

For electron pulses at dose rate up to 2×10^8 rads/sec., $G(Fe^{3+})$ is independent of dose rate but above $\approx5\times10^8$ rads/sec., $G(Fe^{3+})$ diminishes with increasing dose rate (Anderson, 1962; Glazunov and Pikayev, 1960; Rotblat and Sutton, 1960). Accurate and consistent yields are not available but some recent data are assembled in table IC2. Here it is shown that $G(Fe^{3+})$ decreases from 15.6 to 11.3 ± 0.5 at 2.2×10^9 rads/sec. (Anderson, 1962). Consequently the Fricke dosimeter becomes less reliable at these high dose rates since calibration curves of $G(Fe^{3+})$ versus dose-rate are necessary.

The drop in $G(Fe^{3+})$ at dose rates greater than 5×10^8 rads/sec is a manifestation of a general property of aqueous systems. At dose rates of 10^9 rads/sec and higher the hydrogen and hydroxyl radicals are generated in the irradiated solution at such high concentrations that radical-radical reactions compete with the oxidation reactions which take place at lower intensities. The result is a decrease in $G(Fe^{3+})$ which becomes more pronounced as the dose rate increases.

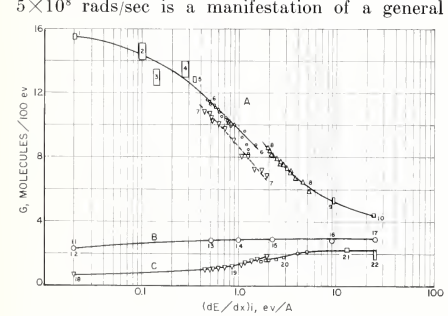

FIGURE IC1. *Oxidation and reduction yields in dosimeter solutions as a function of the initial* LET *of the irradiating particles.*

Curve A: Ferric yields in aerated ferrous sulfate solutions in 0.8*N* sulfuric acid; B: Cerous yields in aerated ceric sulfate solutions in 0.8*N* sulfuric acid; C: Ferric yields in aerated solutions 1 m*M* in ferrous sulfate and 10 m*M* in cupric sulfate, in 0.01*N* sulfuric acid.
Details as to the points indicated by numbers are recorded in table IC1.

2. Ceric Sulfate Dosimeter

For doses higher than $\approx5\times10^4$ rads, which is the upper limit for aerated ferrous sulfate solutions, only the ceric sulfate dosimeter may be regarded as a standard of reference for dosimetry. The ceric sulfate dosimeter may be used in the range 10^5 to 10^8 rads (Taimuty et al., 1959; Harlan and Hart, 1959).

Ceric sulfate dissolved in 0.1 to 0.8 *N* sulfuric acid is reduced to cerous ion with evolution of oxygen by all types of ionizing radiation. Analysis can be carried out spectrophotometrically using the ceric absorption at 320 mμ at which wavelength the molar extinction coefficient is temperature-independent but varies somewhat with pH. Recent values are 5000 ± 50 in 0.1 *N* sulfuric acid (Johnson and Weiss, 1957), and 5580 (Hochanadel and Ghormley, 1953; Medalia and Byrne, 1951), 5600 ± 50 (Johnson and Weiss, 1957) in 0.8 *N* acid. For ceric sulfate solutions above 0.01 *M*, titration with standard ferrous sulfate using 0.001 *M* ferroin as the indicator is preferable to spectrophotometric measurements (Harlan and Hart, 1959). Higher standards of purity than those applying to the ferrous sulfate dosimeter are needed for this system to behave reproducibly. The water must be triply distilled, with the first two distillations from a reagent solution such as alkaline permanganate or acid ceric sulfate. All glassware must be thoroughly cleaned, and before use allowed to stand for some days filled with a ceric sulfate solution. The dosimeter solution itself must stand for about a week; in making dilutions from a concentrated stock solution, it is desirable to use a very dilute (≈50 μM) ceric sulfate solution rather than water which has not previously been standing with ceric ion. Precision of ±1 percent is possible with great care (Taimuty et al., 1959). There is some evidence of a surface effect in the γ-ray induced reaction in that the cerous yield is considerably enhanced in vessels packed with glass beads. It is not certain that this is genuine as it may merely reflect the great difficulty in cleaning surfaces to the necessary extent.

Increasing concentrations of cerous ion reduce the cerous yield by scavenging OH radicals from the particle tracks (Sworski, 1956; Harlan and Hart, 1959). Because $G(Ce^{3+})$ depends on both ceric and cerous ion concentration, the use of ceric sulfate at concentrations above 0.1 *M* requires the use of an empirical equation correcting for the variable $G(Ce^{3+})$. The equation for 0.39 *M* ceric sulfate is

$$D=-2.32\times10^8 \log_{10}(1-1.16\ Ce^{3+})$$

where D is the absorbed dose in rad in the solution

TABLE IC1. *Aqueous solutions for dosimetry*

Reference on figure IC1	Type of radiation	Mode of energy measurement	G	Init. Fe^{3+} concentration	Footnote reference below
		Curve A. Ferrous sulfate solutions			
			Fe^{3+}	*mM*	
(a)	30 Mev electrons	Charge input	16.3±0.3	1	1
(a)	10 Mev electrons	do	15.7±0.3	1	1
1	2 Mev electrons	do	15.45±0.30	1-10	2
(a)	P^{32} β particles	Absolute counting	15.4±0.8	1	3
(a)	Co^{60} γ rays	Calorimetry	15.6±0.3		4
(a)	do	do	15.8±0.3		5
(a)	do	do	15.68±0.07		6
2	100 kvp x rays	Ionization	14.7±0.5		7
3	60 kvp x rays	do	13.1±0.5		7
(a)	35 kvp x rays	do	14.8		8
(a)	14 kvp x rays	do	14.4		8
4	8 kv x rays	do	13.4±0.6		9
5	H^3 particles	Counting and gas density	12.9±0.2		10
6-6 (circles)	4-19 Mev deuterons	Charge input		10	11
7-7 (inverted triangles)	3.5-21 deuterons	do		1	12
(a)	0.3-2 Mev protons	do		10	12
8-8 (triangles)	He ions, 12-32 Mev	do		10	11
9	Po^{210} α particles	Counting	5.1±0.10	10	13
10	B^{10} (n,α) Li^7 recoil radiation	Neutron flux measurement	4.38±0.08	10	14
		Curve B. Ceric sulfate solutions			
			Ce^{3+}		
11	Co^{60} γ rays	Comparison with $FeSO_4$	2.45±0.08		15
	do	do	2.50±0.04		16
12	2 Mev electrons	do	2.31		17
13	18 Mev deuterons	do	2.84		17
14	8 Mev deuterons	do	2.83		17
15	32 Mev He ions	do	2.92		17
16	Po^{210} α particles	do	2.78		18
17	B^{10} (n,α) Li^7 recoil radiations	do	2.95		17
		Curve C. Ferrous-cupric solutions			
			Fe^{3+}		
18	Co^{60} γ rays	Comparison with $FeSO_4$	0.66±0.02		19
19[b] (inverted triangles)	3-22 Mev deuterons	Charge input			12
20 (squares)	0.3-2 Mev protons	do			12
21[c]	3.4 Mev α particles	Comparison with $FeSO_4$	2.3		20
22	B^{10} (n,α) Li^7 recoil radiations	do	2.0±0.2		19

[a] These results are not plotted in figure IC1.
[b] These results are plotted on the same basis of dosimetry as those for ferrous sulfate solutions in the same laboratory (7-7, fig. IC1).
[c] This represents the results of a comparison with the ferrous sulfate dosimeter using Po^{210} α particles which had passed through two mica absorbers. The appropriate ferrous sulfate yield has merely been interpolated from figure IC1.

[1] Minder, 1961.
[2] Schuler and Allen, 1956.
[3] Donaldson and Miller, 1955.
[4] Hochanadel and Ghormley, 1953.
[5] Lazo et al., 1954.
[6] Holm et al., 1961.
[7] Haybittle et al., 1956.
[8] Gevantman and Pestaner, 1959.
[9] Cottin and Lefort, 1956.
[10] McDonell and Hart, 1954.
[11] Schuler and Allen, 1957.
[12] Hart et al., 1956.
[13] Trumbore, 1958.
[14] Schuler and Barr, 1956.
[15] Johnson and Weiss, 1957.
[16] Taimuty et al., 1959.
[17] Barr, 1958.
[18] Anta and Haissinsky, 1954.
[19] Hart and Walsh, 1954.
[20] Miller, 1958.

TABLE IC2. *Effect of dose rate on $G(Fe^{3+})$ for fast electron irradiations*

(Fe^{++}) *mM*	(Cl^-) *mM*	E Mev	Pulse length μ sec	Dose rate rad/sec	$G(Fe^{3+})$	Ref.
1.0	1.0	1.0	Cont)	0.002×10^6	15.6±0.5	1
1.0	1.0	2.0	do)			
3.0	----	4.0	1.7	9.6 ×10^6	14.3	2
3.0	1.0	1.0-1.2	5.0	0.016×10^6	15.0±1.6	3
3.0	1.0	1.0-1.2	5.0	0.18 ×10^6	13.4±0.6	3
3.0	1.0	1.0-1.2	5.0	0.75 ×10^6	10.8±0.9	3
3.0	1.0	1.0-1.2	5.0	2.4 ×10^6	10.1±0.5	3
1.0	1.0	15	1.4	0.091×10^6	15.2±0.4	4
1.0	1.0	15	1.4	0.69 ×10^6	14.5±0.4	4
1.0	1.0	15	1.4	2.26 ×10^6	11.3±0.5	4
1.0	1.0	15	1.4	2.92 ×10^6	12.2±0.5	4
1.0	1.0	15	1.4	8.0 ×10^6	11.8±0.5	5
1.0	1.0	15	1.4	8.0 ×10^6	13.0±0.4	5
1.0	10.0	15	1.4	8.0 ×10^6	8.0±0.5	5

[1] Schuler and Allen (1956).
[2] Keene (1957).
[3] Glazunov & Pikayev (1960).
[4] Anderson (1962).
[5] Thomas (1962).

and Ce^{3+} is the cerous ion concentration (moles/liter) after the solution is irradiated. A precision of 2 percent is reported (Harlan and Hart, 1959). Results are summarized in table IC1 and curve B of figure IC1.

3. Other Chemical Systems

Many chemical systems have been proposed for dosimetry. These systems, calibrated by comparison with the Fricke dosimeter, have applications for which the Fricke dosimeter is less satisfactory or unsuitable. A comparison of some of the more widely used systems with the Fricke and ceric dosimeters is given in table IC3.

An extension of the range of chemical dosimeters to doses below one kilorad has been possible by the use of new systems and by increasing the sensitivity of the Fricke dosimeter. Doses as low

TABLE IC3. *Comparison of chemical dosimeters for Co^{60} gamma rays*

Dosimeter	Dose range (rads x 10^{-6})	Precision %	Postirradiation stability	G	Compound measured	Reference
Benzoic acid	0.000005+	±5	Fair		Fluorescence of oxidation products.	1
Quinine	.00001-.001	do	do	2.3 (max)	Decrease in fluorescence	2
Trichloroethylene	.00001 to 0.005	do	do	Variable	HCl	3, 4
Ferrous sulfate + formic acid + O_2	.0003-0.003	do	do	225	Fe^{3+}	5
Chloroform	.001-0.04		do	25.8	HCl	6
Fricke	.004-0.04	±1	Stable	15.6	Fe^{3+}	7
Formic acid + O_2	.001-0.10	±5	Fair	3.39±0.2	H_2O_2	8
Dyes in gels	.01-0.5		do	135	Dye	9, 10
Ceric sulfate	.05-100	±2	Stable	2.50	Ce^{4+}	7
Ferrous sulfate + cupric sulfate	.1-10	±5	Fair	0.66	Fe^{3+}	7
Oxalic acid	1.6-160		Stable	4.9	Oxalic acid	11
Water + KI	0.1-1000	±5(±2 above 10^6 rads)	do	0.58	I_2	12
Nitrous oxide	.01-3000	±5(±20% above 10^8 rads)	do	12	N_2+O_2	13
Polyisobutylene in heptane	.001-10000	±4 (max)	do	Calibration curve	Viscosity	14

[1] Barr and Stark, (1958).
[2] Barr and Stark, (1960).
[3] Taplin, (1956).
[4] Sigoloff, (1956, 1961).
[5] Hart, (1952).
[6] Teplý & Bednár, (1958).
[7] See Table IC1.
[8] Hart, (1954).
[9] Gevantman, et al., (1957).
[10] Gevantman, (1960).
[11] Draganic, (1959).
[12] Hart and Gordon, (1954).
[13] Harteck & Dondes, (1956).
[14] Wiesner, (1961).

as 100 rads can be measured by using Fe^{59} tracer and extracting the ferric ion into isopropyl ether as its thiocyanate complex (Rudstam and Svedberg, 1953). Even the direct determination of small quantities of ferric ion in the Fricke dosimeter by absorption at 305 mμ by the use of longer absorption cells extends its range downward to 300 rad (Thielens, 1961). Many sensitizers of ferrous ion oxidation increase $G(Fe^{3+})$ by factors of two to fifteen (Hart, 1952; Thielens, 1961), e.g., the ferrous sulfate + formic acid + oxygen dosimeter of table IC3. Sensitive systems not relying on the measurement of ferric ion are represented by the benzoic acid, quinine, trichloroethylene and chloroform systems. Benzoic acid is oxidized to hydroxybenzoates which may be detected in quantities as low as 5×10^{-11} M by fluorimetry. In this way, doses as low as 0.5 rad can be detected and a dose of 5 rad can be determined to ±5 percent precision (Barr and Stark, 1958). Similarly, by measuring the destruction of quinine in aqueous solutions by fluorimetry, doses between 10 and 1,000 rads can be measured conveniently and reproducibly (Barr and Stark, 1960). Aqueous trichloroethylene and chloroform solutions release hydrochloric acid on irradiation. pH-sensitive indicator dyes are used as detectors of hydrochloric acid and an estimate of the dose may be obtained from the change in color (Taplin, 1956; Sigoloff, 1956, 1961).

A second group of systems covering various sections of the range above the Fricke dosimeter to an upper limit of about 10^8 rads, consists of the formic acid + oxygen, dye, ceric sulfate, ferrous sulfate + cupric sulfate and oxalic acid dosimeters. These dosimeters cover a variety of applications. Formic acid + oxygen liberates hydrogen peroxide, carbon dioxide and hydrogen (Hart, 1954). By measuring hydrogen peroxide, doses as low as 1,000 rads can be estimated and if all the products are analyzed, this system may be used for mixed gamma-ray and neutron dosimetry (Hart and Walsh, 1958). Dyes in gels have been used for depth dose measurements. Rigid chemical dosimeters, which can be cut into sections after irradiation, offer obvious advantages in obtaining a picture of the dose distribution in a radiation field. If this distribution is to be related to that in irradiated tissue, the medium has to approach the chemical composition of tissue as nearly as possible. This requirement is met most closely by the use of gels of aqueous gelatin or agar, containing dyes, which are decolorized on irradiation (Day and Stein, 1950; Goldblith, Proctor and Hammerle, 1952; Andrews, Murphy and LeBrun, 1957; Gevantman, 1960). The ceric sulfate, ferrous sulfate + cupric sulfate and oxalic acid systems extend chemical dosimetry reliably into the range between 10^6 and about 10^8 rads. The ferrous sulfate + cupric sulfate dosimeter is particularly valuable when used in conjunction with the Fricke dosimeter to monitor mixed gamma-ray and heavy ionizing particle radiations (Hart and Walsh, 1954). Some results for the ferrous-cupric system are indicated in table IC1 and curve C of figure IC1.

The necessity for monitoring doses above 10^8 rad is rare but the water, nitrous oxide and polyisobutylene dosimeters are available. Of these the water dosimeter has practically no upper limit of dose provided that steps are taken to remove the decomposition products, hydrogen and oxygen, from the radiation field and subsequently to measure them. (Hart and Gordon, 1954; Gordon and Hart, 1958; Hart and Walsh, 1958.) Neutron fluxes may be measured too by adding boric acid or borates to the water. Nitrous oxide gas decomposes into nitrogen, oxygen and nitrogen dioxide and the dose is obtained by the measurement of these gases (Harteck and Dondes, 1956). Another dosimeter useful over a wide range of doses is polyisobutylene dissolved in heptane (Wiesner, 1961). On irradiation, depolymerization takes place and the dose is estimated from viscosity calibration curves. Concentrated solutions of low molecular weight polymers are used for high doses, whereas dilute solutions of high molecular weight polymers are better for the low doses.

D. Photographic Dosimetry

The photographic emulsion is one of the oldest detectors of ionizing radiation. Although the accuracy of photographic dosimetry is relatively low (5 to 10 percent, at best), the method is still widely used for personnel monitoring (Dudley, 1956; Ehrlich, 1954; Rotblat, 1950). Photographic dosimetry is also used for measurements of total exposures up to 10^4 R and more, under conditions for which ruggedness and low cost are important factors, and for mapping of high-energy radiation fields in clinical applications. Recently, a method was developed by which the range of photographic dosimetry can be extended to 1×10^5 R through the use of conventional monitoring film without development (McLaughlin, 1959). Photographic dosimetry has been discussed in detail in the literature (Griffith, 1958). Only some of the more general features will be outlined here.

1. Energy Transfer to a Photographic Emulsion

The energy transferred by ionizing radiation to the photographic emulsion initiates the reduction of the silver halide crystals (grains) of the emulsion to atomic silver. The microscopic silver specks formed in this way are referred to as latent image. Upon processing in special developing solutions, these silver specks then serve as nuclei for a reduction process, leading to the formation of massive silver aggregates which increase the opacity of the developed photographic emulsion. For very large radiation exposures, the reduction by the ionizing radiation alone is large enough to make any further processing unnecessary.

The increase in emulsion opacity (or in optical density, which is equal to the decadic logarithm of opacity) is usually measured by photoelectric means. By appropriate calibration procedures, optical density can be related to exposure, absorbed dose, or incident fluence.

Charged particles transfer their energy to the silver halide grains mainly through collisions leading to atomic excitation and to ionization along the paths of the particles. The photographic effect of charged particles increases with the range of the particles in the emulsion, and—for a given range—with their specific ionization, until one single interaction with a silver halide grain is sufficient to make this grain developable. Any further increase in specific ionization leads to a decrease in the number of grains made developable for any given amount of energy dissipated within the emulsion. Photons, neutrons, and other uncharged particles lose their energy to the emulsion largely through the ionization produced by their charged secondaries.

2. Response to X and Gamma Radiation

The photographic latent image is produced by energy deposited in the grains by secondary and higher order electrons from x- and gamma-ray interactions with the material in the vicinity. Photoelectric absorption in the elements of relatively high atomic number contained in the emulsion causes the ratio of photographic effect to exposure to be up to 30 and more times higher for 40-kev photons than for 1-Mev photons. For dosimetry in the photon energy ranges up to about 200 kev, suitable arrangements of metallic filters aid in reducing this energy dependence, and facilitate the determination of the particular radiation energy (Langendorff, et al., 1952). For higher energies, film response roughly parallels exposure, provided that electronic equilibrium is established at the film in air-equivalent materials.

No rate dependence effects have as yet been demonstrated for the film types usually employed in dosimetry when exposed to low-energy x radiation (Ehrlich, 1956), unless the films were used in contact with scintillators (Ehrlich and McLaughlin, 1959). However, some rate dependence seems to be present for x-ray energies of around 1 Mev. Such rate dependence is particularly likely when the films are processed in weak developers which react mainly with the surface of the silver halide grains.

3. Response to Monoenergetic Electrons and to Beta Rays

Photographic dosimetry of monoenergetic electrons and beta rays is complicated by the relatively high absorption of electrons both in the light-tight wrapping material usually surrounding commercial photographic film and in the emulsion proper. Actually, the ranges of electrons of energies below about 100 kev are smaller than the thickness of the average commercial photographic emulsion. As a consequence, the photographic effect increases with increasing energy up to about 100 kev and also depends strongly on the direction of electron incidence. At higher energies, the photographic effect changes only relatively little with radiation energy and direction of radiation incidence.

In some of the photographic emulsions used for electron investigations, a rate dependence has been found (Digby et al., 1953).

If elements are introduced over the film surface which become beta active upon bombardment with thermal neutrons (such as for instance rhodium), the beta-ray response of suitably calibrated films can also be utilized for thermal-neutron dosimetry.

4. Response to Heavy Charged Particles and to Neutrons

Because of their large specific ionization and the associated waste in energy dissipation on already developable grains, the photographic effect of heavy charged particles is smaller by orders of magnitude than that of x rays and electrons. Where the particle ranges are small compared to the emulsion thickness, the effect is also strongly dependent on the energy and the direction of the incident particles. Furthermore, in some of the

emulsions, the photographic effect is rate dependent. For these reasons, track analysis on nuclear plates, which provides for a detailed study of individual events, is the preferred method of photographic dosimetry of heavy charged particles and also of fast neutrons, whose photographic action is largely due to proton recoils produced in the hydrogenous gelatine. Track analysis for personnel dosimetry of fast neutrons can be simplified by the use of a nuclear-track plate surrounded by essentially tissue-equivalent materials of such thickness that the number of tracks produced in the emulsion per unit absorbed dose is essentially independent of neutron energy (Cheka, 1954). In the 30-micron Eastman NTA emulsion, this method yields about 5 or 6 tracks in an area of 2×10^{-4} cm^2 after the maximum permissible neutron irradiation for a period of 13 weeks, i.e., a dose equivalent of 3 rems.

Analysis of the proton tracks produced by the reaction of thermal neutrons on the nitrogen of the gelatine, or of alpha tracks in lithium- or boron-loaded emulsions, can be used for thermal-neutron dosimetry. The protons produced by the reaction of thermal neutrons on nitrogen produce a slightly larger number of tracks per unit area than the proton recoils from elastic scattering of fast neutrons. The sensitivity of the lithium- or boron-loaded emulsions is about 200 times greater than ordinary emulsions for thermal neutrons.

E. Dose-rate Measurements by Scintillation Techniques

In the scintillation dosimeter, absorbed dose rate is measured in terms of the intensity of luminescence excited within an irradiated scintillator. The latter is usually coupled optically to a multiplier phototube, the increase in whose mean collector current above background level is usually linearly related to the intensity of luminescence and hence to the absorbed dose rate. The method has been reviewed by Rosman and Zimmer (1955, 1956a, 1957).

The scintillation technique has been found useful in a number of practical dosimetric problems, especially for the measurement of x and gamma radiation. Scintillation dosimeters have high sensitivity and a linear response over a wide range of dose rates; they are less dependent on pressure and humidity than are non-sealed ionization chambers. They do however require frequent recalibration because of possible changes in multiplier phototube gain and scintillator performance with time or radiation exposure. The scintillator can be a small block of material mounted at the end of a rigid or flexible light guide which couples it optically to the multiplier phototube; such instruments are useful for the measurement of radiation dose rate in cavities of the human body or for the plotting of radiation fields or isodose curves. Probe dosimeters of this type, incorporating scintillators a few mm in linear dimensions, can be used to measure dose rates down to 1 rad/hour in the scintillating material. (Griffith and Swindell, 1951, Glocker and Breitling 1952; Cole et al., 1952, 1953; Belcher, 1953; Fowler, 1955; Rosman and Zimmer, 1956b, Herbert, 1956; Robson and Gregg, 1956; Shalek and Cole, 1958; Henriksen, 1958; Blanks and Rohrer, 1960).

In many such instruments, a solid rod of methyl methacrylate or quartz is used as a light guide to provide optical coupling between the scintillator and the multiplier phototube. This arrangement is satisfactory in measurements at low photon energies, but at energies above 200 kev visible Čerenkov radiation emitted by secondary electrons in the light guide may be a source of error; the use of an internally polished metal tube to provide optical coupling is then preferable (Cole et al., 1953; Belcher, 1953; Fowler, 1955; Henriksen, 1958).

The insertion of a wavelength shifter such as a mixture of anthracene and tetracene between the scintillator and light guide to transform the blue light emitted by the scintillator to yellow-green, followed by yellow-green filters at both ends of the light guide to exclude the greater part of the Čerenkov radiation provides another method of overcoming this difficulty (Zimmer, 1956; Jahns, 1960).

In most scintillation dosimeters, the multiplier phototube collector current is measured by means of a DC microammeter, valve voltmeter or DC amplifier. Multiplier phototube dark current and direct effects of radiation on the multiplier phototube, both of which contribute to the recorded current, may be sources of error in measurements with such instruments, but the inclusion of a small shutter interrupting the optical path between the scintillator and the multiplier phototube allows the zero to be set before a measurement is made, (Dealler, 1954; Fowler, 1955). In other instruments, a mechanical light-chopping device in the optical path provides an AC signal which can subsequently be amplified by an AC amplifier (Herbert, 1956; Blanks and Rohrer, 1960); in these instruments, dark current and direct effects of radiation on the multiplier phototube do not contribute to the measured current although light emitted by the light guide may still be recorded.

The major disadvantage of scintillation dosimeters for x and gamma radiation lies in their energy dependence. Provided that the dimensions of the scintillator are large compared with the maximum range of the secondary electrons, but small compared to $1/\mu_{en}$, the energy absorbed in the scintillator of a scintillation dosimeter can be related to that absorbed by an air-wall ionization chamber whose sensitive volume has the same dimensions as the scintillator by an expression of the form:

$$\frac{1-e^{-t\mu_{en}}}{t\mu'_{en}}$$

where μ_{en}, μ'_{en} are the linear energy absorption coefficients of the scintillator and air respectively and t is the thickness of the scintillator presented to the

incident radiation. (Brucker, 1952; Ittner and Ter-Pogossian, 1952; Belcher, 1953.)

The variation of the above expression with energy depends on the effective atomic number and hence on the atomic composition of the scintillator and on its thickness. Inorganic scintillators such as calcium tungstate or alkali halides have a response which falls steeply with increase in energy (Brucker, 1952). Organic scintillators such as anthracene have a response which is nearly air-equivalent above 0.1 Mev (Smeltzer, 1950) but which falls at lower energies (Brucker, 1952). By choosing a suitable scintillator or combination of scintillators, the response can be made nearly air- or tissue-equivalent over a wide range of photon energies. Useful combinations include anthracene and calcium tungstate (Cole et al., 1952; Ittner and Ter-Pogossian, 1952); terphenyl dissolved in benzene and chlorobenzene (Breitling and Glocker, 1952); phenanthrene and chlorophenanthrene (Glocker and Breitling, 1952); anthracene and chloroanthracene (Mohr, 1957); polystyrene-based plastic scintillator and calcium tungstate (Rosman and Zimmer, 1956b), and polystyrene-based plastic scintillator and silver-activated zinc sulphide (Belcher and Geilinger 1957). Using mixtures of anthracene, chloroanthracene and calcium fluoride in different proportions, Breitling et al., (1956) have produced combinations equivalent to fat, muscle, and bone.

The above approach to the problem of energy dependence is invalid if the energy of the radiation is so large that the range of the secondary electrons is comparable with the dimensions of the scintillator (Henriksen and Baarli, 1957). In such situations, the effective atomic number of the scintillator depends on its dimensions as well as on its atomic composition. However, by enclosing the scintillator in a sheath of suitable material and thickness, the response may still be made approximately air-equivalent over a limited energy range (Henriksen, 1958).

Scintillation dosimeters have also been used successfully for the measurement of β radiation. Probe dosimeters in which the scintillator is a thin sheet of anthracene (Ittner and Ter-Pogossian, 1954; Sinclair and Trott, 1956) or plastic scintillator (Goodwin, 1956; Brannen and Olde, 1960; Olde and Brannen, 1961) have been used for surface and depth dose measurements on β-ray applicators.

Scintillation dosimeters incorporating homogeneous inorganic or organic scintillators are relatively insensitive to fast neutrons, in the former case because of the low hydrogen content and in the latter because of the low proton sensitivity of the scintillator. Dosimeters incorporating mixtures of powdered inorganic scintillators with hydrogenous materials are however efficient detectors of fast neutrons (Hornyak, 1952; Skjoldebrand, 1955; Brown and Hooper, 1958). Similarly, inorganic scintillators of the alkali halide type in which lithium is the alkali component (Bernstein and Schardt, 1952; Schenck and Heath, 1952), or liquid scintillators containing compounds of boron in solution (Muehlhause and Thomas, 1953) may be used in detectors of slow neutrons. These devices are not air- or tissue-equivalent and must always be calibrated for neutrons of the energy range to be measured. The uses of scintillation counting techniques for neutron flux measurements and for the dosimetry of mixed radiation fields of neutrons and gamma rays are discussed elsewhere in this report.

F. Solid-State Dosimetry

The methods to be discussed here are based upon the following radiation-induced phenomena:

(i) Optical density changes;

(ii) Photoluminescence (i.e., the increase in the ability of the material to fluoresce under ultraviolet light);

(iii) Thermoluminescence (i.e., the emission of light upon heating after exposure to ionizing radiation);

(iv) Conductivity changes (i.e., the temporary increase in electrical conductivity during exposure to ionizing radiation).

Several systems falling into these categories will be briefly discussed in turn in the following sections. They must, of course, be calibrated under appropriate conditions, since none of these dosimetric systems is absolute.

1. Optical Density Methods

a. *Glasses.* The two types of glasses most widely used for dosimetry by this method are silver-activated phosphate glass (Schulman et al., 1955), and cobalt-activated borosilicate glass (Kreidl and Blair, 1956b). Although there are now several types of silver-activated phosphate glass available, only the original "high-Z" glass has been used so far in the optical density method.

This phosphate glass is available in blocks 1 cm$\times$1 cm$\times$3 mm polished on the square surfaces through which the light is passed during the optical density measurement with a spectrophotometer. At 3500Å the dose range for linear response extends from about 5×10^3 to 2×10^6 rads in the glass. With care, 2 percent precision is attainable. The response is independent of the dose rate at least to 4×10^8 rads/hr (Davisson et al., 1956).

Two undesirable features of this glass are the fading of the coloration with time after radiation exposure, and the strong dependence of the response per roentgen upon gamma- or x-ray quantum energy. The coloration fades up to 20 percent in the first 24 hours after exposure. A short heat treatment ($\approx$130 °C for 10 min) accelerates this initial fading and stabilizes the residual optical density (Schulman et al., 1955; Davisson et al., 1956). Alternatively, one can delay the optical density measurement until some arbitrary time (e.g. 24 hours after exposure) when the fading rate is small. Rabin and Price (1955) discuss corrections for fading during long exposure

times. The energy dependence of the glass will be treated in the section on radiophotoluminescence.

Cobalt-activated borosilicate glass (Bausch and Lomb type F–0621) is available in the form of small polished blocks 1.5 mm in thickness. Their radiation induced optical density at 3500Å increases linearly over the range 10^3–10^6 rads (in glass), the sensitivity being somewhat lower than that of the phosphate glass. A precision of ±2 percent is nevertheless attainable. This glass is superior to the phosphate glass both with respect to fading and energy dependence. The fading is only about 2 percent in 24 hours. The atomic numbers in the borosilicate glass are less than 14 except for the small cobalt content. Thus the photoelectric effect will be smaller than in the high – Z phosphate glass, although detailed experimental data on energy dependence are not yet available.

Other dosimetric glasses are described by Kircher et al., (1958), Hedden et al., (1960), Paymal et al., (1960) and Bishay (1961).

b. *Plastics.* Many transparent plastics can be used as radiation dosimeters by virtue of radiation-induced changes in optical density in the ultra-violet or visible spectral region. The useful dose range of any particular material usually extends over about two decades, and these ranges generally lie between 10^5 and 10^8 rads, except for polyethylene terephthalate, which can be used in 6 μ thickness to measure doses up to 10^9 rads (Ritz, 1961).

The response per roentgen is generally constant over a wide range of quantum energies, except where high-atomic-number atoms are present, as in polyvinylchloride.

The main drawback with most plastic dosimeters is the instability of the coloration change. The cellophane-dye system (Henley, 1954; Henley and Richman, 1956) is the only one in which the color change is reported to be permanent, and it is based upon a color-bleaching process. Of the others, polymethylmethacrylate (Boag et al., 1958) is the most stable, showing a slight rise in optical density (<5 percent) in the first 24 hours after exposure, and about 10 percent per month fading after that.

Possible dependence upon dose rate has not been investigated for most of these dosimeters, but the polymethylmethacrylate was found to be independent of rate at least to 3×10^8 rads/sec for 1 μsec pulses of electrons from a linear accelerator (Boag et al., 1958). By contrast polyethylene terephthalate does exhibit such a dependence (Ritz 1961), which limits its usefulness.

2. Radiation-Induced Photoluminescence

The only practical dosimetry system based on radiation-induced photoluminescence has been silver-activated phosphate glass (Schulman, 1950; Schulman et al., 1951, 1953). This glass develops at least two types of centers upon gamma irradiation. One type is chiefly responsible for the coloration effect discussed earlier. The other type of center not only absorbs ultra-voilet light but also emits orange fluorescent light continuously when exposed to ultra-violet light. The intensity of the fluorescence, as determined by a multiplier phototube light-detector, serves as a measure of the absorbed dose in the glass for a given type of radiation. Reproducibility of measurements is usually about ±5 percent, but with sufficient care 2–3 percent is attainable. The dose range covered linearly usually extends from about 10 rad to 10,000 rads or more, depending upon the type of fluorimeter used and the size of the piece of glass (Lee et al, 1961; Schulman and Etzel, 1953; Barr et al., 1961a; Degelman et al., 1957; Bausch and Lomb Optical Co., 1959; Yokota et al., 1961). The longer the optical path of the ultra-violet and the orange light, the more readily the optical absorption begins to cause a saturation effect at the upper end of the response vs dose curve. Lee et al., (1961) have demonstrated that a post-irradiation annealing for 1 hour at 325 °C removes most of the coloration but only a relatively small part of the fluorescing centers. In this way they achieve nearly linear response up to at least 10^5 rads.

Yokota et al., (1961) have recently devised a fluorimeter which, through the selection of optical filters and the enhanced red spectral response of the multiplier phototube, is reported to have extended the usable exposure range down to 50 mR. They make use of a new low-Z type of silver-activated phosphate glass which exhibits greater response to gamma rays than do the other available phosphate glasses.

Silver-activated phosphate glass of either low-Z or high-Z composition and suitable fluorimeters are commercially available. Cylindrical rods of glass 1-mm o.d. by 6-mm length, devised by Schulman and Etzel (1953), are the most widely used form, particularly for application *in vivo*, and to provide a supplementary high-range dosimeter in film badges (Gupton et al., 1961). Other shapes are also available, e.g., blocks such as have been employed in "DT–60"-type casualty-range dosimeters (Schulman et al., 1953) and for use in the optical density method.

The photoluminescence of the irradiated glass is more stable than is the coloration. An initial rise of some 10–20 percent in the radiophotoluminescence is observed in the first few hours after irradiation, after which the signal is reported to be stable in the case of ¾ in. x ¾ in. x 3/16 in. blocks (as used in "DT–60" dosimeters) (Schulman et al., 1953). Some evidence has indicated that a slow fading (~1–3 percent per week) may exist in the glass rods (Hodara et al., 1959; Kondo, 1961). The glass rods have been employed by several investigators for tissue implant dosimetry (Hodara et al., 1959; Fulton et al., 1954; Malsky et al., 1961), and have also been used for dosimetry in the gastrointestinal tract of animals (Nold et al., 1958).

The energy dependence of the glass is regarded as the main hindrance to its use for x-ray measurements where the x-ray spectrum is unknown. The rods of high-Z phosphate glass show 20 to 30 times more response per roentgen at 60 kev than at

1.25 Mev (Co^{60}) (Schulman and Etzel, 1953). For rods of the low-Z glass of Ginther and Schulman (1960), the energy-dependence factor lies between 7 and 13. Day (1956) first designed lead and gold shields to reduce the energy dependence of the high-Z glass rods. Further progress has also been reported (Malsky et al., 1961; Attix, 1961; Thornton and Auxier, 1960) indicating that the excessive response below 100 kev can be eliminated. With low-Z glass rods (Ginther and Schulman, 1960) and partial shields of silver (Attix, 1961), flat response per roentgen within ± 20–30 percent down to 40 kev is probably attainable.

In spite of the energy-dependence of the glass, several studies have shown that, at least under narrow-beam conditions, the response of even the high-Z glass rods follows fairly closely the response of air-equivalent ion chambers or ferrous-sulfate dosimeters in depth-dose curves (Hodara et al., 1959; Riegert et al., 1956; Barr et al., 1961a,b). The use of low-Z glass rods and metal shields would be advisable, however, to minimize the possibility of erroneous measurements due to scattered radiation, particularly under broad beam conditions.

The dose rate independence of the high-Z glass has been verified at rates up to 10^5 rads/sec with respect to coloration (see subsection 1 above, Optical Density Methods). However, the radiophotoluminescence has been investigated only up to 50 rads/sec for continuous radiation, or 500 rad/sec for a γ-ray pulse (Pierson, 1958; Ballinger and Harris, 1959). Kondo (1961) observed a 10 percent dose-rate saturation effect over the range from 4×10^{-2} to 13 rads/sec. Further measurements will be necessary to resolve this discrepancy.

All of the three available types of silver-activated phosphate glass are sensitive to thermal neutrons, the high-Z formulation being least sensitive and the lithium-bearing glass of Yokota et al. (1961) being most sensitive. The response to thermal neutrons also depends upon the size of the piece of glass, so long as it is comparable with the range of the beta-rays emitted by the radioactivated silver in the glass. The response of the glass per rad in tissue is reported to range from several-fold to 100-fold greater for thermal neutrons than for Co^{60} gamma rays. More details are given elsewhere (Attix, 1962).

The fast-neutron response of the high-Z glass is relatively small, being due chiefly to elastic collisions. The fast-neutron response per rad in tissue relative to the response per rad in tissue for Co^{60} gamma rays varies from 0.5 to 0.7 percent for 0.5–1.5 Mev neutrons (Bernard et al., 1961). At 14 Mev the corresponding figure is 3.5 percent (Kondo, 1960a).

The response of the high-Z glass per rad has been reported to be a function of the LET of the radiation, being only one-fifth as large for alpha particles and recoil protons as for fast electrons (Kondo, 1960 a, b, 1961).

3. Radiation-Induced Thermoluminescence

When a thermoluminescent material is exposed to ionizing radiation, the electrons released in the ionization process are trapped at lattice imperfections throughout the crystalline solid. These electrons remain trapped more or less permanently at room temperature, but are released by thermal agitation at some elevated temperature. When thus released, they recombine with opposite charge carriers and emit light in the process. The quantity of light emitted as the material is heated may be measured and related to the absorbed dose in the material. This heating process generally "erases" the phosphor so that it is ready for another exposure.

Of the thermoluminescent phosphors which have been investigated to date (see general references at end of this section), the most promising are synthetic manganese-activated calcium fluoride CaF_2:Mn (Ginther and Kirk, 1956, 1957), and lithium fluoride, LiF (Cameron et al., 1961).

CaF_2:Mn must be enclosed in an evacuated or inert-gas-filled envelope to avoid generation of spurious thermoluminescent signals. The phosphor can be cemented to an ohmic heater within the envelope (Schulman *et al.*, 1960b). The thermoluminescence (blue-green in color) is measured by placing the device in front of a suitable multiplier phototube, and passing electric current through the dosimeter heater element. With 100 mg of CaF_2:Mn in the dosimeter, doses of the order of 10^{-4} rads are detectable and the light output is proportional to dose up to 3×10^5 rad. The response is independent of dose rate at least up to rates of 4×10^5 rads/hr.

The storage of energy in CaF_2:Mn is not entirely stable with time at room temperature. Fading amounts to some 10 percent during the first 16 hours after exposure, 1 percent per day for a few days thereafter, gradually slowing down so that about two-thirds of the original signal remains after 80 days of storage. The energy dependence (response/R) of CaF_2:Mn is roughly the same as that for low-Z silver-activated phosphate glass and can be flattened by appropriate shielding. Response to thermal neutrons is about the same as that of the high-Z phosphate glass. Fast neutron response has not yet been determined, but is expected to be low.

LiF (Cameron et al., 1961) has several advantages over CaF_2:Mn. It requires no envelope, as it is relatively unaffected by atmosphere; its stored signal does not fade at room temperature, and because of its low atomic number it is nearly "air equivalent", exhibiting a response per roentgen only 30 percent greater at 40 kev than at 1,250 kev. The sensitivity of this phosphor is several-fold less than that of CaF_2:Mn, and above a few hundred rads the response rises more rapidly than linearly with dose because of an increase in sensitivity induced by the radiation.

Neither the dose-rate dependence nor the neutron sensitivity have been investigated, but

the latter would be expected to be high because of the lithium content.

Neither of these two phosphors is currently available commercially. At present the techniques for manufacturing the special type of CaF_2:Mn are better understood than for the LiF, because the activators of the latter are not yet well-known. However, it is likely that both phosphors (and perhaps complete dosimetry systems based upon them) will soon be available.

4. Conductivity Induced by Ionizing Radiation

a. *Semiconductor junction detectors.* In operation these devices behave much like solid-state ionization chambers. Although their effective volume is small (≈ 0.1 cm^3 or less), the solid silicon of which they are usually made is some 1,850 times as dense as air at atmospheric pressure. Furthermore the value of "W", the energy necessary to produce a pair of charge carriers, is only about 3.5 ev, or 0.1 that necessary in air. Thus, per unit volume, the yield of charge carriers will be roughly 18,000 times that in an air-filled cavity chamber.

Relatively few applications of semiconductor junction detectors have been made in radiation dosimetry thus far. Friedland *et al.*, (1960) and Jones (1960) have described studies in the development of alpha-, beta-, and gamma-ray survey meters having silicon *p-n* junction detectors. Brownell (1961) has suggested useful medical applications, such as in the study of neutron capture reactions, employing nuclides such as B^{10}, for brain tumor therapy. These semiconductor detectors should prove useful as x- and gamma-ray probes also, for applications where space is at a premium and the dose rate is sufficiently high that measurable ionization currents can be obtained. As a rough guide in gauging the sensitivity to gamma rays, Jones (1960) reports that a 2-cm^2 area silicon *p-n* junction was found to have the same d-c sensitivity to gamma radiation as a 300 cm^3 air ion chamber; i.e., about 10^{-7} amp at 1 R/sec. This would indicate a depletion layer thickness of about 0.1 mm in this case. The lithium-diffused type silicon junction of Baily and Mayer (1961), and Baily et al., (1961) should show even greater gamma-ray current response. Hertz and Gremmelmaier (1960) have reported the application of a *p-n* junction of gallium-arsenide as an x-ray probe in body cavities; current yields of 2×10^{-7} amp per R/sec were obtained.

No attempt will be made here to list the references to existing literature on semiconductor junction detectors. Since the initial work of McKay (1951), hundreds of papers on the subject have appeared. A bibliography by Blankenship (1960) includes references to semiconductor detectors of germanium, diamond, and CdS, as well as silicon.

b. *Cadmium sulfide.* Cadmium sulfide (CdS) crystals have been employed by a number of investigators as sensitive detectors of ionizing radiation (see the bibliography). Instead of behaving strictly as solid state ionization chambers, they amplify the ionization current by up to 4 orders of magnitude. Lucid discussions of the mechanisms involved in radiation-induced conductivity of CdS are given by Garlick (1960)[8] and by Clayton and Briggs (1960).[8]

A "good" CdS crystal can produce currents of 1 μ amp or more in a Co^{60} gamma-ray field of 1 R/hr, with 100 volts imposed across the crystal. It is important to emphasize that as a rule typical CdS photoconductive cells, designed for light detection, exhibit little or no gamma-ray sensitivity. Occasional exceptions are found which can be used as gamma-ray detectors, but the problem of selection makes the effective cost per usable crystal quite high. Three types of CdS photoconductive cells are commercially available; single crystals, sintered layers, and microcrystalline powder dispersed in a binder. The single crystal type generally gives the best gamma-ray performance. Crystals having gamma-ray induced currents of the order of 10^{-9} amp per R/hr at 100 v, together with reasonably short time constants, have been regarded by most of the authors as satisfactory, and were obtained in most cases by selection from larger numbers of crystals. Hollander (1956a) produced CdS crystals having photocurrents as high at 2×10^{-6} amp per R/hr of Co^{60} gamma rays at 100 v. The dark current was less than 10^{-7} amp. The times required to achieve a steady current at 1 R/hr ranged from several minutes to hours, but were shortened considerably by continuous irradiation with a low intensity of radium gamma rays.

The response of CdS crystals is sometimes found to be a function of the age of the crystal and of its prior radiation history.

The response per roentgen of CdS crystals to x rays below 100 kev can be as much as 100-fold greater than for Co^{60} gamma radiation. Shields of high-atomic-number materials can be employed, as with other dosimetry systems, to reduce this dependence.

Recently, Franks (1961) has disclosed the development of ultrasensitive CdS gamma-ray detecting crystals which yield currents as great as 15 μ amp per R/hr of Co^{60} gamma rays at 100 volts. He has found it possible to produce such crystals, falling in the 2–5 μ amp range, routinely and with relatively little selection necessary. Rise times are still in the several-minute range at 1 R/hr and represent the principal remaining shortcoming of these crystals. Nevertheless, they are the best CdS gamma-ray detectors reported to date and are currently obtainable.

5. Bibliography*

Optical Density Method

Artandi, C., and Stonehill, A. A. (1958). Polyvinyl chloride new high level dosimeter, Nucleonics **16** No. 5, 118.

Bauman, R. G. (1956). Glass slides help map gamma fields, Nucleonics **14,** No. 6, 90.

[8] Symposium on Solid State Conductivity, Kings College Hospital, Sept. 25, 1959. Physics in Medicine and Biology **4,** 325 (1960).

*References mentioned in the text will be found in the references at the end of this report.

Birnbaum, M., Schulman, J. H., and Seren, L. (1955). Use of melamine as an x-radiation detector, Rev. Sci Inst. **26,** 457.
Day, M. J., and Stein, G. (1951). Effects of x rays upon plastics, Nature **168,** 644.
Fowler, J. F., and Day, M. J. (1955). High-dose measurement by optical absorption, Nucleonics **13,** No. 12, 52.
Hart, E. J., Koch, H. W., Petree, B., Schulman, J. H., Taimuty, S. I., and Wyckoff, H. O. (1958). Measurement systems for high level dosimetry, Proc. Second Intern. Conf. Peaceful Uses of Atomic Energy, Geneva, **21,** 188.
Henley, E. J., and Miller, A. (1951). Gamma ray dosimetry with polyvinyl chloride films, Nucleonics **9,** No. 6, 62.
Kreidl, N. J., and Blair, G. E. (1956a). A system of megaroentgen glass dosimetry, Nucleonics **14,** No. 1, 56.
Taimuty, S. I., Glass, R. A., and Deaver, B. S. Jr. (1958). High level dosimetry of gamma and electron beam sources, Proc. Second Intern. Conf. Peaceful Uses of Atomic Energy, Geneva, **21,** 204.

Radiation-Induced Photoluminescence

Amato, C. G., and Malsky, S. J. (1961). Radiophotoluminescent gamma-ray dosimetry of mixed neutron gamma-ray fields, Radiology **76,** 290.
Amato, C. G., Malsky, S. J., Bond, V. P., Roswit, B., and Heinze, E. (1961). Multiple implant dosimetry, Radiology **76,** 292.
Amato, C. G., Malsky, S. J., and Roswit, B. (1961). Solid state dosimetry, Trans. New York Acad. Sci., Series II, **23,** 357.
Brustad, T., and Henriksen, T. (1958). Glass dosimetry of soft x-rays, Brit. J. Radiol. **31,** 163.
Bryan, W. C., Annis, M. R., and Cowles, R. (1958). Some possible improvements of the DT–60/PD, CP–95A/PD system, Air Force Special Weapons Center, Kirtland Air Force Base, New Mexico. Rept. No. AFSWC–TN–58–24.
Bryan, W. C., and Schaus, W. P. (1961). Some recent developments in radiophotoluminescent dosimetry, including test results, Air Force Special Weapons Center, Kirtland Air Force Base, New Mexico. Rept. No. AFSWC–TN–61–4.
Caldwell, P. A. (1957). A dosimeter reader for phosphate glass needle dosimeters, U.S. Naval Research Laboratory Memorandum Rept. No. 715.
Etzel, H. W., Kirk, R. D., and Schulman, J. H. (1955). Small volume dosimeter, Ra-Det **8,** No. 2, 49 (Publ. Radiation Instruments Branch, Div. of Biol. & Med., USAEC).
Klick, C. C. (1951). Battery-operated portable reader for radiophotoluminescent glass dosimeters, U.S. Naval Research Laboratory, Rept. No. 3878.
Kondo, S. (1960b). Simultaneous measurement of thermal neutron fluxes and gamma contamination dose by silver-activated phosphate glass, IAEA Symp. Radiation Dosimetry, Vienna.
Malsky, S. J., Amato, C. G., Roswit, B., Reid, C. B., Unger, S. M., Spreckels, C., and Villazon, E. (1959). *In vivo* dosimetry with miniature radioluminescent glass rods, Trans. New York Acad. Sci. **22,** Series II, No. 2, 104.
Malsky, S. J., Amato, C. G., and Reid, C. B. (July 1960). A miniature versatile dosimeter, IRE Trans. Med. Electronics, **ME–7,** 193.
Malsky, S. J., Roswit, B., Amato, C., Reid, C. B., Unger, S. M., and Spreckels, C. (1960). *In vivo* dosimetry with miniature glass rods, Radiology **74,** 107.
Roswit, B., Malsky, S. J., Amato, C. G., Reid, C. B., Maddalone, L., and Spreckels, C. (1961). An ideal *in vivo* dosimetry system for clinical and experimental radiation therapy, Radiology **76,** 295.
Schaffert, J. C. (1956). A portable reader for DT–60 dosimeters, U.S. Naval Research Laboratory Rept. No. 4680.
Schaffert, J. C. (1956). A pulsed-light reader for the DT–60 glass dosimeter, U.S. Naval Research Laboratory Rept. No. 4706.

Radiation-Induced Thermoluminescences

Arkangel'skaya, V. A., Vainberg, B. I., Kodyukov, V. M., and Razumova, T. K. (1960). Luminescence dosimeter based on a $CaSiO_3$: Mn phosphor for gamma rays, beta-particles and neutrons, Atomnaya Energiya, 559.
Burger, H., Lehmann, J., and Mayer, U. (1954). Die Anwendung der Simultandosimetrie bei der Intravaginalen Röntgenbestrahlung der Parametrien, Naturwissenschaften **41,** No. 9, 209.
Daniels, F., Boyd, C. A., and Saunders, D. F. (1953). Thermoluminescence as a research tool, Science **117,** 345.
Daniels, F., and Rieman, W. P. (1954). The thermoluminescence dosimeter, Final Report, Chemical Procurement Agency Contract No. DA18–108–CML–3069, Project No. 4–12–80–001, Univ. Wisconsin.
Grogler, N., Houtermans, F. G., and Stauffer, H. (1958). The use of thermoluminescence for dosimetry and in research on the radiation and thermal history of solids, 2nd Intern. Conf. Peaceful Uses of Atomic Energy, **21,** 226.
Häring, N., and Schön, M. (1961). Dosimetry of ionizing and neutron radiation by thermoluminescence, Ninth Intern. Congress of Radiology. Munich, 1959. **2,** 1388–91, B. Rajewsky, ed. Stuttgart, Georg Thieme Verlag (In German).
Houtermans, F. G., Jäger, E., Schön, M., and Stauffer, H. (1957). Messungen der Thermolumineszenz als Mittel zur Untersuchung der thermischen und der Strahlungsgeschichte von natürlichen Mineralien und Gesteinen, Ann. Physik **20,** No. 6, 283.
Kossel, W., Mayer, U., and Wolf, H. C. (1954). Simultandosimetrie von Strahlenfeldern am lebenden Objekt, Naturwissenschaften **41,** No. 9, 209.
Luchner, K. (1957). Über die Thermolumineszenz von natürlichem Flussspat, Z. Phys. **149,** 435.
Patterson, D. A., and Friedman, H. (1957). Milliroentgen dosimetry with thermoluminescence, J. Opt. Soc. Am. **47,** 1136.
Peter, H. (1960). Thermolumineszenz und Dosimetrie von Samarium-aktiviertem Kalziumsulfat, Atomkernenergie **5,** 453.
Schulman, J. H., Ginther, R. J., Kirk, R. D., and Goulart, H. S. (1959). Thermoluminescent dosimeter, U.S. Naval Research Laboratory Rept. No. 5326.
Schulman, J. H., Ginther, R. J., Kirk, R. D., and Goulart, H. S. (1960). Thermoluminescent dosimeter has storage stability, linearity, Nucleonics **18,** No. 3, 92.

Conductivity Induced by Ionizing Radiation

Becker, J., Scheer, K. E., and Kuber, A. (1952). Ein neues Strahlenmessgerät mit einer biegsamen Kristallmesssonde und seine Anwendung in der Klinik, Strahlentherapie **88,** 34.
Hollander, Jr., L. E. (1956). Photoconductive dose-rate indicator for ionizing radiations, Rept. No. AD 92397, Armed Services Technical Information Agency (Arlington Hall Station, Arlington, Va., U.S.A.)
Hopton, R. L. (1960). A wrist-carried high range gamma-detecting ratemeter, U.S. Naval Radiological Defense Laboratory, Rept. No. TR–488.
Klick, C. C., Peake, H. J., Cole, P. T., Rabin, H., and Lambe, J. J. (1955). Simple fall-out meter uses CdS, Nucleonics **13,** No. 12, 48.
Mauldon, G., and Martin, J. H. (1956). The use of cadmium sulphide crystals in probe and needle dose-measuring systems, Brit. J. Radiol. **29,** 427.
Miller, L. D., and Jaske, A. J. (1960). Summary of the investigation of the response of cadmium sulfide, U.S. Naval Radiological Defense Laboratory, Rept. No. TR–491.
Proceedings of the Second Conference on Nuclear Radiation Effects in Semiconducting Devices, Sept. 17–18, 1959. (Cowan Publ. Corp., New York, N.Y.)

Proceedings of the Conference on Semiconductor Nuclear Particle Detectors, Ashville, N.C., Sept. 28–30, 1960. Natl. Acad. Sci., Natl. Res. Council Publ. No. 871, Washington, D.C. (1961).
Proceedings of the Conference on Solid State Radiation Detectors, Gatlinburg, Tenn., Oct. 3–5, 1960. IRE Trans. Nuclear Sci., **NS–8,** No. 1 (Jan. 1961).
St. John, E. G., and Fish, E. (1960). The use of cadmium sulfide crystals for the measurement of roentgen radiation, Am. J. Roentgenol. Rad. Ther. and Nuclear Med. **83,** 156.
Semiconductor Detectors (1960). Nucleonics **18,** No. 5, 98. Résumé of papers on that subject presented at the Seventh Scintillation Counter Symp., Washington, D.C. Feb. 25–26, 1960.
Symposium on Solid State Conductivity (1960). (Symp. of six papers delivered at the Annual General Meeting of the Hospital Physicists' Association at Kings College Hospital, 25 Sept. 1959), Phys. Medicine Biol. **4,** 325.
Sessoms, III, O. Van P., (1960). Photoconductivity in CdS crystals as a mechanism for gamma ray dosimetry, Wright Air Development Division Tech. Rept. 60–576, Dayton, Ohio.

Systems Based Upon Other Phenomena

Antonov-Romanovsky, V. V., Keirim-Marcus, I. B., Poroshinam, M. S., and Trapeznikova, Z. A. (1956). Dosimetry of ionizing radiation with the aid of infrared sensitive phosphors, Conference of the Academy of Science of the USSR on the Peaceful Uses of Atomic Energy, July 1–5, 1955. English translation by the USAEC (U.S. Government Printing Office).
Attix, F. H. (1959). High level dosimetry by luminescent degradation, Nucleonics **17,** No. 4, 142.
Attix, F. H. (1959). Luminescence degradation, Nucleonics **17,** No. 10, 60.
Attix, F. H. (1960). Dosimetry by luminescence degradation in organics, Wright Air Development Division Rept. No. 60–563, Wright-Patterson Air Force Base, Ohio, U.S.A.
Birks, J. B. (1950). Scintillation efficiency of anthracene crystals, Proc. Phys. Soc. (London) **63A,** 1294.
Cassen, B., Crough, T., and Gass, H. (1955). Semiconductor fast neutron dosimeter, Nucleonics **13,** No. 3, 58.
Loferski, J. J., and Rappaport, P. (1958). Radiation damage in Ge and Si detected by carrier lifetime changes: Damage thresholds, Phys. Rev. **111,** 432.
Moody, J. W., Kendall, G. L., and Willardson, R. K. (1958). Photovoltaic gamma-ray dosimeter, Nucleonics **16,** No. 10, 101.
Scharf, K. (1960). Photovoltaic effect produced in silicon solar cells by x- and gamma rays, NBS J. Research **64A** (Phys. & Chem.) No. 4, 297–307.
Schulman, J. H., Etzel, H. W., and Allard, J. G. (1957). Application of luminescence changes in organic solids to dosimetry, J. Appl. Phys. **28,** 792.

G. Methods of Fast-Neutron and Mixed-Field Dosimetry

1. Calculation of Absorbed Dose in Tissue Exposed to Fast-Neutron Radiation

The absorbed dose may be calculated by first calculating the kerma, and then taking advantage of the fact that the kerma is equal to the absorbed dose (when expressed in the same units) under conditions of charged particle equilibrium. In the case of tissue irradiated by fast neutrons, the ranges of the heavy secondary charged particles (mainly protons) are short relative to the mean free paths of the neutrons, at least up to about 30 Mev (see table IG1). Thus, within this energy range one can assume that charged particle equilibrium exists at any point in a sample, so long as the point is not closer to the sample's surface than the maximum proton range, as shown in table IG1.

a. In applying eq (IG1), it is evident that one must know the energy distribution of the neutrons incident at a point of interest in the tissue. One will know this energy distribution where the primary neutron flux incident upon the tissue sample as a whole is known and is unperturbed by the presence of the sample, i.e., where the sample is small compared with the mean free path of the neutrons in tissue. Table IG1 lists the approximate neutron mean free path in tissue as a function of energy.

The absorbed dose D_i (rad) in a material of type i due to elastic scattering of fast neutrons of energy E_n and under conditions of secondary charged-particle equilibrium is given by

$$D_i = \frac{19.3 \cdot 10^{-9} \cdot \Phi_n \cdot E_n \cdot \sigma_i(E_n) \cdot K_i(E_n)}{(1+A_i)^2} \qquad \text{(IG1)}$$

where

Φ_n = neutron fluence (neutrons/cm^2),
$\sigma_i(E_n)$ = total elastic cross section (barns per atom) for neutrons of energy E_n (Mev),
$\sigma_i(\theta, E_n)$ = differential elastic cross section (barns/atom-steradian) for neutrons of initial energy E_n scattered at angle θ,
$K_i(E_n) = \int_0^{\pi} [\sigma_i(\theta, E_n)/\sigma_i(E_n)]\,(1-\cos\theta) 2\pi \sin\theta d\theta$,
A_i = atomic weight of atoms of type i.

To calculate the absorbed dose it is necessary to multiply the value of the dose from each type of atom by the fractional composition (by weight) of that type and sum the contributions of all types of atoms. Table IG2 lists the quotient, D_i/Φ_n,

TABLE IG1. *Range R(E), in tissue, of most energetic protons generated by neutrons of energy E, and neutron mean free path λ(E), in tissue*

E (Mev)	R(E) (cm)	λ(E) (cm)
0.1	0.00017	0.83
.3	.00060	1.7
1.0	.0029	4.2
3.0	.016	6.7
10.0	.14	17
30.0	1.2	33

TABLE IG2. *Absorbed dose for fast neutrons in tissue calculated from kerma with the assumption of charged particle equilibrium*

Neutron energy (Mev)	Absorbed dose (rad) / Particle fluence, (neutron/cm²)				
	D_H/ϕ	D_C/ϕ	D_N/ϕ	D_O/ϕ	$D_i(E)/\phi$
.01	0.091×10^{-9}	0.001×10^{-9}	0.000×10^{-9}	0.001×10^{-9}	0.093×10^{-9}
.02	$.172\times10^{-9}$	$.002\times10^{-9}$	$.000\times10^{-9}$	$.003\times10^{-9}$	$.177\times10^{-9}$
.03	$.244\times10^{-9}$	$.003\times10^{-9}$	$.001\times10^{-9}$	$.005\times10^{-9}$	$.253\times10^{-9}$
.05	$.369\times10^{-9}$	$.005\times10^{-9}$	$.001\times10^{-9}$	$.008\times10^{-9}$	$.383\times10^{-9}$
.07	$.472\times10^{-9}$	$.006\times10^{-9}$	$.001\times10^{-9}$	$.010\times10^{-9}$	$.489\times10^{-9}$
.10	$.603\times10^{-9}$	$.009\times10^{-9}$	$.001\times10^{-9}$	$.015\times10^{-9}$	$.628\times10^{-9}$
.20	$.914\times10^{-9}$	$.017\times10^{-9}$	$.002\times10^{-9}$	$.031\times10^{-9}$	$.964\times10^{-9}$
.30	1.14×10^{-9}	$.024\times10^{-9}$	$.003\times10^{-9}$	$.046\times10^{-9}$	1.21×10^{-9}
.50	1.47×10^{-9}	$.035\times10^{-9}$	$.003\times10^{-9}$	$.071\times10^{-9}$	1.58×10^{-9}
.70	1.73×10^{-9}	$.043\times10^{-9}$	$.005\times10^{-9}$	$.081\times10^{-9}$	1.86×10^{-9}
1.0	2.06×10^{-9}	$.053\times10^{-9}$	$.006\times10^{-9}$	$.354\times10^{-9}$	2.47×10^{-9}
2.0	2.78×10^{-9}	$.068\times10^{-9}$	$.010\times10^{-9}$	$.135\times10^{-9}$	2.99×10^{-9}
3.0	3.26×10^{-9}	$.078\times10^{-9}$	$.012\times10^{-9}$	$.150\times10^{-9}$	3.50×10^{-9}
5.0	3.88×10^{-9}	$.084\times10^{-9}$	$.009\times10^{-9}$	$.142\times10^{-9}$	4.12×10^{-9}
7.0	4.22×10^{-9}	$.071\times10^{-9}$	$.010\times10^{-9}$	$.310\times10^{-9}$	4.61×10^{-9}
10.0	4.48×10^{-9}	$.105\times10^{-9}$	$.011\times10^{-9}$	$.395\times10^{-9}$	4.99×10^{-9}
14.0	4.62×10^{-9}	$.094\times10^{-9}$	$.014\times10^{-9}$	$.466\times10^{-9}$	5.19×10^{-9}

for each of the important components of tissue as well as their sum, D_f/Φ_n. These are computed from data in BNL 325 (1958, 1960), BNL 400 (1962) and AWRE 0–28/60 (1961) and for a tissue corresponding to the ICRP Standard Man (H=10 percent, C=18 percent, N=3.0 percent and O=65 percent—the other constituents make a negligible contribution to the dose).

b. When the size of the medium under consideration becomes comparable with the mean free path of neutrons in the medium, multiple collision calculations must be made to find the distribution of absorbed dose in the medium. Such calculations have been carried out for a tissue slab which is 30 cm thick in the direction of a collimated broad beam of neutrons (Snyder and Neufeld, 1955; NCRP Report, 1957).

2. The Measurement of Absorbed Dose in a Medium Exposed to Both Neutron and X or Gamma Radiation, and the Distribution of Absorbed Dose With Respect to LET

a. Absorbed dose due to neutrons may be accurately and conveniently determined with ionization cavities employing the Bragg-Gray relation (Gray, 1936, 1944; Zimmer, 1938). The tissue-equivalent ionization chamber (Failla and Rossi, 1950) may be used to determine the total absorbed dose in tissue, and other instruments must be used to evaluate the relative proportions of the radiations making up this total dose. Its sensitivity to neutrons is within 10 percent of its sensitivity to gamma rays, the difference being due to the difference in W for the two cases.

Approximate methods have been devised that permit evaluation of a radiation field in terms of its component primary radiations, especially with regard to the separation of doses due to neutrons and gamma rays. Ionization chambers lined with carbon or conducting teflon and filled with carbon dioxide (Rossi and Failla, 1956) may be expected to yield a good measure of the absorbed dose delivered to tissue by electromagnetic radiations, while being rather insensitive to neutrons. However, these devices do have a certain small neutron sensitivity, k. The coefficient k is defined as the ratio of the reading of a teflon-CO_2 chamber exposed to a neutron fluence which delivers 1 rad to standard tissue, to the reading observed when the chamber is exposed to 1 R of hard x rays. Experimental and computed values of k are given in table IG3 (NCRP Report, 1961). The former were obtained with a chamber made of conducting teflon and filled with carbon dioxide gas, using neutron beams having minimal gamma contamination. However, since the presence of gamma radiation cannot be excluded, these figures must be considered as upper limits only. The computed values for k were obtained by calculations of the type given in NCRP Report (p. 82, 1961) and with the assumption that W is the same for heavy recoils as for protons. They are, therefore, also upper limits.

When a tissue equivalent chamber is exposed to 1 R of gamma rays or hard x rays, the corresponding absorbed dose is 0.96 rad. The same ionization will be produced in this chamber by an absorbed dose of neutrons equal to $\frac{W_\alpha}{W_\beta}\times 0.96$ rad where W_α and W_β are the average energies required from an alpha particle and a beta ray respectively to produce an ion pair in a gas. It is assumed that the value of W in a gas is the same for alpha particles, protons and heavy particles. The ratio of W values will depend slightly upon the gas mixture in the chamber, but will usually lie in the range 1.03 to 1.06,

TABLE IG3. *Maximum k for a teflon-CO_2 chamber*

Neutron energy (Mev)	Observed k	Computed k
0.5	0.08	0.11
1.0	.08	.18
2.0	.09	.13
3.0	.12	.10
4.0	.15	.15
6.0	.20	.16
8.0	.24	.20

Gas	CH_4	CO_2	N_2	air
$\frac{W_\alpha}{W_\beta}$	1.065	1.033	1.05	1.04

If we take the W ratio as 1.04, then the ratio, T, of the ionization produced by Γ rads of hard x rays and N rads of neutrons to the ionization produced in the same chamber by 1 R of hard x rays will be

$$T=\frac{\Gamma}{0.96}+\frac{N}{1.00}=1.04\Gamma+N. \qquad \text{(IG2)}$$

In the teflon-CO_2 chamber the ratio, C, of the ionization produced by the above mixed neutron and x-ray dose to that produced by 1 R of hard x rays will be

$$C=1.04\Gamma+kN. \qquad \text{(IG3)}$$

This procedure makes it possible to evaluate the mixed radiation field on the basis of x-ray calibrations of the two chambers. Direct calibrations may be performed on an absolute basis taking into account chamber volume, gas pressure, electrical capacity, the voltage sensitivity of the detector, and W.

A number of similar schemes (Gray et al., 1940; Dainty, 1950; Bretscher and French, 1944; Marinelli, 1953) involving several ionization chambers have been devised in attempts to separate neutron and gamma doses.

b. Proportional counters may be used to advantage in measuring fast neutron dose in the presence of gamma rays (Hurst, 1954). The Bragg-Gray cavity principle is applied; for example, ethylene gas and polyethylene liners are satisfactory for fast neutrons since the ratio of energy deposited per gram of ethylene to energy dissipated per gram of tissue is substantially independent of neutron energy. The essential departure from the ionization chamber technique

is that the number of ion pairs produced in the gas is determined by a summation of pulse heights, rather than an integration of charge or a current measurement. This fact enables one to integrate only the pulses due to neutrons while rejecting those due to gamma rays, if the dimensions of the gas cavity and the pressure of the gas are chosen so that the pulses due to electrons (from gamma-ray effects) are generally smaller than most of the pulses due to recoil protons (from fast-neutron collisions). If the pulse height is proportional to the number of ion pairs formed, this method of dosimetry is in every way equivalent to the ionization chamber, with the added advantage of being quite insensitive to gamma radiation.

The proportionality between pulse height and number of ion pairs depends on two conditions: (a) there must be no electron attachment, and (b) the height of the pulse at the output of the linear amplifier must not depend on track orientation. Condition (a) may be fulfilled by excluding from the counter such gases as water vapor, oxygen, and some of the halogens, which have very large electron attachment cross sections (Healey and Reed, 1941). Condition (b) may be fulfilled by proper selection of the amplifier rise time and decay time (Hurst and Ritchie, 1953). A variation of the angle between the recoil proton trajectories and the center wire in a proportional counter causes a variation in the pulse profiles. However, it has been shown (Hurst and Ritchie, 1953) that if the rise time and decay time constants (assumed to be equal, which is true for many good linear amplifiers, see Jordan and Bell, 1947) are greater than the collection time of electrons in the counter, the pulse height at the output of the amplifier depends only slightly on the rise time of the proportional counter pulse.

Several variations of proportional counters following these principles have been designed. One of these contains an internal alpha source for calibration. Since the sensitive volume is determined by means of field tubes (Cockroft and Curran, 1951), the mass of gas is known and hence the sensitivity of the detector can be determined without using a known neutron source.

Since dose is proportional to the summation of pulse heights, it is also proportional to the area under the curve showing the number of pulses exceeding a given height, as a function of height. The area may be accurately determined with a planimeter or the summation of pulse heights may be done directly with an electronic pulse integrator (Glass and Hurst, 1952).

The application of a bias energy, B, to discriminate against gamma radiation causes a fraction, f, of the neutron energy to be lost under the bias. Values of f for various values of the bias, B, and neutron energy, E, are given in table IG4. When using the absolute proportional counter with conventional electronic equipment, the value of B may be chosen to suit the particular experimental conditions (Wagner and Hurst, 1959). Factors which govern the choice of B include the following: neutron energy, neutron intensity, gamma-ray energy, and gamma-ray intensity. In any case the discrimination level at which the results may be appreciably affected by gamma radiation may be determined directly for the particular experimental conditions. For example, for Co^{60} gamma-ray dose rates of 1 R/hr or less the bias level required to discriminate against gamma rays is about 0.20 Mev, and the absorbed neutron energy which would be lost under this bias is about 10 percent for 1mrad/hr Po-Be neutrons (see table IG4). On the other hand, if the gamma dose rate were as high as 25 R/hr, the bias level would have to be increased to about 0.36 Mev and the energy lost would be about 20 percent, however this may be estimated by extrapolating the count rate vs pulse height curve for values of pulse height $\leq B$ and then integrating the area under the entire curve. In other words, the values for f given in table IG4 do not necessarily represent errors in the measured dose, but do represent the fraction of the total dose which must be estimated by extrapolation.

A convenient instrument (Wagner and Hurst, 1958) utilizing the absolute counter has been developed. In this instrument, the pulse integrator is a simple four-stage binary circuit (Glass and Hurst, 1952) which gives the area under the integral pulse height curves with very good accuracy, considering the extreme simplicity of the circuit. When using this scheme of pulse height integration, the gamma response corrections mentioned above do not hold, but results for the case of Co^{60} have been reported by Wagner and Hurst (1958).

Proportional counters similar to the above have been used to measure the fast neutron dose as well as the total (neutron + gamma) dose in mixed beams (Slater et al., 1958; Pott and Wagner, 1960).

c. A proportional counter may be used as a dosimeter for gamma rays in the presence of neutrons by pulse height integration of the small pulses due to gamma rays and rejection of the large pulses due to neutrons (Caswell, 1960).

This approach is opposite to that of the use of the proportional counter for fast neutron dosimetry. The instrument consists of a graphite wall, $He\text{-}CO_2$ filled proportional counter operated at low gas pressures (2 to 10 cm Hg). Large pulses

TABLE IG4. *Percent,* f, *of energy spent by recoils losing less than the bias energy,* B, *in the counter*

Bias (B) (Mev)	Fast neutron energy (Mev)							
	0.5	1.0	2.0	3.5	4.8	14	Po-B	Po-Be
0.074	8.9	2.0	1.5	1.3	1.4	2.5	0.6	1.4
.14	19.5	9.4	4.1	3.5	2.8	8.5	2.8	4.5
.21	32.0	12.9	7.6	5.6	5.9	16.2	6.5	10.1
.28	52.6	23.5	12.3	9.1	9.8	25.8	9.9	14.4
.36	73.0	33.3	18.8	12.8	16.2	36.9	15.2	20.5

due to heavy particle recoils, such as C recoils from the walls and C, O, and He recoils from the gas, are discarded. Small pulses due to secondary electrons produced by gamma rays are recorded and their heights are integrated. Maximum pulse-height discrimination between neutrons and gamma rays is obtained at or below pressures where the range of the C recoils is approximately the length of the sensitive volume of the counter.

Gamma-ray response per roentgen is independent of energy to within 5 percent from 1.25 Mev (Co^{60}) to 200 kev and to within 20 percent down to 47 kev. Use of a graphite lining and a thin aluminum wall minimizes production of gamma rays in the walls by inelastic scattering of the incident neutrons (which would enhance the neutron sensitivity of the counter). Response in a 2.5- to 3-Mev H^2 (d, n) He^3 neutron field has been shown experimentally to be ≤ 1 percent of the gamma-ray response for the same kerma in tissue. This type of instrument has relatively high sensitivity, and is therefore useful primarily at gamma-ray exposure rates below 10^{-2} R/min.

d. Another device for measuring ionization which can distinguish between secondary electrons from gamma rays and recoil nuclei from neutrons is the single ionization detector reported by Auxier, Hurst, and Zedler (1958). In this instrument, a cavity of very small linear dimensions and low gas pressure is used. The probability of an electron making an ionizing collision in the gas is low. The probability of more than one collision is correspondingly much lower. On the other hand, fast neutron recoils may lose a large amount of energy in the counter, producing many ion pairs, but still producing only one count per event. The device is therefore very inefficient for neutron recoils. In this way discrimination against neutron radiation is achieved.

The above general ideas have been applied in the development of a very convenient, gamma-ray dosimeter utilizing a commercially available Geiger-Mueller counter (Wagner and Hurst, 1961), shielded with a filter made of Sn and Pb. The instrument measures the exposure in roentgens with nearly uniform response for effective x-ray energies above 200 kev and up to at least 1.2 Mev gamma energies. Calculations show that the fast neutron response is less than 0.15 percent of that for x or gamma radiation, and experiments confirm that this figure is certainly less than 0.5 percent. The response to thermal neutrons is also quite low; 5×10^9 n/cm^2 is equivalent to 1 R of gamma radiation.

e. Discrimination between neutrons and gamma rays in mixed radiation fields may also be achieved with plastics loaded with granular scintillating materials (Hornyak, 1952; Brown and Hooper, 1958). Fast neutrons striking hydrogenous material in the detector button produce proton recoils; these in turn produce light when they strike the phosphor grains, which is then detected by a multiplier phototube. Proton recoils produce large light pulses corresponding to large energy losses in the phosphor grains, whereas secondary electrons from gamma rays produce small pulses corresponding to the low energy per unit track length. The small gamma-ray pulses may be discriminated against electronically. Empirical design of these detectors for measurement of dose in tissue has been discussed by Muckenthaler (1957).

f. Other detectors have been designed to have a response vs neutron energy similar to the dose in tissue while achieving high discrimination against gamma rays in mixed radiation fields. These include the hydrogenous proportional counter (Hurst et al., 1951; Dennis and Loosemore, 1957), the spherical scintillation detector (Skjöldebrand, 1955), and the paraffin-moderated BF_3 counter (DePangher, 1957).

g. The neutron contribution to the absorbed dose may be calculated from measurements of the number and length of the recoil proton tracks produced in photographic emulsion under controlled conditions.

h. The neutron absorbed dose rate in any medium may be calculated from a knowledge of the flux and energy spectrum of the neutron beam at the place of interest. These two quantities may be inferred from the induced activity of a series of "threshold detectors" of Pu^{239} surrounded by B^{10}, Np^{237}, U^{238}, and S^{32} (Hurst et al., 1956; Reinhardt and Davis, 1958).

i. A complete analysis of the radiation field for purposes of radiobiology and protection is one in which the dose delivered at each level of LET is determined. Such an analysis is necessarily very complex and should be reserved for instances where great detail is needed.

A method has been developed in which this "LET spectrum of dose" may be determined experimentally (Rossi and Rosenzweig, 1955a). The detector employed is a spherical proportional counter of tissue-equivalent plastic. The particle spectrum set up in the wall of such a counter will be the same as the one occurring in tissue. The energy deposited by individual charged particles traversing the interior of the counter depends both on LET and the length of the track intercepted. However, the latter geometrical factor may be eliminated on a statistical basis with appropriate mathematical treatment of the pulse height curve that is obtained from the electronic equipment associated with the counter. The analysis is correct only if (1) particles traversing the cavity incur small change in LET, and (2) particle trajectories are essentially straight lines. The first of these requirements may be attained by filling the counter with tissue-equivalent gas at low pressure. The second requirement limits the use of the instrument primarily to positively charged nucleons and mesons. However, only for such particles can the RBE prescribed for protection purposes [9] (NCRP Report, 1954) be more than one. The mean LET of electrons is considered to be less than 3.5 kev/μ of water for purposes of personnel protection. The actual

[9] The new term for this quantity is QF (see appendix I).

LET of electrons can attain values as high as 20 kev/μ. However, the range of electrons having a LET of more than 5 kev/μ is so short that traversal of the counter is impossible under the operating conditions usually chosen. Similarly, the total energy of such electrons is so low that pulses produced by them disappear in the noise. Because of the finite recovery time of the proportional counter, the radiation intensity that may be tolerated without undue "pile-up" is limited, particularly in the case of pulsed radiation sources, However, in the case of protection measurements the count rate recorded is usually adequately low.

Since the instrument is functional for essentially all charged particles having a RBE of more than one, and since the total tissue dose may be determined, using a tissue-equivalent ionization chamber, a combination of these instruments may be used for complete analysis of the radiation field for purposes of protection.

Because of the principles of operation of this device, it is capable of a high degree of differentiation between particles of different LET. For particles of any given LET, only pulses corresponding to a major traversal need be counted, with those imparted by pulses due to shorter traversals being accurately predictable. This almost entirely eliminates the need for a low bias and makes it possible to evaluate the dose delivered by pulses that are normally lost in the electronic noise. Proper mathematical evaluation of the pulse height spectrum usually permits determination of the dose delivered between any two limits of LET. However, complications arise at neutron energies below about 200 kev because even if the instrument is operated at very low pressure, appreciable numbers of particles may stop or start in the cavity. However, because of statistical fluctuations the whole concept of LET loses its meaning for biological structures having diameters less than 1μ.

LET spectra obtained with this instrument (Rossi and Rosenzweig, 1955b) depend somewhat on the gas pressure within it and all differ from LET spectra based on theoretical computations. It has been shown (Rossi and Rosenzweig, 1956) that this effect is due to statistical variations of energy loss of charged secondaries and that such variations do, in fact, result in LET spectra which depend on the size of the "biological sample" to be evaluated. For purposes of protection such variations are usually of little consequence.

A limitation of the device is that with presently available models the maximum dose rate is of the order of 0.5 rad/hr. In addition, multichannel analyzers must be employed to obtain data from sources having variable intensity.

Further details on many of the methods discussed in this section may be found in an NCRP Report (1961).

II. Standards, Instruments and Measurement Techniques for X Rays, Gamma Rays and Neutrons

A. X- and Gamma-ray Standards and Transfer Instruments

1. For a Few Kv to About 0.5 Mv X Rays

a. *Definitions.* The following terms are used in this report: i. *Exposure standard* is an ionization chamber and associated equipment, which allows the direct measurement of exposure. (Frequently referred to as a primary standard.) ii. *Transfer instrument* is an exposure meter of high stability for indirect comparison measurements between two or more exposure standards.

b. *Free-air standards: correction factors and errors.* The free-air ionization chamber provides the exposure standard for the low- and medium-energy x-ray region in all national standardizing laboratories, though in two laboratories pressurized air chambers are being used or investigated for the upper end of this region (for x rays generated at potentials above 250 kv).

The extensive reports on the design of free-air chambers for the measurement of exposures of x rays up to 500 kv (Rajewsky et al., 1955; Wyckoff and Attix, 1957) have been used in designing a number of new chambers, some of which are the first standards to be constructed by the particular national organizations and others of which are improved standards replacing earlier ones now regarded as obsolete. Data concerning the design of chambers for the low-energy region below 100 kv have been given by Ritz (1959, 1960) and by Allisy and Roux (1961).

The examination of the various corrections required for free-air chamber measurements given in these two extensive reports is still valid and investigation of some of the corrections by a number of laboratories in relation to their own chambers has produced results which do not differ significantly from those given in the reports. An errata sheet has been issued for the Wyckoff and Attix report, giving revised values for the secondary photon contribution, the new values making an addition to the correction for this effect of 0.1 to 0.3 percent, the revised values being confirmed by Henry and Garrett (1960). A table of corrections for humidity, based on a theoretical investigation, has been published (Barnard et al., 1960).

An estimate of the maximum uncertainties obtained under optimum conditions for each of the principal factors involved in a free-air chamber determination of the exposure in roentgens is given in table IIA1. The data in this table refers only to medium filtration x rays generated by constant potentials of from 60 to 300 kv. The uncertainties may be larger outside of this range.

c. *Details of national standards.* A list of national exposure standards in current use is given in table IIA2. It has been decided to include as far as possible only the institution in each country

which holds the chambers having the status of national standards and which thus takes part in international comparisons. In a number of countries, there are other institutions also having free-air chambers capable of absolute measurements of exposure, though these are not regarded as national standards.

The literature references in the final column of the table include only papers giving particulars of the chambers in current use. This replaces a similar table incorporated in the previous report (ICRU, 1959) which summarized the information available at that time.

TABLE IIA1. *Estimated uncertainties for principal factors in free-air chamber determination of exposure in roentgens*

Experimental factor	Estimated maximum uncertainty (%)
A. Charge (assumed measured by potentiometer and capacitor)	±0.1
B. Air volume (includes errors in diaphragm area, collecting plate width and alinement and field distortion resulting from other causes)	±0.3
C. Air density and humidity of air (includes pressure, temperature and humidity measurements and uncertainty in humidity correction)	±0.1
D. Saturation of ion collection	±0.1
E. Scattering of x rays by air in the chamber	±0.1
F. Inadequacy of plate separation for electron path length	±0.1
G. Photon beam attenuation in air between diaphragm and collector	±0.2

d. *Recent comparisons of national standards.* The results of a direct comparison between free-air chambers of the National Research Council, Canada, and the U.S. National Bureau of Standards, carried out at Washington in 1959 (Aitken et al., 1962) are given in table IIA3.

One set of indirect comparisons using two of the three-terminal cavity chambers (transfer instruments) described in the last ICRU Report (1959) has been completed. The results of these comparisons are given in table IIA4 (Wyckoff et al., 1963). The estimated maximum uncertainty of about 0.5 percent is somewhat larger than that assigned to direct comparisons, though it is considered that it should be possible to improve such transfer instruments so that indirect comparisons are almost as accurate as direct ones. Taking into account the greater uncertainty in the indirect comparisons by the circulation of these transfer instruments, the results of table IIA4 are consistent, where comparable, with those of earlier comparisons (Aston and Attix, 1956; Allisy et al., 1957).

e. *Future comparisons of national standards.* The Bureau International des Poids et Mesures (BIPM) is taking responsibility for future international comparisons of standards of exposure, and is making available to national standardizing laboratories cavity chambers (transfer instru-

TABLE IIA2. *National Exposure Standards*

Standard No.	Country	Institute and custodian	Radiation range	Type	Literature reference
			kv		
1	Australia	Commonwealth X-ray and Radium Lab., Melbourne, (D. J. Stevens).	30 to 200	Free-air, parallel plate	
2a	Canada	National Research Council, Ottawa, (C. Garrett).	50 to 250	do	Henry and Garrett (1960).
2b	do	do	10 to 50	do	
3a	Bundes-Republik Deutschland.	Physikalisch-Teebnische Bundesanstalt, Braunschweig (W. Hübner).	50 to 400	Free-air, cylindrical	Rajewsky et al., (1955).
3b	do	do	10 to 120	Free-air, parallel plate	Tboraeus et al., (1955).
3c	do	do	5 to 40	do	
4a	France [a]	Laboratoire Central des Industries Electriques, Paris (P. Olmer).	50 to 250	do	
4b	do	Laboratoire de Dosimétrie, Ecole Normale Supérieure, Paris (A. Allisy).	50 to 250	do	Allisy et al., (1957).
4c	do	do	5 to 50	Free-air, parallel plate (special design).	Allisy and Roux (1961).
5	Italy	Instituto Superiore di Sanità, Rome (M. Chiozzotto).	50 to 300	Free-air, parallel plate	Cbiozzotto (1962).
6a	Japan	Electrotechnical Lab., Tokyo (Y. Inoue).	40 to 250	do	Ito, T. and Ito, G. (1941).
6b	do	do	5 to 40	do	Naito et al., (1961).
6c	do	do	200 to 800	10 atm., parallel plate (under construction).	
7a	Netherlands	Rotterdamsch Radiotherapeutisch Inst. Rotterdam (A. Somerwil).	50 to 250	Free-air, parallel plate	deWaard et al., (1958); Somerwil (1959).
7b	do		10 to 50	do	
8	New Zealand	Dominion X-ray Radium Lab. Christchurch (G. E. Roth).	50 to 300	do	
9	Poland	Głowny Urzad Miar, Warsaw (Z. Referowski).	50 to 200	do	
10a	Sweden	Inst. of Radiophysics, Stockholm (R. Thoraeus).	50 to 250	Free-air, cylindrical	Thoraeus (1932, 1954).
10b	do	do	8 to 50	do	Thoraeus (1932, 1954).
11	Union of South Africa.	National Physical Research Lab., Pretoria (M. L. du Preez).	50 to 300	Free-air, parallel plate (under investigation).	
12a	U.S.S.R.	Institute of D. I. Mendeleev, Leningrad (K. K. Aglintsev).		Free-air, cylindrical	Balon (1957).
12b	do		20 to 60	Free-air, parallel plate	Avotina and Ostromukbova (1961).
			250 to 3000	20 atm., parallel plate	Aglintsev and Ostromukhova (1959, 1961).
13a	United Kingdom	National Physical Lab. Teddington (G. H. Aston).	50 to 300	Free-air, parallel plate	Smith, E. E. (1955) Aston and Attix (1956).
13b	do	do	5 to 50	do	
14a	United States	National Bureau of Standards, Washington, D.C. (H. O. Wyckoff).	60 to 250	do	Wyckoff et al., (1954); Aston and Attix (1956).
14b	do	do	20 to 100	do	Ritz (1960).

[a] The French national standard is at Laboratoire Central des Industries Electriques but at present a similar standard at Laboratoire de Dosimétrie is used in international comparisons.

ments) of the type designed by H. O. Wyckoff, National Bureau of Standards and of the type designed by A. Allisy, Laboratoire de Dosimétrie, Institut National D'Hygiène. As an interim measure until the BIPM has facilities for comparisons, a laboratory may request from the BIPM a transfer instrument which has been calibrated at another laboratory. It is thought that eventually the best way of obtaining comparisons between national laboratories may be for each laboratory to provide itself with its own transfer instrument. All of these could be sent to BIPM at the same time. The BIPM could then compare these instruments and return them to the originating laboratories which would then check them for the constancy of their calibrations.

2. For About 0.5 Mv X Rays to a Few Mev Gamma Rays

a. *Types of standards and their correction factors.* The standards which are used for exposure measurement in this energy range are cavity ionization chambers and pressurized-air chambers.

The wall material of a cavity ionization chamber is never truly air equivalent; hence a stopping power correction has to be applied in the calculation of exposure rate. Stopping power data are given in subsection IA2. Corrections for attenuation and scattering in the wall are required, and a correction should be made also for the radiation scattered into the ionization chamber from the stem. This latter correction can be determined by bringing up a second "dummy" stem and observing the increase in ionization current. Figure IIA1 assists in picturing the method of correction for the photon attenuation in the wall of a cavity chamber. It is assumed that the cavity is small enough so that the number of ions produced by electrons generated in the air within it by the photons is negligible, compared with the number of ions produced by the secondary electrons entering the cavity. The ionization current in the cavity initially increases with wall thickness, t, as indicated by the curve AB. This initial portion is followed by a broad maximum B, and a decrease, DE. The slope of the latter portion is controlled by the attenuation of the photon beam in the wall material. When t corresponds to a thickness of wall within the range DE of figure IIA1, the photon attenuation correction depends upon the distance, t', from the outer surface of the wall to the mean position at which the electrons that produce ionization in the cavity are generated. For low-energy photons such electrons are produced very near the inner surface so that $t' \approx t$ and the ionization should be corrected for the attenuation in a thickness t. In such cases one usually assumes that the attenuation of the photons for the thickness t can be obtained by extrapolating DE to zero wall thickness. For high energy photons the difference in attenuation for a thickness t' and a thickness t becomes appreciable. This difference amounts to about 0.5 percent for cobalt-60 gamma rays and 0.2 percent for cesium-137 gamma rays (Wyckoff, 1960. See Burlin, 1959, or Roesch, 1958, for formulation).

With increase in energy this difference increases. Uncertainty in the determination of this difference is one of the principal contributions to the uncertainty of measurements in the megavolt region and tends to set a practical upper limit to such measurements.

Other authors (Tubiana and Dutreix, 1958, and Barnard et al., 1959) have shown an alternative

TABLE IIA3. *Results of comparison of* NRC *and* NBS *free-air chambers* [a]

kv	60	75	100	150	200	250
NRC exposure rate / NBS exposure rate	1.001$_8$	1.002$_9$	1.001$_6$	1.001$_1$	1.001$_4$	1.001$_8$

[a] The ratios given in this table differ from those in the quoted paper because of an additional correction of +0.15 percent for lack of coplanarity of the NBS guard and collector plates.

TABLE IIA4. *Results of indirect comparison of exposure standards*

HVL (mm Cu)	kv	Laboratory [a]	Ratio of calibration factor determined at stated laboratory to that determined at NBS	
			Chamber II	Chamber IX
0.083	60	PTB	0.999	.999
.089	60	LD	.996	----
.103	80	NPL	1.008	1.004
.11	75	PTB	1.000	1.000
.197	100	PTB	1.003	1.002
.20	100	LD	1.001	----
.20	125	NPL	----	1.006
.25	125	NPL	1.000	----
.50	145	NPL	0.995	1.002
.64$_7$	150	PTB	.998	1.004
.65	150	LD	1.000	----
1.02	180	NPL	0.997	1.000
1.2	200	LD	.999	----
1.20$_5$	200	PTB	.998	0.998
1.53	250	NPL	1.008	----
2.11	250	PTB	0.997	0.996
2.19	290	NPL	1.010	1.008
2.55	250	NPL	1.002	----
3.13	250	PTB	0.996	0.995
3.4	290	NPL	1.000	1.009
3.95	300	PTB	(0.992) [b]	(0.998) [b]
4.74	350	PTB	(0.994) [b]	(0.997) [b]

[a] LD = Laboratoire de Dosimétrie, France.
NPL = National Physical Laboratory, United Kingdom.
PTB = Physikalisch-Technische Bundesanstalt, Germany.
[b] Ratio uncertain as extrapolation of NBS data is involved.

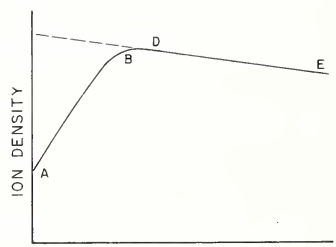

FIGURE IIA1. *The variation in ionization density with wall thickness.*

TABLE IIA5. *Type of standard in the different countries*

Country	Basis for measurement
Canada	Graphite cavity chamber.
Germany	Sources of cobalt-60 and cesium-137 of known exposure rates, which were measured with NBS transfer instruments.
United Kingdom	Graphite cavity chamber.
Japan	Do.
Poland	Graphite cavity chamber based on pressurized air chamber of Institute of D. I. Mendeleev, Leningrad.
Sweden	Graphite cavity chamber based on NBS calibration.
United States	Graphite cavity chambers.
U.S.S.R.	Pressurized air chamber.

approach to the wall attenuation correction. If a value of t is chosen so that the ionization is a maximum, B of figure IIA1, the proper attenuation is for this entire thickness. The two methods should give the same results.

The attenuation in any portions of the chamber wall that are nearly parallel to the radiation beam requires special consideration. Attix and Ritz (1957) found that the calibration of large cylindrical chambers which they used was best obtained when the beam was not parallel to any axis of symmetry of the chamber.

In the pressurized chamber, the air is used at a pressure which depends on the plate separation and the energy of the radiation being measured. Probably the factor giving the largest uncertainty in such determinations is the correction for lack of saturation, which may amount to the order of 10 percent in some circumstances (Wyckoff, 1960). Since most of the electrons which produce the ionization in the collecting region are generated before, and only a few behind the collecting region, the mean position of origin of electrons producing ionization in the collecting region is displaced towards the entrant diaphragm. Therefore, the air absorption correction should be less than that for the distance between the center of the collecting region and the diaphragm. This decrease has been computed to be 0.8 percent for cobalt-60 gamma rays and 0.4 percent for cesium-137 gamma rays (Aglintsev and Ostromukhova, 1959).

The only recent work allowing comparison between these two kinds of standard (Wyckoff, 1960) indicates that there is agreement to about 2 percent. This paper also includes analysis of the errors involved in both methods.

b. *National standards.* Table IIA5 gives the type of standard used in each country for exposure measurements in this energy range. The details of these chambers are indicated in tables IIA6 or IIA7. It is noted that some national laboratories have both cavity and pressurized air chambers but only one type is indicated to be the national standard.

3. For Energies Above a Few Mev

a. *Quantities and units.* It is useful to measure the total beam energy (TBE) of high energy x-ray beams, i.e., the total energy of the photons crossing a plane perpendicular to the beam during the time of interest. Other quantities such as the energy fluence or the intensity can be derived from the TBE with the help of additional measurements. These x-ray beams are bremsstrahlung beams, which are such that at high energies the fluence usually varies over the beam cross section. Moreover, the fluence rate (intensity) varies irregularly with time. The TBE is independent of these variations, and for any irradiation, it can be measured accurately in absolute units. The recommended unit of TBE is the joule although the custom has arisen among nuclear physicists of expressing it either in ergs (1 erg$=10^{-7}$ joules) or in Mev (1 Mev$=1.602\times10^{-13}$ joules).

b. *Methods of measurement.* There are several techniques which have been used to determine the TBE in absolute units; the most direct of which is calorimetry (Laughlin and Beattie, 1951). The usefulness of calorimeter measurements of TBE is limited by low sensitivity and by the need to correct for energy escaping from the calorimeter in the form of neutrons, secondary electrons, and scattered and transmitted photons.

Counting techniques have also been used where the TBE is obtained from knowledge of the number of photons of each energy in the x-ray spectrum. A well-designed pair spectrometer (Walker and McDaniel, 1948) provides this information with high resolution, but its sensitivity is extremely low. A total absorption scintillation crystal (Foote and Koch, 1954) counts the number of incident photons with high sensitivity, but independent knowledge of the shape of the photon spectral distribution is required to obtain the TBE.

There are three other experimental methods which have been used to determine the TBE with less complicated equipment, but which require knowledge of both photon spectral distribution and atomic parameters. The balance converter method (Blocker, Kenney, and Panofsky, 1950) depends upon measurement of ionization current as a function of the atomic number of the front wall of an ionization chamber, and requires mathematical separation of the ionization into components resulting from Compton interactions and from pair production. The shower method (Blocker, Kenney, and Panofsky, 1950) depends upon measurement of ionization current as a function of front-wall thickness, and requires knowledge of electron stopping power ratios. The copper activation method (Loeffler, Palfrey, Tautfest, 1959) depends upon counting the 9.9 min positron activity induced in copper by high energy x rays, and requires knowledge of the differential cross section for the Cu^{63} (γ,n) Cu^{62} reaction.

Each of these techniques requires too much expenditure of time and energy for routine use in the determination of TBE. They have been used to calibrate ionization chambers (transfer instruments) of various designs, so that this determination can be made by measuring the ionization collected during an irradiation. Un-

TABLE IIA6. *Details of cavity chambers used by national laboratories*

Country	Institution	Material	Purity %	Volume cm³	Wall thickness	Corrections used: Stopping power: 2 Mv x rays	Stopping power: Cs^{60} γ rays	Stopping power: Cs^{137} γ rays	Wall absorption: 2 Mv x rays	Wall absorption: Co^{60} γ rays	Wall absorption: Cs^{137} γ rays	References	Compared with	Reference
Canada	National Researcb Council, Ottawa.	Graphite		2.75	3.8 mm		1.003 [a]			1.025			NBS Cavity Chambers.	To be published.
Germany	Physikslisch-Tecbnische Bundesanstalt, Braunschweig.	Graphited Perspex		45.3 6.3										
United Kingdom.	National Pbysical Laboratory, Teddington.	Graphite		2	3 mm	1.010 [b] 1.003 [c]			1.020 [b] 1.012 [c]			Barnard, Axton and Marsh, 1959. Barnard and Marsh, 1959.	NBS Cavity Chambers.	Wyckoff et al., 1963.
Japan	Electrotecbnical Laboratory, Tokyo.	do	99.99	10.84	Variable from 1 to 16 mm.		1.000 [d]	1.027 [e]		0.75%/mm	0.98%/mm			
Poland	Glowny Ursad Mier, Warsaw.	do		65.8	6.1									
Sweden	Institute of Radiophysics, Stockholm.	do		4.3 mm								Thoraeus 1957		
United States.	National Bureau of Standards, Washington, D.C.	do	≥99.9	67.5	0.77 gms/cm²		1.003 [a]	1.007 [a]		1.032 [f,h]	1.042 [f,h]	Attix and Ritz, 1957	NBS Free-Air Cbamber [g] NBS Calorimeter NBS Cavity Chamber	Wyckoff,1960
		do	≥99.9	1.13	0.67 gms/cm²		1.004 [d]	1.008 [d]		1.014 [f]	1.022 [f,h]			Wyckoff et al., 1963

[a] Values based on Bakker-Segrè I values.
[b] These values are used for the calibration of exposure meters against graphite cavity chambers.
[c] In a recent international comparison total correction of 2.0% was used, consisting of +0.3 percent stopping power correction, 1.7 percent for wall absorption and lack of electronic equilibrium, the mean wall absorption correction, taking due account of the curvature of the cylindrical wall, being about 1.25 percent.
[d] Value obtained using Bakker-Segré I values and the Spencer-Attix modification for cbamber size.
[e] From ICRU Report (1959).
[f] These values were determined for a beam incident at approximately 45° to the axis of tbe cylinder. These numbers give the correction for attenuation of the gamma ray beam from the outer wall to the mean position of orgin of the electrons producing the ionization in the cavity.
[g] This comparison was done with a small cobalt-60 and a small cesium-137 source in which the scattering should be minimal.
[h] A weighted mean of the beam calibration data from two cbambers is used.

TABLE IIA7. Pressurized-air chambers

Country	Institution	Radiation range, Mev	Pressure atmos.	Plate separation, cm	Compared with	Reference
Japan	Electro Technical Laboratory, Tokyo.	0.2 to 0.8	Up to 10	40		
U.S.A.	NBS, Washington, D.C.	0.4 to 1.3	Up to 12	44	NBS cavity chambers.	Wyckoff (1960).
U.S.S.R.	Institute of D. I. Mendeleev, Leningrad.	0.25 to 3.0	Up to 20	40		Aglintsev and Ostromukhova (1959, 1961).

fortunately, the calibrations of most ionization chambers depend upon the x-ray beam parameters, maximum photon energy (E_{max}), filtration and diameter, so that a complete empirical calibration program entails the investigation of effects caused by many changes in experimental conditions.

There is one ionization chamber, the quantameter (fig. IIA2) (Wilson, 1957), which does not suffer from these defects. It samples ionization at several depths in a copper medium so that the total ionization current is proportional to the area under a copper transition curve. (The last air cavity is considerably larger, to compensate for transmitted energy.) It may be shown by

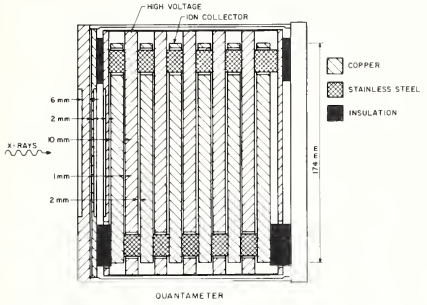

FIGURE IIA2. *Schematic cross section of the quantameter.*

Bragg-Gray cavity ionization theory that this quantity is directly proportional to the energy absorbed in the copper medium, and hence to the incident energy. The quantameter is filled with argon (to reduce ion recombination) to a pressure of 800 mm of Hg (at 20 °C) and with a small admixture of carbon dioxide, to reduce gas multiplication. The quantameter was designed for use above 300 Mev, and at these energies its calibration is independent of the beam parameters to a good approximation. The quantameter response is proportional to the calorimeter response to the extent that both the average electron stopping power ratio and the fraction of energy escaping from the chamber are independent of E_{max}. It corrects for escaping photon and electron energy, but not for energy carried away by neutrons, which introduces an error of a few tenths of one percent. Furthermore, its calibration can be predicted theoretically from knowledge of the chamber dimensions, the energy required to produce an ion pair, and the average stopping power ratio (Komar and Kruglov, 1960). The theoretically calibrated quantameter has been used as an absolute device to calibrate other ionization chambers, and these calibrations have been experimentally verified over a limited range of energies.

c. *Transfer instruments.* Measurements of the TBE have been used to calibrate the four ionization chambers shown in cross section in figure IIA3, each labelled by the name of the institute

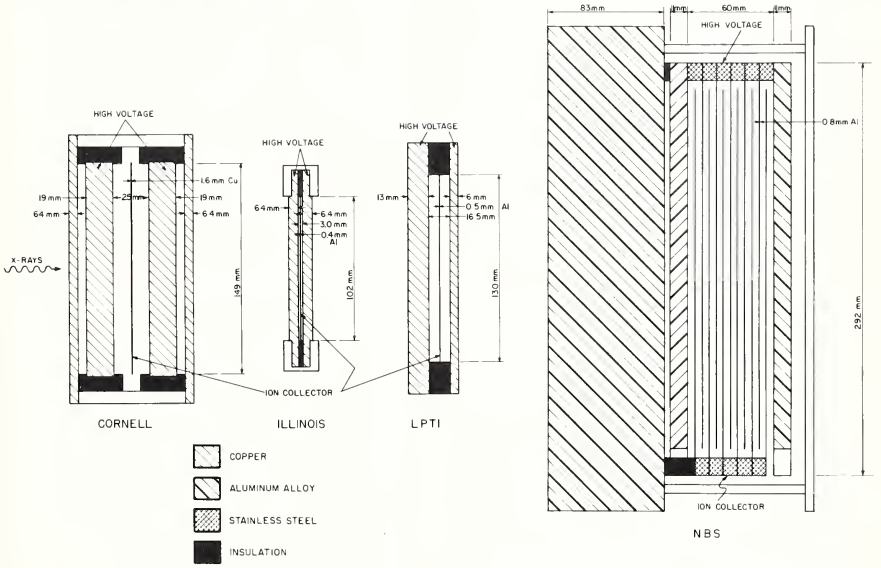

FIGURE IIA3. *Schematic cross sections of the Cornell (Cornell University), Illinois (Univ. of Illinois),* LPTI *(Leningrad Institute of Physics and Technology), and* NBS *(United States National Bureau of Standards) ionization chambers.*

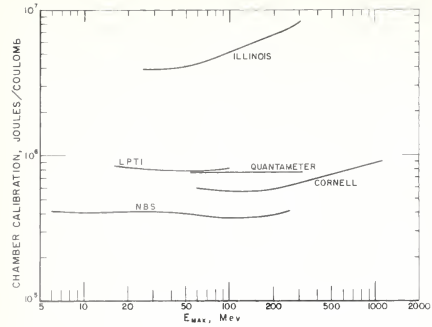

FIGURE IIA4. *Calibration of the Cornell, Illinois,* LPTI, *and* NBS *ionization chambers at 20 °C and 760 mm of* Hg, *and of the quantameter filled with argon to a pressure of 800 mm of* Hg *at 20 °C.*

(Loeffler, Palfrey, and Tautfest, 1959; Pruitt and Domen, 1962; De Wire, 1959; Oakley and Walker, 1955; Edwards and Kerst, 1953; Komar and Kruglov, 1960; Fuller and Hayward, 1961; Leiss, Pruitt, and Schrack, 1958; Pruitt and Domen, 1962; Pruitt and Pohlit, 1960; Wilson, 1957).

where it was first constructed and calibrated. Each of these chambers is of the parallel plate variety, intended for use in x-ray beams of small diameter. Three have copper walls, and the fourth (NBS) has walls of an aluminium alloy (nominally 93.4 percent Al, 4.5 percent Cu, 1.5 percent Mg, and 0.6 percent Mn). All are air filled and open to the atmosphere. Each of these four chambers samples the ionization behind a front wall whose thickness was chosen to reduce the variation of the calibration with E_{max} in the energy range for which it was intended.

The experimental calibration data of these four chambers have been computed in terms of the number of joules of incident energy required to produce one coulomb of ionization charge when measured in air at 20 °C and 760 mm of mercury.

The uncertainties of these calibrations are in the range from 1 to 3 percent and result from a variety of sources, but if these sets of calibrations are plotted as a function of E_{max}, it is possible to fit each set with a smooth curve which passes through almost all of the points to within the quoted error. These curves are shown in figure IIA4. In particular, the quantameter calibration data can be fitted with a straight line of zero slope to within the quoted errors, indicating that no change with E_{max} has been detected between 53 and 315 Mev. Also, it was found that calculated and measured values of the quantameter calibration are in excellent agreement.

The calibrations of the Cornell, Illinois, LPTI, and NBS ionization chambers depend upon the filtration and diameter of the x-ray beam. The variation with filtration arises because these chambers, unlike calorimeters, are sensitive to the photon spectral distribution, as shown by the fact that the relevant curves of figure IIA4 are not flat. The variation with diameter occurs because a fraction of the incident energy scattered

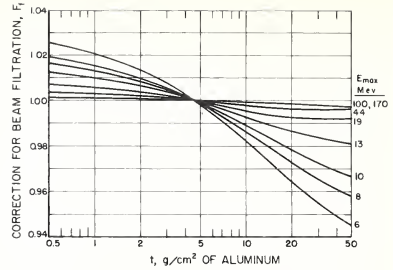

FIGURE IIA5. *Correction factor of* NBS *chamber calibration for a filtration of* t *g/cm² of aluminium relative to calibration for a filtration of 4.5 g/cm² of aluminium.*

in the front wall escapes from the chamber edges without producing ionization in the cavity, and this fraction increases with increasing diameter.

The variation with filtration has been studied for the NBS chamber by calculating the response to monoenergetic x rays, using the bremstrahlung data of figure IIA4 along with the results of additional measurements with Cs^{137} and Co^{60} γ rays and lower energy x rays (Pruitt and Domen, 1962). The results obtained for aluminium filters are shown in figure IIA5, where F_t is the ratio of the calibration in a beam filtered by t g/cm² of aluminium to that in a beam filtered by 4.5 g/cm² of aluminium (the filtration used for the NBS data of fig. IIA4). This curve shows that appreciable changes in the calibration may be expected only if E_{max} is less than about 20 Mev.

The Cornell, Illinois, and LPTI chambers will exhibit the same general type of variation with beam filtration, a variation which becomes less significant at high E_{max}. The quantameter calibration, on the other hand, should be independent of filtration because its calibration curve is flat. This conclusion must break down at some value of $E_{max}<53$ Mev (the lowest experimental calibration in fig. IIA4) but the point at which the calibration factor begins to rise has not yet been determined.

The variation with beam diameter may be obtained from measurements of the relative response of the chamber to a small diameter beam incident at different radii on the chamber face. Measurements of the response to a small diameter beam have been made with the Illinois, LPTI, and NBS chambers, and the results obtained at $E_{max}=85$ Mev for the LPTI chamber (Komar and Kruglov, 1960) and $E_{max}=90$ Mev for the other two (Pruitt and Domen, 1962) are shown in figure IIA6 where r is the radius at which the beam is incident. The change in calibration with beam diameter for a large-diameter centered beam is obtained from such curves by taking into account the variation of beam intensity with radius. The predicted results for the NBS chamber at several energies are shown in figure IIA7 for beams of uniform intensity. The magnitude of the effect decreases as E_{max} is increased.

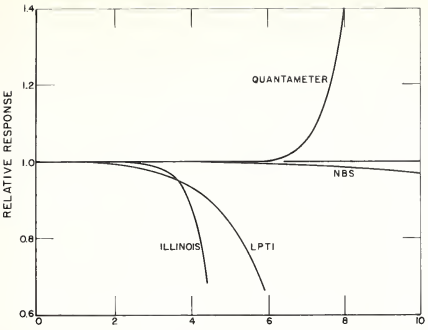

FIGURE IIA6. *Relative response of the Illinois,* LPTI, *and* NBS *ionization chambers and the quantameter to a small-diameter x-ray beam incident at radius* r.

The relative response of the quantameter to a small beam incident at different radii is also shown in figure IIA6 for $E'_{max}=85$ Mev (Komar and Kruglov, 1960). The long flat portion of their curve results from the contribution of the peripheral sensitive volumes which compensate for escaping side-scattered radiation.

Different copies of the same chamber may show differences in calibration. These arise from small variations in dimensions and front wall composition, but experience has shown (DeWire, 1959; Pruitt, Allisy, Joyet, Pohlit, Tubiana, and Zupančič, 1962) that with careful quality control the calibrations of two similar chambers will be the same to within 1 percent. More accurate knowledge of these differences can always be obtained by direct experimental comparison with the original.

B. Measurements of Neutron Flux Density and Neutron Sources

A neutron radiation field may now be described in terms of two alternative concepts. The first is kerma.[10] The second uses neutron flux density, neutron spectrum, and angular distribution (polarization will be ignored in this discussion). In this section of the report the latter approach, which is the traditional approach of neutron physics, will be employed. It should be emphasized that from the information of the type given here, kerma can be calculated if the appropriate neutron cross sections are known.

Neutron flux density information is frequently obtained through knowledge of the strength of neutron sources. The strengths of neutron sources, especially small sources such as radioactive neutron sources and accelerator targets, are customarily expressed as total neutron emission rate in neutrons per second.

The object of this section is to discuss methods

[10] For explanation of terms see appendix 1 of this report.

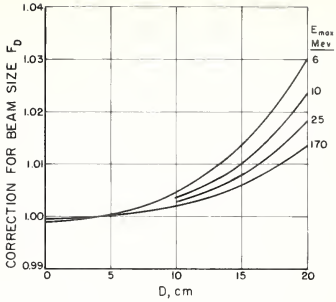

FIGURE IIA7. *Correction factor of* NBS *chamber calibration in a beam of diameter* D *and uniform intensity relative to calibration in a 42 mm diameter x-ray beam.*

of measurement, to review the status of international intercomparisons of measurements, and to make recommendations regarding (1) preferred methods of measurement, (2) possible improvements in measurement techniques, (3) specific areas where further work is needed, and (4) encouragement of international comparisons where needed. A more complete discussion of some of these questions will be found in the report on "Measurement of Neutron Flux and Spectra for Physical and Biological Applications" of the National Committee on Radiation Protection and Measurements in the United States (NCRP 1960).

It is convenient to classify neutrons roughly according to energy. The boundaries between energy ranges, which depend upon the nuclear interaction processes involved, are not sharp. For convenience we shall use the following ranges: thermal neutrons, below cadmium cut off energy (approximately 0.5 ev); intermediate neutrons, cadmium cutoff energy to approximately 10 kev; fast neutrons, above approximately 10 kev.

1. Measurement of Neutron Flux Density

a. *Thermal neutrons*

(1) *Low flux densities*

The absolute measurement of thermal neutron flux density is usually carried out by observing the reaction rate of an element of known cross section. With precise knowledge of the thermal neutron cross sections, elements such as boron, manganese, and gold may serve as standards. To utilize a polyisotopic element such as boron, one must know the isotopic composition accurately. Gold foils are used widely owing to the fact that gold is monoisotopic and has a comparatively large capture cross section for thermal neutrons (98.8 ± 0.3 barns) (Hughes and Schwartz, 1958). The total measured reaction rate is always in part due to non-thermal neutrons. The reaction rate due to thermal neutrons alone may be obtained by means of the cadmium difference method. With gold

detectors it is not sufficient to assume the "1/v law" and use the cadmium difference method to calculate the neutron flux density from the thermal neutron cross section of gold; it is necessary to subtract the low but appreciable ($\sim$1 percent at 0.025 ev) contribution of the resonance cross section. Since the decay scheme of Au^{198} is well known, an absolute determination of the disintegration rate can be performed not only by the 4 pi-beta-counting method but also by a beta-gamma coincidence method (Mosburg and Murphey, 1961). The disintegration rate of Mn foils also may be measured by the 4 pi-beta-gamma coincidence technique with equivalent accuracy despite the complexity of the decay scheme (Axton, 1962). For absolute measurement of thermal neutron flux density manganese has the advantage of a much smaller resonance neutron correction. The B^{10} (n,α) reaction is also useful for absolute determination of thermal neutron flux density since the boron cross section is presumably the best known absorption cross section (755$\pm$2 barns) (Hughes and Schwartz, 1958), and it is strictly 1/v. The problem is in the absolute counting of the alpha particles from the boron disintegrations (De Juren and Rosenwasser, 1954a, 1954b). Recently detectors consisting of a boron layer on a solid-state detector have been developed at Oak Ridge and are available commercially.

In absolute determinations of thermal neutron flux, the depression of the thermal neutron flux density by the detector and the self-shielding effect in the detector should be considered as described in subsection IIB1a(3).

Using a "1/v" detector the measurement done in a thermal neutron flux density determines, in fact, the neutron density at a given point. The so-called "effective flux" is the product of the neutron density and a conventional velocity v_0 (2,200 m/sec, corresponding to the most probable velocity for a Maxwellian distribution at a temperature T_0=20.44 °C). If n is the density of thermal neutrons of various energy, the "effective flux," nv_0, is different from the actual average flux density in the Maxwellian distribution at the temperature T

$$n\bar{v}=\int_0^\infty n(v)v\,dv=(2/\sqrt{\pi})nv_0\sqrt{\frac{T}{T_0}}=1.128nv_0\sqrt{\frac{T}{T_0}}.$$

Direct measurement of the average flux density involves larger uncertainty than determination of nv_0, in view of the difficulty of obtaining exact information about the energy spectrum of a low thermal neutron flux density in a moderator. The most convenient way is to assume that the spectrum is actually Maxwellian with a small $1/E$ flux density component added to the high energy tail of the Maxwellian (above around 0.1 ev) and then to determine the two parameters involved, namely the temperature characteristic of the distribution and the relative contribution of the $1/E$ component. One must also specify the extension in energy, generally the cut-off energy for a stated thickness of cadmium (cf. Westcott et al., 1958).

For comparison of thermal neutron fluxes, measurements of induced activity of a foil irradiated in the fluxes to be compared are most convenient and reliable. In order to reveal all possible errors, the induced activity of the foil should be measured in both of the laboratories taking part in the comparison. Therefore, the half-life of the induced activity should be at least a few days. Au^{198}, which has a half-life of 2.696 days for the induced activity, is preferable to copper for the purpose of an intercomparison because of the presence of two isotopes Cu^{63} (69.1 percent) and Cu^{65} (30.9 percent), with short half-lives (12.8 hours for Cu^{64} and 5.15 min for Cu^{66}). For absolute measurements the absorption cross section of copper for thermal neutrons is small and not well enough known (4.5$\pm$0.1 barns for Cu^{63} and 2.2$\pm$0.2 barns for Cu^{65}) (Hughes and Schwartz, 1958), and the decay scheme of Cu^{64} is complex.

Several comparisons of thermal neutron fluxes have been performed between laboratories as summarized in table IIB1.

Recommendations.

(i) Comparisons of standard neutron flux density measurements between national laboratories using the gold foil method or other adequate methods should be encouraged on a wider basis than has occurred heretofore.

(ii) Work on precise determinations of thermal neutron cross section and decay schemes should be encouraged for some isotopes (for example, the absorption cross section of manganese, and the internal conversion coefficient of the 412-kev gamma rays from Hg^{198} following the decay of Au^{198}), which are used as standards in thermal-neutron flux-density measurements.

(iii) In view of the connection with flux-density measurements in reactors, investigations should be made to obtain more precise descriptions of the standard thermal-neutron flux densities.

(2) *High flux densities*

The special conditions in fields with high neutron flux density, and the strong ionizing radiation associated in most cases, make a direct absolute measurement of thermal neutron flux density more difficult and restrict the applicability of the methods given above. Accordingly direct registration of boron, lithium or fission particles by means of ion-chambers and scintillation- or semi-conducting detectors is not possible. When using activated detectors one must take care that the radioisotope produced, if it has a large capture cross section, not be reduced by double capture in the case of long exposure to a strong neutron field. For example Au^{198} has a peak cross section of 26,000 barns, making double capture probable. The purity of the detector material must be very good, especially since impurities building long-lived activities should not be present. In a strong density gradient, flux anisotropy effects must be considered.

TABLE IIB1. *Intercomparisons of thermal neutron flux density measurements*

Laboratory No. 1	Laboratory No. 2	No. 1 Absolute method and quoted error	No. 2 Absolute metbod and quoted error	Intercomparison method	Ratio R[a] of intercompari-son	Uncer-tainty of intercom-parison	Intercomparison reference
Aktiebolaget Atomenergi, Stockholm, Sweden (Larsson).	JENER, Kjeller, Norway (Grime-land).	Activation of Au foils in thermal column, absolute activity by β-γ coincidence method, $\pm 2\%$.	Activation of NaI crystals and 4π-scintillation counting of induced activity.	Activation of Au foils from Sweden together with NaI crystals at Kjeller.	0.989	$\pm 2\%$	Unpuhlished, 1953.
AERE, Harwell England (Littler, Lockett).	C.E.A., France (Cohen).	Beta counting of Na^{24}, Mn^{56} and Co^{60}, $\pm 3\%$.	Beta activity of Mn^{56} by 4π-counting $\pm 4\%$.	Counting of Cu foils at Cbatillon.	1.06	$\pm 3\%$	Littler and Lock-ett, 1962.
NBS, Washington, D.C., U.S.A. (DeJuren).	Oak Ridge, Tenn., U.S.A. (Klema, Ritchie).	Absolute counting of I^{126} (n,α) re-action, $\pm 2\%$.	β-γ coincidence counting of Au foils activated in standard graphite pile.	End-window beta counting of Au foils.	0.98	$\pm 2.5\%$	DeJuren and Rosenwasser, 1954b.
NBS, Washington, D.C., U.S.A. (DeJuren).	C.E.A., France (Cohen).	----do----	Beta activity of Mn^{56} by 4π-counting, $\pm 4\%$.	4π-counting of thick Cu foils.	0.968	$\pm 1.5\%$	Murphey and Cbin, 1962.
NBS, Washington, D.C., U.S.A. (Mosburg).	Electrotechnical Laboratory, Tokyo, Japan (Teranishi, Michikawa).	Activation of Au foils, absolute activity by 4π β-γ coincidence method, $\pm 1.5\%$.	Activation of Au foils in standard graphite pile, absolute activity by 4π β-γ coinci-dence method, $\pm 1.9\%$.	Exchange of activated Au foils and $4\pi\beta$-counting at NBS and ETL.	0.986 (NBS) 0.994 (ETL)	$\pm 1.5\%$	Do.
NBS, Washington, D.C., U.S.A. (Chin).	NPL, Teddington, U.K. (Axton).	----do----	Activation of Gold foils, absolute activity by 4π β-γ coincidence.	Exchange of activated Au foils and 4π β-counting.	0.983 (0.987) mod	----------	Do.

[a] $R = \frac{\text{value determined for given arbitrary thermal neutron flux density by laboratory No. 1}}{\text{value determined for given arbitrary thermal neutron flux density by laboratory No. 2}}$, each value based on the absolute flux determination of the particular laboratory.

On the other hand, in high fluxes only a little detector substance is needed, so that the self-shielding and flux depression described in subsection IIB1a(3) become negligible. For a direct absolute determination of the activity of the sample by counting, it may be preferable to use an element with a small capture cross section. A negligible resonance-activation is usually associated with this, so that a Cd-measurement is not needed. Na^{23} seems to be suitable for accurate absolute measurements (Littler and Lockett, 1952; Wolf, 1961). The most recent value for capture cross section, 531 ± 8 mb related to the value of 98.7 barns for Au^{197} (Wolf, 1961), differs considerably from the Brookhaven compilation value for the absorption cross section, 505 ± 10 mb (Hughes and Schwartz, 1958), but not from the activation cross section of 536 ± 10 mb given in the same reference. A further independent determination may be desirable.

Wire made of spectroscopically pure Co^{59} from Johnson and Matthey, London, with diameters 0.005 in., 0.018 in. and 0.025 in. with a very good uniformity are used successfully at Chalk River (Jervis, 1957) while Euratom uses foils from the same producer with an 1/10 mm thickness. For Co^{59} a cross section of 38.0 ± 0.5 barns has been reported (Wolf, 1961), compared with 36.3 ± 1.5 barns from Brookhaven compilation and 38.0 ± 0.7 barns from Euratom. Better accuracy in the knowledge of the cross section is desirable. Also the purity of the cobalt does not seem to be satisfactory. The use of the monoisotopic Sc^{45}, cross section 28.3 ± 0.7 barns, has been reported (Wolf, 1961).

For use of elements with a larger capture cross section, the detector must be made very thin for a direct counting. Gold samples of 100 and 300 $\mu g/cm^2$, evaporated on plastics have been found suitable (Stephens et al., 1961). If the activity is too great for direct counting the sample may be put into solution and an aliquot calibrated by absolute counting, or the dilute solution may be directly irradiated.

In many cases indirect methods may be used to measure a neutron field known at one location by absolute calibration. The requirements for a single kind of distintegration, on the monoisotopic constitution, and on the purity of the sample material are not so high. Tungsten cables, made of 7 wires, each 0.006 in. diameter, nickel and manganese-nickel alloys with 10 percent nickel in form of wires, 0.02 in. diameter (Abson et al., 1958) and in form of foils with a thickness of 100 mg/cm^2 (Stephens et al., 1961) have been used for fluxes up to 10^{15} neutrons/cm^2 sec. Copper foils also are suitable, selectively counting the Cu^{64} annihilation radiation with a coincidence method (Maier-Leibnitz, 1961). The fission process has been used by measuring the fission products outside the reactor. In one of the experiments the rare gaseous fission products from a little probe were transported outside of the reactor by a gas current and measured in a gas ion chamber (Koch et al., 1958; Stephenson, 1958). Another method uses a thin sample of fissile material surrounded by plastic foils. The activity of the fission particles contained in the foils is measured. Another possible method is measurement of changes in isotopic abundance of materials.

Accuracies of about one percent in the neutron flux density have been obtained by measuring calorimetrically the heat produced in a sample. Thermocouples are used for temperature indication. With 4 percent B^{10} in $CaSO_4$ a thermocouple voltage of 3 mv corresponding to a 10 °C temperature difference and to an absorption of 0.1 watt was reached in a field of 10^{12} neutrons/

cm^2 sec. Only 2 percent of this heat originated from the gamma-radiation (Jaques et al., 1953; Abson et al., 1958). An arrangement with one mg U^{235} in a sample consisting of an uranium-aluminum sinter-alloy uses the greater energy of fission (Schilling, 1960).

(3) *Flux perturbation (self-shielding and flux depression) corrections*

The inner layers of a detecting foil placed in a uniform neutron field are shielded by the outer layers (the self-shielding effect); in addition the foil as a whole behaves as a negative source which depresses the neutron flux density in the neighborhood of the foil (the flux depression effect). The observed foil activity must therefore be increased to yield the true neutron flux density in the absence of the detector.

On the basis of first order diffusion theory, Bothe (1943) calculated the ratio of $\bar{\varphi}$, the average flux density in a foil of radius a and thickness t, to φ_0, the initially unperturbed flux density as:

$$\bar{\varphi}/\varphi_0=\frac{\frac{1}{\tau}\left[\frac{1}{2}-E_3(\tau)\right]}{1+\left[\frac{1}{2}-E_3(\tau)\right]\left(\frac{a}{\lambda_s}\cdot\frac{3L}{2a+3L}-1\right)} \quad \text{for } a>>\lambda_s$$

$$=\frac{\frac{1}{\tau}\left[\frac{1}{2}-E_3(\tau)\right]}{1+\left[\frac{1}{2}-E_3(\tau)\right](0.46a/\lambda_s)} \quad \text{for } a<<\lambda_s,$$

where $\tau=t\Sigma_a^D$,

Σ_a^D is the disappearance cross section per cm^3 of foil,

λ_s is the scattering mean free path of the neutrons in the medium,

L is their diffusion length given by $L=\frac{1}{\sqrt{3\Sigma_s\Sigma_a}}$

Σ_a, Σ_s are the absorption and scattering cross sections of the medium surrounding the foil,

$E_3(\tau)$ is the third order exponential integral defined by $E_n(x)=\int_1^\infty \frac{e^{-xu}}{u^n}du$ where $n=3$ and $x=\tau$.

The factor $\frac{1}{\tau}\left[\frac{1}{2}-E_3(\tau)\right]$ represents the self-shielding effect while the remainder of the equation accounts for the flux depression,

$\frac{1}{\tau}\left[\frac{1}{2}-E_3(\tau)\right]$ may be written as

$$\frac{1}{2\tau}\left[1-e^{-\tau}(1-\tau)-\tau^2\int_\tau^\infty \frac{e^{-s}}{s}ds\right].$$

The calculation was made for a spherical detector and then modified to apply to plane foils. Bothe's measurements on thin dysprosium foils in aluminum supported his calculations within experimental error.

Tittle (1951) applying later values for the medium constants to Bothe's original data concluded that better agreement was obtained if Bothe's original sphere formula were used (corresponds to replacing a in the above formula by $\frac{3}{2}a$), and λ_s replaced by λ_{tr}, the transport mean free path. $\lambda_{tr}=\lambda_s/(1-\bar{\mu})$ where $\bar{\mu}$ is obtained by averaging the cosine of the scattering angle over the neutron scattering angular distribution.

The self-shielding factor $\frac{1}{\tau}\left[\frac{1}{2}-E_3(\tau)\right]$ is probably low, since it was calculated for foils of infinite radius, but the error is negligible except for foils of very small radius (Sola, 1960).

An alternative correction for very thin foils was derived by Skyrme (1943) on the basis of one-speed transport theory,

$$\bar{\varphi}/\varphi_0=1-\tau\left[\frac{1}{2}E_1(\tau)+A(g)+D_1-D_1'\right] \text{ for } \tau<1.$$

$A(g)$ is a function of $g=a\Sigma_a$ and is presented graphically by Skyrme. For $g>\sim 2$, $A(g)=\frac{3}{4}$. Skyrme also gives values for D_1, a function of the constants of the medium, and indicates that D_1' is negligible compared with D_1.

A comparison between the Bothe and Skyrme formula and a more accurate solution of the transport equation has been published by Ritchie and Eldridge (1960) (see also NCRP, 1960). They suggest the following equation for $a\neq\infty$.

$$\bar{\varphi}/\varphi_0=\frac{\frac{1}{\tau}\left[\frac{1}{2}-E_3(\tau)\right]}{1+\left[\frac{1}{2}-E_3(\tau)\right]\left[\frac{3L}{2\lambda}S\left(\frac{2a}{L}\right)-K\left(\frac{2a}{\lambda},\gamma\right)\right]}$$

where the functions $S(x)=1-\frac{4}{\pi}\int_0^1\sqrt{1-t^2}e^{-xt}dt$ and $K(x,\gamma)$ are presented graphically in figures IIB1 and IIB2. The quantity γ is the ratio of scattering to total cross section in the medium.

Ritchie and Eldridge compared the predictions of the theories with experimental results by Klema and Ritchie (1952) and by Thompson (1956); the measurements concerned gold and indium foils in graphite, where the flux depression effect is in any case small compared with the self-shielding effect. They concluded that the available data were insufficient to judge the relative accuracy of the theories.

To test the prediction of the Bothe and Skyrme theories, Sola measured a large number of gold foils of different radius and thickness in graphite. The data are reproduced in table IIB2.

A more comprehensive treatment of the flux perturbation has recently been published by Dalton and Osborn (1961), and some corrections and discussions of their papers by Ritchie and Dalton (1961). Meister (1958) has used Ra-Be(α,n) sources with paraffin or graphite

moderators and indium foil detectors, and has developed a theory to compare with his experiment. The method is based on the solution of the transport equation for specific cases by means of a digital computer; nonisotropic neutron scattering in the medium, and scattering in the foil are permitted, all dimensions of the detector may be varied, and the neutron flux density may be mapped at points inside and outside the detector.

Scattering in the detector is shown to be unimportant, but nonisotropic scattering in the medium may involve errror. For example, differences of 3 percent are obtained for 5 mil (127μm) gold foils in water, depending on the value taken for $\overline{\mu}$, the average cosine of the scattering angle. Typical results are shown in figures IIB3 to IIB6 for coin- and wire-shaped detectors in water and graphite. These plots are valid provided that

$$1.0 \leq \Sigma_a^D \leq 10.0 \text{ cm}^{-1} \text{ and } \Sigma_s^D << \Sigma_a^D.$$

The value for $\overline{\mu}$ was taken as zero for these plots, so the results may be up to 3 percent low for thick foils or wires in water. Examples of flux density mapping inside and outside detector foils are reproduced in figures IIB7 and IIB8. They illustrate the undesirability of attempting to separate the perturbation into separate self-shielding and flux depression effects.

Measurements of flux depression and self-shielding for gold foils of 0.5 cm to 3 cm diameter in

TABLE IIB2. *Flux perturbation (flux depression plus self shielding) for circular gold foils in graphite*

Perturbation factor for various foil thicknesses								
μm	25.4	50.8	76.2	101.6	127	254	481	508
in.	.001	.002	.003	.004	.005	.010	.015	.020
Foil radius ½ in. (1.27 cm)								
Measured*	0.945	0.916	0.892	0.870	0.850	0.775	0.712	0.656
Bothe**	.965	.931	.907	.883	.860	.773	.708	.647
Skyrme	.958	.926	.896	.868	.843	.727	.624	.514
Ritchie and Eldridge	.950	.914	.880	.851	.825	.718	.639	.575
Dalton and Osborn	.934	.894	.862	.834	.811	.754	------	------
Foil radius ¼ in. (0.635 cm)								
Measured*	0.951	0.925	0.905	0.883	0.864	0.788	0.733	0.683
Bothe**	.968	.936	.915	.893	.872	.792	.731	.675
Skyrme	.962	.933	.907	.883	.862	.763	.678	.587
Ritchie and Eldridge	.958	.927	.899	.875	.852	.761	.692	.634
Dalton and Osborn	.950	.912	.883	.859	.838	.781	------	------
Foil radius ⅛ in. (0.318 cm)								
Measured*	0.957	0.931	0.910	0.890	0.872	0.799	0.747	0.704
Bothe**	.969	.938	.917	.898	.876	.798	.740	.681
Skyrme	.964	.936	.912	.890	.870	.780	.701	.620
Ritchie and Eldridge	.962	.934	.909	.888	.868	.786	.722	.668
Dalton and Osborn	.960	.928	.903	.881	.862	.804	------	------
Foil radius 1/16 in. (0.159 cm)								
Measured*	0.963	0.936	0.914	0.895	0.878	0.811	0.762	0.726
Bothe**	.970	.939	.919	.898	.878	.802	.744	.689
Skyrme	.966	.937	.913	.891	.872	.784	.708	.628
Ritchie and Eldridge	.968	.947	.928	.911	.896	.834	.784	.740
Dalton and Osborn	.966	.938	.914	.893	.876	.820	------	------

*Measurements are by Sola (1960). The total standard deviations are less than 2 percent.
**Modified by Tittle.

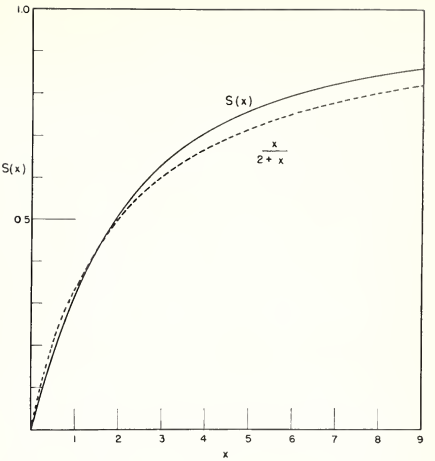

FIGURE IIB1. *The Skyrme function* $S(x) = 1 - (4/\pi) \int_0^1 e^{-xt}\sqrt{1-t^2}dt$. *(Ritchie and Eldridge, 1960) and an approximate function,* $\frac{x}{2+x}$.

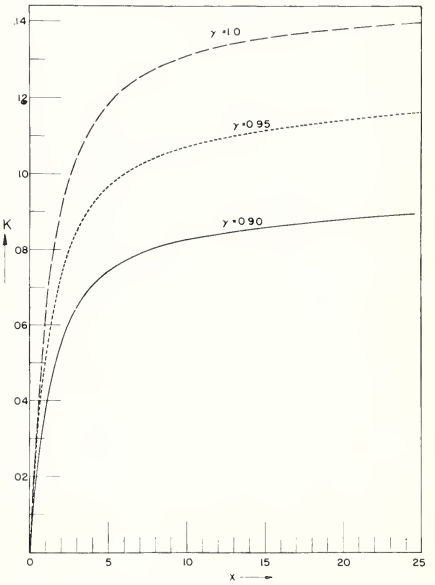

FIGURE IIB2. *The transport correction term,* $K(x,\gamma)$, *versus* x.
(Ritchie and Eldridge, 1960).

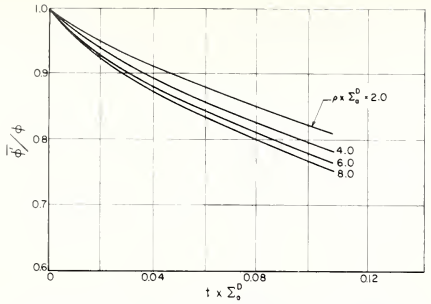

FIGURE IIB3. *The average normalized flux density in a coin-shaped detector in graphite for various radii ρ and thickness* t.

(Dalton and Osborn, 1961).

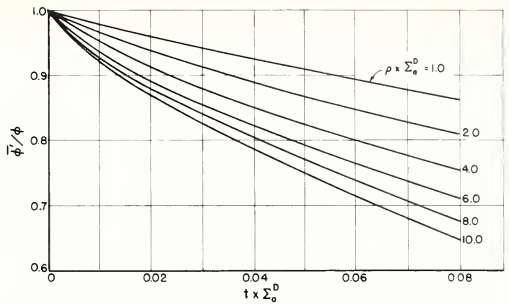

FIGURE IIB4. *The average normalized flux density in a coin-shaped detector in water for various radii ρ and thickness* t.

(Dalton and Osborn, 1961).

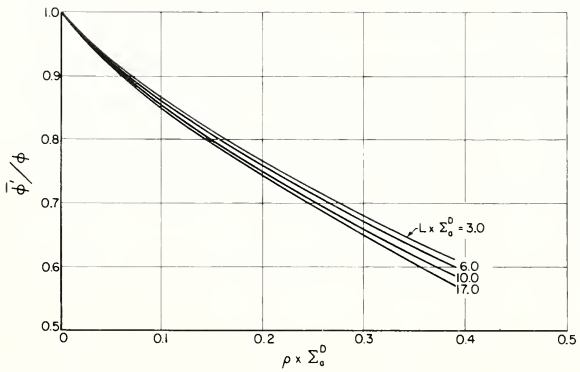

FIGURE IIB5. *The average normalized flux density in a wire-shaped detector in water for various lengths* L *and radii ρ.*

(Dalton and Osborn, 1961).

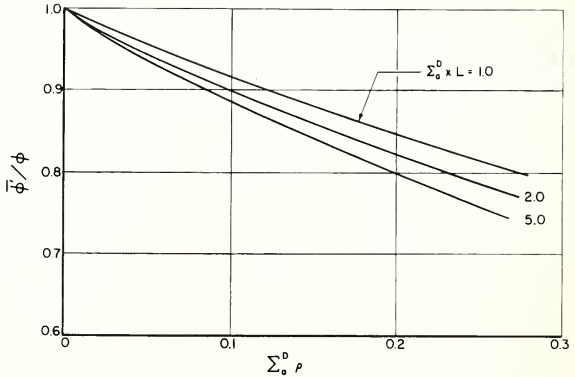

FIGURE IIB6. *The average normalized flux density in a wire-shaped detector in graphite for various radii ρ and lengths* L.

(Dalton and Osborn, 1961).

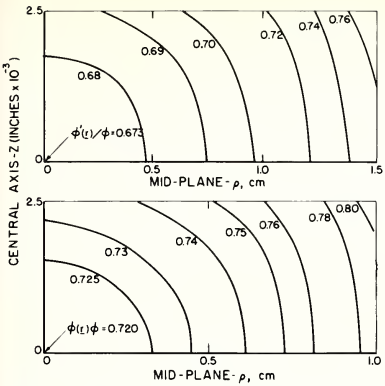

FIGURE IIB7 a and b. *A map of the normalized flux density within a coin-shaped gold detector in water.*

(a) Radius of 1.5 cm and thickness of 5 mils (127 μm). (Dalton and Osborn, 1961). (b) Radius of 1.0 cm and thickness of 5 mils (127 μm). (Dalton and Osborn, 1961).

water have been made recently by Zobel (1961) to test the various theories discussed here. Best agreement is obtained for the Ritchie and Eldridge calculation and for the Dalton and Osborn calculation with isotropic scattering. Data for the case of 2-cm diameter foils is shown in figure IIB9. More comprehensive experimental data are required to judge the recent calculations of flux perturbation by detector foils by Ritchie and Eldridge (1960) and Dalton and Osborn (1961).

(4) *Choice of effective disappearance cross section*

In the case where flux depression is small, an approximate treatment may be used to evaluate self-shielding. A one-speed treatment is used where a careful choice must be made for the absorption cross section for use in evaluating τ. An approximate procedure is to use the cross section applicable to the mean velocity $\bar{v}$ of the Maxwellian spectrum, viz., $(\sqrt{\pi}/2)\sigma_0$ where σ_0 at room temperature is the customarily tabulated 2,200 m/sec cross section. However, as has been pointed out (Hanna, 1961; Zahn, 1937), a thin 1/v detector reduces a normally incident Maxwellian flux by the factor $(1-(\sqrt{\pi}/2)t\Sigma_a^D)$, but reduces the response of a thin 1/v detector to this flux by $(1-(2/\sqrt{\pi})t\Sigma_a^D)$, where t is thickness in cm and Σ_a^D is in cm^{-1}. It might be expected, therefore, that in calculating the flux perturbation correction factor for an isotropic Maxwellian neutron distribution, a cross section value of $(\sqrt{\pi}/2)\sigma_0$ should be used for calculating the flux depression, and one of $(2/\sqrt{\pi})\sigma_0$ for the activation depression.

The last two values are applicable only for the case of a very thin detector, and will reduce as the lower energy neutrons are preferentially absorbed and spectral hardening occurs.

For example, in calculating self-shielding effects

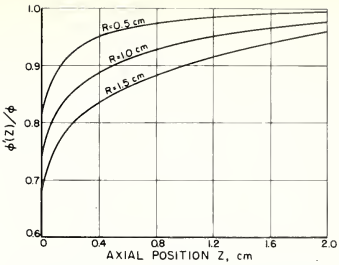

FIGURE IIB8. *A plot of the normalized flux densities along the central axis outside of a set of gold coin-shaped detectors of radius* R *in water, thickness of 5 mils (127 μm).* (Dalton and Osborn, 1961).

in gold foils used to calibrate the NBS standard thermal neutron flux, Mosburg (1961) used an integration method to calculate the average activity in a foil in a Maxwellian spectrum of neutrons. He showed that a value of 1.08 σ_0 was appropriate for the range of thickness used ($\tau \leq .09$). With thicker foils, this effective cross section would decrease as spectral hardening occurred within the foil.

(5) *Cadmium absorbers*

Thermal-neutron flux-density measurements are normally carried out in the presence of a non-thermal component of flux which is allowed for by cadmium difference experiments. The neutron flux density below the effective cadmium cut-off energy is obtained by subtraction of the activity obtained with the foil encased in a certain thickness of cadmium. The thickness of the cadmium cover should be stated because it affects the effective cadmium cut-off energy. Effective cut-off energies both for beam and for isotropic neutron fields have been published by Westcott et al., (1958), and by Hickman and Long (1961).

With non-1/v detectors, it is necessary to apply a correction factor, to the cadmium-covered activity for absorption of the resonance neutrons in the cadmium cover. This correction can be obtained either from computation of the absorption of resonance neutrons in the cadmium or from measurement of the attenuation of resonance neutrons in a further equal thickness of cadmium (Axton, 1962).

If the neutron spectrum is assumed to take the form of a Maxwellian distribution at temperature T_0 °Kelvin plus a non-thermal component proportional to dE/E which is cut off sharply near $5kT$, the cadmium ratio may be written

$$R_{Cd}(\delta)=\frac{\dfrac{F}{r\sqrt{\dfrac{T}{T_0}}}+G_t\dfrac{s_0}{g}}{f(\delta)\,G_t\left(\dfrac{s_0}{g}-W\right)+\dfrac{1}{K(\delta)}} \qquad \text{(IB1)}$$

(Walker et al., 1960)

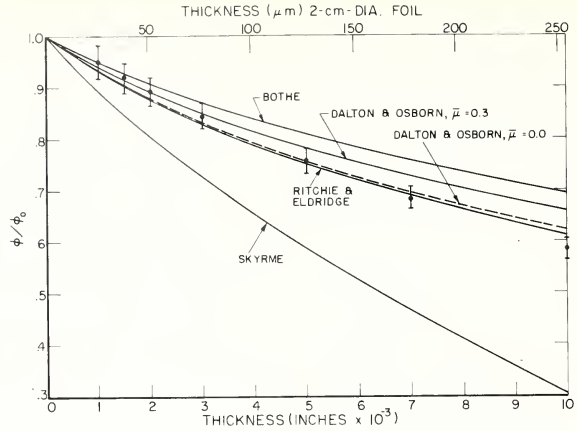

FIGURE IIB9. *Flux perturbation (flux depression and self-shielding) for gold foils in water.*

(Zobel, 1961).

where t is the thickness of the foil,

δ is the thickness of the cadmium cover,

$R_{Cd}(\delta)$ is the ratio of the activity produced in a bare foil to that produced in a foil covered with cadmium of thickness δ,

F is the thermal neutron flux perturbation factor,

r is the non-thermal flux parameter which is a measure of the relative importance of the dE/E component of the spectrum,

g and s_0 are functions of the resonance integral, and are a measure of the departure of the absorber cross section from 1/v law in the thermal and non-thermal energy regions, respectively. They are tabulated by Westcott (1960),

W is a small correction which arises when σ is not proportional to $g\sigma_0 v_0/v$ in the energy region between the dE/E cut-off and the cadmium cut-off energies,

$K(\delta)=4\sqrt{E_0/\pi E_{Cd}(\delta)}$ where $E_{Cd}(\delta)$ is the effective cut-off energy and $E_0=kT_e$,

G_t represents the attenuation due to self-shielding in a foil of thickness t of the resonance neutrons,

$f(\delta)$ represents the attenuation in a cadmium cover of thickness δ of the resonance neutrons.

The correction factor $F_{Cd}(\delta)$ is given by

$$F_{Cd}(\delta)=\frac{G_t\left(\frac{s_0}{g}\right)+1/K(\delta)}{f(\delta)G_t\left(\frac{s_0}{g}-W\right)+1/K(\delta)}$$

An approximate value $F_{Cd}(\delta)$ may be obtained experimentally as follows, from measurements of foil activity obtained with various thicknesses of cadmium. Note that $F_{Cd}(\delta)$ is not obtained directly from this measurement.

If $f(\delta)$ is small so that $f(2\delta)=f^2(\delta)$ one may write

$$\frac{f^2(\delta)G_t\left(\frac{s_0}{g}-W\right)+1/K(2\delta)}{f(\delta)G_t\left(\frac{s_0}{g}-W\right)+1/K(\delta)}=f(t) \qquad \text{(IB2)}$$

where $f(t)$ is the measured ratio of activities for a foil of thickness t. $f(\delta)$ may then be obtained from the equation if all the other quantities are known. G_t may be obtained from the equations of Roe (1954). Alternatively, G_t may be obtained from cadmium ratio measurements.

$R_{Cd}(\delta)$ is measured for very thin foil ($G_t=1$) and eq (IB1) is solved for $r\sqrt{\frac{T}{T_0}}$ using for $f(\delta)$ its approximate value $f(t)$. G_t may then be evaluated from eq (IB1) for a foil of thickness t and used in eq (IB2) to obtain a better value for $f(\delta)$. Eventually all the quantities involved are obtained by successive approximation. Martin (1955) obtained a value of 1.02 for $(1/f(t))$ for a gold foil.

(6) *Calculation of* $f(\delta)$

$f(\delta)$ is given approximately by the equation

$$f(\delta)=\frac{E_3(a)-E_3(a+b)}{\frac{1}{2}-E_3(a)} \qquad \text{(IB3)}$$

where $a=t\Sigma_{Foil}$ and $b=\delta\Sigma_{Cd}$.

Σ_{Foil} is the effective foil absorption cross section at the effective resonance energy. Σ_{Cd} is usually taken as the effective cadmium cross section for the capture of neutrons at the effective resonance energy. Some possible uncertainties are: (1) the choice of the effective energy (does this depend on foil thicknesses?); (2) the evaluation of the effective capture cross section for cadmium at this energy; (3) whether or not Σ_{Cd} should include a proportion of the scattering cross section (does

this proportion vary with t?); (4) whether or not K depends on foil thickness. For very small a eq (IB3) becomes $f(\delta)=E_2(b)$ as suggested by Walker et al., (1960). For very large a it becomes $f(\delta)=2E_3(b)$ which is the expression suggested by Tittle (1951). If b is small the equation becomes

$$f(\delta)=1-2b\frac{1-E_2(a)}{1-2E_3(a)}.$$

To satisfy experimental results (e.g., Martin 1955) with this equation, it is necessary to include some scattering in Σ_{Cd}. A theoretical calculation and further experimental results are needed to determine F_{Cd} for various cadmium thicknesses, foil thicknesses, materials and neutron spectral distributions.

b. *Intermediate energy neutrons*

(1) *Low flux densities.*

A simple approach to the measurement of neutron flux density is by use of a detector whose response is independent of energy. If the detector contains a material whose neutron cross section is sufficiently large so that all neutrons interact in the detector, then the efficiency is flat with energy since the probability of a neutron interaction is 100 percent. The efficiency of the detector, however, is in general less than 100 percent since not every interaction produces an event which is finally recorded. As long as the final detection probability is independent of the energy of the neutron causing the event, the detector's response is flat. An advantage of this method is that it does not depend upon precise knowledge of a neutron cross section, but requires only that the neutron cross section be large enough. These detectors are called "black" detectors since they absorb all neutrons incident upon them. The nuclear reactions commonly used for black detectors are the $B^{10}(n,\alpha)Li^7$ and the $Li^6(n,\alpha)H^3$ reactions. Both of these reactions have a large neutron reaction cross section extending from thermal neutron energies into the kilovolt neutron energy region. Both reactions produce charged particles which are readily detectable, and the boron reaction is followed by a 0.48 Mev gamma ray from an excited state of Li^7 in 94 percent of the cases which also may be detected. The flatness of response of detectors made of 10 g/cm^2 thickness of natural lithium, natural boron, Li^6 and B^{10} is shown in figure IIB10. As can be seen from the figure, the detection efficiency with separated isotopes is flat to considerably higher neutron energies than with the natural elements. The response of B^{10} and Li^6 detectors are essentially flat to 1 kev and the B^{10} detector is only down 3.4 percent in response at 10 kev. These detectors are well suited to low flux density neutron measurements because they tend to have high efficiencies.

Work has been done on suitable detectors containing boron and lithium because they are also useful as detectors for intermediate energy neutron time-of-flight systems where their high efficiency is very desirable. Unfortunately, most of these detectors are also efficient detectors of gamma rays, which are invariably present in neutron radiation fields.

A new approach with the same disadvantage of sensitivity to gamma rays may be carried out using a mixture of rare earths (gadolinium, europium, samarium) placed at the center of a big liquid scintillator tank. Such a detector should be black in the region of 10 kev because of the overlapping of extremely numerous neutron resonance levels.

(a) *Indirect detection method*

In this method a sample of B^{10} is placed in the neutron beam. Gamma rays following the reactions of neutrons with the B^{10} are observed with

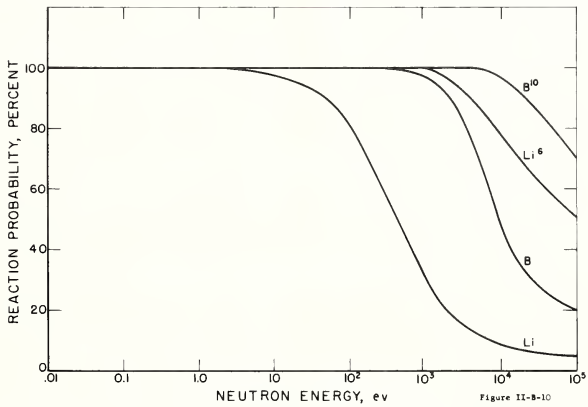

FIGURE IIB10. *Response of a 10 gram-cm^{-2} "black" detector as a function of energy.*

one or more shielded NaI crystals. By setting a differential pulse height selector or "window" on the 0.48 Mev gamma ray peak, other gamma rays can be discriminated against to some degree. Bollinger et al., (1957), report an estimated error of 0.5 percent but do not state the efficiency of the detector. Rae and Bowey (1953) reported an efficiency of 2.6 percent using a sample of amorphous B^{10} in a thin-walled aluminium cylinder 3 in. diameter by 1¼ in. deep viewed by two 1¾ in. diameter by 2 in. deep NaI scintillation crystals. The boron plate may be placed at an angle to the incident neutron beam to increase its effective thickness without loss of detection efficiency, and the efficiency may be improved by increasing the solid angle for detection of gamma rays. The instrument may be calibrated by placing it in a known thermal neutron flux density.

(b) *Direct detection method*

A number of methods have been developed for placing the lithium or boron directly in a scintillator. With these detectors efficiencies approaching 100 percent may be achieved at low neutron energies. However, the efficiency does not remain constant to as high energies as with a pure sample. Many kinds of scintillators have been used: inorganic crystals such as $Li^6I(Eu)$ (Schenck, 1953; Murray, 1958); boron-loaded liquids (Bollinger and Thomas, 1957); cerium-activated B^{10}-loaded scintillating glass (Bollinger et al., 1959), and cerium-activated Li^6-loaded scintillating glass (Firk et al., 1961). All of these detectors respond to gamma rays; however, the lithium-loaded scintillators can discriminate against moderate fields of low energy gamma rays (around 10 mR/hr) because of the 4.78 Mev of energy release in the $Li^6(n, \alpha)H^3$ reaction. The boron-loaded liquid scintillator assembly is efficient, but rather complex and requires considerable care in operation. The LiI(Eu) crystals have a rather slow decay time (1.2 μsec), require careful mounting, and the crystals available are rather small. Their energy resolution (the thermal neutron resolution is about 6–8 percent in pulse height) is improved by operation at liquid nitrogen temperatures. The glass scintillators are faster (decay time about 100 ns for Li^6 loading). While B^{10}-loaded glasses have a factor of 4.5 in their favor because of the larger cross section, the Li^6-loaded glasses have the advantages of better time resolution, better gamma-ray discrimination, ease of manufacture, and better pulse-height resolution. The α-particle and the Li^7 recoil with a total kinetic energy of 2.3 Mev contribute only 250 kev of equivalent electron energy in the boron glass. Either detector requires only simple associated electronics.

(2) *High flux densities*

The intermediate neutron energy range at high flux densities is difficult to investigate, even for relative measurements. It is always possible to restrict the methods to relative measurements and to calibrate the detector using absolute measurement in a thermal neutron flux or with a monoenergetic source of neutrons (for example, a Sb-Be (γ,n) neutron source).

A convenient solution in some cases is to determine the flux integrated over a broad energy spectrum and to know simultaneously the shape of the energy spectrum. For example, the flux density may be measured for all neutrons with an energy above the cadmium cut-off. The spectral shape is calculated from the configuration of the investigated medium (reactor lattice, etc.), or it is measured with the help of an open beam going outside of the medium. The measurements on an open beam are done on low fluxes and these measurements are relatively easy.

If one wishes specifically to do measurements at a location where the flux density is high, it is necessary to distinguish between two cases, according to the energy range of neutrons: (a) Neutron energy below several kev: corresponding roughly to the domain where neutron resonance detectors are useful. (b) Neutron energy between 1 and 50 kev: In this domain the energy is too low for the techniques available for fast neutrons and generally is too high for the resonance detectors.

(a) *Neutron energy below several kev*

Detectors are generally made from thin sheets on a metal or plastic (mylar or polystyrene) backing or even from thin foils without backing. The detector is thin enough (about 100 $\mu g/cm^2$) to reduce the neutron self-shielding corrections.

The activity is measured following an irradiation of the detector covered by cadmium. If desired, absolute measurements of the activity can be made. However, an absolute value of the flux density does not result from such a measurement, unless the activation cross section in the resonance spectrum is well known. If the activation cross section is not accurately known, only relative measurements can be made.

If one is trying to correlate the result of the measurement with fairly well defined neutron energy, useful nuclei are those having a single first resonance giving the main contribution (In, 1.46 ev; Au, 4.8 ev.; Co, 13 ev; Mn, 330 ev; Na, 2 kev).

It is also conceivable to restrict the measurements to the "effective integral" over all the intermediate neutron resonances.

(b) *Neutron energy between 1 and 50 kev*

A satisfactory solution does not exist today. Rough estimates only are feasible. For example, a foil detector may be covered with a sheet of 2 g/cm^2 of B^{10}, in order to perform an integral measurement in the energy domain under study without any contributions from the neutrons below 1 kev.

A thick iron shield provides a way to generate an "energy gate" around the mean value 25 kev

the iron cross section is very low just at this energy). If a black B^{10} detector (viewed by a NaI (Tl) crystal) is placed behind this shielding, its output will be largely due to neutrons of about 25 kev.

Activation of medium-weight nuclei in the energy domain under study gives low counting rates and is therefore difficult to use.

New techniques are certainly needed to improve measurement of intermediate energy neutrons.

c. *Fast neutrons*

(1) *Low flux densities*

Relatively accurate methods of absolute fast neutron flux density measurement do not exist, except for proton-recoil counters and telescopes and associated particle counting, which in general requires great care in use and well-defined sources or beams (see NCRP, 1960; Johnson, 1960). Associated particle counting can be used only with certain suitable reactions such as $H^2(d,n)He^3$ and $H^3(d,n)He^4$ with an ion accelerator, and requires great care in beam line-up and in the prevention of observation of neutrons from extraneous sources, such as the accelerator itself and diaphragms for the charged particle beam (when accelerating deuterons, any matter struck by the beam is a potential source of $H^2(d,n)He^3$ neutrons).

A relative or transfer instrument of wide applicability is the "long counter" of Hanson and McKibben (1947). In spite of the large size of this detector (length and diameter about 40 cm), the long counter is used widely because of its high efficiency for fast-neutron detection, its rather uniform energy response and its excellent discrimination against gamma radiation. Recently DePangher (1961) has proposed a revision of this instrument called the "precision long counter" of improved mechanical design and excellent reproducibility for neutron sensitivity (better than one percent).

Although this instrument has been calibrated absolutely versus energy with radioactive neutron sources (see fig. IIB11), unfortunately no careful calibration with methods such as the counter telescope and associated particle counting mentioned above has yet been carried out. The calibrations with radioactive neutron sources are not too meaningful because the neutrons are spread through a wide range of energies and because of large uncertainties in the number of neutrons below 1 Mev (De Pangher, 1959; Hess, 1957). The precision long counter is provided with a 1 gram Pu^{239}-Be (α,n) source of neutron emission rate about 10^6 neutrons/sec for day to day checks on sensitivity. To maintain calibration, it is essential that the emission rate of this source not change with time. In the future perhaps an Am^{241}-Be (α,n) source should be used for monitoring since most Pu^{239}-Be (α,n) sources have significant neutron emission growth rates which depend upon the purity of the plutonium.

Information on the energy response of long counters is presented in figure IIB11. The curve is based on data from Harwell (Allen and Ferguson, 1957) for one long counter and from Los Alamos (Bame, et al., 1957) for another long counter with accelerators. The points shown in figure IIB11 for radioactive neutron sources are shown at calculated values of the average energy for the sources based on measurements by moderation methods of determining neutron energy (DePangher, 1959). Calibration over a wide range of energies requires an accelerator with energies above 10 Mev such as the tandem accelerator or variable energy cyclotron. This energy range should extend from around 10 kev, to overlap the energy range of the "black" detector to about 20 Mev to determine the useful upper energy limit for the detector.

A careful calibration at several energies in several laboratories seems very desirable. Laboratories contemplating construction of a long counter should consider this standard design, since interlaboratory comparisons will be facilitated and one may expect to benefit from the energy calibrations recommended here. A

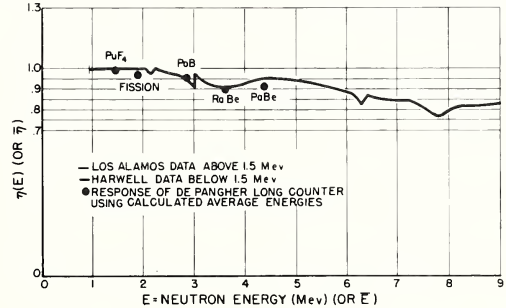

FIGURE IIB11. *Energy response of "long counters."*
The ordinate is the relative count rate for a given incident neutron flux density.

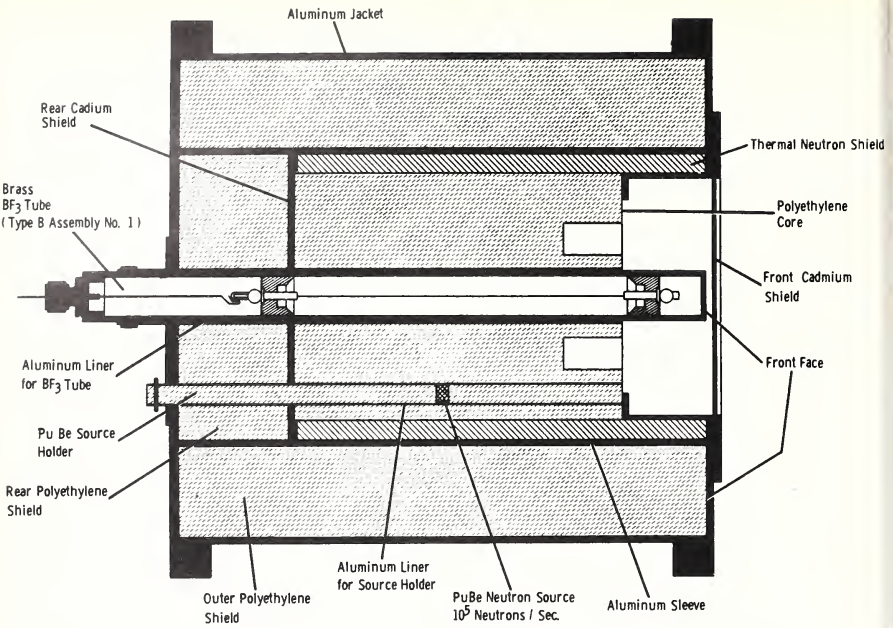

FIGURE IIB12. *Precision long counter of DePangher (1961).*
The length and diameter are each about 40 cm.

schematic diagram of the counter is shown in figure IIB12. Design drawings may be obtained by writing to W. C. Roesch, Hanford Laboratories, Richland, Washington, U.S.A.

The main features of the new counter compared to the Hanson-McKibben design are:

(a) use of polyethylene as the moderating material,
(b) a larger diameter BF_3 tube (1½ inches),
(c) a machineable thermal neutron shield of low-molecular weight polyethylene impregnated with 5.0 percent boron,
(d) a retractable one-gram Pu-Be (α,n) neutron source for the calibration of the BF_3 counter,
(e) extensive use of aluminium alloy for the confinement of the polyethylene,
(f) a larger cadmium shield on the front of the counter, and a rear cadmium shield instead of a rear B_2O_3 shield,
(g) an annular region instead of eight holes cut out of the central core to provide the augmentation of low energy neutron response.

To a good approximation the long counter acts as a point detector, with the effective center deeper in the counter the higher the neutron energy. For the DePangher long counter the relation between distance, c, in *cm* from the front face to the effective center is given approximately by the relation $c=7.8+1.1E$ where E is the neutron energy in Mev.

Recent developments in solid state counters indicate that these devices will be of increasing importance in fast neutron flux density measurement. Solid state detectors have been applied to associated particle counting (Cedarlund et al., 1961). Reactions in the silicon of the detector such as $Si(n,p)$ and $Si(n,\alpha)$ present interesting possibilities, and a proton recoil counter had been reported (Dearnaley and Whitehead, 1961).

(2) *High flux densities*

For intense fast neutron flux densities the measurement of total neutron flux density is inseparable from the measurement of spectrum. Many methods which are suitable in low fluxes or in collimated beams become impossible at high fluxes. Threshold detectors, which are too insensitive at low fluxes, provide a satisfactory method to obtain both flux density and spectrum in the same measurement and they are unaffected by pulsing (see Trice, 1957; Hurst et al., 1956; Delattre, 1961). Activation detectors are generally used for absolute flux density measurements, the activity being counted after the

irradiation. Fission counters are used chiefly for relative measurements, since the amount of fission material permissible in the counter is extremely small at high fluxes. Threshold detectors have two disadvantages: they have low resolution, and they require precise knowledge of the neutron cross sections of the detectors used. These cross sections are not sufficiently well known (Moteff and Beever, 1960), frequent discrepancies in the mean cross sections of greater than 10 percent being reported. Fission cross sections are known to somewhat better than 10 percent.

Often the data is analyzed by the assumption of a constant cross section above threshold. Polynomial expansion methods which can take advantage of detailed knowledge of the cross sections above threshold have been given by Trice (1957), Hartmann (1957), and Uthe (1957). These methods require the use of electronic computers for efficient fast neutron spectrum determination.

A list of threshold detectors with approximate threshold energies is given in table IIB3. For cross section values, the reader is referred to the compilations by the various cross section committees such as BNL–325 and supplements (Hughes and Schwartz, 1958), and the Euratom report (Liskien and Paulsen, 1961).

TABLE IIB3. *Threshold detectors*

Detector	Reaction	Product	Half-life	Approx. threshold energy*
				Mev
Np^{237}	(n,f)	Many	Many	0.2
In^{115}	(n,n')	In^{115m}	4.5 hr	.45
Ba^{137}	do	Ba^{137m}	2.6 min	.60
U^{238}	(n,f)	Many	Many	.7
Th^{232}	do	do	do	1.3
S^{32}	(n,p)	P^{32}	14.3 days	1.7
Ni^{58}	do	Co^{58}	71.3 days	1.7
P^{31}	do	Si^{31}	2.6 hr	1.8
Fe^{54}	do	Mn^{54}	290 days	1.8
Al^{27}	do	Mg^{27}	10 min	2.6
Si^{28}	do	Al^{28}	2.27 min	4.4
Fe^{56}	do	Mn^{56}	2.6 hr	5.0
Mg^{24}	do	Na^{24}	15.06 hr	6.3
Al^{27}	(n,α)	Na^{24}	15.06 hr	6.5
Cu^{63}	(n,2n)	Cu^{62}	10 min	11.4
C^{12}	do	C^{11}	20.5 min	20

*These threshold values will be usually lower than the "effective" threshold To evaluate the "effective" threshold in a given experiment, it is suggested that the cross section curve be used together with any spectral information available.

2. Neutron Sources

a. *Status of neutron source calibrations and intercomparisons.* Desirable features of a neutron source which is to serve as a standard include:

neutron emission rate independent of time,
reproducible manufacture and neutron emission rate,
monoenergetic neutrons of known energy,
negligible gamma-ray output,
high neutron emission rate,
transportable,
small size,
negligible self absorption and scattering of neutrons,
isotropic emission of neutrons, and
ease of preparation.

No source has all of these features, but several, which have been used as standards or which offer outstanding promise as source standards, are given in table IIB4.

The most desirable neutron standard source would have a known emission rate of neutrons of definite and variable energy. Accelerators furnish monoenergetic neutrons of a wide range when use is made of the $T(p,n)He^3$, $D(d,n)He^3$, and $T(d,n)He^4$ reactions. For particular applications associated with reactor uses, a fission neutron spectrum is desirable. Such a spectrum is emitted

TABLE IIB4. *Characteristics of neutron sources important for standardization*

Source	Chief advantages	Chief disadvantages	Important data
Ra^{226}-Be(α,n)	Large neutron yield, small, most widely measured standard source.	Too much gamma radiation, unknown spectrum, not reproducible except for Ra-Be F_4, strength changes with time due to Po growth.	$T\frac{1}{2}$=1622yr, $\approx 1.5\times10^7 n$/sec curie.
Pu^{239}-Be(α,n)	Few gamma rays, long half-life	Not monoenergetic, significant self-absorption, large bulk, neutron emission grows with time if Pu^{239} is not pure.	$T\frac{1}{2}$=24,400yr $\approx 1.5\times10^6 n$/sec curie.
Am^{241}-Be(α,n)	Small, few gamma rays	Significant self-absorption, not monoenergetic.	$T\frac{1}{2}$=458y,$2.0\times10^6 n$/sec curie.
Ra^{226}-Be(γ,n)	Reproducible, isotropic	Too many gamma rays, polyenergetic spectrum below 0.7 Mev, lower neutron yield than the (α,n) source.	$T\frac{1}{2}$=1622yr,$1.2\times10^6 n$/sec curie.
Pu^{240}(Spontaneous fission)	Long half-life (6600 yr) fission spectrum, few gamma rays.	Expensive, low neutron yield	$\approx 7\times10^3 n$/sec g.
Cm^{244}(Spontaneous fission)	Fission spectrum, low mass	Expensive, difficult to obtain	$T\frac{1}{2}$=18.4yr,$1\times10^7 n$/sec g.
$Li^7(p,n)$	Monoenergetic neutrons, few gamma rays.	Requires accelerator, knowledge of flux is not too good, anisotropic, not transportable.	$\approx 10^5 n$/microcoulomb at 2 Mev; threshold energy 1.881 Mev.
$H^3(p.n)$	Same as $Li^7(p,n)$	Same as $Li^7(p,n)$	$\approx 2\times10^6 n$/microcoulomb at 2 Mev; threshold energy 1.02 Mev.
$H^2(d,n)$	Lowest gamma ray contamination, monoenergetic neutrons.	Requires accelerator, anisotropic, associated particle counting possible, but requires knowledge of $H^2(d,n)$ and $H^2(d,p)$ relative cross sections and angular distributions.	$\approx 2\times10^6 n$/microcoulomb at 2 Mev (thick target).
$H^3(d,n)$	Low gamma-ray output, large neutron yield for low deuteron energies, monoenergetic, rather isotropic.	Requires accelerator, excellent for associated particle counting for flux determination.	Neutron energies roughly 10–20 Mev, $\approx 10^5 n$/microcoulomb at 2 Mev (thick target).

by the spontaneous fission sources like the Cm^{244} source. In spite of the main requirements concerning the neutron standard, the Ra-Be(α, n) source with its wide energy spectrum, and the Ra-Be(γ, n) source with its tremendous gamma-ray output have become the most widely used standard neutron sources. Measurements with Ra-Be sources are important because:

(i) international comparisons of national standard sources ensure that the same flux scale is used in different countries and different laboratories,

(ii) agreement between absolute measurements by different methods and in different laboratories strengthens our confidence that the measurements are correct.

The Ra-Be(α, n) like the Ra-Be(γ, n) source, has the main disadvantage of a high gamma output. The Ra-Be(α, n) has the disadvantage of a greater variation in time of the neutron emission rate, and perhaps also of the spectrum. The Ra-Be(α, n) source neutron emission rate increases with time because of the growth of Po.

Correction for the latter effect must be made to obtain the emission rate at a later date according to the formula:

$$Q_{t_1}=Q_{t_0}\frac{1+0.14[1-e^{-0.0357(t_0+t_1)}]}{1+0.14[1-e^{-0.0357t_0}]}$$

where Q_{t_0} is the absolutely measured emission rate at a time t_0 years after the sealing of a Ra^{226} source (RaD must have been extracted), and t_1 is the time elapsed after the calibration date in years. The factor 0.14 is derived from neutron emission rate considerations at different α-particle energies (compare NRCP, 1960) and 0.0357 is the appropriate disintegration constant for formation of polonium based on a RaD half-life of 19.4 years.

A considerable number of standard neutron sources have been absolutely calibrated during the period 1950–60. Several of these sources have also been compared in a series of *direct* comparisons such that no cumulative errors might arise from the comparison series as was the case in earlier measurements. As to the *absolute calibrations* most of the techniques used in absolute particle counting have been explored. The main groups of neutron detection techniques used are as follows.

(i) Associated particle techniques. The Ra-Be(α, n) source of NRC, Canada, has been absolutely calibrated by comparison with the yield of the $F^{19}(\alpha, n)Na^{22}$ reaction. The activity of Na^{22} was determined absolutely by $4\pi\beta$-counting. The Ra-Be(α, n) source of AB Atomenergi, Sweden, has been calibrated by comparison of its emission rate with the neutron emission rate from the $T(d, n)He^4$ reaction. α-particles from this reaction were absolutely counted in a proportional counter within a known solid angle. The RdTh-D_2O source of Oxford, U.K., has been absolutely calibrated by counting the number of protons from the $D(\gamma, n)H$ reaction in an ion chamber. These measurements are cross section independent.

(ii) Recoil particle techniques. The emission rate of the Oxford RdTh-D_2O source was absolutely determined by comparison to a measured neutron flux density from the $Li(p,n)$ and $T(p,n)$ reactions, the flux density being absolutely determined by recoil proton counting in hydrogen and methane filled ion chambers. The Hanson-McKibben long counter was used for the comparison. The emission rate of the Swedish source was determined by comparison of its output to that of the $T(d,n)$ reaction by measuring the recoil proton ion current in a homogeneous ion chamber. These measurements are dependent on the (n,p) scattering cross section.

(iii) Thermalization techniques. Most absolute calibrations are performed by integrating the total neutron absorption rate in an essentially infinite moderator. Either the absorption rate of the thermalized neutrons is determined from the activity induced in the absorber (Mn-bath methods) or the absorption rate is deduced from an absolute determination of the spatial neutron density integral. The absolute part of the measurement involves $4\pi\beta$-counting, β-γ coincidence technique, the counting of $B^{10}(n,\alpha)Li^7$ reactions in a known volume, etc. Most of these measurements are dependent on the neutron disappearance cross sections of H^1, Mn^{55}, Au^{197}, etc.

The results of a great number of source calibrations are collected in table IIB5. As will be seen in column 3 of this table, where the results of the absolute neutron emission rate determinations of the different national standard sources are listed, the errors quoted for these separate determinations cluster about ± 2 or ± 3 percent. In order to investigate if these limits of error are realistic or not, a considerable number of source strength comparisons have been made. Examples of the more important direct comparison measurements are listed in columns 4–8 of the table. Only those measurements are listed which involve direct comparison of two sources. Also only comparison measurements made in 1956 and later have been included as the addition of old and obsolete data would have obscured the trend of modern measurements. To make the absolute source strength values commensurable, all those source strength values depending upon the absorption cross section σ_{Au} of gold and σ_H of hydrogen have been corrected to the values obtained if $\sigma_{Au}=98.8$ barns and $\sigma_H=0.332$ barns (Hughes and Schwartz, 1958). Also all the corrections for polonium growth have been recalculated using the formula given above with the more accurate constant 0.14 instead of the previously used value of 0.17.

Numerous methods are involved in the comparison series.

(i) The sources are immersed in a large moderator volume containing a solution of a Mn-salt. The relative source strengths follow from the activity produced in the solution. An accuracy of about ± 0.5 percent is possible when sources of similar spectra are compared.

(ii) The sources are immersed in a large moderator and the neutron density integrated by the aid of BF_3 counters. An accuracy of ± 0.8 percent is possible when sources of similar spectra are compared.

TABLE IIB5. *International intercomparisons of national standard neutron sources*

Neutron source Q_s	Date of absolute calibration	Absolute emission rate n/sec×10^6	Emission rate Q_s as measured by comparison to standard source Q_x from the place X. The ratio $\frac{Q_s}{Q_x}$ is also given					U. K. (Richmond, 1957)	Sweden (Larsson, 1958) Revised 1961	Canada (Geiger, 1960)	Least squares estimate of error of absolute value (Axton, 1961)
Belgium, U.M., Brussels	Dec. 1952	Ra-α-Be [1] 7.88±2%	PTB, Germany 7.88±2% 1.000±0.3%					0.997	1.015	1.012	+1.9%
Canada Natl. Research Council.	July 1958	Ra-α-Be [2] 3.20±1.5%	Stockholm, Sweden. 3.182 ±2.2% 1.008 ±0.8%	PTB, Germany. 3.227 ±2.2% 0.994 ±0.3%	U.M. Belgium. 3.234 ±2% 0.992 ±0.3%	NPL, U. K. 3.142 ±1.5% 1.021 ±0.5%	NBS, U.S.A. 3.13 ±3% 1.026 ±1%		1.008	1.000	+0.7%
Germany, Physikalish-Technische Bundesanstalt, Braunschweig.	Aug. 1958	Ra-α-Be [3] 1.95 ±2%	Stockholm, Sweden. 1.937 ±2.2% 1.007 ±0.8%	U.M., Belgium. 1.975 ±2% 0.987 ±0.3%					1.007	1.006	+1.3%
Italy, CISE, Milan.	Sept. 1960	Ra-α-Be [4] 7.73 ±3.5%	Stockholm, Sweden. 8.05 ±2% 0.960 ±0.8%						0.960		
Japan, ETL, Tokyo.	1958	Ra-α-Be [5] 14.8s ±3%	Brussels, Belgium. 1.50 ±5% 1.008 ±5% (through intermediate source).						1.007		
Sweden, AB Atomenergi, Stockholm.	Oct. 1954	Ra-α-Be [6] 2.65 ±2%	Moscow, U.S.S.R. 2.634 ±3.1% 1.006 ±0.5%	PTB, Germany. 2.658 ±2% 0.997 ±3%	U.M., Belgium. 2.689 ±2% 0.985 ±0.3%				1.000	0.992	−0.1%
Switzerland, Physical Institute of the University Basel.	April 1955	Ra-α-Be [7] 1.52$_4$ ±2.8%	Stockholm, Sweden. 1.516 ±2.2% 1.005 ±0.8%	Harwell U.K. 1.560 ±1.7% 0.977 ±0.5%	CISE, Italy. 1.504 ±4% 1.025 ±2.3%			0.979	1.005		−1.9%
U.K. Oxford via Harwell.	1951 (1956)	RdTh-D_2O [8] Ra-α-Be 9.08 ±1.7%	Stockholm, Sweden. 9.15 ±2.2% 0.992 ±0.8%					1.000	0.992		−0.1%
U.K. National Phys. Laboratory, Teddington (secondary source).	1960	Ra-γ-Be [9] 0.1664 ±2%	NRC, Canada. 0.1668 ±3% 0.998 ±1.7%	NBS, U.S.A. 0.1695 ±1.7% 0.982 ±0.24%				0.991		0.979	−1.0%
U.S.A. National Bureau of Standards, Washington, D.C. (Source II).*	1955	Ra-γ-Be [10] 1.18$_7$ ±1.8%	Stockholm, Sweden. 1.166 ±3.5% 1.018 ±3.1%	NRC, Canada. 1.176 ±1.6% 1.010 ±0.8%	Harwell (Oxford) U.K. 1.179 ±1.7% 1.007 ±0.5%	NPL, UK. 1.164 ±2.0% 1.019 ±0.1%		1.007	1.018	1.010	+0.6%
U.S.S.R., Moscow Inst. of Physics, Moscow.	June 1951	Ra-α-Be [11] 5.96 ±3%	Stockholm, Sweden. 6.00 ±2.2% 0.994 ±0.8%						0.994		−1.3%
U.S.S.R., Joint Inst. for Nuclear Research, Dubna.	March 1952	Ra-α-Be [11] 0.486 ±7%	Stockholm, Sweden. 0.490 ±2.2% 0.992 ±0.8%						0.992		

*Reference standard available for comparisons.

[1] del royer, A., and Tavernier, G. C. (1954).
[2] Geiger, G. W., and Whyte, G. N. (1959), Geiger, K. W. (1959, 1960).
[3] von Droste, Dr., and Kolb, M. (1960).
[4] Felcher, G. P., Germagnoli, E., and Musci, M. (1960).
[5] Michikawa, T., Teranishi, E., Tomimasu, T., and Inoue, Y. (1959).
[6] Larsson, K. E. (1954, 1955, 1958).
[7] Von Planta, C., and Huber, P. (1956).
[8] Richmond, R. (1958).
[9] Axton, E. J., and Cross, P. (1961); Axton, E. J. (1961).
[10] DeJuren, J. A., Padgett, D. W., and Curtiss, L. F. (1955); DeJuren, J. A., Chin, J. (1955); Mosburg, E. R. (1959).
[11] Erozolimsky, B. G., and Spivak, P. E. (1957); Bezotosnii, V. M., and Zamyatnin, Yu. S. (1957).

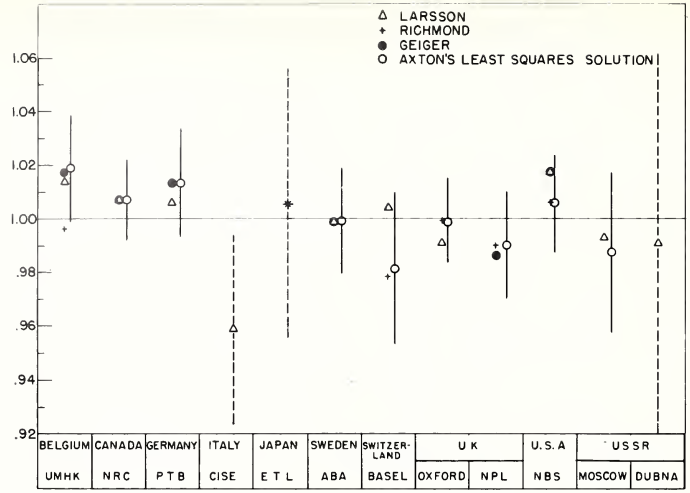

FIGURE IIB13. *Results of some international intercomparisons of standard neutron sources*
See table IIB5 for detailed explanation.

(iii) The sources are directly compared in air by use of long counters. The accuracy reached is strongly dependent on any asymmetry of the neutron yield of the source. The accuracy attainable is of the order of ± 0.5 percent for similar sources using the same nuclear reaction. If different sources are used and even if all necessary corrections are made, the error may be as high as 5 percent.

(iv) The sources are compared using the effect of the source neutrons on the reactivity of an almost critical reactor. With extreme care the accuracy attainable may be as good as ± 0.5 percent.

(v) The sources are placed in the center of a moderator such as graphite with thermal neutron detectors located at large distances from the source if energy independence is desired (Macklin, 1957; Walker, 1946).

From table IIB5 there appears to be a much greater uncertainty in the intercomparison of (γ,n) sources with (α,n) sources than is the case when similar sources are compared. The (γ,n) sources involved in the series are the Ra-Be sources of NBS, USA and NPL, UK and the RdTh-D_2O source of Oxford, U.K. It should be noted that a systematic error may be common to many absolute calibrations since a number of identical corrections have been applied. These corrections need not be applied in the relative calibration of photoneutron sources, but they do appear in the relative comparison with Be(α,n) sources. The main difficulties seem to be fast neutron absorption effects and leakage of fast neutrons. Both of these effects are negligible when sources of similar spectra are compared. As shown by the ratio of the absolute measurements Q_s/Q_z given in columns 4–8 most of these fall within limits ± 0.8 percent, $0.992 \leq Q_s/Q_z \leq 1.008$, with only two exceptions when Ra-Be(α,n) sources are compared. When Ra-Be(α,n) sources are compared to Ra-Be(γ,n) sources the same ratio varies within limits $0.977 \leq Q_s/Q_z \leq 1.028$; i.e., almost ± 3 percent.

Results of three comparison series are reported in table IIB5 of which the Swedish Ra-Be(α,n) source is involved in the longest series. This source has been directly compared to nine sources from eight countries. The comparisons have been made in Stockholm as well as at other places such as Braunschweig, Germany, Brussels, Belgium, and Moscow, USSR. The source strength value of the appropriate source has been arbitarily set equal to 1.000 and the other source calibrations are expressed in terms of it. Results are given in columns 9, 10, and 11 of the table and in figure IIB13. The result of a least squares analysis of source intercomparisons (Axton, 1961) is also reported. As is most clearly shown by the figure, the spread of the absolute values is small, all values except one falling within ± 1.5 percent. The error bars shown in the figure are those given by the authors of the different absolute calibration reports.

Conclusion and Recommendations:

(i) All careful absolute neutron source strength determinations listed are capable of about ± 1.5 percent accuracy.

(ii) Any new standard source may be compared to any of the sources listed in the table and the figure. The establishment of a world average

seems inopportune because of the need for investigation of possible systematic errors.

(iii) High precision is obtained only when comparing sources of similar spectra. Careful studies should be made of the reasons why the comparison results of sources of widely different spectra scatter so much. Efforts should be made to study effects of (n,α)-, (n,p)-, (n,γ)-reactions at higher energies as well as of the processes (γ,n) and $(n,2n)$. The $O^{16}(n,\alpha)$ reaction is very important at energies above 5 Mev. Also when neutron moderation techniques are used, the comparisons should be made in such a way that fast neutron leakage from the standard moderator is negligible.

b. *Some data on radioactive neutron sources and spontaneous fission sources.* A large number of possible (α,n) and (γ,n) neutron sources are listed in tables IIB6 and IIB7. Examples of the neutron spectra emitted by these sources are given in subsection IIB2c.

TABLE IIB6. *Data on some* (α,n) *sources*

Source	Half-life	Maximum neutron energy (Mev)	Average neutron energy (Mev)	Yield $n/\sec\times10^{-6}$ / Curie	Neutron spectrum
Po^{210}-Li	138. 4*d*	1. 32	0. 48	0. 05	Figure IIB21.
Po^{210}-Be	2. 93*y*	10. 6			Not measured.
Po^{210}-Be	138. 4*d*	10. 8	4. 3 [9]	2. 5	Figures IIB19, 20.
RaDEF-Be	19. 4*y*	10. 8	4. 5	2. 5	Similar to Po-Be.
Ra^{226}-Be	1622*y*	13. 2	3. 6 [9]	15	Figure IIB14, 15.
Rn^{222}-Be	3. 825*d*	13. 2		12	Not well known.
Ac^{227}-Be	21. 8*y*	12	4. 6	25 [1]	Figure IIB16.
Pu^{238}-Be	90*y*	11		2. 8 [1]	Not measured.
Pu^{239}-Be	24. 400*y*	10. 6	4. 5	2. 0 [1]	Figure IIB17, 18.
Am^{241}-Be	458*y*	11		2. 0	Not measured.
Cm^{242}-Be	163*d*	11. 6		4. 0 [1]	Do.
Ra-BeF$_4$	1622*y*	13. 2		2. 53 [2]	Do.
Po^{210}-B^{10}	138. 4*d*	6. 1	2. 8 [9]	. 8 [3]	Figure IIB22a.
Po^{210}-B	138. 4*d*	5. 0		. 2 [4]	Figure IIB22.
Po^{210}-B^{11}	138. 4*d*	6. 1		. 8 [4]	Figure IIB22b.
Po^{210}-O^{18}	138. 4*d*	4. 3 [5]		1. 0 [5]	Figure IIB23.
Po^{210}-F^{19}	138. 4*d*	2. 8	1. 4	. 1* [6]	Figure IIB24.
Po^{210}-Na	138. 4*d*			. 04 [7]	Not measured.
Po^{210}-Mg	138. 4*d*			. 03 [7]	Do.
Po^{210}-Al	138. 4*d*	2. 7 [3]		. 02 [7]	Do.
Po^{210} (mock fission).	138. 4*d*	10. 8	1. 6	about 0. 4	Simulated fission spectrum. [8]

*With CaF_2 as target material.
[1] Runnals, O. J. C., and Boucher, R. R. (1956).
[2] Feld, B. T. (1953).
[3] Roberts, J. H. (1947).
[4] Geiger, K. W., and Jarvis, J. (1962).
[5] Khabakhpashev, A. G. (1960).
[6] Szilvasi, A. J. D., Geiger, K. W., and Dixon, W. R. (1960).
[7] Breen, R. J., and Hertz, M. R. (1955).
[8] Tochilin, E., and Alves, R. V. (1958).
[9] DePangher, J. (1959).

(1) $(\alpha,\ n)$ *sources*

Any α-emitter may be mixed with a suitable substance like beryllium to produce neutrons, if the $(\alpha,\ n)$ reaction is energetically possible. As seen from table IIB6 the $Be(\alpha,n)$-reaction gives the highest neutron emission rate. This increases steeply with α-energy. The following empirical expression for the maximum thick target neutron emission rate, Q_{max}, has been given by Runnals and Boucher (1956):

$$Q_{max}=0.\ 152\ E^{3.65}\ \text{neutrons per million alphas}$$

where the α-energy E is expressed in Mev.

The yield for $B(\alpha,n)$ and $O^{18}(\alpha,n)$ is about one third of that for $Be(\alpha,n)$. The yield for $F^{19}(\alpha,n)$ is somewhat lower. For the remaining light elements the yield is much lower.

For the majority of (α,n) sources, neutron emission may leave the residual nucleus in an excited state which may decay by particle or gamma emission. Breen and Hertz (1955) have published data on gamma-ray emission. Examples for particle emission are the $Be^9(\alpha,n)$ 3α reaction and the $B^{10}(\alpha,np)C^{12}$ reaction (Geiger and Jarvis, 1962).

It is therefore expected that the neutron spectrum from such sources is rather complex. Only a Po-$B^{11}(\alpha,n)$ source gives a simple spectrum, showing a single peak. Here the probability of

TABLE IIB7. *Characteristics of some important* (γ,n) *sources*

Sources	Half-life	E_γ [a] Mev	E_n calculated [a] Mev	E_n observed [b] Mev	Standard yield [b, f]	Actual source yield [g]
Na^{24}+Be	15. 0*h*	2. 757	0. 966	0. 83	13	
Na^{24}+D_2O	15. 0*h*	2. 757	. 261	. 22	27	
Al^{28}+Be	2. 30*m*	1. 782	. 103			
Cl^{38}+Be	37. 3*m*	2. 15	. 430			
Mn^{56}+Be	2. 58*h*	1. 77, 2. 06, 2. 88	. 092, 0. 350, 1. 076	. 15, 0. 30	2. 9	
Mn^{56}+D_2O	2. 58*h*		. 320	. 22	0. 31	
Ga^{72}+Be	14. 2*h*	1. 87, 2. 21, 2. 51	. 181, 0. 484, 0. 750		5	
Ga^{72}+D_2O	14. 2*h*		. 140	. 13	6. 9	
As^{76}+Be	26. 6*h*	1. 77, 2. 06	. 089, 0. 350			
Y^{88}+Be	104*d*	1. 853	. 166, 0. 972	. 158±0. 005	10	
Y^{88}+D_2O	104*d*		. 265		0. 3	
In^{116}+Be	54*m*	2. 090	. 377	>0. 15, 0. 30	. 82	
Sb^{124}+Be	60*d*	1. 70	. 031	. 0248±0. 0024 [c]	19	1. 6 [c]
La^{140}+Be	40. 2*d*	2. 51, 3. 0	. 747	. 62	0. 3	
La^{140}+D_2O	40. 2*d*		. 140	. 13, 0. 15	. 7	
RdTh+D_2O	1. 90*y*	2. 623 (ThC″)				1. 2 [d]
MsTh+Be	6. 7*y*	2. 614, 1. 8 (ThC″)		. 827± 030	3. 5	
MsTh+D_2O	6. 7*y*			. 197± 010	9. 5	1. 2 [d]
Ra^{226}+Be	1622*y*	1. 690, 1. 761, 1. 820, 2. 090, 2. 200, 2. 420		. 7 max	1. 2	1. 3
Ra^{226}+D	1622*y*			. 12	0. 1	

[a] For references see Amaldi (1959).
[b] For references see Amaldi (1959) and Wattenberg (1949).
[c] U.S. Atomic Energy Commission Isotopes catalog.
[d] Ms-Th and Rd-Th sources emit some neutrons through $(\alpha,\ n)$ reactions with light elements in the carrier and container walls (Littler, 1957).
[e] Schmitt (1960).
[f] This is the neutron yield$\times10^{-4}$ for a 1-curie gamma source with 1g of target material placed 1cm away from the gamma source (Wattenberg, 1949).
[g] 10^6n/sec per curie.

forming an excited N^{14} nucleus is only 5 percent. In the usual neutron source, consisting of a mixture of target material and α emitter, considerable broadening of a peak in the neutron spectrum occurs, compared to the peak observed in thin target geometry. There are two reasons for this broadening.

(i) The α particles are slowed down in the source material and all α energies from zero to the maximum energy occur.

(ii) In a source the observed neutrons are emitted at all angles with respect to the α particles.

Consequently, monoenergetic neutron emission can never be expected from the usual (α,n) source.

Table IIB6 also lists the average neutron energy because of its importance for neutron dosimetry.

Examination of table IIB6 shows that Pu^{238}-Be or Am^{241}-Be appear to be most suitable for the purpose of neutron standards. These materials can be prepared isotopically pure. The half-lives are well-known and can, for a given source, be verified by a calorimetric method. However, many countries have regulations regarding these materials which makes the acquisition and export of such sources difficult.

As seen from table IIB6 most of the α-n sources except the Ra-Be source have inconveniently short half-lives. Also the yield figures are considerably lower than those of Ra-Be sources. The neutron spectra emitted by Be(α,n)-sources are all of the very complex type as illustrated by the results on Ac-Be, Pu-Be, and Po-Be sources given in figures IIB16 to IIB20. The spectra are on the whole rather badly known.

(2) (γ,n) *sources*

Radioactive (γ,n) sources use only Be$(Q=-1.666$ Mev) and $D(Q=-2.226$ Mev). The neutron emission rate is relatively low, about 10–1,000 times smaller than that of a (α,n) source. The accompanying γ-radiation is very intense. For monochromatic gamma-ray emitters the energy of the photoneutrons extends only over a small range since little linear momentum is transferred to the residual nucleus. From conservation laws it follows that the relative energy spread of neutrons is only ± 14 percent in the case of D and ± 1.5 percent in the case of Be, for the gamma-ray energy at threshold (Amaldi, 1959). This spread becomes even smaller for higher gamma-ray energies. It has been assumed, however, that the gamma-ray and neutron energies are not being degraded in the target by scattering. Therefore it must be expected that bulky sources emit neutrons down to lower energies than the energy values indicated in table IIB7. Cloud chamber measurements show relatively broad spectra (Eggler and Hughes, 1950), but this probably indicates the difficulties of measurement of neutrons in the presence of a large gamma-ray background, rather than lack of energy homogeneity of the neutrons from the source. Complex gamma-ray spectra cause complex neutron spectra; this applies particularly to sources containing Ra and Th and is evident from figure IIB25.

Table IIB7, listing some important data on (γ,n) sources, shows that except for the Ra-Be (γ,n) source all the (γ,n) sources have inconveniently short half-lives for use as standard sources. For some applications it is of importance that the energy of the neutrons from most (γ,n) sources is much smaller than from (α,n) sources.

(3) *Spontaneous fission sources*

For a class of heavy even-even nuclei the process of spontaneous fission becomes energetically possible. Neutron sources made of such materials have not been in common use in spite of their merits, low gamma-radiation and well-known spectral distribution of the type $\sqrt{E}e^{-E/T}$, where T is a characteristic nuclear temperature of the order of 1.3 Mev. The reason for this is that most of the suitable materials have not been available in large enough quantities or have not been available with sufficient purity. A number of possible nuclides together with some pertinent data are given in table IIB8. The Cm^{244} source, which has a copious yield, is attractive as a possible standard source. Two grams of Cm^{244} would emit about 2×10^7 n/sec or the same amount as a 1 gram Ra-α-Be source. As these sources could be made very small, the chance that the emitted neutrons make any inelastic collision before leaving the sources would be small and the

TABLE IIB8. *Characteristics of some important spontaneous fission neutron sources*

Nuclide	Half-life (spontaneous fission) [a]	Half-life (α decay) [a]	Alphas per fission [b]	Neutrons per fission [c]	Neutrons per g sec
U^{232}	$8\times10^{13}y$	$74y$	$\left\{\begin{array}{l}1.1\times10^{12}\\ 6.5\times10^{12}, \text{ after aging with 1.9 yr half-life.}\end{array}\right.$		
Pu^{236}	$3.5\times10^{9}y$	$2.7y$	1.3×10^{3}	1.9	3.1×10^{4}
U^{238}	$8.3\times10^{15}y$	$4.51\times10^{9}y$	1.8×10^{6}		
Pu^{238}	$4.9\times10^{10}y$	$89.6y$	5.5×10^{8}	2.0	2.3×10^{3}
Pu^{240}	$1.3\times10^{11}y$	$6600y$	1.9×10^{7}	2.1	7.0×10^{2}
Pu^{242}	$7.2\times10^{10}y$	$3.8\times10^{5}y$	1.9×10^{5}	2.3	
Cm^{242}	$7.2\times10^{6}y$	$162.5d$	1.6×10^{7}	2.3	1.8×10^{9}
Cm^{244}	$1.4\times10^{7}y$	$18.4y$	7.6×10^{5}	2.6	1.0×10^{7}
Cf^{252}	$66y$	$2.2y$	30		2.6×10^{12}
Cf^{254}	$60d$	$60d$	≈0	3.5	

[a] Sullivan, W. H. (1957).

[b] The number of alphas/fission is an inverse "figure of merit." A source with a low number of alphas per fission has relatively many fissions and the neutron spectrum is not likely to be contaminated with (α,n) neutrons.

[c] Crane, W. W. T., Higgins, G. H., and Bowman, H. R. (1956).

spectrum would be a true virgin fission spectrum. The report of a serious attempt to construct and calibrate a spontaneous fission source (Pu^{240}) has been published by Richmond (1958). It is highly recommended that increased efforts be made to establish a standard spontaneous fission neutron source.

c. *Neutron spectra.* Because of the very unfavorable ratio of gamma-to-neutron yield of Ra-Be neutron sources, very few spectrum measurements have been performed on them. The only technique applied to these spectrum measurements is the recoil proton registration. The measurements made so far on Ra-Be(α,n) sources have been collected by Hess (1957) and Medveczky (1961). Hess has also performed a calculation of the spectrum as well as of the spectra of other (α,n) sources. The calculation is based on a knowledge of range energy relations of α-particles in beryllium and of the cross section for the (α,n) reaction as a function of energy.

The results of the calculations as well as of a recoil proton measurement is given in figure IIB14. Other results gained on Ra-Be(α,n) neutron spectra are collected in figure IIB15. As shown by the figures the status in this field is not satisfactory. An additional low energy neutron component ($E_p < 0.5$ Mev) was estimated by DePangher (1959) to be 26 percent of the whole spectrum.

A measured spectrum for the Ra-Be(γ,n) source is shown in figure IIB25. Comparison of the figures IIB15 and IIB25 indicates the difficulty of comparing Ra-Be(α,n) to Ra-Be(γ,n) sources due to very different initial neutron energies involved in the slowing down process.

The status of these particular neutron spectrum measurements merely illustrates the general great need for a neutron spectrometer of high efficiency able to work in a field of strong gamma-radiation. Research in this field is strongly recommended.

The spectra of some important radioactive neutron sources are shown in figures IIB16 to IIB25.

The existence of a low energy neutron component for Be(α,n) sources is controversial in the case of polonium or plutonium as alpha-emitter, because the alpha-energy is very close to the threshold for the break-up reaction. Results of DePangher for the case of the Po-Be source spectrum support the absence of such a component. But recent results concerning the Pu-Be(α,n) source of St. Romain et al., (1962) claim evidence for an intense low energy component not visible on the earlier curve of Stewart (see fig. IIB17). For Ac^{227} (+ decay products) with an average alpha-energy of 6.4 Mev, the low energy component is to be expected.

Typical reactor and accelerator neutron spectra are given in figures IIB26 and IIB27.

For further information the reader is referred to NCRP (1960).

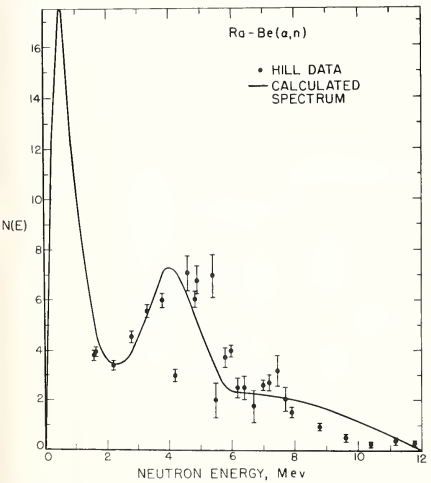

FIGURE IIB14. *Calculated neutron spectrum (Hess, 1959) for a Ra-α-Be source.*
Experimental data from Hill (1947).

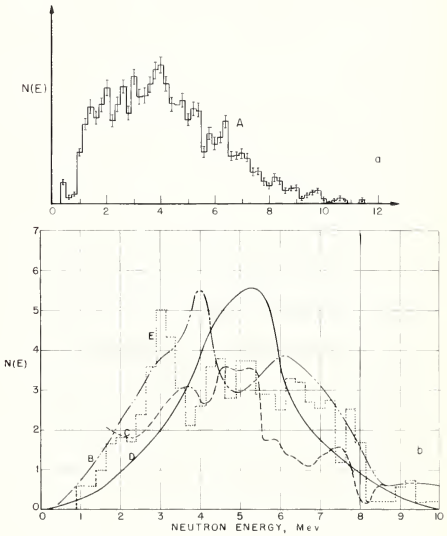

FIGURE IIB15. *Neutron spectrum for Ra-Be(α,n).*
Curve A was measured with nuclear emulsions (Medveczky, 1961); Curve B with nuclear emulsions (Houtermans and Teucher, 1951); Curve C with a counter-absorber arrangement called the "Ranger" (Hill, 1947); Curve D with nuclear emulsions (Demers, 1945); and Curve E with nuclear emulsions (Watson, 1958).

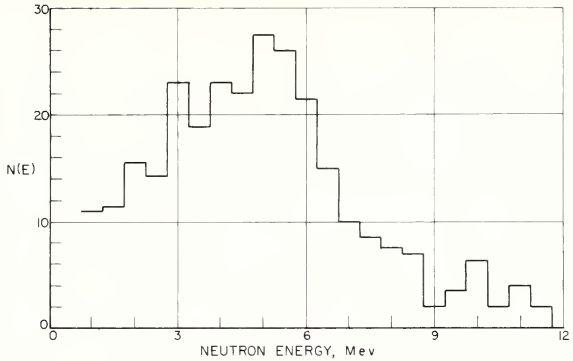

FIGURE IIB16. *Neutron energy spectrum of Ac-Be(α,n).*
Nuclear emulsions were used for the measurement (Dixon, Bielesch, and Geiger, 1957).

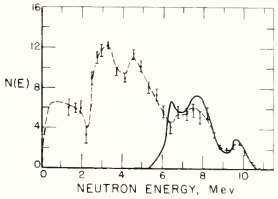

FIGURE IIB18. *Neutron energy spectrum of a Pu-Be(α,n) source (Broek and Anderson, 1960).*

An organic scintillation crystal was used for the measurement. The measurement is shown dotted, and the solid curve is a calculated part of the spectrum due to Be^9 (α,n) leaving C^{12} in its ground state.

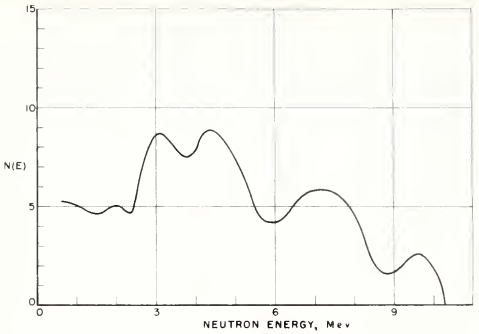

FIGURE IIB17. *Neutron energy spectrum of Pu-Be(α,n).*
Nuclear emulsions were used for the measurement (Stewart, 1955).

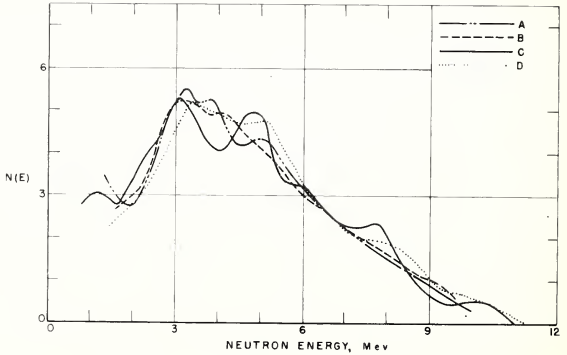

FIGURE IIB19. *Neutron energy spectra of Po-Be(α,n).*

Curve A was measured with a proton recoil proportional counter telescope (Cochran and Henry, 1955); curve B was determined by a similar method (Breen, Hertz, and Wright, 1956); curve C with nuclear emulsions (private communication from author, 1960, indicates that the all quoted energies should be increased by 3 percent, Whitmore and Baker, 1950); curve D with Li^6I scintillation crystal spectrometer (Murray, 1958).

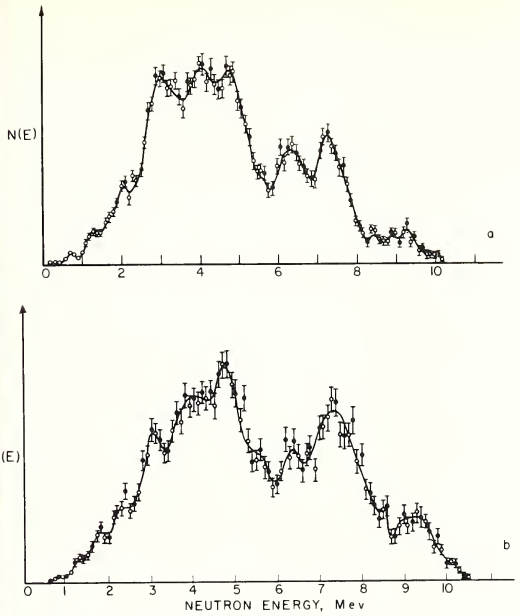

FIGURE IIB20. *Neutron spectrum of Po-Be(α,n).*

Nuclear emulsions were used for the measurement (Medveczky, 1961). Curve a is for a source with carrier while curve b is for a carrier free source. Significant differences are observed.

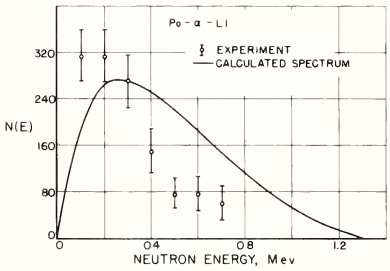

FIGURE IIB21. *Neutron spectrum of Po^{210}-Li(α,n) (Barton, 1953).*

The calculated curve is from Hess (1959).

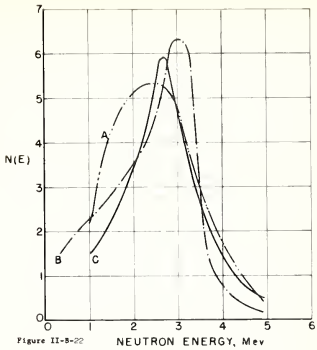

FIGURE IIB22. *Neutron spectrum of Po-B(α,n).*

Curve A is the result of a measurement with nuclear emulsions (Perlman, Richards, and Speck, 1946); curve B was also by nuclear emulsions (Staub, 1947); curve C by proton recoil counter telescope (Cochran and Henry, 1955).

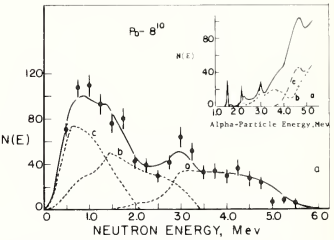

FIGURE IIB22a. *Calculated neutron spectra for a Po-B^{10}(α,n) source for transitions into the ground state (a), 2.4-Mev state (b), and 3.54-Mev state (c), where the relative neutron yields (curves a, b, and c), as shown in the inset, are used in the calculation.*

Also shown are the sum of these three calculated spectra (solid line) and the experimental points from emulsion data, corrected for a small contribution from the B^{11} impurity in the actual source (Geiger and Jarvis, 1961).

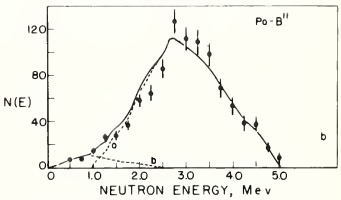

FIGURE IIB22b. *Calculated neutron spectra for a Po-B^{11}(α,n) source for transitions into the ground state (a) and the 2.3-Mev state (b).*

The sum of the two curves and the experimental points from emulsion data are also shown (Geiger and Jarvis, 1962).

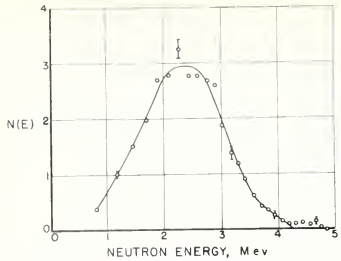

FIGURE IIB23. *Neutron spectrum of* Po^{210}-O^{18} (α,n), *(Khabakhpashev, 1960).*

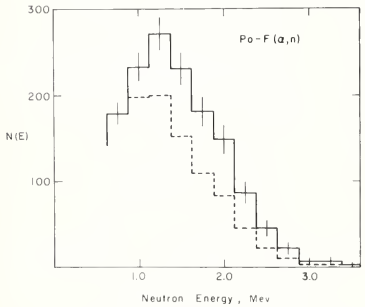

FIGURE IIB24. *Neutron spectrum of* Po^{210}-F^{19} (α,n).

Dashed histogram shows the neutron spectrum obtained from these results after correcting for the neutron-proton scattering cross section and the escape of proton tracks from the nuclear emulsion (Szilvasi, Geiger, and Dixon, 1960).

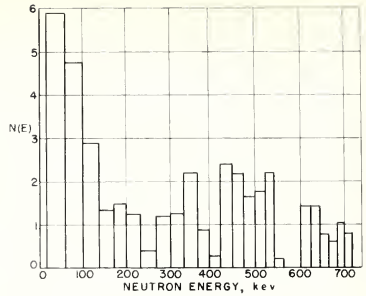

FIGURE IIB25. *Neutron energy spectrum of a Ra-Be*(γ,n) *source.*

A cloud chamber was used for the measurement (Eggler and Hughes, 1950).

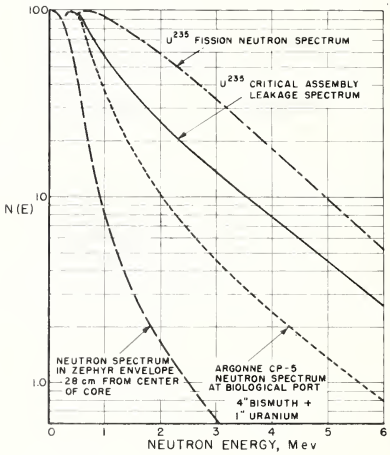

FIGURE IIB26. *Neutron fission spectra from reactors.*

References: Watt, 1952; Rosen, 1956; USNRDL measurement on CP-5 spectrum (unpublished); Codd, Sheppard, and Tait, 1956.

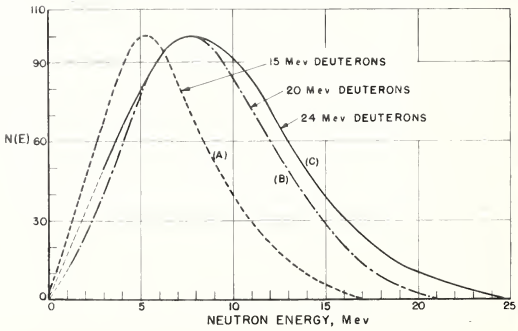

FIGURE IIB27. *Neutron energy spectra for 15, 20, and 24 Mev deuterons on thick* Be *target.*

Measurement for 15 Mev was by Cohen and Falk, 1951; for 20 and 24 Mev by Tochilin and Kohler, 1958.

III. Practical Measurement of Exposure

A. Definitions

The following terms are used in this section.

(i) *Exposure standard* is an ionization chamber and associated equipment, which allows the direct measurement of exposure. (Frequently referred to as a primary standard.)

(ii) *Reference instrument* is an exposure or exposure-rate meter of good stability which is calibrated as accurately as possible against an exposure standard and used only for the calibration of field instruments. (The reference instrument is frequently referred to as a secondary standard or substandard.)

(iii) *Field instrument* is an exposure or exposure-rate meter used for routine measurements.

B. Field Instrument Requirements

An exposure or exposure-rate meter should have—

(i) a minimum variation in sensitivity over the energy range of interest,

(ii) been calibrated against an exposure standard or reference instrument for all the qualities of interest,

(iii) appropriate constancy and means for checking same,

(iv) minimum stem "leakage,"

(v) suitable range and dimensions.

Restrictions on the size of the ionization chamber are less stringent for in-air measurements than for those in a phantom. Volumes of a few cm^3 are permissible except for measurements in a phantom or at the ends of closed applicators. For such measurements the depth of the chamber should not be more than a few millimeters. The wall thickness should be no greater than is necessary to provide both electronic equilibrium [11] and sufficient mechanical strength.

A typical thimble chamber used for measurements of filtered 100 to 250 kv x rays has a wall thickness of about 0.1 g/cm^2.

Examples are given below of the minimum wall thickness required in graphite cavity chambers used with higher photon energies:

approx. 0.2 g/cm^2 for cesium-137 gamma rays
approx. 0.5 g/cm^2 for cobalt-60 gamma rays
approx. 1.5 g/cm^2 for 4 Mv x rays.

For other radiation qualities it may be necessary to determine experimentally the minimum wall thickness required. Suitable materials include polystyrene, Perspex (Lucite), nylon, or bakelite. The thickness (in g/cm^2) required for a given photon energy is nearly the same for these and other low-atomic-number materials.

C. Instrument Calibration

This subsection deals with the calibration of reference and field instruments against exposure standards. Such calibrations are obtained by a substitution technique. The beam output is first measured with the standard and a reading of the reference or field instrument then obtained at the same position in the beam. The calibration factor is computed from these data.

The information presented here with subsequent comments is derived from a questionnaire sent to all exposure standard custodians listed in the 1959 ICRU Report. Useful information was received from ten calibration laboratories.

---

[11] *Electronic equilibrium and electron contamination.* As the photon energy is increased, the range of the secondary electrons is also increased and electrons from outside of the ionization chamber are more likely to reach the ionization chamber and penetrate its walls. Thus, if one considers the usual chamber wall thickness, this factor becomes more significant at energies above 1 Mev, where electronic equilibrium rather than mechanical strength determines the thickness. Before the equilibrium thickness is reached, the chamber is able to collect and record electrons from the various sources indicated in subsection IIIE. The presence of these electrons therefore affects the shape of the build-up curve and may affect the magnitude of the equilibrium thickness. When equilibrium thickness has been reached, the wall of the chamber is sufficiently thick to prevent these electrons from contributing significantly to the ionization within the chamber.

The amount of electron emission from irradiated material depends on whether it is "emergence emission"—in the direction of the primary radiation—or "incidence emission"—in the opposite direction to the primary radiation (Wilson, 1941). The relation between the amount of this emission and the atomic number of the irradiated material also varies with the direction of the emission. Under the conditions in which output or half-value-layer measurements are normally made, the electron emission may be regarded chiefly as emergence emission. Under these conditions, it has been shown that for radium gamma rays, for cobalt-60 gamma rays and for 1–2 Mv x rays, the amount of electron emission is a function of atomic number of the irradiated material such that it is minimal for materials of intermediate atomic number such as copper, iron, brass, etc. (Wilson, 1941; Wilson and Perry, 1951; Wyard, 1951). The same finding may be inferred to hold for cesium-137 gamma rays and recent work suggests that it holds also for 4 Mv x rays (Martin and Muller, 1961). This, of course, is the basis of the accepted procedure of using intermediate atomic number filters on the nosepieces of beam equipment that must be close to the skin. Quite a small thickness of suitable material, such as brass, will absorb the electron emission from the heavy high-atomic-number diaphragm material, and will itself produce a minimum of such emission.

The exact amount of electron emission incident upon an ionization chamber will depend, of course, upon the geometry of the irradiated surfaces and intervening air and their relation to the chamber.

In order to minimize the effect of electron contamination in radiotherapy, it has been shown that a certain clearance between the end of the collimator and the patient is desirable. Although the distance to insure the maximum buildup factor will increase with increased primary radiation energy, a distance of about 15 to 20 cm is adequate for cesium-137 equipments (Burns, unpublished), cobalt-60 (Johns et al., 1952a; Kemp and Burns, 1958), and 4 My accelerators (Jones, unpublished).

1. Exposure Meters Used for a Few Kv to About 0.5 Mv X Rays

a. *Tube output constancy.* In a few laboratories output constancies within 0.1–0.2 percent during calibration are claimed. If, however, the output of the x-ray tube cannot be kept at a high degree of constancy throughout the calibration, the use of a monitor chamber is recommended. The majority of the laboratories use monitor chambers.

b. *Monitor chambers.* These chambers and their measuring accessories should be at least of the same precision as the exposure standard.

If appreciable drift in radiation quality can occur during a calibration, the quality dependence of the monitor chamber over the drift region should not exceed that of the instrument to be calibrated. The presence of the monitor in the beam between the source and the chamber should not impair the uniformity of the field. A flat chamber with thin but firm flat walls at right angles to the beam axis can serve this purpose. Such chambers have been described by Thoraeus (1956), Worthley et al., (1957), and Henry and Aitken (1961). Monitor filtration should be included in the total filtration.

For very soft radiations (5–50 kv x rays), Allisy and Roux (1961) report the use of a free-air monitor chamber.

c. *Sources of error.* When calibrating an instrument against a standard, it is important that the exposure it receives per unit time (or, if a monitor is used, per unit charge collected in the monitor) is the same as that of the standard. There are at least three possible sources of error: nonuniformity over the beam cross-section, scattered radiation, and timing of exposure.

(1) *Nonuniformity.* When the cross-section of the beam covering the chamber to be calibrated is not identical with that covering the standard chamber aperture, the average exposure rate over these two cross-sections may not be the same.

Four laboratories stated that the uniformity of the cross-section of the beam had been investigated. Three other answers only estimated the uniformity of the beam cross-section; the rest of the answers presented no definite data.

Recommendation:

Radiation field uniformity over the beam cross-section used in calibration should be tested.

Several methods have been used to investigate the uniformity of the beam. In one method three apertures of different diameters were used with the standard chamber to find out whether the ionization current was proportional to the aperture area. Another method (communicated by Aston, 1961) involves the exploration of a diameter of the beam with a restricted part of an ionization chamber, this restriction being obtained by a diaphragm with a slit of uniform width approximately equal to that of the chambers of the exposure meters to be calibrated. It was found that the average exposure rate over the chamber of the largest instrument used for therapy did not differ by more than 1 part in 1,000 from the average exposure rate over the aperture of the standard. The spread of rates so determined amounted in some cases to several parts in 1,000. Stevens and Richardson (1961) made radiographs at right angles to the central ray and measured the density of the image at a great number of points using densitometers with 1 and 2 mm aperture diameters. McLaughlin (1962) also used a photographic method and concluded that the relative exposure rate across the beam could be determined with an accuracy of 1 percent.

(2) *Scattered radiation.* The monitor may receive a different amount of scattered radiation when the standard is in the measuring position than when the chamber to be calibrated is in the measuring position. This error may be important when large monitor chambers are used or if the distance from the monitor to the standard is small. To avoid this, Rajewsky et al., (1955) placed a diaphragm between the monitor and the chamber. The answers to the questionnaire of most laboratories and the measurements of Stevens and Richardson (1961), and Henry and Aitken (1961), however, lead to the following conclusion:

If the distance between monitor and standard chamber is at least 50 cm and the monitor chamber diameter not substantially larger than that of the beam, this error is of minor importance.

(3) *Timing errors.* If the irradiation interval is defined by switching the x-ray tube on and off, or by unearthing the meters and switching off the x-ray tube, difference in energy dependence between the monitor and the other chambers may cause errors during x-ray tube potential buildup, and the grounding switches for the monitor and standard may not work simultaneously. These errors are difficult to evaluate and are greater when the timing is different for the standard and the reference or field instrument

Recommendation:

A mechanical shutter should be used. If a mechanical shutter is used and the arrangement of the monitor or the chamber to be calibrated is not symmetrical about the beam axis passing through the standard aperture, slight irregularities in the irradiation timing may arise if the shutter moves to and fro. In asymmetrical arrangements, the shutter therefore should always move in the same direction, or high speed shutter mechanisms should be used.

The timing errors may be evaluated by comparing the average ionization current collected for two different shutter-controlled timing periods. Timing errors introduced by shutter operation may be reduced to an acceptable level by lengthening the exposure period. If the operation of the shutter [12] requires more than a fraction of a second, exposures of several minutes' duration may be required.

The shutter error may be avoided for those

[12] Publication of the details of acceptable shutter designs is encouraged.

instruments that have a charge or current indicator which is connected during instrument exposure. In this case the time is taken from the time at which the detector is ungrounded to the time at which it is grounded. The beam is "on" during this procedure.

d. *Off-focus radiation.* In order that the monitor, the standard, and the instrument to be calibrated "see" the same source of radiation, and to prevent too great a beam divergence inside the standard chamber, it is usually considered wise to reduce the effect of off-focus radiation as much as possible. This may be accomplished by placing the first diaphragm as close to the tube window as possible. In addition, it will be worthwile to place a second diaphragm between this one and the monitor chamber. This second diaphragm will further reduce the amount of off-focus radiation "seen" by the monitor. Such an arrangement might place the monitor chamber at a larger distance from the source and therefore reduce its sensitivity somewhat, but it has the added advantage of being further removed from the heat which is developed within the tube. Under these conditions the temperature of the monitor will be more nearly constant.

e. *Exposure rates used for calibrations.* Calibrations with the large free-air chambers necessary in the medium energy region call for relatively large distances between the chamber and the tube focus in order to keep the beam divergence inside the chamber within permissible limits. For this reason instruments will, as a rule, be calibrated at low exposure rates. Maximum exposure rates among the standardization laboratories who answered the questionnaire range between 2 and 20 R/min at medium filtration. At the heaviest filtration used, maximum exposure rates obtainable at the calibration position were sometimes as low as 0.1 R/min.

These exposure rates have the disadvantage of being generally much lower than those for which the instruments will be used. Furthermore, the calibration of insensitive instruments will take considerable time, which may introduce appreciable errors due to instability and leakage. In order to investigate these sources of error, it is recommended that, in addition to calibration, the relevant tests from those mentioned below (Testing Procedures Associated with Calibration) should be performed.

For the calibration of a high sensitivity instrument very low exposure rates may be required. These exposure rates can be obtained by high filtration, but the resulting spectral distribution may differ appreciably from that for which the instrument is to be used in the field. If the calibration factor for the instrument is very energy dependent, such a modification of the spectrum may not be acceptable. In such a case one of the following methods may be preferred.

(i) Low x-ray tube current. This can be recommended where unstable leakage currents or other causes do not render the maintenance of a sufficiently constant low tube current difficult.

(ii) Large distance between the tube and the calibration position. This can be recommended if sufficient space is available and backscatter from surrounding materials is negligible. As this method tends to give greater field uniformity for large instruments it may be especially useful for their calibration. Due to the relatively low sensitivity of the standard it may be necessary to use a shorter target distance for the standard than for the sensitive field instrument. If so, correction has to be made both for the inverse square and air absorption effect on the exposure. Alternatively a sensitive reference instrument may be used for the beam measurement at the place of interest.

The following evaluation has no reference to these low exposure-rate calibrations.

f. *Evaluation of exposure-meter calibration accuracy for the region from about 60 to about 400 kv x rays.* An estimation of maximum uncertainty in calibration procedure with good techniques at medium exposure rates gives the following figures:

	Percent
Exposure standards*	±1.0
Monitor, during calibration:	
Volume fluctuations	.1
Air density	.2
Charge measurement	.1
Distance	.1
Shutter operation	.1
Stray radiation	.1
Irradiation field nonuniformity	.2
Total	±1.9

*See subsection IIA for components of this uncertainty.

This evaluation does not take into account the uncertainty in the reading of the instrument to be calibrated. The estimated maximum[13] uncertainty therefore is:

±(1.9 percent+reading uncertainty of instrument to be calibrated).

2. Exposure Meters Used for 0.5 to a Few Mev

This section deals with the calibration of reference and field instruments against exposure standards in the energy range from about 0.5 to a few Mev. These exposure standards, which are described in section IIA2, are graphite ionization chambers, except in the U.S.S.R. where a pressurized air chamber is used. There has for some time been discussion as to which point in a cavity ionization chamber should be taken as the effective point of measurement but it is now generally accepted that the center of the chamber should be taken as this point (Burlin, 1959). It is the practice of all the standardizing laboratories to place the center of the ionization chamber of the reference instrument at the specified point in the beam of radiation. The source-chamber distance used in the various laboratories varies from 70 to 180 cm and the field

[13] With the best techniques, some of these errors can be reduced. For example, in the case of a highly stabilized output, the total monitor-induced uncertainty can be reduced to about 0.1 percent. However, for x rays generated by potentials of less than 60 kev, the total uncertainty may be larger.

sizes at the calibration positions from 4.5×4.5 cm to 33×33 cm. One laboratory has published an account of its calibration technique (Barnard et al., 1956).

There is no general agreement on the uncertainties associated with such calibrations. The major source of disagreement arises from the uncertainties associated with the exposure standard.

3. Exposure-Rate Meters

For the calibration of an exposure rate meter, its position, P, in the x-ray beam and the target current are so adjusted that the desired scale reading is obtained. When high stability tube output is used, the exposure rate in the beam at this position is then determined by the standard or by a reference instrument. It should be noted that the time enters here only in the measurement with the standard or reference instrument and not with the instrument to be calibrated. Therefore, an absolute value determination is necessary. Thus, when an exposure standard for 60 to 400 kv x rays is used, the estimated maximum uncertainty found for the calibration of exposure meters will be augmented by ±0.2 percent for time measurements, giving a total of ±(2.1 percent+reading uncertainty of instrument to be calibrated).

When, however, a reference instrument is used, which has been calibrated with good techniques, the evaluation will be:

	Percent
Calibration of reference instrument	±1. 9
Reading error with reference instrument	. 2
Time measurements	. 2
Monitor	*. 4
Distance	. 1
Shutter operation	. 1
Stray radiation	. 1
Irradiation field nonuniformity	. 2
Total	±3. 2

*If a monitor is used, the exposure rate (L) is found by the formula

$$L=\frac{E}{Q_1}\times\frac{Q_2}{t},$$

where E=the exposure measured by the standard or reference instrument in position P during the time in which a charge Q_1 is collected in the monitor. Q_2=the charge collected in the monitor during a time t in which the instrument to be calibrated, in position P, is kept exactly at the desired scale reading by manual regulation of the target current.

This figure also is to be augmented by the reading uncertainty of the instrument to be calibrated.

At high exposure rates care should be taken that saturation conditions in the reference instrument, as well as in the monitor, are satisfied.

4. Testing Procedures Associated with Calibration

A common experience of standardization laboratories is that during calibration a number of instruments to be calibrated show irregularities of some kind, which make calibration difficult or impossible. Furthermore, the presence of stem leakage and the like will have a certain influence upon the calibration results. It is, of course, largely a question of policy of the individual standardization laboratories as to whether they can investigate such irregularities in detail. If such service is not available at the calibration center, the owner may wish to perform his own special tests or have them done elsewhere.

In a number of cases, however, conditions during calibration will make it imperative that the standardization laboratories test at least some of the instruments' properties before calibration. All tests should be done after proper warming-up time and, if possible, repeated after an interval.

a. *Zero drift.* In instruments where the radiation sensitive part (e.g., the ionization chamber) is permanently connected to the measuring instrument, zero drift should be determined. This test should be carried out after a period of at least 12 hours during which the exposure meter has not been irradiated.

b. *Leakage in ionization chamber exposure meters.* Ordinary leakage, due to inadequate insulation, can be determined by giving the collector system a charge which produces a reading of about ⅔ total scale or more and observing during an adequate period whether there is any appreciable loss.

Stem leakage in exposure or exposure rate instruments, due to ionization gains or losses in insufficiently shielded air cavities in the stem can be determined by placing the ionization chamber together with the stem in a uniform beam of radiation of sufficient diameter. Readings are to be taken with shielded and unshielded stem. Care must be exercised to assure that scattering from the shield does not adversely affect the results.

This test is also appropriate for exposure-rate meters. If insufficiently-shielded preamplifiers are housed in the stem, even weak stray radiation may have appreciable effects. In this case the stem may have to be shielded from all sides to find these effects.

If an appreciable stem leakage is found, this should be stated in the calibration report, as well as the length of the part of stem exposed during calibration. DIN 6817 (1962) requires that, if the ionization chamber is shielded while other irradiation conditions remain the same, no reading may be detectable. This procedure, apt though it may be to detect any spurious charges leaking to the collector part of the instrument, is unable to detect any *loss* of charge through leakage to earth. To cover both possibilities, this test would have to be done with and without an initial charge on the collector.

c. *Exposure-rate dependence.* Many exposure or exposure-rate meters are of a design which makes the determination of saturation curves by a standardization laboratory impracticable. Moreover, lack of saturation need not be the only cause of exposure-rate dependency.

The only decisive way of testing exposure rate dependence is a calibration both at high and low exposure rates.

d. *Radiation-quality dependence.* Standardizing laboratories will in general calibrate exposure

or exposure-rate meters only at the radiation qualities requested. It is, however, recommended, if an instrument is to be calibrated at one fixed quality in a region where quality dependence may be suspected, that the standardization laboratory advise the owner to have the instrument calibrated at some adjacent qualities, in order to obtain an idea about the instrument's quality dependence.

e. *Anisotropy.* Ionization chambers which are apparently axially symmetrical sometimes show marked nonuniformity of wall thickness. Also, the collector electrode may be eccentrically positioned. Either of these may cause a sensitivity shift when the orientation of the chamber in the beam is changed. The standardization laboratory should either measure the influence of these factors, especially when low-energy radiation is used, or indicate the orientation of the chamber relative to the beam when the chamber was calibrated.

f. *Scale characteristics.* If one or more points on the scale of an exposure meter have been calibrated, the rest of the scale of those instruments where the chamber or other radiation sensitive part is continuously connected to the measuring part may be tested by means of a constant exposure rate, e.g., from a radioactive source. The chamber should be exposed to this radiation in such a way that the pointer moves slowly (e.g., 1–2 scale divisions per minute). Variation of the timing for different parts of the scale is then a measure of the lack of uniformity of the scale.

D. Instrument Performance

1. Requirements

The requirements are of necessity a compromise between the wishes of the user and the ability of the manufacturer to satisfy them. For clinical instruments, the limits of the user's needs can, to a certain degree, be derived from an inquiry made by Ellis (1959) and from the inquiry mentioned below.

General requirements can be found, for instance, in the Report of the ICRU (1959), the "Code of Practice for X-ray Measurements" prepared by the Hospital Physicists' Association (1960) and, in more detail, in the draft DIN 6817 (1962) of the German Standardization Commission.

An inquiry was made among a number of radiologists, physicists, and institutions in Belgium, Germany, Italy, the Netherlands, Sweden, and the United Kingdom in order to obtain information about their requirements regarding sensitivity, accuracy, and other physical properties of the instruments. The information obtained was partly collected by and discussed with representatives of industrial firms, in order to know to what extent commercial instruments could meet the users' demands.

It was found that the requirements regarding acceptable uncertainty had a rather large spread lying partly within the limits of maximum calibration error as evaluated in the preceding section. According to this inquiry, the acceptable uncertainty for reference and field instruments in the range between 100 kv and a few Mv varied generally between 2 and 5 percent. This means that generally high accuracy was required.

The industry stated that it is not in a position to meet the extremes of the users' requirements. It claimed, however, to be able to meet them to a large extent.

This statement can easily be confirmed as far as measuring range and sensitive volume dimensions are concerned. It has, however, been shown (ICRU Report, 1959, section 7.2) that the accuracy of commercial instruments has in a number of cases been overrated. Therefore, in the next section recommendations have been made for the performance of reference instruments.

2. Performance of Reference Instruments [14]

a. *Calibration.* All reference instruments should be calibrated and a written report of the results should be available.

This report should indicate: (i) The correction factors by which the readings are to be multiplied to obtain the exposure or exposure rate for each radiation quality at which the instrument was calibrated; (ii) scale readings of the calibration point(s) or interval(s); (iii) for unsealed chambers, temperature and pressure (corrected for humidity) for which the correction factors are valid; (iv) readings shortly before or after calibration with any checking device provided with the instrument; (v) the exposure standard against which the instrument was calibrated; and (vi) the date of calibration.

The correction factors should enable the user to measure exposure with a maximum uncertainty of ± 3 percent at the qualities and readings indicated. (This uncertainty applies in the range where the calibration uncertainty against the exposure standard is about ± 2 percent.)

b. *Scale characteristics.* The scale error depends on the reading and indication uncertainty and scale nonlinearity of the measuring device (electrometer, scaler, potentiometer, etc.). It should not exceed ± 1 percent of the full scale reading.

c. *Leakage.* Errors may result from insulation effects (inherent and induced leakage and electrical aftereffects) and stem leakage. The latter may cause errors of considerable amount in a condenser ionization chamber using high energy x and gamma radiation (Braestrup and Mooney, 1958).

Leakage should be tested routinely. The correction due to leakage should not exceed 1 percent of the value measured.

d. *Exposure-rate dependence.* Errors due to exposure-rate dependence generally result from saturation defects or dead-time effects. It is recommended that the operating instructions of the instrument should state over what range the error due to exposure-rate dependence does not exceed 1 percent.

[14] This subsection includes excerpts from ICRU Report (1959).

e. *Energy dependence.* It is not possible to make an ionization chamber of the cavity type with an energy-independent response over a wide range of radiation quality. It is therefore recommended that the instrument should not be used outside the quality range for which it has been calibrated unless the energy dependency there is sufficiently well known for the desired measuring accuracy.

f. *Incident-beam-direction dependency.* Errors due to this source may be eliminated by irradiating the chamber in the same orientation relative to the beam as during its calibration against the exposure standard.

g. *Atmospheric temperature, pressure and humidity.* If the chamber is not hermetically sealed, it is recommended that accurate instruments be available for the measurement of atmospheric conditions to determine the correction factor. After moving the instrument to a new location, it should be permitted time to attain temperature and pressure equilibrium before measurements are made. Attention is called to the possibility that chambers usually not sealed may inadvertently become sealed because of a very tight-fitting outer wall or other defects.

h. *Operation and constancy checks.* It is recommended that a carefully constructed checking device containing a radioactive source for the irradiation of the chamber in a fixed geometry be available. If the chamber is not hermetically sealed, readings must be corrected for temperature, humidity, and pressure.

E. Measurement Techniques

1. Composition of the Radiation Beam

The beam includes:

(i) primary radiation (including any off-focus emission),

(ii) scattered radiation which is able to reach the ionization chamber from any part of the collimating system, including applicators (cones), etc., and from the irradiated air,

(iii) corpuscular radiation (electrons) arising from similar places and able to reach the chamber. (Normally, these electrons are almost completely absorbed in the wall of the chamber and therefore do not contribute significantly to its reading; see footnote 11 at beginning of this section for a detailed discussion of electron contamination).

2. Field and Point of Measurement

The exposure rate in air at a point on the central ray increases with the area of the beam, due to the increased contribution of off-focus emission and radiation scattered from the diaphragm system, from the irradiated air and from other objects. This is exemplified in figure IIIE1 for a 250 kv x ray machine (Farr, 1955a).

More marked variation is introduced by scattered radiation from the walls and end plate of an applicator (cone). The magnitude of the effect depends upon the design of the applicator; representative figures for 50–250 kv x rays have been given by Bradshaw (1953) and Bailey and Beyer (1957).

The presence of such scattered radiation may be demonstrated by measuring the exposure rate at points along the central ray and plotting the product of the exposure and the square of the distance to the source, versus distance. Typical results are shown in figure IIIE2 for 250 kv x rays and a closed-ended applicator (Farr, 1955a).

In the megavoltage region, the amount of radiation scattered by the irradiated material is less dependent upon the atomic number of the material but more of the low energy scattered radiation is absorbed by a higher than by a low atomic number scatterer. The radiation observed from a high atomic number scatterer may thus have a higher average energy than that for a low atomic number (Martin and Muller, 1961). The amount of scatter produced from source capsule, diaphragms, etc., depends less on the type of materials used than on the geometrical construction. Published data of the dependence of output from various megavoltage apparatus upon the beam size confirm this. The data also show that the proportion of scattered radiation in the beam does not vary very widely with energy from 1–4 Mev. They also suggest that the actual geometrical relationships between the source, diaphragm, and chamber may affect the amount of scatter only by a few percent of the total radiation, provided care is taken to minimize this in the diaphragm design. This is illustrated in figure IIIE3.

In radiotherapy, the exposure rate in air is commonly measured either at a point corresponding to the surface of the object to be irradiated or at the center of revolution of a moving source. Where no applicators are used, the point of

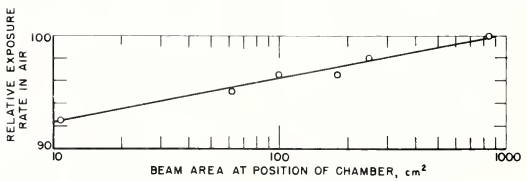

FIGURE IIIE1. *Variation of relative exposure rate in air with field area (source-chamber distance, SCD, 50 cm; HVL 1.8 mm Cu), the beam being defined by a simple diaphragm 21 cm from the source (Farr, 1955a).*

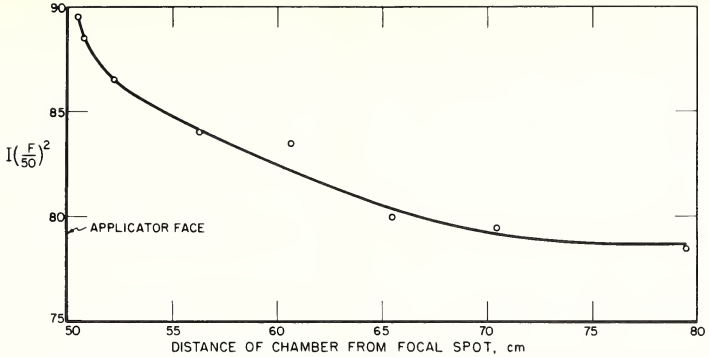

FIGURE IIIE2. $I(F/50)^2$ *plotted against* F *for a closed ended applicator (SCD 50 cm, 10 cm diameter, HVL 1.8 mm* Cu) *where* I *is the measured exposure rate on the central ray at distance* F *from the source (Farr, 1955a).*

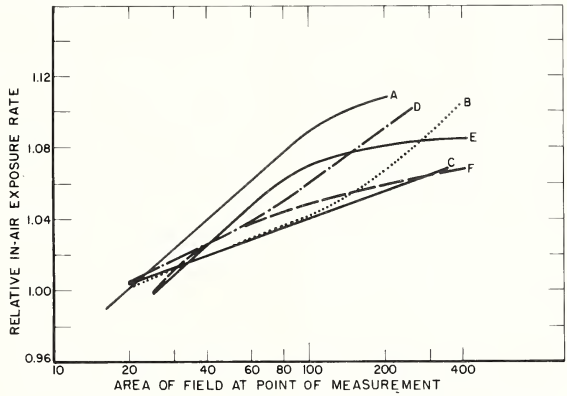

FIGURE IIIE3. *Variation of relative exposure rate with field area for various equipments, designated by reference letters only.*

Curves A: Co–60 (type 'A'). A good fit for data at 60, 70 and 75 cm source-chamber distance (SCD) (Wilson, unpublished). Data for a Cs^{137} gamma beam apparatus also fit this curve (Burns, unpublished); B: 2 Mv generator (type 'B'), 100 cm SCD, (Burns, unpublished); C: Co^{60} (type 'C'). SCD 80 cm, multivane diaphragm (Kemp and Burns, 1958). This data is also a close fit for 4 Mv data; D: Co^{60} (type 'D'), SCD 60 cm (Burns, unpublished). For curves A, B, C, and D relative outputs are taken as unity for a 4x4 cm field; E: 300 kv generator (type 'E'). 4 mm Cu HVL, SCD 50 cm (Trout, Kelley, and Lucas, unpublished); and F: 2000 kv generator (type 'F'). 7 mm Pb HVL, SCD, 100 cm (Trout et al., unpublished). For curves E and F relative outputs are taken as unity for a 5x5 cm field.

measurement will be freely accessible. When open-ended applicators are used, the ionization chamber should be placed in the middle of the x-ray field with its center as nearly as possible in the place of the end of the applicator (Hospital Physicists' Association, 1960).

With closed-ended applicators, the exposure rate in air at the surface may be obtained with sufficient accuracy (Hospital Physicists' Association, 1960) for most purposes by making measurements in the middle of the field with the chamber (or its stem) in contact with the surface and applying a simple inverse-square-law correction. This correction does not take into account the effect of the scattered radiation from the applicator sides and end which may introduce an error of a few percent, and which will increase with chamber size. For higher accuracy an extrapolation technique may be applied.

3. Special Problems Relating to Low-Voltage X Rays

The measurement of exposure rate in air at the open end of an applicator presents particular problems in the 5–50 kv range. This is due to (a) the short SSD in comparison with the diameter

of typical thimble chambers, and (b) their wavelength dependence in this energy region. For the design of special chambers for this purpose, consideration must be given to (i) minimizing the absorption in the chamber walls, and (ii) ensuring saturation at high dose rates. The exposure rate in air may be measured with a compact free air chamber (Greening, 1960), but this may not, for reasons of geometry, include the soft secondary radiation from the walls of such an applicator (Meredith, 1940). Suitable secondary chambers have been described by Oosterkamp and Proper (1952) and Tranter (1961).

4. Output Measurement Technique

The specification of the output of an x-ray tube or gamma-ray beam source requires a statement of the measurement conditions. These include (i) the voltage, tube current, filter, HVL, and other pertinent operating conditions of the x-ray machine, or the nuclide(s) and the date in the case of a gamma-ray beam source; (ii) the source-chamber distance, the beam dimensions employed, and the type of collimator.

The following precautions should be taken in the measurement of output.

(i) Care should be taken to minimize extraneous radiation from nearby objects.

(ii) Sufficient time must be allowed for the exposure meter to achieve temperature and pressure equilibrium with its surroundings. Appropriate corrections for the actual temperature and pressure conditions must be applied to the readings obtained.

(iii) The measurement should be made at the point of interest. The location of this point has been discussed in section IIIE2. In using published depth-exposure data, it should be recognized that the exposure at the surface is affected more by the scatter contributions from the collimating system (including applicators) than is the exposure in a depth. In view of this variation, a measurement taken at 5 cm depth in water (equivalent) phantom may be a more reliable basis for use of published depth-exposure data in radiotherapy.

(iv) The field size should not be so large as to produce undue scattered radiation and to irradiate unnecessarily large parts of the exposure-meter insulator.[15] On the other hand, the beam size should not be so small as to prevent the whole of the effective volume of the chamber seeing the entire source. The measurement, therefore, inevitably includes a small percentage of scattered radiation. The field size employed should be as close as practicable to that used in the calibration of the chamber though, in general, a field size of 10×10 cm, or 10-cm diameter, is recommended for 250-kv equipment (Farr, 1955a) and for gamma-beam equipments (Braestrup and Mooney, 1958).

[15] Useful figures for typical radiation-induced leakage have been given by Braestrup and Mooney (1958) for a common type of condenser chamber exposure meter.

(v) Measurements should be repeated from time to time to determine possible variations in output. The output of an x-ray tube often decreases throughout its useful life due to increased absorption caused by the roughening of the target and by the deposition of tungsten on the tube window, and to other factors. The drop in output is usually greatest with low filtration. The output of some multisection x-ray tubes has been found to vary with tube angulation. When determining the reduction in output, due to radioactive decay of a cesium source, it is necessary to take account not only of the decay of the Cs^{137} (half-life 30 yr), but also of any contamination by Cs^{134} (half-life 2.3 yr) (Wheatley et al., 1960).

F. Exposure Distribution in the Beam

This subsection considers the distribution of exposure or exposure rate in a plane normal to the central ray, at the usual SSD in air. If the distribution of exposure rate is circularly symmetrical about the central ray, then it is necessary only to map the distribution along one line perpendicular to the central ray. Such symmetry usually exists for a transmission x-ray target. If, however, the electrons do not all have the same velocity and if they are bent by a magnetic field before striking the target, some asymmetry may be introduced into the exposure distribution (Newberry and Bewley, 1955). The distribution of exposure rate from a reflection x-ray target does not usually show such circular symmetry and it is necessary to map it along two lines, perpendicular to the central ray. One of these lines should be parallel and the other perpendicular to the tube axis.

1. Gamma Beam Equipment

The distribution of exposure rate is usually symmetrical but tends to drop more rapidly toward the periphery of the field than would be expected from the inverse square law.

2. Transmission X-Ray Targets

For high-energy generators which use transmission targets the distribution of exposure rate is usually symmetrical but shows a greater falloff toward the edge of the field than is the case with a gamma-ray beam equipment. It is governed principally by the physical laws of bremsstrahlung and, to a lesser extent, by obliquity of filtration of the x rays in their passage through the target and other filters. Fortunately, such generators are able to produce copious output and it is usual to employ a conical filter so shaped as to make the exposure rate in air nearly constant across the field. For example, the exposure rate may be made uniform across a 30-cm-diameter field at 100-cm SSD by sacrificing one-third of the output on the central ray of a 4-Mv linear accelerator (Greene and Tranter, 1956).

3. Reflection X-Ray Targets

The distribution of exposure rate from a reflection target has neither the symmetry nor comparative uniformity of that from a gamma-ray beam equipment. Nor is there usually available the high output to permit the use of a flattening filter, such as is provided by the high energy x-ray machine.

a. *Exposure distribution along a line perpendicular to the tube axis.* The exposure rate usually decreases symmetrically on either side of the central ray by an amount determined by (i) the inverse square law, (ii) obliquity of filtration, and (iii) the design of the tube, and the windows of tube and housing. Tubes of different makes may vary in this respect (fig. IIIF1), a particularly poor distribution being produced (curve IV) by a reentrant oil displacement cone (Farr, 1955b).

b. *Exposure distribution along a line parallel to the tube axis.* The exposure rate does not usually decrease symmetrically on either side but falls off more rapidly in either the cathode or the anode direction, depending on the target angle of the tube. (The target angle is the angle between the direction of the electron stream and the normal to the target face.)

Figures IIIF2 and IIIF3 illustrate the wide range of distributions which can be shown by tubes of different makes operating at the same voltage. These curves indicate that these distributions are the product of three effects depicted diagrammatically in figure IIIF4 and discussed by Farr (1955b).

(i) The symmetrical factors, identical with those affecting the distribution of exposure rate along the line perpendicular to the tube axis, would produce a similar distribution along this line (curve a).

(ii) The predominantly forward emission of x rays generated at any point within the target

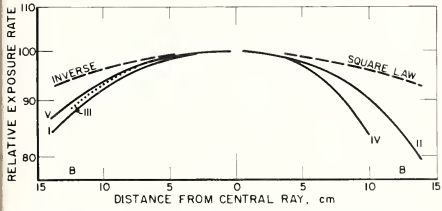

FIGURE IIIF1. *Relative exposure rate along a line perpendicular to both the tube axis and the central ray (50 cm source-chamber distance, 200-265 kv, HVL 1.7 mm* Cu) *for a number of different makes of tube.*

Dashed line shows effect of inverse square law (Farr, 1955b).

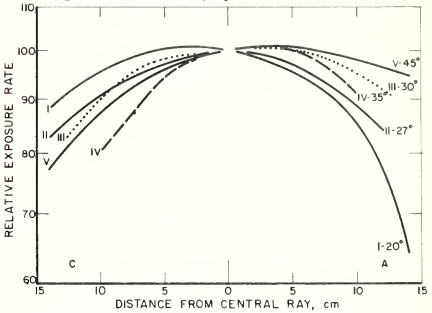

FIGURE IIIF2. *Relative exposure rate along a line perpendicular to the central ray and parallel to the tube axis (otherwise same conditions as figure IIIF1) for a number of tubes of different makes and target angles. (Farr, 1955b).*

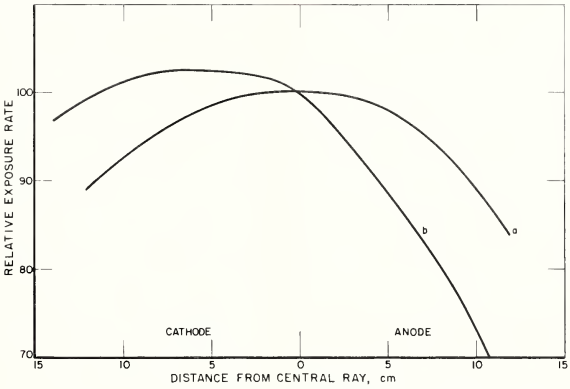

FIGURE IIIF3. *Relative exposure rate distribution across the field of an x-ray tube operated at 100–140 kv.*

(a) Parallel to tube axis of 45 degree target.
(b) Perpendicular to tube axis of 20 degree target (Farr, unpublished).

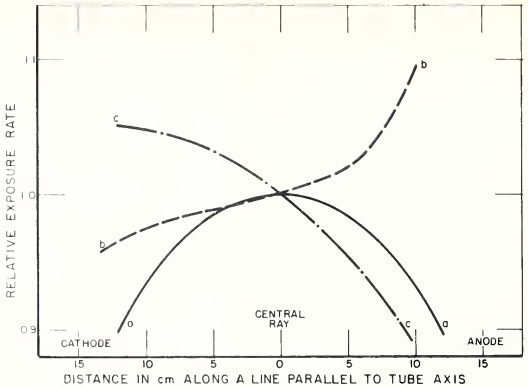

FIGURE IIIF4. *Diagrammatic representation of (a) symmetrical factors applying to distribution along any line, (b) emission effect, (c) heel effect applying to distribution of exposure rate along a line parallel to the tube axis.*

produces a rise of exposure rate from the cathode to the anode end of the field (curve b). The magnitude of this "forward emission" effect increases with tube voltage.

(iii) The absorption of the rays, generated at a depth within the target, increases as the angle made with the target face by the emergent ray decreases. This "heel effect" causes a decrease of exposure rate from the cathode to the anode end of the field (curve c), and becomes less marked the greater the filtration.[16] The absorption, in the target, of x radiation which originates from its interior is too complex for satisfactory theoretical treatment. It has been estimated (Farr, 1955b) that the effective depth of penetration of the cathode stream at 250 kv is about 5 microns and that, in a typical tube, this produces an equivalent filtration of the central ray of about 0.2 mm Cu. The corresponding equivalent filtration for a tube operated at 10–50 kv has been estimated (Jennings, 1953) as 0.04 mm aluminum.

c. *Optimum target angle.* The above considerations suggest that it may be possible to choose the target angle (in relation to tube voltage and filtration) so as roughly to balance the two unsymmetrical curves b and c and thus produce a nearly symmetrical distribution of exposure rate along the line parallel to the tube axis. Indeed, it appears (Farr, 1955b) that at 250 kv the heel and emission effects can be balanced so that the distribution along that line follows curve a, the same as that along the line perpendicular to the tube axis.

With low filtration (HVL=0.5 mm copper) this is achieved at 250 kv by a target angle of about 30 degrees. With increasing filtration, the heel effect becomes less pronounced, and the optimum angle becomes somewhat smaller (Farr, 1955b).

[16] The "heel effect" also results in an increase of HVL from cathode to the anode side of the beam (see section IV).

At lower kilovoltages, similar considerations hold. The optimum angle at 140 kv and HVL 3 mm aluminum is about 45 degrees (Farr, 1955b). Atlee and Trout (1943) recommend the use of a curved target.

4. Desirable Distribution of Exposure Rate in Air

a. *Radiotherapy.* Undue variation of exposure rate in air across the section of the beam distorts the isodose curves in a phantom in such a way to make the application of general isodose curves uncertain (Farr, 1955b). The distribution of exposure rate in air should therefore be as uniform as can be obtained by reasonable care in the design of the tube and the housing window. They should be designed so as to produce as uniform as possible a distribution of exposure rate along a line perpendicular to the tube axis, and the angle of the target should be chosen to give, for the desired quality range of radiation, a distribution of exposure rate along a line parallel to the tube axis as symmetrical as possible. In this way, the distribution can be made approximately symmetrical about the central ray with some decrease in exposure rate at the periphery.

If a single x-ray tube is used over a wide range of voltages, e.g., 100–300 kv, account must be taken of the change of exposure distribution which may occur over that range. Under these circumstances, the tube should have a target angle appropriate to the lower voltage; i.e., 45 degrees. It is possible to design an aluminum filter for use at the higher voltage which will compensate for the unsymmetrical distribution of exposure rate in the anode-cathode direction. Similarly, it is possible to design special filters to make the exposure rate in air constant over the useful beam, which may be desirable for some purposes (Farr, 1955b).

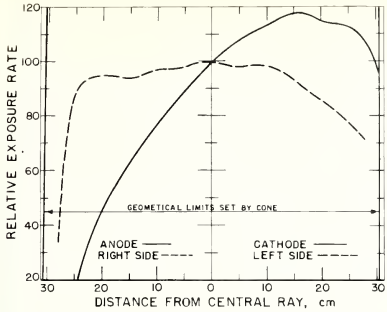

FIGURE IIIF5. *Distribution of exposure rate across the field of a diagnostic x-ray tube (Kemp, 1946).*

Full line indicates anode-cathode distribution; dotted line, normal to above.

b. *Radiography.* In radiography the desirable target angle is governed by other considerations. For this application the angle is usually small and the "heel" effect pronounced. There is a marked fall of exposure rate towards the anode end of the field (fig. IIIF5) which becomes more pronounced as the target roughens during the life of the tube (Beetlestone and Thurmer, 1958). Because of the latitude of films and the tolerance of the human eye, the heel effect is generally of little account in radiography. It is sometimes turned to good purpose if gross variations in the thickness of the subject can be matched by variations of exposure dose rate across the field.

A tube designed for radiography, with a steep target, is unsuitable for therapy or other applications where a uniform field is required (fig. IIIF2 and IIIF3).

IV. The Specification and Measurement of Radiation Quality

A. Introduction

A complete specification of x and gamma radiation at the place of interest must include not only an expression of quantity, such as exposure or energy fluence, but also information as to the quality of the radiation. Such information is required to predict the penetration of a beam of radiation, to calculate differential absorption in various materials and in attempting to explain variations in biological effectiveness. As a measure of the penetrating ability of a beam, it has been the practice to express the quality in terms of the half-value layer (HVL). This single parameter is usually inadequate and additional parameters are required. A discussion of the HVL and related ways of expressing the quality of a radiation beam is given in subsection IVB.

A more complete expression of the quality of x and gamma rays is the spectral distribution of fluence, energy fluence, or exposure as a function of photon energy. Spectral distributions of radiation beams and of the radiation at points within an irradiated medium are discussed in subsection IVC. If the spectrum of the incident radiation is known, the scattered radiation within the medium may be calculated under certain conditions of radiological interest. Some equivalent HVL's of the total radiation for various fields are also given.

The relative biological effectivess of various radiations is best correlated with the radiation quality expressed in terms of the microscopic distribution of energy along the tracks of the ionizing particles. Subsection IVD contains a brief discussion of the initial distribution of electrons set in motion in an irradiated medium and of the energy deposition by these electrons.

B. Quality of the Incident Beam Expressed in Terms of Potential, Half Value Layer and Other Parameters

1. Specification of Quality by a Single Parameter

a. *Tube potential.* In the case of radiation from high-energy x-ray machines (1 to 4 Mv), quality is frequently described simply by a statement of the accelerating potential, provided such beams are heavily filtered by the transmission target. The choice of this somewhat inadequate specification of quality may be attributed to the less rapid variation of attenuation coefficients with energy in this region, thus rendering the methods of quality specification based on attenuation less precise than at lower energies. The same quality specification is frequently used at lower energies when the radiation suffers considerable attenuation, such as in certain problems in radiation protection and x-ray diagnosis.

b. *Half value layer (HVL).* The HVL is that thickness of material necessary to produce a reduction to 50 percent of the initial exposure rate. Suitable materials for such measurements, and details of recommended techniques, are discussed in subsection IVB6. This method has been very widely used for x rays, especially in the field of radiation therapy where is has been most useful. However, it is not always an adequate specification for the determination of percentage depth dose (Jennings, 1950; Trout et al., 1962) or backscatter factor (Greening, 1954; Trout et al., 1962). HVL can be improved as a specification of quality by restricting the combination of filter and kv used to produce such a value of HVL (Thoraeus, 1936, 1958), but in such circumstances the specifications almost fall into the category discussed below (tube potential and HVL).

For gamma ray beams identification of the source(s) is generally sufficient, although attenuation measurements of gamma ray beams are sometimes made and the HVL quoted. Even with good geometry, it is not possible to eliminate scattered radiation entirely. The observed HVL is therefore somewhat less than that calculated for the known source energy levels (see subsection IVB6a(2)).

c. *Attenuation coefficient.* If a tangent is

drawn to an attenuation curve plotted semilogarithmically, the slope of this tangent gives the attenuation coefficient of the radiation after passing through the absorber thickness at which the tangent was drawn. Special cases are tangents at the origin (Taylor, 1931) and at very large absorber thicknesses.

d. *Equivalent wavelength or equivalent energy.* One of the oldest methods of specifying the quality of a heterogeneous radiation beam is to express it in terms of wavelength or energy of that monochromatic radiation which would show the same particular property as the heterogeneous radiation; e.g., same HVL in a certain absorber. This wavelength or energy is then called the equivalent wavelength or equivalent energy of the heterogeneous radiation. It is essential in any such statement of quality to indicate the respect in which the radiations are equivalent, as different equivalent wavelengths or energies will result from consideration of different properties of the radiations.

2. Specification of Quality by Two Parameters

a. *Tube potential and HVL.* Bell (1936) thought that these two parameters were sufficient to give the spectral distribution of the radiation, but Jones (1940) showed this to be inadequate for some purposes. However, for most clinical purposes these two parameters give an appropriate specification of radiation quality and are recommended in preference to a statement of HVL only.

b. *HVL and homogeneity coefficient, h.* The HVL is that thickness of material necessary to reduce the initial exposure rate to 50 percent, and the second HVL is the *additional* thickness necessary to reduce the exposure rate to 25 percent of the initial value. The ratio of the first to the second HVL is termed the homogeneity coefficient, h, and is unity for monoenergetic rays.

Figures IVB1a and IVB1b (Hettinger and Starfelt, 1958a) show the spectral distributions of radiations produced by 100 kv and 220 kv accelerating potentials, respectively. These radiations have approximately the same HVL (0.59 and 0.55 mm of copper) but obviously very different spectral distributions. This difference is characterized by their very different homogeneity coefficients of 0.88 and 0.40, respectively. Trout et al., (1962) have made a detailed examination of the homogeneity coefficient for many radiation beams. A few of their data are shown in figures IVB2 and IVB3 which give homogeneity coefficients as a function of HVL in copper and aluminum respectively for x-ray beams produced between 100 and 300 kv.

When x-ray beams contain an appreciable amount of characteristic radiation with an energy considerably different from the peak of the continuous spectrum, the significance of the homogeneity coefficient must be reconsidered. As Zieler (1954, 1957) has shown, the intense L-characteristic radiations from tungsten are largely transmitted by tubes containing only 1 mm Be filtration, yielding relatively homogeneous beams.

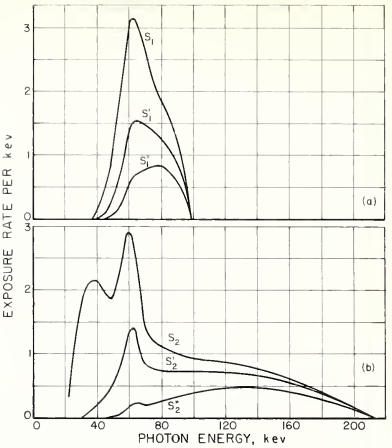

FIGURE IVB1 a and 1b. *Spectral distribution of exposure rate for x rays produced by (a) 100 kv accelerating potential, 4 mm* Al *inherent + 1.67 mm* Al + *0.87 mm* Cu *filtration (curve* S_1*) and (b) 220 kv, 4 mm* Al *inherent filtration only (curve* S_2*). (Hettinger and Starfelt, 1958a).*

Curves S′ and S″ are the calculated spectral distributions after the radiation has passed through 1 and 2 HVL of Cu, respectively.

Increasing aluminum filtration results first in a less, and then in a more homogeneous beam. Thus the coefficient h will possess first a maximum, and then a minimum, with increasing filtration (see also Wagner, 1957). A similar effect would be expected to occur with lightly filtered x rays above 200 kv (see, for example, fig. IVB1b), in which there is an appreciable amount of K-characteristic radiation. Under these conditions, the homogeneity coefficient, h, is no longer a useful concept.

3. Specification of Quality in Terms of Depth Dose in Tissue

For low voltage x-ray treatments, a measure of radiation penetration in soft tissue forms a useful concept of "quality". If this were to be a measure of the radiation beam leaving the tube, it would have to be expressed in terms of percentage depth dose for zero field area and infinite SSD. Such a concept has little advantage over attenuation measurements in aluminum or copper for a fixed target-chamber distance. On the other hand, the percentage depth dose given for specified field areas and SSD is useful and of direct meaning to the clinician.

The specification adopted may take the form of a complete depth-exposure curve from the surface (100 percent) to the level at which the exposure rate is reduced, say, to 10 percent; or it may be restricted to one or two selected points. The depth at which the exposure rate has been reduced to 50 percent of the surface value is termed *half-*

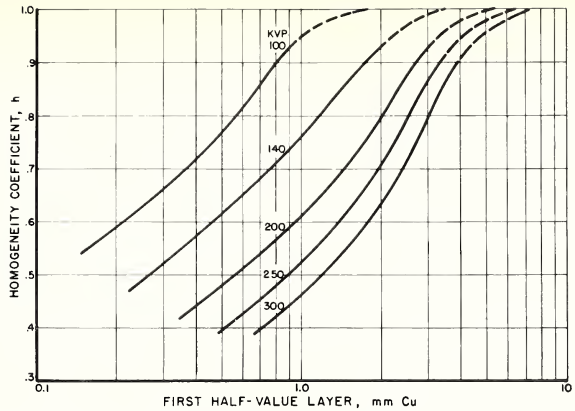

FIGURE IVB2. *Homogeneity coefficient as a function of HVL in copper for radiations generated at 100 to 300 kv.*

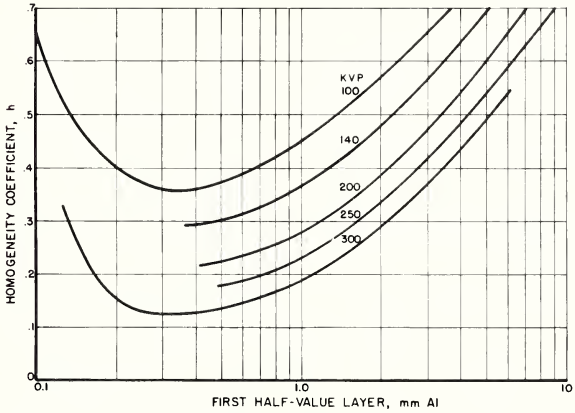

FIGURE IVB3. *Homegeneity coefficient as a function of HVL in aluminum for radiations generated at 100 to 300 kv.*

value-depth or HVD or $D_{\frac{1}{2}}$ (Mayneord, 1940) and this has been advocated as a useful concept (see, for example, Smithers (1946), Jennings (1950; 1951), Proppe and Wagner (1954)).

However, at low energies, it has been found that (a) the HVD in tissue can vary for a given HVL in aluminum, and (b) the depth at which the exposure rate is reduced to 10 percent of the surface value ($D_{\frac{1}{10}}$) can vary for a given HVD in tissue. Both of these factors are dependent on the kv-filter combination used to obtain the HVL or HVD. Their significance for radiations generated under 50 kv is shown in tables IVB1 and IVB2.

Thus, a two-point specification is desirable. This may consist of HVD together with the potential employed, or the $D_{\frac{1}{2}}$ and the $D_{\frac{1}{10}}$. The ratio $D_{\frac{1}{10}}/D_{\frac{1}{2}}$ termed the "Fall-off" Ratio (F.O.R.) has been studied by Jennings (1950) and Tuddenham (1957), and figures are included in tables IVB1 and IVB2.

4. Distribution of Quality Over Field Area in Air

The predominantly forward emission of x rays generated at a point within a reflection target causes a *decrease* of the exposure rate from the cathode to the anode side of the field, as discussed in section III. At the same time, a phenomenon (called the "heel" effect) results in an *increase* in the HVL of the beam from cathode to anode side of the field on account of the internal filtration at the target. This is exemplified in figure IVB4 for a diagnostic x-ray tube, and in figure IVB5 for two deep-therapy x-ray tubes with different target angles.

5. Choice of Appropriate Quality Specification

The more rapidly the penetration of the beam varies with energy, the more detailed the knowledge of radiation quality required. However, for most clinical purposes a statement of the potential and HVL is recommended. The choice of method is given below in order of successive stages of complexity:

a. *Specification of nuclide.* In gamma-ray beam equipment, identification of the source(s) is generally an adequate specification of quality, except for those sources where filtration or scattering affects the quality.

b. *Tube potential.* When the spectral distribution (and hence subsequent penetration) changes slowly with filtration (over ≈ 1 Mv), the quality may be specified by the accelerating potential alone. This statement may be useful also for highly filtered low-voltage beams, but for most applications, this specification is insufficient.

c. *Half value layer.* A statement of HVL alone may be sufficient if the kv-filter combinations are those normally employed clinically.

d. *Half value depth in "tissue," HVD.* For low voltage x-ray treatments, the concept of HVD in mm "tissue" forms a useful quality specification of direct meaning to a clinician. However, this specification is not restricted to the incident beam (except for zero area and infinite SSD) because the HVD is related to a selected field area and SSD.

e. *Equivalent wavelength or energy.* The equivalent wavelength or energy can be determined from the attenuation curve, though care must be taken in selecting the point on the curve. For example, if only a small fraction of the radiation is absorbed in producing the effect, such as the calibration of exposure meters, the exposure of photographic emulsions, or the irradiation of thin specimens, one may choose an equivalent wavelength or energy derived by drawing a tangent near the origin. On the other hand, in some protection work and in some diagnostic x-ray measurements in which the radiation is heavily attenuated, the equivalent wavelength should be derived from a point of low percentage transmission on the curve. This method is infrequently used in clinical work.

f. *Tube potential and HVL.* At potentials under ≈ 0.5 Mv, and in other applications where the addition of filtration or small changes in potential can materially alter the penetration, a statement of potential and HVL is suitable, and is generally recommended for clinical work.

g. *HVL and homogeneity coefficient,* h. When unusual kv-filter combinations are employed, and the potential is not accurately known, a statement of the HVL and homogeneity coefficient, h, is desirable.

h. *Complete attenuation curve.* If a complete attenuation curve is measured with sufficient accuracy, it can be employed to obtain the spectral distribution of the radiation beam by absorption analysis (see section IVC2a). A few points only on the attenuation curve are sufficient when less detailed information is required.

i. *Spectral distribution.* The most complete statement of radiation beam quality is given by the spectral distribution obtained, as discussed in section IVC. This knowledge makes it possible to calculate the relative amount and quality of the scattered radiation at various points in a medium. Such information is useful, for example, in estimating the dose in nonwater-equivalent tissues, in allowing for energy dependence in films and other dosemeters, and in calculating electron and linear-energy-transfer distributions.

TABLE IVB1. *Two examples of the variations in $D_{1/2}$ and $D_{1/10}$ for a given HVL in Al. All the data relates to a 5-cm-diameter field at 10 cm SSD*

HVL mm Al	kv(p)	Added filtration mm Al	HVD (or $D_{1/2}$) mm "tissue"	$D_{1/10}$ mm "tissue"	F.O.R. (see text)
0.3	50	0.40	5.2	28.6	5.5
	30	.44	4.7	22.6	4.8
	20	.60	4.0	16.0	4.0
0.5	50	.55	7.1	34.1	4.8
	30	.74	6.7	27.5	4.1
	20	1.3	6.2	22.0	3.55

NOTE: Although the 2 HVD ranges above do not overlap, those for $D_{1/10}$ do. Thus it is possible to have 0.3 mm Al HVL yielding a more "penetrating" beam than one of 0.5 mm Al HVL.

TABLE IVB2. *Two examples of the variations in $D_{1/10}$ for a given HVD in "tissue", the data relating to a 5-cm-diameter field at 10 cm SSD*

HVD mm "tissue"	kv(p)	Ext. filtration mm Al	$D_{1/10}$ mm "tissue"	F.O.R. (see text)
2.0	37	0.1	10.4	5.2
	20.5	.2	9.7	4.85
	16.5	.3	9.2	4.6
	14	.4	8.0	4.0
10	45	1.0	40	4.0
	32	1.5	37	3.7
	27	2.0	35.5	3.55

NOTE: Possible variations in $D_{1/10}$ depths are reduced by specifying HVD in "tissue" instead of HVL in Al, but the F.O.R. remains as variable (and HVD is a function of field size and SSD). Jennings (1951); see also Wagner (1953).

6. The Measurement of HVL

a. *Materials.* Materials chosen for HVL meas-

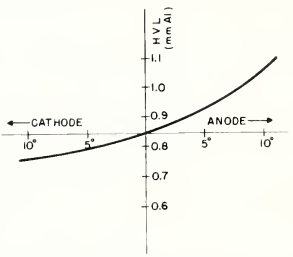

FIGURE IVB4. *Distribution of HVL from the cathode to anode side of a beam from a diagnostic x-ray tube (Kemp, 1946).*

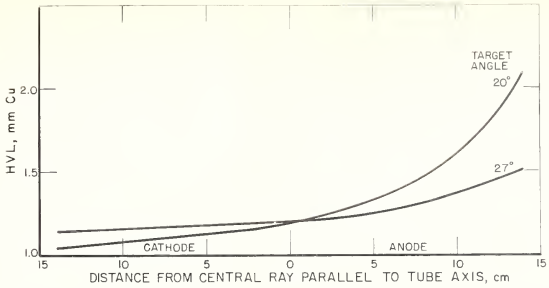

FIGURE IVB5. *Distribution of HVL along a line parallel to the tube axis and perpendicular to the central ray (200–230 kv, 20 degree and 27 degree targets) (Farr, unpublished).*

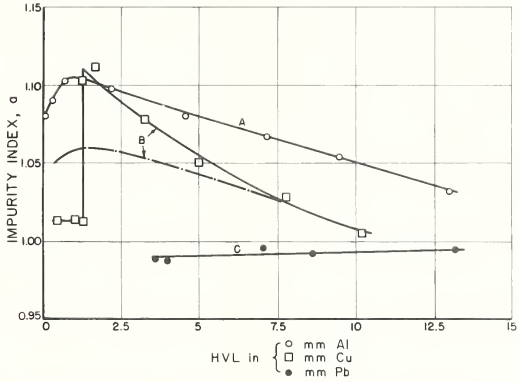

FIGURE IVB6. *Impurity index,* a, *as a function of HVL*

A. Impurity of 1 percent Cu in Al (HVL in mm Al)
B. Impurity of 1 percent Pb in Cu (HVL in mm Cu)
C. Impurity of 1 percent Fe in Pb (HVL in mm Pb)

The plotted values and full-line curve (*B*) apply to monoenergetic radiation (discontinuity arises from Pb *K*-edge); the chain-dotted curve attempts to display values appropriate to continuous x-ray spectra.

urements should be solids of definite composition and density and which can be made into thin sheets of uniform thickness.

The quality range over which a given material can yield unequivocal values of HVL will depend upon the shape of the graph relating the total absorption coefficient for the material to the energy of the radiation. The occurrence of discontinuities at the lower energies (absorption edge phenomena), or of minimum values at the higher energies (caused by the onset of pair-production process) will help to define the useful quality range.

Although tin has sometimes been used for HVL measurements, reference to a variety of tabulated data indicates that its density can vary over rather a wide range, being dependent on crystalline form. Moreover, at the lower energies its range of usefulness is limited by the energy of its K-absorption edge (29 kev). Therefore, tin cannot be recommended as a standard material for HVL measurement.

The chemical purity of the material must also be considered, particularly at the lower energies, where the absorption processes are governed more by atomic number than by electron density.

(1) *Chemical purity.* Hübner (1958) derived expressions which enable the influence of known amounts of impurities to be evaluated numerically. In particular, he obtained an expression for a dimensionless constant, *a*, which gives directly the factor by which the HVL as measured with impure material must be multiplied to give the corresponding value for the pure material. This constant serves also as a numerical index of the effect of the impurities. Jones (1961) has evaluated *a* on the assumption that a given material (Al, Cu, or Pb) contains an impurity

688-008 O - 64 - 6

element, differing in atomic number from that of the basic material by as much as is likely, and amounting in each case to 1 percent by weight. The results are shown graphically in figure IVB6, where a is plotted as a function of HVL ,the latter being derived from the relationship $HVL = 0.69\,\mu^{-1}$ where μ is the linear attenuation coefficient. The latter is determined from the product of the mass attenuation coefficient (White Grodstein, 1957) and the density of the pure metals. The densities used were 2.70 g/cm^3 for aluminum, 8.93 for copper, and 11.35 for lead (*International Critical Tables*, 1926). Since a varies very nearly linearly with percentage impurity, a-values appropriate to other impurity levels are easily derived.

It is concluded (Jones, 1961) that as regards impurity effects, generally available grades of lead (99.9 percent pure) and copper (99.2 percent pure) are adequate, whereas for aluminum, grades must be selected which are at least 99.8 percent pure.

For the specification of HVL, "effective" thicknesses of attenuators[17] should be used. These are the quotient of the measured mass per unit area by the density of the material.

(2) *Useful quality range.* Jones (1961) considers the extent to which absorption edges can set a lower limit to the energy at which aluminum, copper and lead should be used for HVL determination. As a rough guide the x-ray generating potential should be not lower than about four times the characteristic K-absorption limit. It follows that the lower limits for copper and lead are 35 and 350 kv, respectively. For aluminum this limit is too low to be of significance (6 kv). An upper limit will occur where the onset of pair production causes a minimum in the attenuation coefficient. To avoid the confusion arising from there being two energy values related to the same absorption coefficient, the peak energy of the x-ray beam should be below the energy at which the minimum is reached for the attenuating medium concerned. The minima are found at about 3.5 Mev for lead, at 8 Mev for copper, and at about 20 Mev for aluminum.

In consequence of the above considerations, it is necessary to restrict the ranges over which these materials are used for HVL measurements, and the following table summarizes the position:

	Acceptable range for HVL measurements
Aluminum	10 kv-10 (or more) Mv
Copper	35 kv-8 Mv
Lead	350 kv-3.5 Mv

Practical considerations may further limit this useful range.

For cobalt-60 gamma rays, aluminum, copper and lead are equally satisfactory attenuating media, provided that the measurements are carried out under conditions of good geometry. Due to the presence of scattered radiation, the observed HVL is somewhat less than that calculated for the source energy levels. For example, Johns et al., (1952a) found 10.5 ± 0.1 cm for the HVL in water as compared with 11.0 cm calculated for the known average energy of 1.25 Mev. Jones (1961) gives the following experimental values of HVL for a cobalt-60 beam: 4.47 cm aluminum, 1.40 cm copper, and 0.96 cm lead, for which the associated equivalent energies are: 1.15, 1.12, and 1.13 Mev, respectively. The HVL in water quoted by Johns et al., is consistent with 1.13 Mev.

b. *HVL measurement technique.* A determination of HVL entails the measurement of exposure rate at a selected point as increasing thicknesses of appropriate attenuating material are placed in the path of the beam. A monitoring chamber may be useful with x rays to permit correction for any variation in exposure rate. It should be placed so that its readings are independent of the amount of absorbing material placed in the beam. The chamber used for the attenuation measurements should have a minimum quality dependence over the range concerned.

Consideration must be given to the conditions required to minimize the influence of the scattered radiation emitted by the attenuator which would otherwise increase the HVL obtained. Thus Farr (1955a) investigated the effect of variations in field size, and of source-attenuator-chamber spacing, on the HVL obtained, and Trout et al., (1960, 1961) have demonstrated how a unique HVL can be derived for the 100–300 kv range.

(1) *100–300 kv x-ray beams.* In order to minimize the influence of scattered radiations, the following conditions should be observed: Limiting of the field size reduces the amount of scattered radiation that reaches the exposure meter, but the field must be large enough so that the chamber "sees" all of the source. Great care must be taken with alinement (e.g., radiographic check). The diaphragm must be of sufficient thickness to absorb the primary beam. In order to avoid transmission through the edge of the collimator, a slightly conically shaped aperture is advantageous at the higher energies.

Figure IVB7 (Somerwil, 1957) illustrates the extent by which the measured HVL decreases with decreasing field diameter, d, at the attenuator. The figure also shows that for d less than 5 cm, the attenuator-chamber distance, b, should be at least equal to the source-attenuator distance, F, which in this case was 20 cm. This condition is to be expected when the source may be considered as a point source for the geometrical arrangement concerned. However, when the source and chamber sizes are significant in relation to the diaphragm dimensions at the attenuator, then the optimum position of the attenuator may be about half way between the source and the chamber (Tarrant, 1932; Seeman, 1938; Hettinger and Cormack, private communication, 1962). Hence, as a general rule, the attenuating material should be placed approximately midway between the source and the chamber, and for this quality range, a source-chamber distance of at least 50 cm should be used (Farr, 1955a).

For clinical purposes, HVL derived in this way

[17] Less precise (measured) thicknesses may be adequate for clinical needs.

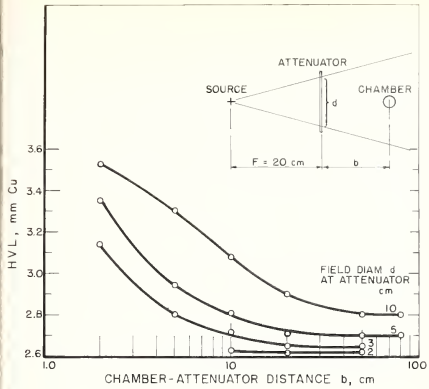

FIGURE IVB7. *Variation of HVL with field diameter,* d, *at the attenuator, and with chamber-attenuator distance,* b.

250 kv, 2 mm Cu filtration, source-attenuator distance F=20 cm. (Somerwil, private communication, 1957).

will be of sufficient accuracy (H.P.A. Code of Practice, 1960) because the percentage depth dose data are not critically dependent on HVL; see, for example, "Depth Dose Tables for use in Radiotherapy" (fig. D.1, Hospital Physicists' Association, 1961).

When greater precision is necessary, a "unique" HVL can be arrived at by a method developed by Trout et al., (1960). This consists in deriving the zero-field-area value, either by an extrapolation technique, or by applying correction factors based on such measurements, thus eliminating the effects of the otherwise unavoidable scattered radiations. By measuring HVL for at least two, and preferably three or more diaphragm sizes, a linear extrapolation of a plot of HVL against the aperture diameter will yield the zero-area value. To derive the zero-area HVL from a single HVL measurement, correction factors should be applied depending on the field area, source-attenuator and source-chamber distances employed. If the measurements are made with a source chamber distance of 50 cm and the attenuators placed midway between them, then the curves of figure IVB8 can be applied for any field diameter up to 10 cm (at the attenuator position) to correct to zero-area. For other source attenuator and source-chamber distances, additional correction factors are provided in the papers of Trout et al., (1960, 1961).

(2) *Under ≈100 kv x-ray beams.* In addition to observing the points stated in the previous section, particular attention should be given to any effect of chamber wavelength dependence. Morrison and Reed (1952) have shown that corrections of 5–10 percent may be required for HVL measured in the 0.5–2 mm aluminum HVL range with chambers whose readings have to be corrected for quality. The corrections can be derived by a method of successive approxima-

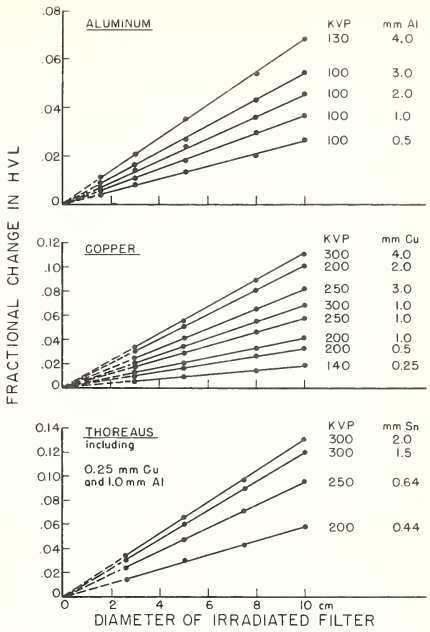

FIGURE IVB8. *Fractional change of HVL with diameter of irradiated absorber, for the indicated potentials and filtrations with* F=b=*25 cm.*

(See Figure IVB7 for definitions of *F* and *b*).
Aluminum and copper curves from Trout et al., (1960); Thoraeus curves from Trout et al., (1961).

tions, provided an absolute calibration curve (to correct for readings obtained at known HVL's) is available for the chamber. A transmission curve is first obtained in terms of the observed readings without correction, from which a series of apparent HVL's can be obtained for a range of added filtrations. Correction factors for these HVL's are then read from the calibration curve, and applied to the original readings to give a second percentage transmission curve. This process can be repeated, the new factors obtained being applied to the original readings, though in practice, a single approximation curve is usually sufficient.

At a lower end of the range (under ≈0.5 mm aluminum HVL) the relation of HVL to filtration for a given kv undergoes a double bend (see Jennings, 1950, fig. 22 and Zieler 1956, fig. 8). This is due to the contribution of L-characteristic radiations from tungsten, as discussed in subsection IVB2.

(3) *Over ≈300 kv x-ray beams and gamma-ray beams.* As in the 100–300 kv range extraneous scatter should be reduced to a minimum, and the diaphragm placed about midway between the

688-008 O - 64 - 7

source and the chamber. Under these circumstances, Jones (1961) has shown for a Co^{60} beam that if the semiangle subtended by the irradiated filter at the chamber position does not exceed $\tan^{-1}$ 0.02 (1 degree), then the HVL obtained (in aluminum, copper or lead) will be within 0.5 percent of the zero-area value.

If larger fields are employed, correction to zero-area values—the unique HVL—can be achieved by extrapolation. Jones (1961) finds that a plot of the HVL obtained is linear with the square of the aperture diameter. Trout, Kelley, and Lucas (private communication, 1961) find that this relationship holds for angles up to 0.08 steradians corresponding to an attenuator area of ≈ 50 cm^2 at a source-attenuator distance of 27 cm. For this area, the fractional change in HVL is ≈ 6 and 10 percent for lead and copper, respectively.

Measurements made by Trout et al., (private communication, 1961) with 1 and 2 Mv x-ray generators, indicate a more restricted range of linear extrapolation, but greater attenuator areas can be employed with the greater spacing practicable at the higher energies. For small angles (under 0.04 steradians), the fractional increase in HVL is ≈ 1 percent per 0.01 steradians, using copper or lead attenuators, and for both equipments.

C. Spectra of X and Gamma Radiation

1. Introduction

In this subsection both primary and secondary radiation are considered. Secondary radiation arises when material is irradiated and consists mainly of photons degraded in energy by one or more Compton scattering processes. In some cases the characteristic (fluorescent) radiation from heavier materials may give considerable contribution to secondary radiation. At a point within the irradiated medium secondary radiation will be incident from all possible directions and may have a different spectral distribution in each direction.

2. Methods of Determining Photon Spectra

a. In *absorption analysis* the spectral distribution is calculated from a transmission curve which must be measured with high accuracy. In practice it is necessary to measure the transmission through a suitable absorber under conditions of good geometry until less than 10 percent of the incident radiation remains. The radiation detector should have an essentially uniform response to radiation of all energies in the beam. The transmission curve can then be fitted to one of about four different functions which have been suggested, each having usually two adjustable constants. These constants, when determined, are substituted in corresponding functions (actually the inverse Laplace transformations) in order to calculate the spectral distribution. The theory of absorption analysis is given by Silberstein (1932), Jones (1940), and Greening (1947, 1950, 1952) among others. Cormack et al., (1955) and Wang et al., (1957b) compared spectra obtained by the attenuation method with those obtained by scintillation spectrometry, and found good agreement for 280 kv and 50 kv x rays, respectively. Other recent determinations of x-ray spectra with the use of absorption analysis have been made by Burke and Pettit (1960) and Trout et al., (1961). Greening (1951) determined the spectrum of primary and secondary x radiation within a block of irradiated material. He used spherical ionization chambers enclosed in shells of absorbing materials.

The amount of spectral information obtainable by this method is limited by the accuracy to which the transmission curve can be measured and by the limited number of parameters used in the curve fitting. The method is usually limited to relatively simple spectra although Greening (1947) has developed a method allowing for the presence of characteristic radiations.

b. *Scintillation spectrometry* has become a common method of determining photon spectra. A sodium iodide crystal is the most commonly used scintillator. When such a crystal is irradiated each absorbed photon gives rise to a light pulse or scintillation, which can be observed by a multiplier phototube and converted into an electric pulse with a height nearly proportional to the absorbed energy. After amplification the electric pulses are sorted in a pulse-height analyzer. The recorded pulse-height distribution constitutes the response of the detector to the whole radiation spectrum and has to be corrected for distortions such as those due to statistical fluctuations and incomplete absorption of the incident photon energy. The pulse-height distribution may be represented as a column matrix P, where each element indicates the number of pulses within a certain pulse height interval. The unknown radiation spectrum may in an analogous way be represented as another column matrix N, with the same number of elements as matrix P. With this notation the relation between P and N, with a small approximation, may be written in the following way:

$$P = M \cdot N$$

where M is a quadratic response matrix. Symbolically the unknown spectrum N can be written as

$$N = M^{-1} \cdot P$$

where M^{-1} is the inverse response matrix. If the energy intervals are chosen large enough the response matrix is nonsingular and its inverse can be calculated. However, objection may be raised against correction of the pulse-height distribution for the statistical spread with the inverse matrix method (Dixon and Aitken, 1958). It is more suitable to correct the pulse-height distribution for such spread through some kind of analytical or numerical solution of the Fredholm integral equation that describes the statistical spread in pulse height (Lidén and Starfelt, 1954 and Dixon and Aitken, 1958). After this correction the in-

verse matrix method may be applied to correct for the escape effects (Rawson and Cormack, 1958 and Hubbell, 1958). It is also possible to obtain the radiation spectrum by applying successive approximations of the noninverted matrix equation (Hettinger and Starfelt, 1958a and Skarsgard et al., 1961).

If one measures radiation spectra, which are smooth and broad, and uses a total absorbing scintillation detector (Hettinger and Starfelt, 1958b), the Gaussian spread has little influence on the spectra. If the correction for the spread is omitted and the pulse-height distributions set equal to the radiation spectra, the introduced error is unimportant (Hettinger and Lidén, 1960).

Primary and secondary radiation are usually measured with different experimental arrangements. The measured spectra of secondary radiation have to be normalized with regard to the flux of the primary radiation. Either both primary and secondary radiation have to be measured in absolute units (photons per kev, cm^2, second and unit solid angle) or the normalization factor must be calculated from tabulated or measured exposure data. If the spectral distributions are measured in absolute units, conventional depth dose tables and backscatter data can be used as a check of the obtained spectra with regard to magnitude and shape (Hettinger and Lidén, 1960; Hettinger, 1960b; and Skarsgard and Johns, 1961).

c. *Theoretically calculated spectra* of scattered radiation of radiological interest have been published by Bruce and Johns (1960). The distributions of scattered x rays were determined through a combination of analytic and Monte Carlo methods. The contribution of once-scattered radiation was calculated analytically and added to the results of Monte Carlo calculations of multiple scatter.

3. Spectra of Primary Radiation

a. *Spectra of x rays,* 20–400 kv. A number of experimental determinations of the radiation emitted by x-ray tubes with thick targets have been made, the majority of the work being done in the past few years. An attempt will be made to survey the published data, to compare some spectra measured in various laboratories and to assess the applicability of the relation of Kulenkampff (1922) and Kramers (1923). The discussion will be concerned with the shapes of the spectra and with the absolute magnitude of the bremsstrahlung and the characteristic radiation from the target.

Table IVC1 lists present available data concerning primary spectra of x rays generated at potentials from 20 kv to 400 kv. It will be noted that spectra have been reported for a wide variety of makes and types of generator and for various voltage wave-forms; they are expressed as various kinds of distributions. Most spectra measured with scintillation spectrometers are presented as number fluence distribution (N_k) as a function of photon energy (k), whereas spectra derived from absorption analysis are usually given as an exposure distribution against wave length (X_λ vs λ). The filtration of the primary beam varies considerably from one spectrum to another. The most appropriate form in which a spectrum is finally presented will depend upon the use to be made of it. The choice among distributions of number fluence, energy fluence and exposure against photon energy will depend upon the particular circumstances.

It would be highly desirable to obtain a general empirical relation which would describe the shape of radiation spectra in terms of peak kilovoltage, waveform and filtration. A relation which has sometimes been used as a basis of comparison and which has the great advantage of simplicity is the thick-target formula found experimentally for x rays up to 40 kv by Kulenkampff (1922) and derived theoretically by Kramers (1923). This formula may be written as follows:

$$I_k = A(k_0 - k)$$

where I_k is the intensity distribution function, e.g., erg cm^{-2} sec^{-1} kev^{-1}, A is the constant for a given spectrum, k is the photon energy at which I_k is evaluated and k_0 is the maximum value of k.

TABLE IVC1. *Thick target primary spectra*

Reference	Method	Generator	kv	Wave form
Kulenkampff (1922)			20–50	
Greening (1947)	Abs		90, 220	C.P.
Greening (1950)	do	G.E. Maximar	150, 220	λ/2.
Johansson (1951)	Scint	Phil. Metalix	75, 100	C.P.
Ehrlich (1955)	do	Exp. Be window	20–100	C.P.
Kolb, Jaeger (1955, 1956)	do		25–50	C.P.
Cormack et al., (1955, 1958)	do	Picker Vanguard	280	λ/2.
Cormack et al., (1957a, b)	do	G.E. Maximar	400	λ/2.
Wang et al., (1957)	Abs. & Scint	Machlett OEG 60		λ/2.
		Machlett OEG 50	50	C.P.
Hettinger and Starfelt (1958a)	do	Philips MG 300	100–250	C.P.
		Siemens Tutomat	47, 75	λ.
Villforth et al., (1958)	do	West. Quandrocondex	30–250	C.P.
Aitken and Dixon (1958)	do	G.E. Be window	30–100	λ/2, C.P.
Cormack and Burke (1960)	do	Picker Vanguard	140	λ.
Burke and Pettit (1960)	Abs	G.E. XRD-3	20, 30, 50	λ.
Skarsgard and Johns (1961)	Scint	Siemens	250	C.P.
Trout et al., (1961)	Abs		200, 300	λ/2.

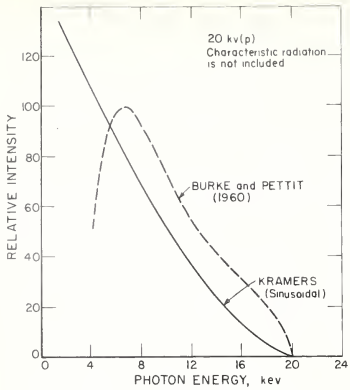

FIGURE IVC1. *Comparison of experimental spectrum (dotted line) and spectrum calculated from the Kulenkampff-Kramers formula (solid line) modified for filtration and voltage wave form.*

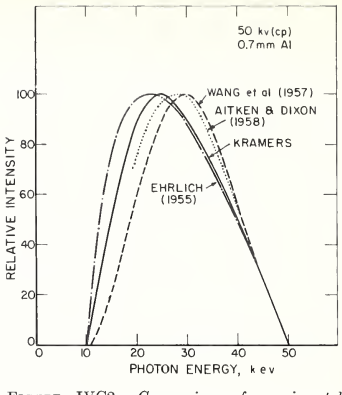

FIGURE IVC2. *Comparison of experimental spectra (dotted lines) and spectrum calculated from the Kulenkampff-Kramers formula (solid line) modified for filtration and voltage wave form.*

This relation refers to the thick target bremsstrahlung unaffected by the photon absorption within the target. The absorption within the target and the electron backscatter reduce mainly the low energy part of the spectrum. For purposes of comparison, some of the measured spectra are represented together with spectra calculated from the Kulenkampff-Kramers formula modified for pulsating wave form and for filtration of all materials between the target and the detector.

Burke and Pettit (1960) have used absorption analysis to measure x-ray spectra from tubes operated at 20, 30, and 50 kv. In order to separate the continuous and characteristic components of the spectra, they collected absorption data on various tubes which differed from each other only in target material. Their 20 kv spectrum is shown in figure IVC1 together with a theoretical spectrum averaged over the sinusoidal voltage waveform and decreased in correspondence to the attenuation of the tube window.

Hettinger and Starfelt (1958a) have carried out a series of measurements of primary spectra generated at constant potentials ranging from 45 to 250 kv. Several measurements have been made by other workers of spectra generated at 50 kv. An intercomparison between these spectra and the theoretical spectrum for a filtration of 0.7 mm Al is shown in figure IVC2. Wang et al., (1957a) also made measurements with lower filtration (0.0127 mm Al+1 mm Be) and estimated the contribution of characteristic radiation. Analysis of the shape of the scintillation spectrum indicated that 30 percent of the total intensity was due to characteristic radiation. Greening's (1947) method for analyzing the shape of the absorption curve indicated that characteristic radiation accounted for 40 percent of the total intensity.

At 45 and 50 kv there appears to be rather good agreement among the spectra of Hettinger and Starfelt, of Aitken and Dixon, and of Wang et al. The spectra obtained by all these workers have peaks at considerably higher photon energy than that predicted by the Kulenkampff-Kramers formula. The discrepancy between the theoretical and the experimental curves in figure IVC2 is less than in figure IVC1. As pointed out by Cormack (1960, 1961), the above-mentioned modified formula may be used for an approximate prediction of the spectral shapes of x rays for voltages above 100 kv. Figures IVC3, IVC4, IVC5, and IVC6 illustrate this condition at 140 kv (constant potential), 140 kv (sinusoidal voltage waveform), 250 kv (cp) and 280 kv (p), respectively. The peaks at about 60 kev are due to characteristic K-radiation from the tungsten target. When heavier filtration is used the agreement with the theoretical formula is very much improved.

Some spectra have been measured in absolute units. Figure IVC7 shows a comparison of a 100 kv (cp) spectrum calculated by Ehrlich (1955) and one measured by Hettinger and Starfelt (1958a). The experimental intensity distribution was corrected for the absorption in the window which was equivalent to about 4 mm Al.

Figure IVC8 shows the relative number of tungsten K-photons emitted along the central ray from an x-ray tube with an inherent filtration of 4 mm Al and operating at various constant voltages. According to earlier measurements (Compton and Allison, 1935), the absolute intensity of characteristic radiation varies with the difference between the exciting and critical voltages raised to a power of 1.6, Hettinger (1960a) found the value of this exponent to be 1.2 ± 0.1 (fig. IVC9).

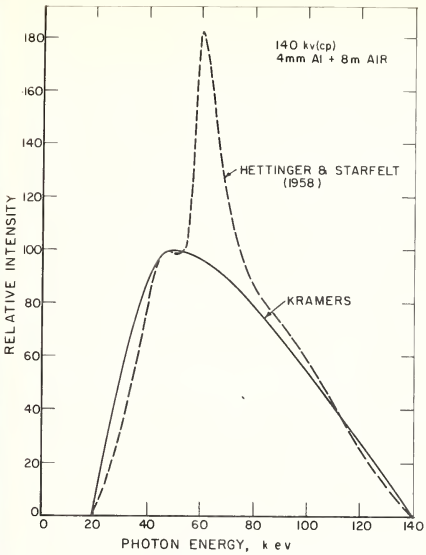

FIGURE IVC3. *Comparison of experimental spectrum (dotted line) and spectrum calculated from the Kulenkampff-Kramers formula (solid line) modified for filtration and voltage wave form.*

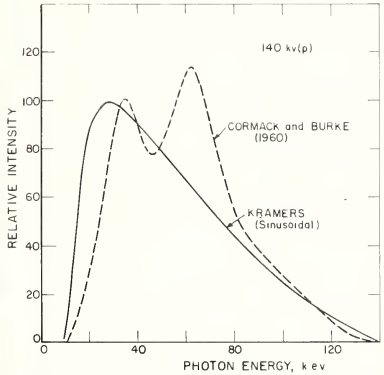

FIGURE IVC4. *Comparison of experimental spectrum (dotted line) and spectrum calculated from the Kulenkampff-Kramers formula (solid line) modified for filtration and voltage wave form.*

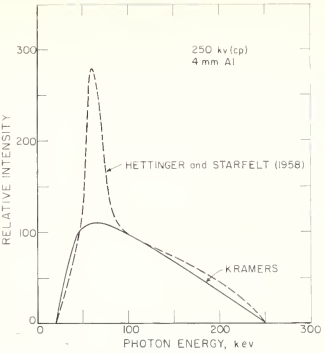

FIGURE IVC5. *Comparison of experimental spectrum (dotted line) and spectrum calculated from the Kulenkampff-Kramers formula (solid line) modified for filtration and voltage wave form.*

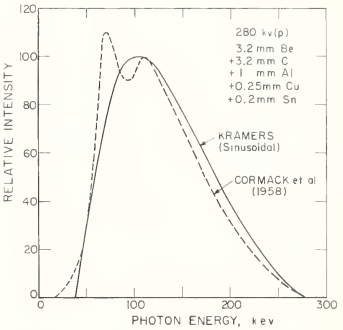

FIGURE IVC6. *Comparison of experimental spectrum (dotted line) and spectrum calculated from the Kulenkampff-Kramers formula (solid line) modified for filtration and voltage wave form.*

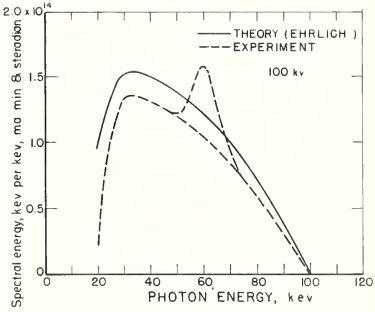

FIGURE IVC7. *Comparison between theoretical and experimental spectrum of 100 kv thick target bremsstrahlung. The peak at 60 kev in the experimental curve is due to characteristic tungsten K-radiation.*

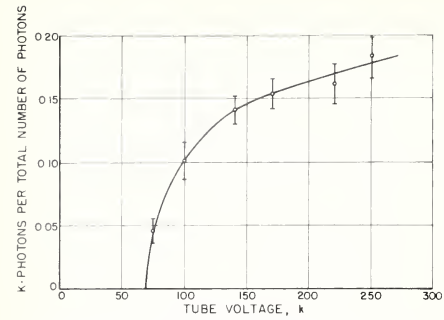

FIGURE IVC8. *The number of tungsten K-photons per total number of photons versus tube voltage (Hettinger and Starfelt, 1958a).*

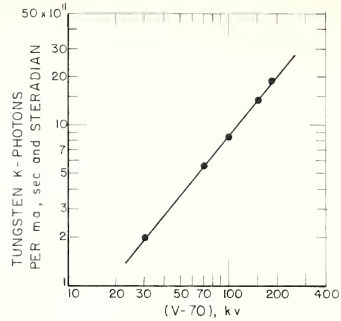

FIGURE IVC9. *The tungsten K-radiation intensity plotted against the difference between exciting voltage and critical voltage (70 kv) from Hettinger (1960a).*

TABLE IVC2. *Sources of experimental spectra for potentials of 1 Mv or greater*

Accelerating potential Mv	Machine type	Target		Method	Reference
		Material	Thickness		
1.0 1.25 1.4	Constant potential	W	2.8 mm/cos 45°	Compton	Miller et al., (1954).
1.0 1.5 2.0	Constant potential Van de Graaff	(Styrene Al Cu Ag Au	Approx. equal to electron range.	Scintillation	Edelsack et al., (1960).
2.8	Betatron	W Be	0.020″ 2.63 mg/cm²	Compton	Lasich and Riddiford (1947).
2.72 4.54 9.66	do	Al Au W	0.878 mg/cm² 0.209 mg/cm² 0.240 mg/cm² 0.489 0.5800	Scintillation	Starfelt and Koch (1956).
9	Linear accelerator	Cu	0.375″	Photo-protons	Phillips (1954).
11	Betatron			do	Wang and Wiener (1949).
11	do	W	0.060″ wire	Compton	Motz et al., (1953.)
17.5	do	Mo	0.002″ 0.005″ 0.022″	Pairs	Warner and Schrader (1954).
17.8	do	W	0.005″	Compton	Robson and Gregg (1957).
18.5	do	W	0.010″	Photo-protons	Phillips (1952).
19.5	do	Pt	0.005″	Pairs	Koch and Carter (1950).
22	do	Pt	Thin (see paper for details).	Photo-protons	Weinstock and Halpern (1955).
65	Synchrotron	W	0.005″	Pairs	Stokes (1951).
70	do	W	0.25″ diameter (but see paper).	do	McDiarmid (1952).

b. *Spectra of x rays*, 1–100 Mv. Data are less plentiful and generally less accurate in this energy range than they are below 0.4 Mv. Spectra have been obtained by means of scintillation spectrometry and by measuring the energies of Compton-recoil electrons, electron-positron pairs or photo-protons from deuterium. The last two methods preclude the detection of photons with energies below the thresholds of these reactions. Scintillation spectrometry gives better statistical accuracy and makes possible the detection of the, often important, low-energy photons.

Details of some experimentally determined spectra available in the literature are given in table IVC2, the better established ones between 1 and 10 Mv being shown in figures IVC10, IVC11, IVC12, and IVC13.

Spectra depend upon the thickness of target used, as this determines the extent to which the accelerated electrons are slowed down and scattered, and the absorption of photons in the target. The effective target thickness is often uncertain with betatrons and synchrotrons, and care should be exercised in applying the results obtained with one machine to a problem associated with another.

Above 10 Mv, and with thin targets, the theory of Schiff (1951) predicts spectral shapes which are in fair agreement with experiment. Hisdal (1957) has considered the effect of multiple scattering within the target on Schiff's theory. A comprehensive discussion of the bremsstrahlung spectra generated by electron energies of 1–100 Mev has been given by Koch and Motz (1959).

c. *Spectra of gamma-ray beams.* The radioactive nuclides which have been used as sources for beam therapy are listed in table IVC3 together with some of their physical properties. For such

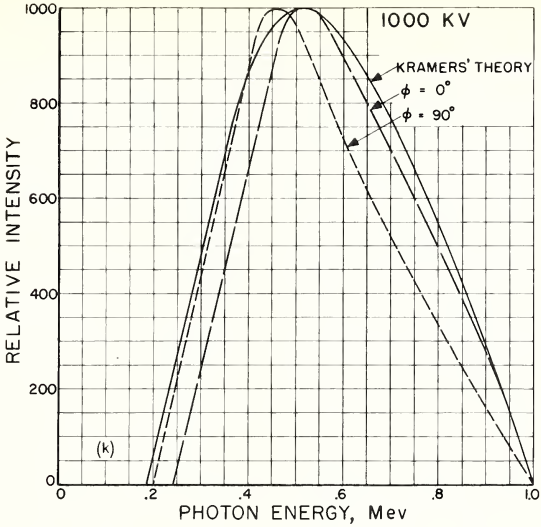

FIGURE IVC10. *X-ray spectra obtained at 1000-kv tube potential.*

Filtration: 2.8 mm W+2.8 mm Cu+18.7 mm water+2.1 mm brass. Dashed curves: spectra measured by Compton spectrometer (the ordinate is photon energy multiplied by number of photons of that energy) (Miller et al., 1954). Angles refer to direction of x rays relative to initial electron direction. Solid curve: spectrum calculated by Kramers' method (1923).

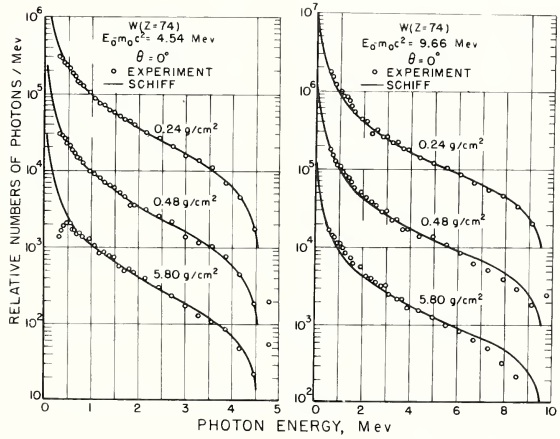

FIGURES IVC11 and IVC12. *Relative x-ray spectra (in photon/Mev interval) from a betatron (Starfelt and Koch, 1956).*

Curves are given for three tungsten target thicknesses: 0.24 g/cm², 0.48 g/cm², and 5.80 g/cm². Only the curve shapes, not their relative positions, are significant. The points were obtained with a scintillation spectrometer. The solid curves were calculated from the thin target formula of Schiff (1951), and normalized to the experimental data.

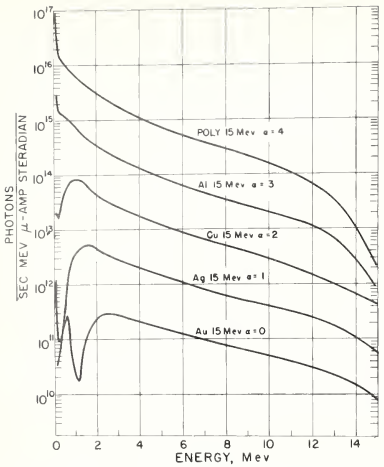

FIGURE IVC13. *Family of bremsstrahlung spectra for 1.5 Mev electrons on thick targets of different Z.*

The measurement is made at zero degrees relative to the incident electron direction. Each curve is multiplied by 10^{α} for clarity of presentation. (Edelsack et al., 1960).

use the radioactive material is enclosed in a metal capsule which effectively absorbs the beta radiation. The beam from a teletherapy unit will therefore contain primary gamma and possibly some characteristic radiation from the source, secondary radiation scattered within the source, the treatment head and the collimating system and electrons generated in any material through which the beam passes.

The gamma-ray spectrum from a radioactive nuclide consists of one or more discrete lines. The quantum energies are of interest in nuclear physics and have been determined to a high degree of precision. The gamma rays emitted by a radium source are largely due to the beta-active daughters Ra B (Pb^{214}) and Ra C (Bi^{214}) and form a complicated spectrum of some twenty lines ranging in energy from 0.05 Mev to 2.2 Mev. The average is roughly 1 Mev. Iridium-192 has rather a complicated spectrum with an intense group of lines at about 0.3 Mev, a strong line at 0.47 Mev and several other lines between 0.14 and 0.62 Mev. Cobalt-60 has a much simpler spectrum, 1.17 and 1.33 Mv gamma rays in cascade, while cesium-137 has a single gamma-ray line at 0.662 Mev. Cesium-137 units may contain some of the isotope cesium-134 whose principal gamma rays have energies of 0.57, 0.60 and 0.79 Mev and whose half life is 2.3 years.

The secondary radiation scattered from the source material and from the treatment head may constitute an appreciable fraction of the total radiation. It is therefore of importance to know the spectral distribution of the secondary

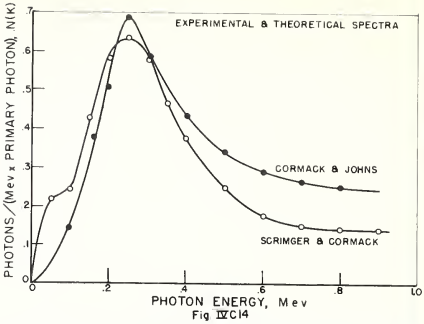

FIGURE IVC14. *Spectral distribution of the degraded radiation emerging from the source and collimator of a cobalt-60 therapy unit.*

TABLE IVC3. *Radionuclides used as teletherapy sources*

Nuclide	Gamma energy (Mev)	Half life	Specific gamma ray constant [a]
Ra^{226}	0.2–2.2	1620 y	0.825 [b]
Co^{60}	1.17 (100%) 1.33 (100%)	5.26 y	1.30
Ir^{192}	0.31, 0.47 (0.14–1.2)	74 d	
Cs^{137}	0.662 (84%)	30 y	0.326

[a] Roentgens per hour at 1 meter from 1 curie. This assumes no attenuation in source, its capsule or in air.
[b] Roentgens per hour at 1 meter from 1 gram of radium after filtration through 0.5 mm platinum.

radiation and also the quantity of such radiation with respect to the primary. Cormack and Johns (1958) have made approximate calculations of the Compton scattered radiation from a cobalt source 2.5 cm in diameter and 1.3 cm thick and from a tapered lead collimator. Recently, Costrell (1962) has made measurements of the scattered components in the spectra from various calibration sources of cobalt-60. The intensity of the scattered radiation was found to vary from 3 percent of the total incident intensity for a bare source 17 mm in diameter and 2.5 mm thick to 15 percent for a source simulating cobalt pellets in a capsule 5 cm in diameter and 5 cm thick mounted in a collimating head. The shapes of the spectra are very similar to those calculated by Cormack and Johns (1958). Scrimger (1962) has measured the spectrum of scattered radiation in the beam for a therapy unit containing a cobalt-60 source 2.5 cm in diameter and 1.3 cm thick in a standard capsule. The spectrum is shown in figure IVC14 and is compared with the calculated spectrum of Cormack and Johns. The spectrum was found to be almost independent of field size from 4×4 cm to 20×20 cm at 80 cm SSD. Additional studies of the radiation from various collimators are required.

Johns et al., (1959) have measured the spectrum from a cesium-137 unit by using a scintillation spectrometer. On comparison with the spectrum from a small, relatively low activity cesium-137 source the scattered spectrum from the larger

therapy source was calculated. The scattered spectrum is of nearly the same height from 0.6 Mev down to 0.2 Mev where it falls abruptly. The scattered exposure was found to be 27 percent of the primary. Costrell (1962) finds scattered contributions ranging from 8 to 21 percent of the total beam intensity for CsCl sources of various dimensions with the average energy of the scattered photons ranging from 0.3 to 0.45 Mev. Recent work of Bruce et al., (1962) shows the marked influence of radiation scattered from the collimator of a cesium-137 therapy unit.

4. Spectra of Secondary Radiation

a. *Introduction.* Several spectra of scattered radiation have lately been determined for different geometrical conditions. Most of the phantoms were of radiologic type with regard to geometrical dimensions. In most cases water was used as a soft-tissue-equivalent material. The point of observation was on the front or back surface of the phantom or within it. The spectral distributions depend on several variables; viz, the energy of the primary radiation, the source-surface distance, the field size, the depth of the point of observation and its position in relation to the beam axis, and the size and composition of the phantom. The spectrum of scattered radiation seems to be independent of the distance between source and observation point, provided the beam area at this point is kept constant. Johns et al., (1958) have indicated that this condition holds for first-order scattered radiation.

The secondary radiation in soft tissue consists essentially of photons which have undergone one or more Compton-scattering processes. The multiply-scattered photons become more important with increasing field size and depth of the observation point. The total number of scattered photons in relation to the primary flux, i.e., the number buildup, shows a similar trend. However, the number buildup seems to be roughly independent of the primary photon energy when this is between 50 and 250 kev. Hettinger and Lidén (1960), Hettinger (1960b), and Bjärngard and Hettinger (1961) found this condition to be valid when the point of observation was on the front of, within, and on the back of the phantom. These authors also studied the angular distribution of the scattered radiation within a radiologic phantom, the forward scattered photons being more numerous with increasing field size and depth.

Most spectra reported refer to points along the central axis. Mak and Cormack (1960) have measured 140 kv(p) and 280 kv(p) x rays and found that the spectra at points lying off the beam axis, but within the primary beam, agree very well in shape with those at points at the same depth on the central axis.

b. *Spectral distributions.* Table IVC4 surveys measured and theoretically calculated spectra of secondary radiation of interest for radiology. Most of the measurements were carried out with scintillation spectrometers. Bruce and Johns (1960) have performed Monte Carlo calculations and their spectra cover a wide range of primary photon energies, field sizes and depths. Most of the spectra mentioned in table IVC4 refer to a geometrical arrangement, where the source of primary radiation is outside the phantom and the central ray of the primary beam is perpendicular to the surface.

Figure IVC15 shows some typical spectra calculated by Bruce and Johns (1960). The spectra refer to different depths (0, 2, 5, and 10 cm) when a parallel primary beam is perpendicularly incident on a semi-infinite water scatterer. The beam is 25, 100, 400 cm^2 or infinite, and the energy of the initial photons is 100 kev. The spectral fluence is given in units of kev cm^{-2} $(kev)^{-1}$. The ordinate is normalized with regard to an incident primary fluence of 1 photon per cm^2. The smooth curve including the dashed line represents the contribution of multiply-scattered radiation to which the discontinuous singly scattered distribution has been added. The area under the curve gives the energy of the

TABLE IVC4. *Spectra of secondary radiation*

Reference	Primary photon energy	Geometry	Method
Payne-Scott (1937)	x rays	First order scatter considered within phantom	Theoretical.
Greening and Wilson (1951)	do	Within radiol. phantom	Abs. analysis.
Greening (1951)	do	do	Do.
Lindell (1954)	70–160 kv x rays	Backscatter	Scint.
Goldstein and Wilkins (1954)	250 kev–10 Mev	Within semiinfinite media	Theoretical.
Hine and McCall (1954)		Backscatter	Scint.
Berger and Dogget (1956)	0.66, 1 and 4 Mev	Infinite field size, backscatter and transmission	Monte Carlo.
Cormack et al., (1957)	400 kvp x rays	Within radiol. phantom	Scint.
Peelle et al., (1957)	Co^{60} radiation	Source and detector within an infinite water tank	Compton spectromet.
Cormack et al., (1958b)	280 kvp x rays	Within radiol. phantom	Scint.
Hettinger and Starfelt (1959)	50–250 kev	do	Do.
Hettinger and Lidén (1960)	50–250 kev	do	Do.
Cormack and Burke (1960)	140 kvp x rays	do	Do.
Mak and Cormack (1960)	140 kvp and 280 kvp x rays	Within radiol. phantom at points lying off the beam axis.	Do.
Hettinger (1960b)	50–250 kev	Backscatter from radiol. phantom	Do.
Berger and Raso (1960)	20 kev–2 Mev	Backscatter	Monte Carlo.
Bruce and Johns (1960)	50, 100, 200, 500, and 1250 kev	Backscatter from and scatter within an irradiated medium.	Do.
Baarli (1961)	0.2–1 Mev	Backscatter	Scint.
Skarsgard and Johns (1961)	250 kv radiation	Backscatter from and scatter within radiol. phantom	Do.
Bjärngard and Hettinger (1961)	50–250 kev	Transmitted radiation scattered from radiol. phantom	Do.
Bruce and Pearson (1962)	Cs^{137} radiation	Within radiol. phantom	Do.

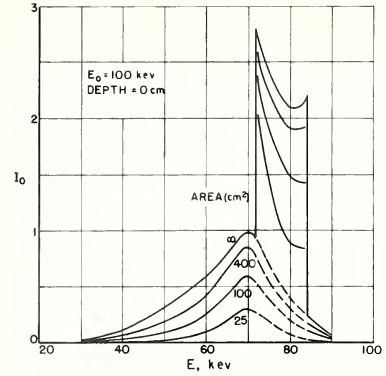

FIGURE IVC15a. *Spectral distribution of scattered radiation at the surface of a water phantom from an incident fluence of one 100 kev photon per cm². The ordinate is in units of kev cm⁻² (kev)⁻¹. (Bruce and Johns, 1960).*

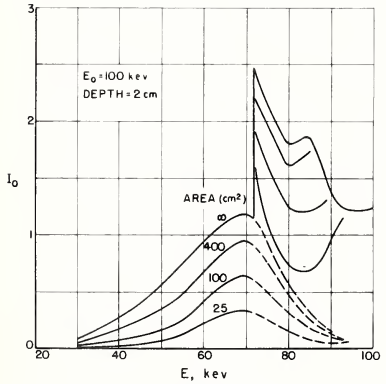

FIGURE IVC15b. *Spectral distribution of scattered radiation at a depth of 2 cm in a water phantom from an incident fluence of one 100 kev photon per cm². The ordinate is in units of kev cm⁻² (kev)⁻¹. (Bruce and Johns, 1960).*

scattered radiation. Inspection shows that about half of the scattered energy is due to singly scattered photons. The effective lower energy limit of the spectra is at about 25 kev. At about this photon energy the photo-electric absorption becomes so important that further energy degradation through scattering processes becomes very unlikely.

From their calculated spectra, Bruce and Johns (1960) have made matrices useful for determining spectra of scattered radiation resulting from any arbitrary continuous primary spectrum with photon energies below 400 kev.

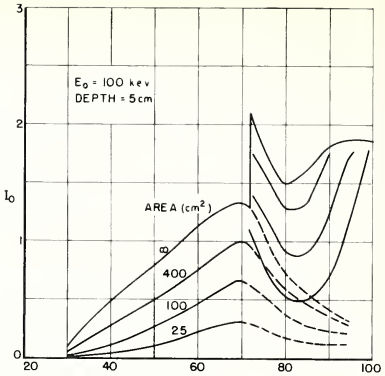

FIGURE IVC15c. *Spectral distribution of scattered radiation at a depth of 5 cm in a water phantom from an incident fluence of one 100 kev photon per cm². The ordinate is in units of kev cm⁻² (kev)⁻¹. (Bruce and Johns, 1960).*

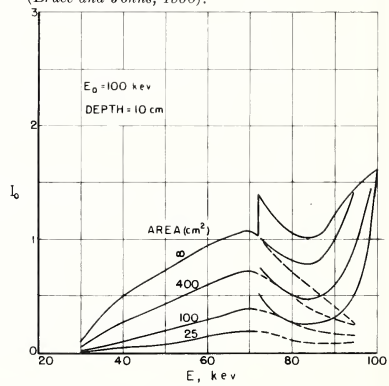

FIGURE IVC15d. *Spectral distribution of scattered radiation at a depth of 10 cm in a water phantom from an incident fluence of one 100 kev photon per cm². The ordinate is in units of kev cm⁻² (kev)⁻¹. (Bruce and Johns, 1960).*

Figure IVC16 shows some scattered spectra measured with a scintillation spectrometer. The spectra refer to primary 250 kv radiation with a HVL of 2.4 mm copper. From the spectrum at 6 cm depth and 200 cm² field size it can be calculated that the energy absorption in compact bone is somewhat more than twice that in soft tissue.

c. *Comparison of experiment and calculations.* Cormack (1960) has compared some spectra from Bruce and Johns (1960) with the secondary photon spectra measured by Hettinger and Starfelt (1959) and by himself (1958). In the former comparison the secondary spectra resulting from x-ray beams

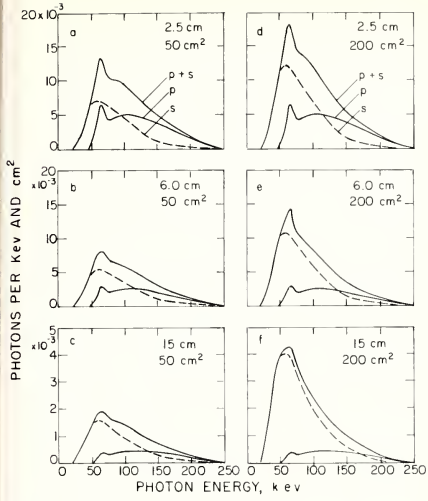

FIGURE IVC16. *Spectral distribution of primary and secondary 250-kv (cp) radiation at different depths (2.5, 6.0, and 15 cm) when the field size at the phantom surface is 50 cm² (a, b, and c) and 200 cm² (d, e, and f).*

The focus-surface distance is 67.5 cm; one primary photon per cm² is incident upon the phantom surface. The upper curve in each diagram corresponds to the total radiation, i.e., is the sum of primary and secondary photons. The ordinate scale in diagram c and f have been enlarged 4 times (Hettinger and Lidén, 1960).

with effective energies of 63, 113, and 184 kev were compared with the theoretical spectra for monoenergetic sources of the equivalent energy. Agreement in magnitude and general shape was good although the measured spectra did not display the discontinuities of the theoretical as they were not from monoenergetic primaries (fig. IVC17). Cormack's second comparison was for a scattered spectrum generated by 280 kv(p) x rays with HVL of 2.6-mm copper. The agreement in the shape of the spectra was good but no test was made of the absolute magnitude.

Bruce et al., (1962) have made a comparison of their Monte Carlo results (1960) with the secondary x rays measured by Skarsgard and Johns (1961) and with their own measurements of cesium-137 and cobalt-60 spectra. The calculated and measured spectra agree within the limits of error.

d. *Equivalent energy or HVL in a medium.* Although the half value layer is strictly defined only for a nearly monodirectional beam of radiation, an equivalent HVL or energy may be used as a partial description of the quality of the multidirectional radiation within an irradiated medium. Values of the equivalent energy have been measured using double ionization chambers by Bruzau (1929), Wilson (1939), Clarkson and Mayneord (1939), Greening and Wilson (1951), and Schaal (1956). Values of the equivalent HVL may also be calculated from the complete spectral distribution making use of tabulated attenuation coefficients. Table IVC5 shows values of the equivalent HVL determined in this way by a number of workers for water phantoms irradiated with x rays.

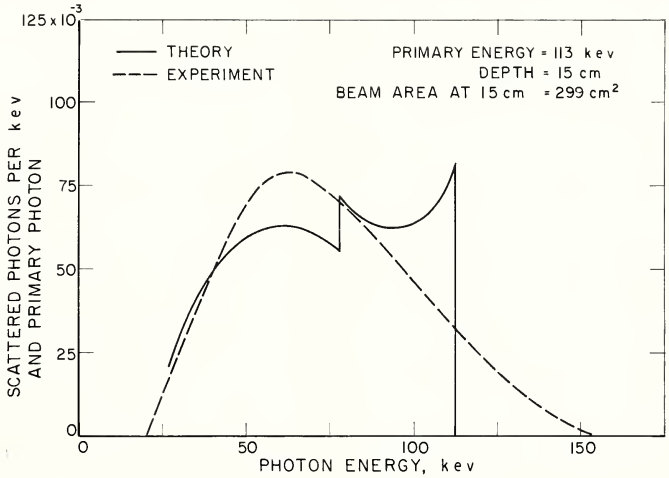

FIGURE IVC17. *Comparison between an experimental spectrum and one calculated with a Monte Carlo method. The secondary radiation is integrated over space. (Hettinger, 1960a).*

TABLE IVC5. *HVL in irradiated water—values in table give HVL in mm Cu for total radiation*

(a) 400 kv (p), Primary HVL 3.8 mm Cu, Cormack et al., (1957)

Depth (cm) \ Area (cm²)	0	50	100	400
0	3.8	3.5	3.4	3.2
2	3.9	3.4	3.2	3.1
6	4.1	3.3	3.1	2.8
15	4.3	3.2	2.9	2.6

(b) 280 kv (p) Primary HVL 2.6 mm Cu, Cormack et al., (1958b)

2	2.7	2.0	1.7
5	2.8	2.0	1.5
15	3.0	1.7	1.2

(c) 250 kv (cp), Primary HVL 2.4 mm Cu, Hettinger and Lidén (1960)

2.5	2.4	1.7	1.4
6	2.5	1.6	1.3
15	2.8	1.6	1.1

(d) 250 kv (cp), Skarsgard and Johns (1961)

Primary HVL—1.25 mm Cu

Depth (cm) \ Area (cm²)	0	25	50	100	200	500
0	1.28	0.98	0.92	0.87	0.84	0.82
2.5	1.38	.85	.72	.66	.61	.58
5.0	1.55	.82	.72	.63	.56	.52
10.0	1.83	.90	.75	.62	.49	.46
15.0	2.24	.99	.75	.60	.50	.47

Primary HVL—2.20 Cu

0	2.26	1.89	1.80	1.70	1.62	1.54
2.8	2.39	1.72	1.55	1.41	1.23	1.15
5.0	2.53	1.70	1.48	1.21	1.08	1.00
10.0	2.67	1.54	1.29	1.06	.88	.80
15.0	2.90	1.48	1.20	.98	.81	.66

Primary HVL 3.20 Cu

0	3.16	2.78	2.67	2.56	2.45	2.37
2.5	3.19	2.45	2.26	2.09	1.93	1.81
5.0	3.26	2.46	2.22	1.91	1.70	1.56
10.0	3.33	2.31	1.98	1.69	1.44	1.27
15.0	3.46	2.11	1.75	1.45	1.18	.86

The hardening effect of the passage of the primary beam through the water and its effect on the overall quality of the radiation is particularly striking in the work of Skarsgard and Johns.

D. Electron Spectra in an Irradiated Medium

In a medium irradiated with x or gamma rays, electrons are set in motion as a result of the photoelectric, Compton and pair production processes. The distribution of initial energies given to these electrons at some point may be calculated from the photon spectrum at that point. Nelms (1953) has given a comprehensive set of graphical data of the distribution of Compton-recoil electrons. Johns et al., (1954) have presented tables for calculating the distributions of photoelectrons, Compton-recoil electrons and positron-electron pairs generated by continuous photon spectra.

The energy deposition along the tracks of the electrons may be described in various ways (see also subsection IAlg). McGinnies (1959) gives tables based on the theory developed by Spencer and Fano (1954) of the energy spectrum of electrons as they slow down from a number of initial energies. Burch (1957) has derived a method of progressively calculating for a complete initial energy spectrum the energy dissipated by small collisions in each of a number of electron energy intervals. A graphical summary of various electron-dissipation distributions as a function of linear energy transfer has been presented by Howard-Flanders (1958). Rossi et al., (1961) have critically discussed the specification energy deposition in a small volume with particular attention to the statistical fluctuations and to the combined effect of more than one traversing particle. Rossi also measured energy deposition distributions of electrons set in motion by gamma rays and for protons set in motion by fast neutrons.

In the present state of knowledge it does not appear useful to present here a detailed description of methods for determining energy deposition distributions nor to summarize existing data.

References

Abson, W., Cox, R. L., and Gray, A. L. (1958). Neutron flux instrumentation, Proc. Intern. Conf. on Peaceful Uses of Atomic Energy, 15/P/56 Geneva.

Aglintsev, K. K., and Ostromukhova, G. P. (1959). The distribution of ionization along a beam of γ-radiation and the determination of radiation dose with normal ionization chambers, Soviet J. Atomic Energy **6,** No. 1, 33.

Aglintsev, K. K., and Ostromukhova, G. P. (1961). Roentgen readings in the γ-radiation range, with quantum energy of 0.25–3 Mev, Tr. Vses. Nauchno.-Issle. Inst. Metodiki (Bull. Mendeleev Inst.) **55**, No. 115, 55.

Aitken, J. H., and Dixon, W. R. (1958). X-ray spectra from a 100 kv machine, NRC (Can.) Report 4864.

Aitken, J. H., DeLaVergne, L., Henry, W. H., and Loftus, T. P., (1962). Comparison of United States and Canadian free-air ionization chambers, Brit. J. Radiol. **35,** 65.

Allen, A. O., Hogan, V. D., and Rothschild, W. G. (1957). Studies in the radiolysis of ferrous sulfate solutions; effect of acid concentration in solutions containing oxygen, Radiation Res. **7**, 603.

Allen, A. O., and Rothschild, W. G. (1957). Studies in the radiolysis of ferrous sulfate solutions; effect of oxygen concentrations in 0.8*N* sulfuric acid, Radiation Res. **7**, 591.

Allen, W. D., and Ferguson, A. T. G. (1957). The fission cross sections of U^{233}, U^{235}, U^{238} and Pu^{239} for neutrons in the energy range 0.030 Mev to 3.0 Mev., Proc. Phys. Soc. (London) A**70**, 573.

Allisy, A., and Astier A. (1958). Determination of the absorbed dose/exposure dose ratio in bone and muscle by the method of equivalent gases, J. Radiol. Electrol. Nucl. Med. **39,** 340.

Allisy, A., DeLaVergne, L., and Wyckoff, H. O. (1957). International comparison of French and U.S. roentgen-ray standards, Acta Radiol. **48**, 484.

Allisy, A., and Roux, A. M. (1961). Contribution à la mesure des rayons roentgen dans le domaine de 5 a 50 kv, Acta Radiol. **55**, 57.

Amaldi, E. (1959). The production and slowing down of neutrons, Encyclopedia of Physics **38/2,** Springer-Verlag.

Anderson, A. R. (1962). A calorimetric determination of the oxidation yield of the Fricke dosimeter at high dose rates of electrons, J. Phys. Chem. **66,** 180.

Andrews, H. L., Murphy, R. E., and Lebrun, E. J. (1957). Gel dosimeter for depth-dose measurements, Rev. Sci. Instr. **28**, 329.

Anta, M. C., and Haissinsky, M. (1954). Sur la réduction des sels cériques par les rayons α du polonium preparé par dépot anodique, J. Chim. Phys. **51**, 33.
Astier, A., and Allisy, A. (1959). Quelques données récentes sur la conversion roentgen—rads dans l'os et le muscle, J. Radiol. Electrol. Med. Nucl. **40**, 379.
Aston, G. H. (1961). Private Communication.
Aston, G. H., and Attix, F. H. (1956). An intercomparison of the roentgen standards of Gre at Britain and U.S.A. Acta Radiol. **46**, 747.
Atlee, Z. J. and Trout, E. D. (1943). A study of roentgen ray distribution at 60–140 kvp, Radiology **40**, 375.
Attix, F. H., and Ritz, V. H. (1957). A determination of the gamma-ray emission of radium, J. Research NBS **59,** 293, RP2801.
Attix, F. H. (1961). Unpublished experiments at U.S. Naval Research Laboratory, reported at 2nd Microdosimetry Conference, Rochester, N.Y.
Attix, F. H. (1962). Dosimetry by solid state devices, U.S. Naval Research Laboratory Report No. 5777.
Auxier, J. A., Hurst, G. S., and Zedler, R. E. (1958). A single ion detector for measurement of γ-ray ionization in cavities, Health Phys. **1**, 21.
Avotina, M. P., and Ostromukhova, A. P. (1961). An installation for the absolute measurement in roentgens for X-radiation in the 20–60 kv range, Tr. Vses. Nauchno.-Issle. Inst. Metodiki (Bull. Mendeleev Inst.) **55**, No. 115, 35.
AWRE 0–28/60 (1961). Neutron cross sections of selected elements and isotopes for use in neutronics calculations in the energy range 0.025 ev–15 Mev. Atomic Weapons Research Establishment.
Axton, E. J. (1961). Neutron source calibrations: a review, Nucleonics **19**, No. 3, 90.
Axton, E. J., and Cross, P. (1961). The establishment of an absolutely calibrated neutron source, J. Nucl. Energy **15**, 22.
Axton, E. J. (1962). Private communication, National Physical Lab., Teddington, England.
Baarli, J. (1961). An experimental study of gamma-ray backscattering using scintillation gamma-ray spectroscopy, Arkiv Math. Naturvidenskap, Band **LV**, No. 8, Oslo.
Back, M. H., and Miller, N. (1957). Use of ferrous sulfate solutions for x-ray dosimetry, Nature **179,** 321.
Baily, N. A. and Beyer, N. S. (1957). The influence of treatment cones on dose rate, Am. J. Roentgenol, Radium Therapy Nucl. Med. **77,** 873.
Baily, N. A., and Mayer, J. W. (1961). A P–N junction semiconductor radiation detector for use with beta- and gamma-ray-emitting isotopes, Radiology **76,** 116.
Baily, N. A., Grainger, R. J., and Mayer, J. W. (1961). Capabilities of lithium drifted P–I–N junction detectors when used for gamma-ray spectroscopy, Rev. Sci. Instr. **32,** 865.
Ballinger, E. R., and Harris, P. S. (1959). Field study of the $AgPO_3$ glass personnel dosimeter, Los Alamos Scientific Laboratory Rept. No. LA 2298.
Balon, Z. P. (1957). Researches in the area of ionizing radiations, Tr. Vses. Nauchno.-Isse. Inst. Metodiki (Bull. Mendeleev Inst.) **30,** No. 90, 70.
Bame, S. J., Jr., Haddad, E., Perry, J. E., Jr., and Smith, R. K. (1957). Absolute determination of monoenergetic neutron flux in the energy range 1 to 30 Mev., Rev. Sci. Instr. **28,** 997.
Barber, W. C. (1955). Specific ionization by high-energy electrons, Phys. Rev. **97,** 1071.
Barnard G. P., Axton, E. J., Belcher, D. S. C., and Marsh, A. R. S. (1956). The present status of calibrations of ionization dosimeters with high-voltage X-rays, Phys. Med. Biol. **1,** 18.
Barnard, G. P., Axton, E. J., and Marsh, A. R. S. (1959). A study of cavity ion chambers for the use with 2 Mv X-rays: equilibrium wall thickness; wall-absorption correction, Phys. Med. Biol. **3,** 366.
Barnard, G. P., and Marsh, A. R. S. (1959). The stopping power correction for graphite cavity chambers used with 2Mv x rays, Phys. Med. Biol. **4,** 33.
Barnard, G. P., Aston, G. H., and Marsh, A. R. S. (1960). Effects of variations in the ambient air on the calibration and use of ionization dosimeters, Her Majesty's Stationery Office, London, England.
Barr, N. F. (1958). Private communication.
Barr, N. F., and Stark, M. B. (1958). The destruction of the fluorescence of quinine in acid solution by 250 kvp x-rays, Radiation Res. **9,** 89.
Barr, N. F., and Stark, M. B. (1960). Chemical dosimetry with fluorescence compounds: The destruction of the fluorescence of quinine by gamma rays, Radiation Res. **12,** 1.
Barr, N. F., Stark, M., Hands, J., Laughlin, J. S. (1961b). Dosimetry with small silver-activated glass rods, Health Phys. **7,** 48.
Barr, N. F., Stark, M., and Laughlin, J. S. (1961a). A comparison of two fluorometers designed to measure the radiation-induced fluorescence of silver-activated glass rods, Radiology **76,** 113.
Barton, David M. (1953). Measurement of the neutron spectrum from a Po-Li^7 low energy neutron source, AEC Los Alamos Report LA–1609.
Bausch & Lomb Optical Co. (1959). Commercial microdosimeter uses glass fluorescence, Nucleonics **17,** No. 9, 128.
Bay, Z., Mann, W. B., Seliger, H. H., and Wyckoff, H. O. (1957). Absolute measurement of W_{air} for sulfur-35 beta rays, Radiation Res. **7,** 558.
Bay, Z., Newman, P. A., and Seliger, H. H. (1961). Absolute measurement of W for Po^{210} alpha particles in air, nitrogen and carbon dioxide, Radiation Res. **14,** 551.
Beetlestone, A., and Thurmer, G. (1958). Some considerations of focal spot sizes, Brit. J. Radiol. **31,** 492.
Belcher, E. H. (1953). Radiation dosimetry with scintillation detectors, Brit. J. Radiol. **26,** 455.
Belcher, E. H., and Geilinger, J. E. (1957). Improved scintillating media for radiation dosimetry, Brit. J. Radiol. **30,** 103.
Bell, G. E. (1936). Spectral distribution in the continuous X-ray spectrum and the specification of X-ray quality, Brit. J. Radiol. **9,** 680.
Berger, M. J., and Dogget, J. (1956). Reflection and transmission or gamma radiation by barriers: Semi-analytic Monte Carlo calculation, J. Research NBS **56,** 89, RP2653.
Berger, M. J., and Raso, D. (1960). Monte Carlo calculations of gamma ray backscattering, Radiation Res. **12,** 20.
Berger, R. T. (1961). The x- or gamma-ray energy absorption or transfer coefficient: tabulation and discussion, Radiation Res. **15,** 1.
Bernard, C. H., Thornton, W. T., and Auxier, J. A. (1961). Silver metaphosphate glass for x-ray measurements in coexistent neutron and x-radiation fields, Health Phys. **4,** 236.
Bernier, J. P., Skarsgard, L. D., Cormack, D. V., and Johns, H. E. (1956). A calorimetric determination of the energy required to produce an ion pair for cobalt-60 gamma rays, Radiation Res. **5,** 613.
Bernstein, W., and Schardt, A. W. (1952). Activation of LiI crystal phosphors, Phys. Rev. **85,** 919.
Bezotosnii, V. M., and Zamyatnin, Yu S. (1957). Measurement of absolute intensities of neutron sources, At. Energ. **2,** 313; (1958) J. Nucl. Energy **6,** 237.
Biber, C., Huber, P., and Müller, A. (1955). Arbeit pro Ionenpaar von mehratomigen Gasen für Po-α-Teilchen, Helv. Phys. Acta **28,** 503.
Bichsel, H. (1961). Outer shell corrections for stopping powers, Bull. Am. Phys. Soc. **6,** 46.
Bishay, A. M. (1961). A bismuth lead borate glass dosimeter for high-level gamma measurements, Phys. Chem. Glasses **2,** No. 2, 33.
Bjärngard, B., and Hettinger, G. (1961). Spectra of scattered radiation behind slabs of water irradiated by X-rays, Arkiv Fysik **20,** 517.
Blankenship, J. L., Bibliography on semiconductor nuclear radiation detectors, Rept. No. TID–3907, Dec. 6, 1960 (Office of Technical Services, Department of Commerce, Washington 25, D.C.)
Blanks, B. A., and Rohrer, R. H. (1960). A sensitive gamma ray dosimeter, Am. J. Roentgenol., Radium Therapy and Nucl. Med., **83,** 581.

Blocker, W., Kenney, R. W., and Panofsky, W. K. H. (1950). Transition curves of 330 Mev Bremsstrahlung, Phys. Rev. **79,** 419.
BNL 325 (1958). Neutron cross sections. Brookhaven National Laboratory.
BNL 325 (1960). Neutron cross sections, supplement number 1. Brookhaven National Laboratory.
BNL 400 (1962). Angular distribution in neutron-inducted reactions. Brookhaven National Laboratory.
Boag, J. W. (1954). The distribution of linear energy transfer or "ion density" for fast neutrons in water, Radiation Res. **1,** 323.
Boag, J. W. (1956). Chapt. 4, Radiation Dosimetry, Hine and Brownell, Academic Press, Inc., New York, N.Y.
Boag, J. W., Dolphin, G. W., and Rotblat, J. (1958). Radiation dosimetry by transparent plastics, Radiation Res. **9,** 589.
Bollinger, L. M., Saplakoglu, A., Coceva, C., Cote, R. E., and Thomas, G. E. (1957). Precision thermal fission cross sections by a new method, Bull. Am. Phys. Soc. **112,** 196; Argonne National Laboratory Physics Division Summary Report, January through March 1957, ANL–5698, p. 2, Argonne National Laboratory, Lemont, Ill.
Bollinger, L. M., and Thomas, G. E. (1957). Boron-loaded liquid scintillation neutron detectors, Rev. Sci. Instr. **28,** 489.
Bollinger, L. M., Thomas, G. E., and Ginther, R. G. (1959). Glass scintillators for neutron detection, Rev. Sci. Instr. **30,** 1135.
Bortner, T. C., and Hurst, G. S. (1954). Ionization of pure gases and mixtures of gases by 5-Mev alpha particles, Phys. Rev. **93,** 1236.
Bothe, W. (1943). Zur Methodik der Neutronensonden, Z. Physik. **120,** 437.
Bouzigues, H., Scheidhauer, J., Brian, R., and Messainguiral, L. (1961). Enlarged sensibility of the Fricke dosimeter by utilization of the orthophenanthroline reagent, pp. 331–5 of "Selected Topics in Radiation Dosimetry," Vienna, International Atomic Energy Agency.
Bradshaw, A. L. (1953). The wall effect of applicators, Hosp. Phys. Assoc. Bull. **1,** pt. 1, 4.
Braestrup, C. B., and Mooney, R. T. (1958). Cobalt 60 radiation measurements, Radiology **70,** 516.
Brandt, W. (1958). Tight-binding corrections of stopping powers, Phys. Rev. **112,** 1624.
Brannen, E., and Olde, G. L. (1960). Electron dosimetry in phantoms using thin scintillator sheets, Phys. Med. Biol. **5,** 37.
Breen, R. J., and Hertz, M. R. (1955). Gamma radiation from polonium neutron sources, Phys. Rev. **98,** 599.
Breen, R. J., Hertz, M. R., and Wright, D. U. (1956). The spectrum of polonium-beryllium neutron sources, U.S. Atomic Energy Commission Report MLM–1054.
Breitling, G., and Glocker, R. (1952). Über die Wellenlängenabhängigkeit von Szintillationszählern im Röntgengebiet, Naturwissenschaften **39,** 84.
Breitling, G., Glocker, R., and Mohr, H. (1956). Die Messung der Röntgendosis in Fett, Muskel, Knochen mit Hilfe von Leuchtstoffen verschiedener Zusammensetzung, Fortschr. Gebiete Röntgenstrahlen Nuklear-Med. **84,** 561.
Bretscher, E., and French, A. P. (1944). British Atomic Energy Project Report 386; The measurement of a neutron flux in the presence of gamma rays, British Atomic Energy Project Rept. BR–517.
Broek, H. W., and Anderson, C. E. (1960). The stilbene scintillation crystal as a spectrometer for continuous fast-neutron spectra. Rev. Sci. Instr. **31,** 1063.
Brown, B., and Hooper, E. B. (1958). Plastic phosphor matrix for fast neutron detection, Nucleonics **16,** No. 4,96.
Brownell, G. L. (1961). Medical applications of semiconductor nuclear particle detectors, Publ. No. 871, Natl. Acad. Sci.-Natl. Res. Council, Wash., D.C., U.S.A.
Bruce, W. R., and Johns, H. E. (1960). The spectra of X-rays scattered in low atomic number materials, Brit. J. Radiol. Suppl. No. 9.
Bruce, W. R., Pearson, M. L., and Johns, H. E. (1962). Comparisons of Monte Carlo calculations and experimental measurements of scattered radiation produced in a water phantom by primary radiations with half value layers from 1.25 mm Cu to 6 mm Pb, Radiation Res. **17,** 534.
Bruce, W. R., and Pearson, M. L. (1962). Spectral distribution of scattered radiation in a water phantom irradiated with Cs^{137} gamma rays, Radiation Res. **17,**555.
Brucker, G. (1952). Energy dependence of scintillating crystals, Nucleonics **10,** No. 11, 72.
Bruzau, M. (1929). Sur la distribution du rayonnement dans les milieux dispersifs, Ann. Phys. **11,** 5.
Brynjolfsson, A. (1960). Calorimetric measurements of gamma-rays in the Co-60 irradiation facility of Risø, Risø Report **16**.
Burch, P. R. J. (1955). Cavity ion chamber theory, Radiation Res. **3,** 361.
Burch, P. R. J. (1957). Some physical aspects of relative biological efficiency, Brit. J. Radiol. **30,** 524.
Burke, E. A., and Pettit, R. M. (1960). Absorption analysis of X-ray spectra produced by beryllium window tubes operated at 20 to 50 kvp., Radiation Res. **13,** 271.
Burlin, T. E. (1959). The measurement of exposure dose for high energy radiation with cavity ionization chambers, Phys. Med. Biol. **3,** 197.
Burlin, T. E. (1961). An experimental examination of theories relating to the absorption of gamma-ray energy in a medium to the ionization produced in a cavity, Phys. Med. Biol. **6,** 33.
Burlin, T. E. (1962). An experimental examination of theories relating ionization in a cavity to radiation dose, Ph.D. Thesis, London University, London, England.
Burns, J. E., Perry, B. J., Pierce, N. H., Trotman, R. E., and Wilson, C. W. (1959). A kilocurie caesium 137 beam unit at Westminster Hospital: Physical aspects, Brit. J. Radiol. **32,** 215.
Cameron, J. R., Daniels, F., Johnson, N., and Kenney, G. (1961). Radiation dosimeter utilizing the thermoluminescence of lithium fluoride, Science **134,** 333.
Caswell, R. S. (1960). Neutron-insensitive proportional counter for gamma-ray dosimetry, Rev. Sci. Instr. **31,** 869.
Cedarlund, R., Horn, A., and Scolnick, M. (1961). Solid-state detector for monitoring 14-Mev neutron production, Nucl. Instr. Methods **13,** 305.
Cheka, J. S. (1954). Recent developments in film monitoring of fast neutrons, Nucleonics **12,** 40.
Chiozzotto, M. (1962). La camera a ionizzazione ad aria libera dell' Instituto Superiore di Sanità, Instituto Superiore di Sanità, Rome, Italy.
Clarkson, J. R., and Mayneord, W. V. (1939). The quality of high voltage radiations, Brit. J. Radiol. **12,**168
Clarkson, J. R., Leech, H. J., Taylor, A. G. C., and Mason. S. W. A. (1959). A moving-beam caesium 137 telecurie, unit, Brit. J. Radiol. **32,** 798.
Cochran, R. G., and Henry, K. M. (1955). Proton recoil fast-neutron spectrometer, Pt. II, Experimental, Rev. Sci. Instr. **26,** 757.
Cockroft, A. L., and Curran, S. C. (1951). The elimination of the end effects in counters, Rev. Sci. Instr. **22,** 37.
Codd, J., Shepherd, L. R., and Tait, J. H. (1956). The physics of fast reactors, Progr. Nuclear Energy, **1,** Ser. 1, 251, Pergamon Press, Inc., London, England.
Cohen, B. L., and Falk, C. E. (1951). (d,n) reactions with 15-Mev deuterons; II Neutron energy spectra and yields, Phys. Rev. **84,** 173.
Cole, D. P., Duffy, P. A., Hayes, M. E., Lusby, W. S., and Webb, E. L. (1952). The phosphor-phototube radiation detector, Elec. Eng. **71,** 935.
Cole, A., Moore, E. B., and Shalek, R. J. (1953). A simplified automatic isodose recorder, Nucleonics **11** No. 4, 46.
Cole, A., Sinclair, W. K., Fletcher, G. H., and Johnson, G. C. (1960). Physical studies on a short-treatment-distance cesium 137 teletherapy unit, Radiology **74,** 731.
Compton, A. H., and Allison, S. K. (1935). X rays in theory and experiment, 2nd ed., p. 81, D. van Nostrand Co., New York, N.Y.
Cormack, D. V., Till, J. E., Whitmore, G. F., and Johns, H. E. (1955). Measurements of continuous x-ray spectra with a scintillation spectrometer, Brit. J. Radiol. **28,** 605.
Cormack, D. V. (1956). Distribution of energy losses of the electrons set in motion by radiation, Indian J. Radiol. Souvenir No. 576.

Cormack, D. V., Griffith, T. J., and Johns, H. E. (1957). Measurement of the spectral distribution of scattered 400 kvp x-rays in a water phantom, Brit. J. Radiol. **30,** 129.
Cormack, D. V., and Johns, H. E. (1958). Spectral distribution of scattered radiation from a kilocurie cobalt unit, Brit. J. Radiol. **31,** 497.
Cormack, D. V., Burke, D. G., and Davitt, W. E., (1958a). Spectral distribution of 140 kvp x rays, Radiology **70,** 91.
Cormack, D. V., Davitt, W. E., Burke, D. G., and Rawson, E. G. (1958b). Spectral distribution of 280 kvp x-rays, Brit. J. Radiol. **31,** 565.
Cormack, D. V., and Burke, D. G. (1960). Spectral distributions of primary and scattered 140 kvp x-rays, Radiology **74,** 743.
Cormack, D. V. (1960). A comparison of calculated and measured scattered spectra, J. Can. Assoc. Radiol. **XI,** 40.
Cormack, D. V. (1961). Spectral distributions in a medium irradiated with X- or gamma-rays, Trans. IX Intern. Cong. Radiology, p. 1400.
Costrell, L. (1962). Scattered radiation from large Co^{60} calibrating sources, Health Phys. **8,** 261.
Costrell, L. (1962). Scattered radiation from large Cs^{137} sources, Health Phys. **8,** 491.
Cottin, M., and Lefort, M. (1956). Etalonnage absolu du dosimètre au sulfate ferreux avec rayons x mous de 10 et 8 Kev, J. Chim. Phys. **53,** 267.
Crane, W. W. T., Higgins, G. H., and Bowman, H. R. (1956). Average number of neutrons per fission for several heavy-element nuclides Phys. Rev. **101,** 1804.
Dainty, J. (1950). Report on fast neutron dosimetry, CRM–482.
D'Ans, J., and Lax, E. (1949). Handbook for Chemistry and Phys., 2nd ed., Springer-Verlag, Berlin, Germany.
Dalton, G. Ronald and Osborn, Richard, K. (1961). Flux perturbations by thermal neutron detectors, Nucl. Sci. Eng. **9,** 198.
Davisson, S., Goldblith, S. A., and Proctor, B. E. (1956). Glass dosimetry, Nucleonics **14,** No. 1, 34.
Day, M. J., and Stein, G. (1950). Chemical effects of ionizing radiation in some gels, Nature **166,** 146.
Day, F. H. (1956). Unpublished work, National Bureau of Standards.
Dealler, J. F. (1954). An optical shutter for scintillation meters, Brit. J. Radiol. **27,** 646.
Dearnaley, G., and Whitehead, A. B. (1961). Two semiconductor detectors for fast neutrons. AERE–R 3662, Harwell, U. K. See also: Dearnaley, G., and Ferguson, A. T. G. (1962). Nucleonics **20,** No. 4, 84.
Degelman, J., Callahan, A. B., and Fulton, G. P. (1957). An improved fluorometer for miniature glass rod radiation detectors, Radiation Res. **6,** 548.
DeJuren, J. A., and Rosenwasser, H. (1954a), Pulse-height measurements of recoils from B^{10} (n,α) Li^7. Phys. Rev. **93,** 831; (1954b), Absolute calibration of the NBS standard thermal neutron density, J. Research NBS **52,** 93, RP2477.
DeJuren, J. A., Padgett, D. W., and Curtiss, L. F. (1955). Absolute calibration of the National Bureau of Standards photoneutron standard, I. J. Research NBS **55,** 63, RP2605.
DeJuren, J. A., Chin, J. (1955). Absolute calibration of the National Bureau of Standards photoneutron standard; II. Absorption in manganese sulfate, J. Research NBS **55,** 311, RP2635.
Delattre, P. (1961). Les méthodes de détermination des spectres de neutrons rapides á l'aide de détecteurs à seuil, Rapport C.E.A. No. 1979, C.E.N. de Saclay, Gif-sur-Yvette, France.
Demers, J. P. (1945). Photographic emulsion studies of Po-Be neutrons, MP–74 and Energy distribution of neutrons from Ra-Be sources, MP–204. Montreal Report.
Dennis, J. A., and Loosemore, W. R. (1957). A fast neutron counter for dosimetry, A.E.R.E. EL/R 2149.
DePangher, J. R. (1957). Double moderator neutron detector, HW–54584.
DePangher, J. (1959). Double moderator neutron dosimeter, Nucl. Instr. Method **5,** 61.
DePangher, J. (1961). A reproducible precision polyethylene long counter for measuring fast neutron flux, Hanford Laboratories, Richland, Wash.
deTroyer, A., and Tavernier, G. C. (1954). Absolute measurement of the Union Minière neutron standard, Bull. Classe Sci., Acad. Roy. Belg., Ser. 6, **40,** 150.
de Waard, R. H., Oosterkamp, W. J., and Somerwil, A. (1958). Mededeling van de Dosimetrie-commissie van de Nederlandse Vereniging voor Electrologie en Röntgenologie, J. Belge Radiologie **41,** No. 6, 41.
Dewhurst, H. A. (1952). Effect of aliphatic alcohols on the γ-ray oxidation of aerated aqueous ferrous sulfate, Trans. Faraday Soc. **48,** 905.
De Wire, J. W. (1959). Private communication.
Digby, N., Firth, D., Hercock, R. J. (1953). The photographic effect of medium energy electrons, J. Phot. Sci. **1,** 194.
DIN 6817, (1962). Dosimeter mit Ionisationskammern fur Röntgen- und Gammastrahlen, Regeln für die Herstellung, Fachnormenausschuss Radiologie in Arbeitsgemeinschaft mit der Deutschen Röntgengesellschaft.
Dixon, W. R., Bielesch, Alice, and Geiger, K. W. (1957). Neutron spectrum of an actinium-beryllium source, Can. J. Phys. **35,** 699.
Dixon, W. R., and Aitken, J. H. (1958). The resolution correction in the scintillation spectrometry of continuous X-rays, Can. J. Phys. **36,** 1624.
Dolphin, G. W., and Innes, G. S. (1956). A calorimetric method used in the dosimetry of x-ray beams from a 1 Mev generator, Phys. Med. Biol. **1,** 161.
Donaldson, D. M., and Miller, N. (1955). Etudes quantitatives des reáctions radiochimiques, III Oxydation de sulfate ferreux par les particles β, J. Chim. Phys. **52,** 578.
Draganic, I. (1959). Action des rayonnements ionisants sur les solutions aqueuses d'acide oxalique: acide oxalique utilisé comme dosimètre chimique pour les doses entre 1.6 et 160 M rads, J. Chim. Phys. **56,** 9.
von Droste, G. and Kolb, M. (1960). Unpublished.
Dudley, R. A. (1956). Photographic film dosimetry, Chapt. 7, Radiation Dosimetry, Hine and Brownell, Academic Press Inc., New York, N.Y.
Edelsack, E. A., Kreger, W. E., Mallet, W., and Scofield, N. E. (1960). Experimental investigation of thick target bremsstrahlung radiation produced by electrons of 1.00, 1.50, and 2.00 Mev, Health Phys. **4,** 1.
Edwards, P. D., and Kerst, D. W. (1953). Determination of photon flux for energies between 150 Mev and 300 Mev, Rev. Sci. Instr. **24,** 490.
Eggler, C., and Hughes, D. J. (1950). The neutron spectrum of a radium-beryllium photo source, U.S. Atomic Energy Commission Report ANL 4476.
Ehrlich, M. (1954). Photographic dosimetry of X- and gamma rays, NBS Handb. 57.
Ehrlich, M. (1955). Scintillation spectrometry of low-energy bremsstrahlung, J. Research NBS **54,** 107, RP2339.
Ehrlich, M. (1956a). National Bureau of Standards. Private communication.
Ehrlich, M. (1956b). Reciprocity law for X-rays, Part I: Validity for high-intensity exposures in the negative region, J. Opt. Soc. Am. **46,** 797.
Ehrlich, M., and McLaughlin, W. (1959). Photographic dosimetry at total exposure levels below 20 mr, NBS Tech. Note 29 (1959) (PB151388).
Erozolimsky, B. G., and Spivak, P. E. (1957). The standardization of neutron sources using the graphite stack of a reactor, Atomnaya Energiya **2,** 1327 (1957); J. Nucl. Energy **6,** 243 (1958).
Ellis, F. (1959). The use of the rad in clinical practice, Brit. J. Radiol. **32,** 588.
Failla, G., and Rossi, H. H. (1950). Dosimetry of ionizing particles, Am. J. Roentgenol. Rad. Therapy Nucl. Med., **64,** 489.
Fano, U. (1953). Gamma ray attenuation, Nucleonics **11,** No. 8, 8.
Farr, R. F. (1955a). The specification of roentgen ray output and quality, Acta Radiol. **43,** 152.

Farr, R. F. (1955b). The distribution of dose rate across the field of an X-ray therapy tube, Brit. J. Radiol. **28,** 364.

Felcher, G. P., Germagnoli, E., and Musci, M. (1960). On the absolute calibration of a Ra-Be neutron source, Energia Nucl. **7,** 31 and 738.

Feld, B. T. (1953). The neutron. E. Segrè, Exp. Nuclear Phys. **II,** 208.

Firk, F. W. K., Slaughter, G. G., and Ginther, R. J. (1961). An improved Li^6-loaded glass scintillator for neutron detection. Submitted to Nuclear Instr. Method.

Foote, R. S., and Koch, H. W. (1954). Scintillation spectrometers for measuring the total energy of X-ray photons, Rev. Sci. Inst. **25,** 746.

Fowler, J. F. (1955). Problems in the design of a fluorescence meter for interstitial therapy, and a practical design of instrument, Brit. J. Radiol. **28,** 104.

Franks, J., Associated Electrical Industries (Woolwich) Ltd., Harlow Research Laboratory, West Road Temple Fields, Harlow, Essex, England. (Private communication.)

Fricke, H., and Morse, S. (1929). The actions of x rays on ferrous sulfate solutions, Phil. Mag. **7,** 129.

Friedland, S. S., Mayer, J. W., and Wiggins, J. S. (1960). Tiny semiconductor is fast, linear detector, Nucleonics **18,** No. 2, 54.

Fry, W. H., Miller, H., and Orton, K. F. (1955). A 50 curie cobalt-60 teletherapy unit, Brit. J. Radiol. **28,** 8.

Fuller, E. G., and Hayward, E. (1961). Calibration of a monitor for use in bremsstrahlung beams, J. Research NBS **65A** (Phys. & Chem.), No. 5, 401 (Sept.-Oct. 1961).

Fulton, G. P., Schulman, M. H., Lutz, B. R., and Arendt, K. A. (1954). Minute radiophotoluminescent glass implants for *in Vivo* radiation dosimetry, Federation Proc. **13,** 50.

Geiger, K. W. (1959). Absolute standardization of radioactive neutron sources. II. The use of the $F^{19}(\alpha,n)Na^{22}$ reaction, Can. J. Phys. **37,** 550.

Geiger. K. W., and Whyte, G. N. (1959). Absolute standardization of radioactive neutron sources. I. Activation of manganese bath, Can. J. Phys. **37,** 256.

Geiger, K. W. (1960). The status of the Canadian neutron standard, Can. J. Phys. **38,** 569.

Geiger, K. W., and Jarvis, C. J. D. (1962). Neutrons and gamma rays from Po^{210}-B^{10} (α,n) and Po^{210}-B^{11} (α,n) sources, Can. J. Phys. **40,** 33.

Genin, R. (1956). Energie moyenne d'ionisation dans les gaz. Défaut d'ionisation, J. Phys. Radium **17,** 571.

Genna, S., and Laughlin, J. S. (1955). Absolute calibration of a cobalt-60 gamma-ray beam, Radiology **65,** No. 3, 394.

Genna, S., and Laughlin, J. S. (1956). Calorimetric measurement of energy locally absorbed in an irradiated medium, AEC Contract Report AT (30–1) 1451.

Gevantman, L. H., Chandler, R. C., and Pestaner, J. F. (1957). Tridimensional examination of chemical systems irradiated in gel media, Radiation Res. **7,** 318.

Gevantman, L. H., and Pestaner, J. F. (1959). Ferric ion yields in ferrous sulfate solutions irradiated with low energy x-rays, J. Chem. Phys. **31,** 1140.

Gevantman, L. H. (1960). Radiation effects in gels, Radiation Res. Suppl. **2,** 608.

Geygy, J. R. (1955). Ed., Wissenschaftliche Tabellen, J. R. Geygy, Inc., Zurich, Switzerland.

Ginther, R. J., and Kirk, R. D., Thermoluminescence of CaF_2:Mn and its application to dosimetry, Report of Progress, U.S. Naval Research Laboratory, Sept. 1956, p. 12.

Ginther, R. J., and Kirk, R. D. (1957). The thermoluminescence of CaF_2:Mn, J. Electrochem. Soc. **104,** 365.

Ginther, R. J., and Schulman, J. H. (1960). New glass dosimeter is less energy-dependent, Nucleonics **18,** No. 4, 92.

Glass, F. M., and Hurst, G. S. (1952). A method of pulse integration using the binary scaling unit, Rev. Sci Instr. **23,** 67.

Glazunov, P. Ya, and Pikayev, A. K. (1960). An investigation of the radiolytic oxidation of divalent iron with irradiation doses of high power, Dokl. Akad. Nauk SSSR **130,** 1051.

Glocker, R., and Breitling, G. (1952). Der Kristall-Szintillationszähler als neues Dosismessverfahren, Strahlentherapie **88,** 92.

Goldblith, S. A., Proctor, B. E., and Hammerle, O. A. (1952). Evaluation of food-irradiation procedures utilizing high energy cathode rays, Ind. Eng. Chem **44,** 310.

Goldstein, H., and Wilkins, Jr., J. E. (1954). Calculations of the penetration of gamma rays, U. S. Atomic Energy Commission Report NYO–3075.

Goodwin, P. N. (1956). Scintillation counter for beta-ray dosimetry, Nucleonics **14,** No. 9, 120.

Goodwin, P. N. (1959). Calorimetric measurements on a cesium-137 teletherapy unit, Radiation Res. **10,** 6.

Gordon, S., and Hart, E. J. (1958). Radiation decomposition of water under static and bubbling conditions, 2d Intern. Conf. Peaceful Uses of Atomic Energy, Geneva, P/952, **29,** 13.

Gray, L. H. (1936). An ionization method for the absolute measurement of γ-ray energy, Proc. Roy. Soc. (London), **A.156,** 578.

Gray, L. H., Mottram, J. C., and Read, J. (1940). Some experiments upon the biological effects of fast neutrons, Brit. J. Radiol. **13,** 371.

Gray, L. H. (1944). The ionization method of measuring energy, Proc. Cambridge Phil. Soc. **40,** 72.

Greene, D., and Tranter, F. W. (1956). Dosage data for 4,000,000 volt X-rays, Brit. J. Radiol. **29,** 193.

Greening, J. R. (1947). The determination of x-ray energy distributions by the absorption method, Brit. J. Radiol. **20,** 71.

Greening, J. R. (1950). The determination of X-ray wavelength distributions from absorption data, Proc. Phys. Soc. **63A,** 1227.

Greening, J. R. (1951). A method of determining the wavelength distribution of the X-radiation at a point in a scattering medium, Brit. J. Radiol. **24,** 204.

Greening, J. R., and Wilson, C. W. (1951). The wavelength of the X-radiation at a depth in water irradiated by beams of X-rays, Brit. J. Radiol. **24,** 605.

Greening, J. R. (1952). The spectral distribution of radiation from X-ray tubes, J. Opt. Soc. Am. **42,** 685.

Greening, J. R. (1954). A survey of surface backscatter factors for radiations generated at 200 to 250 kv, Brit. J. Radiol. **27,** 532.

Greening, J. R. (1960). A compact free air chamber for use in the range 10–50 kv, Brit. J. Radiol. **33,** 178.

Griffith, H. D., and Swindell, G. E. (1951). Measurement of skin dose in radium therapy, Brit. J. Radiol. **24,** 337.

Griffith, G. H. (1958). Bibliography on photographic film dosimetry, WADC Tech. Note 58–105, ASTIA Document No. 155571.

Gross, W., Wingate, C., and Failla, G. (1957). Average energy lost by sulfur-35 beta rays per ion pair produced in air, Radiation Res. **7,** 570.

Gupton, E. D., Davis, D. M., and Hart, J. C. (1961). Criticality accident application of the Oak Ridge National Laboratory badge dosimeter, Health Phys. **5,** 57.

Haeberli, W., Huber, P., and Baldinger, E. (1953). Arbeit pro Ionenpaar von Gasen und Gasmischungen für α-Teilchen, Helv. Phys. Acta **26,** 145.

Hall, E. J., and Oliver, R. (1961). A pitfall to avoid in ferrous sulphate dosimetry, Brit. J. Radiol. **34,** 397.

Hanna, G. C. (1961). The depression of thermal neutron flux and density by absorbing foils, Nucl. Sci. Eng. **11,** 338.

Hanson, A. O., and McKibben, J. L. (1947). A neutron detector having uniform sensitivity from 10 kev to 3 Mev, Phys. Rev. **72,** 673.

Harlan, J. T., and Hart, E. J. (1959). Ceric dosimetry: Accurate measurement at 10^8 rads, Nucleonics **17,** No. 8, 102.

Hart, E. J. (1952). Mechanisms of the gamma-ray-induced chain oxidation of aqueous ferrous sulfate-formic acid-oxygen solutions, J. Am. Chem. Soc. **74,** 4174.

Hart, E. J. (1954). Gamma-ray-induced oxidation of aqueous formic acid-oxygen solutions, Effect of oxygen and formic acid concentrations, J. Am. Chem. Soc. **76,** 4312.

Hart, E. J., and Gordon, S. (1954). Gas evolution for dosimetry of high gamma, neutron fluxes, Nucleonics **12**, No. 4, 40.
Hart, E. J., Ramler, W. J., and Rocklin, S. R. (1956). Chemical yields of ionizing particles in aqueous solutions; effect of energy of protons and deuterons, Radiation Res. **4**, 378.
Hart, E. J., and Walsh, P. D. (1954). A molecular product dosimeter for ionizing radiations, Radiation Res. **1**, 342.
Hart, E. J., and Walsh, P. D. (1958). Dosimetry of gamma ray and neutron fluxes in CP–5, Proc. 2d Intern. Conf. Peaceful Uses of Atomic Energy, Geneva, P/763, **29**, 38.
Hart, E. J., Koch, H. W., Petree, B., Schulman, J. H., Taimuty, S. I., and Wyckoff, H. O. (1958). Measurement systems for high-level dosimetry, Proc. 2d Intern. Conf. Peaceful Uses of Atomic Energy **21**, 188.
Harteck, P., and Dondes, S. (1956). Nitrous oxide dosimeter for high levels of betas, gammas, and thermal neutrons, Nucleonics **14**, No. 3, 66.
Hartmann, S. R. (1957). WADC Technical Report 57–375, U.S. ASTIA Document AD–142029.
Haybittle, J. L., Saunders, R. D., and Swallow, A. J. (1956). X- and gamma irradiations of iron sulphate, J. Chem. Phys. **25**, 1213.
Healey, R. H., and Reed, J. W. (1941). The behaviour of slow electrons in gases, Amalgamated Wireless Valve Co., Sydney, Australia.
Hedden, W. A., Kircher, J. F., and King, B. W. (1960). Investigation of some glasses for high-level gamma-radiation dosimeters, J. Am. Ceram. Soc. **43**, No. 8, 413.
Heller, P. (1958). Private communication.
Henley, E. J. (1954). Gamma-ray dosimetry with cellophane-dye systems, Nucleonics **12**, No. 9, 62.
Henley, E. J., and Richman, D. (1956). Cellophane dye dosimeter for 10^5 to 10^7 roentgen range, Anal. Chem. **28**, 1580.
Henriksen, T. (1958). A scintillation dosimeter for 31 MeV betatron radiation, Acta Radiol. (Stockh.) **49**, 377.
Henriksen, T., and Baarli, J. (1957). The effective atomic number, Radiation Res. **6**, 415.
Henry, W. H., and Garrett, C. (1960). The Canadian standard free-air chamber for medium quality X-rays, Can. J. Phys. **38**, 1677.
Henry, W. H., and Aitken, J. H. (1961). Monitoring ionization chamber for an X-ray generator, Brit. J. Radiol. **35**, 516.
Herbert, R. J. T. (1956). A scintillation dose-rate meter using a tuned low frequency amplifier, Brit. J. Radiol. **29**, 345.
Hertz, C. H., and Gremmelmaier (1960). Miniature semiconductor dose-rate meter, Acta Radiol. **54**, 69.
Herwig, L. O., and Miller, G. H. (1954). Alpha-particle ionization in a gridded chamber, Phys. Rev. **94**, 1183.
Hess, W. N. (1957). Neutrons from (α,n) sources. Ann. Phys. **6**, 116.
Hettinger, G., and Starfelt, N. (1958a). Bremsstrahlung spectra from roentgen tubes, Acta Radiol. **50**, 381.
Hettinger, G., and Starfelt, N. (1958b). Inproved NaI scintillation spectrometer for the study of continuous X-ray spectra, Nucl. Instr. **3**, 25.
Hettinger, G., and Starfelt, N. (1959). Energy and angular distribution of scattered radiation in a water tank irradiated by X-rays, Arkiv. Fysik **14**, 497.
Hettinger, G. (1960a). Spectra of primary and secondary roentgen radiation, Radiation Physics Department, Lund.
Hettinger, G., and Lidén, K. (1960). Scattered radiation in a water phantom irradiated by roentgen photons between 50 and 250 kev, Acta Radiol. **53**, 73.
Hettinger, G. (1960b). Angular and spectral distribution of backscatter radiation from slabs of water, brass and lead irradiated by photons between 50 and 250 kev, Acta Radiol. **54**, 129.
Hickman, G. D., and Leng, W. B. (1961). The calculation of effective cutoff energies for cadmium, and gadolinium, samarium, Trans. Am. Nucl. Soc. **4**, 154.
Hill, D. L. (1947). Studies with the "Ranger", U.S. Report AECD–1945 (rev.).
Hine, G. J., and McCall, R. C. (1954). Gamma ray backscattering, Nucleonics **12**, No. 4, 27.
Hisdal, E. (1957). Bremsstrahlung spectra corrected for multiple scattering in the target, Phys. Rev. **105**, 1821.
Hochanadel, C. J., and Ghormley, J. A. (1953). A calorimetric calibration of gamma-ray actinometers, J. Chem. Phys. **21**, 880.
Hodara, M., Friedman, M., and Hine, G. J. (1959). Radiation dosimetry with fluorods, Radiology **73**, 693.
Hollander, L. E., Jr. (1956). Special CdS cells have high x- and γ-ray sensitivity, Nucleonics **14**, No. 10, 68.
Holm, N. W., Brynjolfsson, A., and Maul, J. E. (1961). Absolute measurements on the Co^{60} irradiation facility at Risø, p. 371–6 of Selected Topics in Radiation Dosimetry, Vienna, International Atomic Energy Agency.
Hornyak, W. F. (1952). A fast neutron detector, Rev. Sci. Instr. **23**, 264.
Hospital Physicists' Association (1960). A code of practice for X-ray measurements, Brit. J. Radiol. **33**, 55.
Hospital Physicists' Association (1961). Depth dose tables for use in radiotherapy, Brit. J. Radiol. Suppl. No. 10.
Houtermans, F. G., and Teucher, M. (1951). Das Primarspektrum der schnellen Neutronen einer (Raα+Be)-quelle und deren unelastischen Stosse in Pb. II. Z Physik **129**, 365.
Howard-Flanders, P. (1958). Physical and chemical mechanisms in the injury of cells by ionizing radiations, Advan. Biol. Med. Phys. **6**, 553.
Hubbell, J. H. (1958). Response of a large sodium-iodide detector to high energy X-rays, Rev. Sci. Instr. **29**, 65.
Hübner, W. (1961). Private communication.
Hübner, W. (1958). Uber den Einfluss von Fremdstoffen in Filtersubstanzen bei Schwächungs-und Halbwerte schichtmessungen, Fortschr. Gebiete Röntgenstrahlen Nuklearmed **89**, 629.
Huffman, R. E., and Davison, N. (1956). Kinetics of the ferrous iron-oxygen reaction in sulfuric acid solutions, J. Am. Chem. Soc. **78**, 4836.
Hughes, D. J. (1953). Pile neutron research, Addison-Wesley Publ. Co., Cambridge, Mass.
Hughes, D. J., and Schwartz, R. B. (1958). Neutron cross sections, BNL–325, 2d ed.
Hurst, G. S., Ritchie, R. H., and Wilson, H. N. (1951). A count-rate method of measuring fast neutron tissue dose, Rev. Sci. Instr. **22**, 981.
Hurst, G. S., and Ritchie, R. H. (1953). On energy resolution with proportional counters, Rev. Sci. Instr. **24**, 664.
Hurst, G. S. (1954). An absolute tissue dosimeter for fast neutrons, Brit. J. Radiol. **27**, 353.
Hurst, G. S., Harter, J. A., Hensley, P. N., Mills, W. A., Slater, M., and Reinhardt, P. W. (1956). Techniques of measuring neutron spectra with threshold detectors—tissue dose determination, Rev. Sci. Instr. **27**, 153.
ICRU (1957). Report of the International Commission on Radiological Units and Measurement, 1956 NBS Handb. 62.
ICRU (1959). Report of the International Commission on Radiological Units and Measurements, NBS Handb. 78.
ICRU Report 10a (1962). Radiation Quantities and Units, NBS Handb. 84.
ICRU Report 10d (1962). Clinical Dosimetry, NBS Handb. 87.
International critical tables of numerical data (1926–30). Publ. for National Research Council by the McGraw-Hill Book Co. Inc., New York, N.Y.
Ishiwari, R., Yamashita, S., Yuasa, K., and Miyake, K. (1956). On the ionization-energy relation for alpha-particles in air, J. Phys. Soc. Japan **11**, 337.
Ito, T., and Ito, G. (1941). Special edit. Commemorating 50th anniv. of Electrotechnical Lab., Tokyo, Japan, p. 11.
Ittner, W. B., and Ter-Pogossian, M. (1952). Air-equivalence of scintillation materials, Nucleonics **10**, No. 2, 48.
Ittner, W. B., and Ter-Pogossian, M. (1954). Scintillation probe for determining relative beta ray intensities, Nucleonics **12**, No. 5, 56.

Jaeger, R., and Kolb, W. (1956). Scintillationsspektrometrie weicher Röntgenstrahlung, Sonderbände Strahlenther. **35,** 285.
Jaffe, G. (1929). Columnar ionization in gases at high pressures, Physik. Zeitschr. **30,** 849.
Jaques, T. A. J., Bollinger, H. A., and Wade, F. (1953). Neutron detector for reactor instrumentation, Proc. Inst. Elec. Engrs. **100**, Pt. I, 110.
Jahns, E. (1960). Bau und Erprobung eines Lumineszenz-Dosimeters für Messungen in Körperhöhlen, Diploma Thesis, University of Heidelberg.
Jennings, W. A. (1950). Physical aspects of the roentgen radiation from a beryllium window tube operating over the range 2–50 kvp for clinical purposes, Acta Radiol. **33,** 435.
Jennings, W. A. (1951). Low voltage X-ray therapy with a beryllium window tube part 2, the achievement of optimum depth dosage distribution, from the physical standpoint, Brit. J. Radiol. **24,** 135.
Jennings, W. A. (1953). A theoretical study of radiation outputs and qualities from a beryllium window tube operated at low kilovoltage, Brit. J. Radiol. **26,** 193.
Jentschke, W. (1940). Messungen an harten H-Strahlung, Physikal Zeits. **41,** 524.
Jervis, R. E. (1957). A cobalt irradiation-monitoring technique. Report Atomic Energy of Canada, CRDC–730.
Jesse, W. P., and Sadauskis, J. (1953). Alpha particle ionization in pure gases and the average energy to make an ion pair, Phys. Rev. **90,** 1120.
Jesse, W. P., and Sadauskis, J. (1955). Ionization in pure gases and the average energy to make an ion pair for alpha and beta particles, Phys. Rev. **97,** 1668.
Jesse, W. P. (1958). Absolute energy to produce an ion pair in various gases by beta particles from S^{35}, Phys. Rev. **109,** 2002.
Jesse, W. P. (1960). The ionization by polonium alpha particles in air and the average energy to make an ion pair, Radiation Res. **13,** 1.
Johansson, S. A. E. (1951). The use of scintillation counters in the measurement of the energy of X-rays and low energy gamma rays, Arkiv Fysik **3,** 533.
Johns, H. E., Epp, E. R., Cormack, D.V., and Fedoruk, S. O. (1952a). Depth dose data and diaphragm design for the Saskatchewan 1000 curie cobalt unit, Brit. J. Radiol. **25,** 302.
Johns, H. E., Fedoruk, S. O., Kornelsen, P. O., Epp, E.R., and Darby, E. K. (1952b). Depth dose data, 150 kvp to 400 kvp, Brit. J. Radiol. **25,** 542.
Johns, H. E., Till, J. E., and Cormack, D. V. (1954). Electron energy distributions produced by gamma-rays, Nucleonics **12,** No. 10, 40.
Johns, H. E., Bruce, W. R., and Reid, W. B. (1958). The dependence of depth dose on focal skin distance, Brit. J. Radiol. **31,** 254.
Johns, H. E., Hunt, J. W., and Skarsgard, L. D. (1959). A cesium 137 teletherapy unit for use at a source-to-skin distance of 35 cm, Brit. J. Radiol. **32,** 224.
Johnson, C. H. (1960). Recoil telescope detectors, Chapter II C in Fowler, J. L., and Marion, J. B., Fast Neutron Physics, Part I, Interscience Publ. Inc., New York.
Johnson, G. R. A., and Weiss, J. (1957). The actions of X-rays (200 kv) and γ rays (^{60}Co) on dilute aqueous solutions of ceric salts, Proc. Roy. Soc. (London) **A240,** 189.
Jones, A. R. (1960). Uses of semiconductor detectors in health physics monitoring, Nucleonics **18,** No. 10, 86.
Jones, D. E. A. (1940). The determination from absorption data of the distribution of X-ray intensity in the continuous X-ray spectrum, Brit. J. Radiol. **13,** 95.
Jones, D. E. A. (1961). The suitability of materials used for the measurement of the half-value thickness of X-ray beams, Brit. J. Radiol. **34,** 801.
Jordan, W. H., and Bell, P. R. (1947). A general purpose linear amplifier, Rev. Sci. Instr. **18,** 703.
Joyet, G., Trumpy-Eggenberger, C., and Mauderli, W. (1953). Article in The Brown Boveri Betatron, Brown, Boveri & Co., Ltd., Baden, Switzerland.
Kara-Michailova, E., and Lea, D. E. (1940). The interpretation of ionization measurements in gases at high pressures, Proc. Cambridge Phil. Soc. **36,** 101.
Keene, J. P. (1957). Oxidation of ferrous ammonium sulfate solutions by electron irradiation at high dose rates, Radiation Res. **6,** 424.
Kemp, L. A. W. (1946). The physicist in the radiodiagnostic department, Brit. J. Radiol. **19,** 304.
Kemp, L. A. W., and Burns, J. E. (1958). Physical measurements on the London Hospital Picker C3000 cobalt unit, Acta Radiol. **49,** 471.
Khabakhpashev, A. G. (1960). Neutron spectrum of a Po-α-O source, Soviet J. Atomic Energy (Transl.) **7,** 591.
Kircher, J. F., King, B. W., Oestmann, M. J., Schall, P., and Calkins, G. D. (1958). Recent research in high-level gamma dosimetry, Proc. 2d Intern. Conf. Peaceful Uses of Atomic Energy **21,** 199.
Klema, E. D., and Ritchie, R. H. (1952). Thermal neutron flux measurements in graphite using gold and indium foils, Phys. Rev. **87,** 167.
Koch, H. W., and Carter, R. E. (1950). Determination of the energy distribution of bremsstrahlung from 19.5 Mev electrons, Phys. Rev. **77,** 165.
Koch, L., Labeyrie, J., and Tarassenko, S. (1958). Nouvelle méthode de mesure de flux de neutrons, Conf. Rept. Geneva, 15/P/1207.
Koch, H. W., and Motz, J. W. (1959). Bremsstrahlung cross-section formulas and related data, Rev. Mod. Phys. **31,** 920.
Kolb, W. (1955). Scintillationsspektrometrie weicher Röntgenstrahlung, Naturwissenschaften **43,** 53.
Komar, A. P., and Kruglov, S. P. (1960). Quantameter for measuring energy flux of bremsstrahlung from betatrons and synchrotons and an investigation of this instrument, Zh. Tekh. Fiz. **30,** 1369 (Soviet Phys.-Techn. Phys. **5,** 1299, 1961).
Kondo, S. (1960a). Neutron response of silver-activated phosphate glass, Health Phys. **4,** 21.
Kondo, S. (1961). Response of silver-activated phosphate glass to α,β,γ rays and neutrons, Health Phys. **7,** 25.
Kramers, H. A. (1923). On the theory of X-ray absorption and of the continuous x-ray spectrum, Phil. Mag. **46,** 836.
Kreidl, N. J., and Blair, G. E. (1956b). Recent developments in glass dosimetry, Nucleonics **14,** No. 3, 82.
Kulenkampff, H. (1922). Über das kontinuierliche Röntgenspektrum, Annal. Phys. **69,** 548.
Langendorff, H., Spiegler, G., and Wachsmann, F. (1952). Strahlenschutzueberwachung mit Filmen, Fortschr. Gebiete Roentgenstrahlen Nuklearmed **77,** 143.
Larson, H. V. (1958). Investigation of the energy loss per ion pair in air for protons in various gases, Phys. Rev. **112,** 1927.
Larsson, K. E. (1954). A critical comparison between some methods for measuring the strength of a Ra-Be neutron source absolutely, Arkiv. Fysik **7,** 323.
Larsson, K. E. (1955). The use of the T^3 (d,n) He^4 reaction for the comparison of some methods for the absolute measurement of a fast neutron flux, Arkiv. Fysik **9,** 293.
Larsson, K. E. (1958). Present status in the field of neutron source calibrations, J. Nucl. Energy **6,** 322.
Lasich, W. B., and Riddiford, L. (1947). Note on the 2.8 Mev Betatron, J. Sci. Instr. **24,** 177.
Laughlin, J. S., and Beattie, J. W. (1951). Calorimetric determination of the energy flux of 22.5 Mev x rays, Rev. Sci. Instr. **22,** 572.
Laughlin, J. S., Beattie, J. W., Henderson, W. J., and Harvey, R. A. (1953). Calorimetric evaluation of the roentgen for 400 kv and 22.4 Mev roentgen rays, Am. J. Roentgenol., Radium Therapy, Nucl. Med. **76,** No. 2, 294.
Laughlin, J. S., and Genna, S. (1956). Calorimetric Methods, Chapt. 9. Radiation Dosimetry, Hine and Brownell, Editors, Academic Press, Inc., New York, N.Y.
Laughlin, J. S., Zsula, J., and Liuzzi, A. (1957). Oxidation of ferrous sulfate by high-energy electrons and the influence of the polarization effect, Radiation Res. **7,** 327.

Laurence, G. C. (1937). The measurement of extra hard x rays and gamma rays in roentgens, Can. J. Res. **A15,** 67.
Lazo, R. M., Dewhurst, H. A., and Burton, M. (1954). The ferrous sulfate radiation dosimeter, a calorimetric calibration with gamma rays, J. Chem. Phys. **22,** 1370.
Lee, P. K., Ballinger, E. R., and Schweitzer, W. H. (1961). A heat treatment which extends the usable range of $AgPO_3$ glass dosimeters, Los Alamos Scientific Laboratory Rept. No. LA2575.
Leiss, J. E., Pruitt, J. S., and Schrack, R. A. (1958). Private Communication.
Lidén, K., and Starfelt, N. (1954). Scintillation spectrometry of continuous gamma- and X-ray spectra below 1 Mev, Arkiv Fysik **7,** 427.
Lindell, B. (1954). Secondary roentgen radiation, Acta Radiol. **41,** 353.
Liskien, H., and Paulsen, A. (1961). Compilation of cross sections for some neutrons induced threshold reactions, Euratom, Central Bureau for Nuclear Measurements, Geel (Belgium).
Littler, D. J., and Lockett, E. E. (1952). The measurement of an absolute thermal neutron density in G. L. E. E. P., AERE RIR 961 Appendix 3.
Littler, I. J., and Thomas, R. H. (1952). Absolute neutron density determinations using cobalt, AERE R/R 1019.
Littler, D. J. (1957). Report on a conference on neutron source preparation and calibration held at Buckland House on the 8th and 9th of July 1954, British Report AERE NP/R 1577.
Loeffler, F. J., Palfrey, T. R., and Tautfest, G. W. (1959). The energy dependence of the Cornell thick-walled ionization chamber, Nucl. Inst. Methods **5,** 50.
MacLaughlin, W. L. (1962). Radiation beam mapping with photographic film, Radiology **78,** 119.
Macklin, R. L. (1957). Graphite sphere neutron detector, Nuclear Inst. **1,** 335.
Maier-Leibnitz (1961). Reaktor München, Private communication.
Mak, S., and Cormack, D. V. (1960). Spectral distributions of scattered X-rays at points lying off the beam axis, Brit. J. Radiol. **33,** 362.
Malsky, S. J., Amato, C. G., Reid, C. B., Spreckels, C., and Maddalone L. (1961). *In Vivo* dosimetry with miniature glass rods, Parts I (Physical Aspects) and II (Clinical Application), Am. J. Roentgenol. Radium Therapy, Nucl. Med. **85,** 568–582.
Marinelli, L. D. (1953). Radiation dosimetry and protection, Annual Review of Nuclear Science, **3,** 249 (Annual Reviews, Inc., Stanford, Calif.)
Martin, D. H. (1955). Correction factors for Cd-covered foil measurements, Nucleonics **13,** No. 3, 52.
Martin, J. H., and Muller, G. W. (1961). Quantity and quality of scattered X-rays, Brit. J. Radiol. **34,** 227.
Mayneord, W. V. (1940). Energy absorption, Brit. J. Radiol. **13,** 235.
McDiarmid, I. B. (1952). The X-ray spectrum from a 70 Mev synchrotron, Phil. Mag. **43,** 1003.
McDonell, W. R., and Hart, E. J. (1954). Oxidation of aqueous ferrous sulfate solutions by charged particle radiation, J. Am. Chem. Soc. **76,** 2121.
McElhinney, J., Zendle, B., and Domen, S. (1956). A calorimeter for measuring the power in a high-energy x-ray beam, J. Research NBS **56,** No. 1, 9, RP2642.
McElhinney, J., Zendle, B., and Domen, S. R. (1957). Calorimetric determination of the power in a 1400 kv x-ray beam, Radiation Res. **6,** 40.
McGinnies, R. T. (1959). Energy spectrum resulting from electron slowing down, NBS Circ. 597.
McKay, K. G. (1951). Electron-hole production in germanium by alpha-particles. Phys. Rev. **84,** 829.
McLaughlin, W. L. (1959). Photographic methods in measuring large radiation doses, Nucleonics **17,** No. 10, 58.
Medalia, A. I., and Byrne, B. J. (1951). Spectrophotometric determination of cerium (IV), Anal. Chem. **23,** 453.
Medvecsky, L. (1961). Energy spectrum of neutron sources Be(α,n), Atomki Kozeemenyek **III,** 2–3 (Debrecen, Hungary).
Meister, Von H. (1958). Die Aktivierungsquerschnitte von Mn^{55}, Cu^{63}, Pd^{108} und In^{115} für thermische neutronen. Z. Naturforsch. **13a,** 820.
Meredith, W. J. (1940). Percentage depth doses in low voltage X-ray therapy, Brit. J. Radiol. **13,** 320.
Michikawa, T., Teranishi, E., Tomimasu, T., and Inoue, Y. (1959). The absolute calibration of a Ra(α)-Be neutron source, Bull. Electrotech. Lab. (Tokyo) **23,** 223.
Michikawa, T., Furubayashi, B., Teranishi, E., and Inoue, Y. (1961). Absolute calibrations of thermal neutron flux densities. Bull. of the Electrotech. Lab. (Tokyo), to be published.
Miller, W., Motz, J. W., and Cialella, C. (1954). Thick target bremsstrahlung spectra for 1.00, 1.25 and 1.40 Mev electrons, Phys. Rev. **96,** 1344.
Miller, N., Part III, Chapter 2, Actions chimiques et biologiques des radiations 2me série Hassinsky, Masson et Cie, Paris, p. 161 et seq., 1956.
Miller, N. (1958). Radiation yield measurements in irradiated aqueous solutions. II. Radical yields with 10.9 Mev deuterons, 21.3 and 3.4 Mev alpha particles, and B(n,α)Li recoil radiations, Radiation Res. **9,** 633.
Milvy, P., Genna, S., Barr, N., and Laughlin, J. S. (1958). Calorimetric determination of local absorbed dose, Proc. 2d Intern. Conf. Peaceful Uses of Atomic Energy **21,** 142.
Milvy, P., Barr, N., Geisselsoder, J., and Laughlin, J. S. (1960). Calorimetric determination of local absorbed dose, IXth Intern. Cong. Radiology, Trans., George Thieme Verlag, Stuttgart, Germany.
Minder, W. (1961). Chemical dose measurements of high energy photons and electrons, p. 315–23 of Selected Topics in Radiation Dosimetry, Vienna, International Atomic Energy Agency.
Moe, H. J., Bortner, T. C., and Hurst, G. S. (1957). Ionization of acetylene mixtures and other mixtures by Pu^{239} α-particles, J. Phys. Chem. **61,** 422.
Mohr, H. (1957). Vergleichende Dosismessungen im Phantom mit Leuchtstoffdosimeter und Ionisationskammer, Fortschr. Röntgenstr. **85,** 486.
Morrison, M. T., and Reed, G. W. (1952). A note on the determination of half-value layers of soft X-rays, Brit. J. Radiol. **25,** 270.
Mosburg, E. R. Jr. (1959). A scintillation counter method of intercomparing neutron source strengths by means of a manganous sulfate bath, J. Research NBS **62,** 189, RP2952.
Mosburg, E. R. (1961). Notes on self-shielding corrections for 1/v detectors in a Maxwellian flux. Private communication, National Bureau of Standards.
Mosburg, E. R., and Murphey, W. (1961). A recalibration of the NBS standard thermal neutron flux. Reactor Sci. Technol. (J. Nucl. Energy, Parts A/B) **14,** 25–30.
Moteff, J. and Beever, E. R. (1960). Proc. Symp. Selected Topics in Radiation Dosimetry, I.A.E.A., Vienna, Austria, p. 383.
Motz, J. W., Miller, W., and Wyckoff, H. O. (1953). Eleven-Mev thick target bremsstrahlung, Phys. Rev. **89,** 968.
Muckenthaler, F. J. (1957). Applied nuclear physics annual progress report, p. 270, ORNL–2389.
Muehlhause, C. O., and Thomas, G. (1953). Two liquid scintillation neutron detectors, Nucleonics **11,** No. 1, 44.
Murphey, W. M. and Chin, J. (1962). Intercomparisons of the Standard Thermal Neutron Flux Density of the National Bureau of Standards. Proc. IAEA Symp. Neutron Detection, Dosimetry and Standardization held at Harwell, England, Dec. 10–14, 1962.
Murray, R. B. (1958). Use of Li^6I(Eu) as a scintillation detector and spectrometer for fast neutrons. Nucl. Instr. Methods **2,** 237.

688–008 O—64——8

Myers, I. T., Le Blanc, W. H., Fleming, D. M., and Wyckoff, H. O. (1961). An adiabatic calorimeter for high precision standardization and determination of W(air), paper presented at meeting of Radiation Research Society, Washington.
Naito, M., Inoue, Y., Ibaraki, Y., and Moriuchi, Y. (1961). Present status of standardization of exposure dose in Japan, Proc. Symposium on Selected Topics in Radiation Dosimetry (Vienna, 1960), IAEA.
NCRP Report, 1954, Permissible dose from external sources of ionizing radiation, NBS Handb. 59.
NCRP Report, 1957, Protection against neutron radiation up to 30 million electron volts, NBS Handb. 63.
NCRP Report, 1960, Measurement of neutron flux and spectra for physical and biological applications, NBS Handb. 72.
NCRP Report, 1961, Measurement of absorbed dose of neutrons and of mixtures of neutrons and gamma rays, NBS Handb. 75, p. 82.
NCRP Report, 1961, Stopping powers for use with cavity ionization chambers, NBS Handb. 79.
Nelms, A. T. (1953). Graphs of the Compton energy-angle relationship and the Klein-Nishina formula from 10 kev to 500 Mev, NBS Circ. 542.
Nelms, A. T. (1958). Energy loss and range of electrons and positrons, Suppl. NBS Circ. 577.
Newbery, G. R., and Bewley, D. K. (1955). The performance of the medical research council 8 Mev linear accelerator, Brit. J. Radiol. **28,** 241.
Nold, M. M., Hayes, R. L., and Comar, C. L. (1958). Tissue dose from internally administered Y^{90}, Radiation Res. **9,** 190 (Abstracts).
Oakley, D. C., and Walker, R. L. (1955). Photoproduction of neutral pions in H; magnetic analysis of recoil protons, Phys. Rev. **97,** 1283.
Olde, G. L., and Brannen, E. (1961). Surface dose measurements with a scintillation dosemeter, Phys. Med. Biol. **6,** 325.
Oosterkamp, W. S., and Proper, J. (1952). Free-air and thimble ionization chambers for Grenz-ray dosimetry, Acta Radiol. **37,** 33.
Paymal, M., Bonnaud, M., and LeClerk, P. (1960). Radiation dosimeter glasses, Proc. Intern. Symp. Selected Topics in Radiation Dosimetry, IAEA, Vienna, Austria, June 7–13.
Payne-Scott, R. (1937). The wave length distribution of the scattered radiation in a medium traversed by a beam of X or gamma rays, Brit. J. Radiol. **10,** 850.
Peelle, R. W., Maienschein, F. C., and Love, T. A. (1957). Energy and angular distribution of gamma radiation from a Co^{60} source after diffusion through many mean free paths of water, ORNL Rept. 2196.
Peirson, D. H. (1958). The phosphate glass dosimeter, Atomic Energy Research Establishment, Harwell Rept. No. AERE–EL/R 2590.
Perlman, Richards, and Speck (1946). U.S. Atomic Energy Commission Rept. MDDC–39.
Petree, B. (1958). Absorbed dose calorimetry for high dose rates, Abs. No. 215, Radiation Res. **9,** 166.
Phillips, K. (1952). The experimental determination of the spectra of a betatron, Proc. Phys. Soc. **65A,** 57.
Phillips, K. (1954). On the thick target bremsstrahlung spectrum at relativistic energies, Proc. Phys. Soc. **67A,** 669.
von Planta, C., and Huber, P. (1956). Bestimmung der Quellstarke einer Be-Photo-und einer Ra-Be-Neutronenquelle, Helv. Physica Acta **29,** 375.
Pott, F. Rh., and Wagner, S. (1960). Die selektive Messung von Neutronen-und Photonendosen mit einem Äthylendosimeter, Nukleonik **2,** No. 7, 271.
Proppe, A., and Wagner, G. (1954). Die Bedeutung der Halbwerttiefe für die dermatologische Röntgentherapie, Z. Haut Geschlechtskrankh. **16,** 289.
Pruitt, J. S., and Pohlit, W. (1960). Vergleichsmessungen mit Intensitäts-standards fur energiereiche Bremsstrahlung, Z. Naturforsch. **15b,** 617.
Pruitt, J. S., and Domen, S. R. (1962). Determination of total X-ray beam energy with a calibrated ionization chamber, NBS Mono. 48.
Pruitt, J. S., Allisy, A., Joyet, G., Pohlit, W., Tubiana, M., and Zupančič, C. (1962). Transfer of NBS high energy X-ray calibrations to European betatron laboratories, J. Research NBS **66C** (Eng & Instr), No. 2, 107 (Apr.-June 1962).
Rabin, H., and Price, W. E. (1955). Mapping radiation fields with silver-activated phosphate glass, Nucleonics **13,** No. 3, 33.
Rae, E. R., and Bowey, E. M. (1953). A scintillation detector for neutrons of intermediate energy, Proc. Phys. Soc. (London), **A66,** 1073.
Rawson, E. G., and Cormack, D. V. (1958). A matrix to correct for scintillator escape effects, Nucleonics, **16,** No. 10, 92.
Rajewsky, B., Bunde, E., Dorneich, M., Lang, D., Sewkor, A., Jaeger, R., and Hübner, W. (1955). Darstellung, Wahrung und Übertragung der Einheit der Dosis für Röntgen-und Gammastrahlen mit Quantenenergien zwischen 3 kev und 500 kev (Physikalisch-Technische Bundesanstalt, Braunschweig, Germany).
Reid, W. B., and Johns, H. E. (1961). Measurement of absorbed dose with calorimeter and determination of W, Radiation Res. **14,** 1.
Reinhardt, P. W., and Davis, F. J. (1958). Improvements in the threshold detector method of fast neutron dosimetry, Health Phys. **1,** 169.
Richardson, J. E., Kerman, H. D., and Brucer, M. (1954). Skin dose from a cobalt-60 teletherapy unit, Radiology **63,** 25.
Richmond, R. (1958). The standardization of neutron sources, Progr. in Nucl. Energy, Series I, Phys. and Math., **II,** 165.
Riegert, A. L., Johns, H. E., and Spinks, J. W. T. (1956). Ag-phosphate glass needles for measuring gamma dose, Nucleonics **14,** No. 11, 134.
Ritchie, R. H., and Dalton, G. R. (1961). Re: Thermal neutron flux depression by absorbing foils and flux perturbations by thermal neutron detectors, Nucl. Sci. Eng. **11,** 451.
Ritchie, R. H., and Eldridge, H. B. (1960). Thermal neutron flux depression by absorbing foils, Nucl. Sci. Eng. **8,** 300.
Ritz, V. H. (1959). Design of free-air ionization chambers for the soft X-ray region (20–100 kv), Radiology **73,** 911.
Ritz, V. H. (1960). Standard free-air chamber for the measurement of low energy x-rays (20–100 kilovolts-constant potential), J. Research NBS **64C** (Eng. & Instr.), No. 1, 49.
Ritz, V. H. (1961). A note on Mylar film dosimetry, Radiation Res. **15,** 460.
Roberts, J. H. (1957). Absolute flux measurement of anisotropic neutron spectra with proton recoil tracks in nuclear emulsions, Rev. Sci. Instr. **28,** 677.
Robson, J. W., and Gregg, E. C. (1956). A scintillation crystal roentgen ray dosimeter, Am. J. Roentgenol, Radium Therapy, Nucl. Med. **76,** 979.
Robson, J. W., and Gregg, E. C. (1957). Bremsstrahlung measurements with a Compton electron spectrometer, Phys. Rev. **105,** 619.
Roe, G. M. (1954). The absorption of neutrons in Doppler broadened resonances. KAPL 1241.
Roesch, W. C. (1958). Dose for nonelectronic equilibrium conditions, Radiation Res. **9,** 399.
Rosen, L. (1956). Techniques for measurement of neutron cross sections and energy spectra for sources which are continuous in energy and time, Proc. Intern. Conf. Peaceful Uses of Atomic Energy, **4,** paper P/582, United Nations, New York, N.Y.
Rosman, I. M., and Zimmer, K. G. (1955). O primenenii Stsintillyatorov v dosimetrii, Vestnik Rentgenologii i Radiologii, No. 1, 63.
Rosman, I. M., and Zimmer, K. G. (1956a). Über die Anwendung von Szintillatoren in der Dosimetrie, Z. Naturforsch, **11B,** 46.
Rosman, I. M., and Zimmer, K. G. (1956b). An isodose plotter of simple design, Brit. J. Radiol. **29,** 688.
Rosman, I. M., and Zimmer, K. G. (1957). Über die Anwendung von Szintillatoren in der Dosimetrie—II. Atomkernenergie **2,** 429.

Rossi, H. H., and Rosenzweig, W. (1955a). A device for the measurement of dose as a function of specific ionization, Radiology **64,** 404.
Rossi, H. H., and Rosenzweig, W. (1955b). Measurements of neutron dose as a function of linear energy transfer, Radiation Res. **2,** 417.
Rossi, H. H., and Rosenzweig, W. (1956). Limitation of the concept of linear energy transfer (LET), Radiology **66,** 105.
Rossi, H. H., and Failla, G. (1956). Tissue-equivalent ionization chambers, Nucleonics **14,** No. 2, 32.
Rossi, H. H., Biavati, M. H., and Gross, W. (1961). Local energy density in irradiated tissues, I. Radiobiological significance, Radiation Res. **15,** 431.
Rotblat, J. (1950). Photographic emulsion technique, Chapter 3, Progress in Nuclear Phys. **1,** Academic Press, Inc., New York, N.Y.
Rotblat, J., and Sutton, H. C. (1960). The effects of high dose rates of ionizing radiations on solutions of iron and ceric salts, Proc. Roy. Soc. (London) **A255,** 490.
Rudstam, G., and Svedberg, T. (1953). Use of tracers in chemical dosimetry, Nature **171,** 648.
Runnalls, O. J. C., and Boucher, R. R. (1956). Neutron yields from actinide-beryllium alloys, Can. J. Phys. **34,** 949.
Rosenzweig, W., and Rossi, H. H. (1959). Determination of the quality of the absorbed dose delivered by monoenergetic neutrons. Radiation Res. **10,** 532, and Private communication.
St. Romain, F. A., Bonner, T. W., Bramblett, R. L., and Hanna, J. (1962). Low-energy neutrons from the reaction $Be^9(\alpha,n)C^{12}$, Phys. Rev. **126,** 1794.
Schaal, A. (1956). Messung der Strahlenhärte innerhalb eines streuenden Mediums in der Röntgen-Tiefentherapie, Strahlentherapie **99,** 561.
Scharf, K., and Lee, R. M. (1961). Investigation of the spectrophotometric method of measuring the ferric ion yield in the ferrous sulfate dosimeter Radiation Res. Abstract No. 135, **14,** 498.
Schenck, J., and Heath, R. L. (1952). Tin activation of LiI, Phys. Rev. **85,** 923.
Schenck, J. (1953). Activation of lithium iodide by europium, Nature **171,** 518.
Schiff, L. I. (1951). Energy-angle distribution of thin target bremsstrahlung, Phys. Rev. **83,** 252.
Schilling, W. (1960). Neutron flux measurements at the FRM with a thermocouple. Kerntechnik **2,** 398.
Schmidt-Rohr, U. (1953). Ein Spektrometer für schnelle Neutronen und das Neutronenspektrum von Ra-α-Be, Z. Naturforschung **8a,** 470.
Schmitt, H. W. (1960). Determination of the energy of antimony-beryllium photoneutrons, Nuclear Phys. **20,** 220.
Schneider, D. O., and Cormack, D. V. (1959). Monte Carlo calculations of electron energy loss, Radiation Res. **11,** 418.
Schuler, R. H., and Allen, A. O. (1956). Yield of the ferrous sulfate radiation dosimeter: an improved cathode-ray determination, J. Chem. Phys. **24,** 56.
Schuler, R. H., and Barr, N. F. (1956). Oxidation of ferrous sulfate by ionizing radiations from (n,α) reactions of boron and lithium, J. Am. Chem. Soc. **78,** 5756.
Schuler, R. H., and Allen, A. O. (1957). Radiation chemistry studies with cyclotron beams of variable energy: Yields in aerated ferrous sulfate solution, J. Am. Chem. Soc. **79,** 1565.
Schulman, J. H. (1950). Dosimetry of x rays and γ rays, U.S. Naval Research Laboratory Rept. No. 3736.
Schulman, J. H., Ginther, R. J., Klick, C. C., Alger, R. S., and Levy, R. A. (1951). Dosimetry of x rays and γ rays by radiophotoluminescence, J. Appl. Phys. **22,** 1479.
Schulman, J. H., Shurcliff, W., Ginther, R. J., and Attix, F. H. (1953). Radiophotoluminescent dosimetry system of the U.S. Navy, Nucleonics **11,** No. 10, 52.
Schulman, J. H., and Etzel, H. W. (1953). Small volume dosimeters for x-rays and gamma-rays, Science **118,** 184.
Schulman, J. H., Klick, C. C., and Rabin, H. (1955). Measuring high doses by absorption changes in glass, Nucleonics **13,** No. 2, 30.
Schulman, J. H., Attix, F. H., West, E. J., and Ginther, R. J. (1960b). New thermoluminescent dosimeter, Rev. Sci. Inst. **31,** 1263.
Schwarz, H. A. (1954). Temperature coefficient of the radiation induced oxidation of ferrous sulfate, J. Am. Chem. Soc. **76,** 1587.
Scrimger, J. W. (1962). The measurement of cobalt-60 output spectrum. Thesis. University of Saskatchewan.
Seeman, H. E. (1938). Secondary radiation intensity as a function of certain geometrical variables, Am. J. Roentgenol. **39,** 628.
Shalek, R. J., and Cole, A. (1958). A scintillation probe for the measurement of radiation dose in body cavities, Am. J. Roentgenol. **79,** 450.
Sharpe, J. (1952). Energy per ion pair for argon with small admixture of other gases, Proc. Phys. Soc. (London) **A65,** 859.
Sigoloff, S. C. (1956). Fast-neutron insensitive chemical gamma-ray dosimeter, Nucleonics **14,** No. 10, 54.
Sigoloff, S. C. (1961). Chemical and colorimetric dosimetry: the tetrachloroethylene chemical dosimeter system, p. 337–59 of Selected Topics in Radiation Dosimetry, Vienna, International Atomic Energy Agency.
Silbertstein, L. (1932). Spectral composition of an X-ray radiation determined from its filtration curve, Phil. Mag. **15,** 375.
Sinclair, W. K., and Trott, N. G. (1956). The construction and measurement of beta-ray applicators for use in ophthalmology, Brit. J. Radiol. **29,** 15.
Skarsgard, L. D., Bernier, J. P., Cormack, D. V., and Johns, H. E. (1957). Calorimetric determination of the ratio of energy absorption to ionization for 22-Mev x rays, Radiation Res. **7,** 217.
Skarsgard, L. D., and Johns, H. E. (1961). Spectral flux density of scattered and primary radiation generated at 250 kv, Radiation Res. **14,** 231.
Skarsgard, L. D., Johns, H. E., and Green, L. E. S. (1961). Iterative response correction for a scintillation spectrometer, Radiation Res. **14,** 261.
Skjöldebrand, R. (1955). A fast neutron scintillation counter with tissue equivalent response, J. Nucl. Energy **1,** 299.
Skyrme, T. H. R. (1943). Reduction in neutron density caused by an absorbing disk, British Report MS–91.
Slater, M., Bunyard, G. B., and Randolph, M. L. (1958). Combination ion chamber-proportional counter dosimeter for measuring gamma-ray contamination of neutron fields, Rev. Sci. Instr. **29,** 601.
Smeltzer, J. C. (1950). Energy dependence of the naphthalene scintillation detector, Rev. Sci. Instr. **21,** 699.
Smith, E. E. (1955). The standardization of X-ray dosimeters, Brit. J. Radiol. **28,** 662.
Smithers, D. W. (1946). X-ray treatment of accessible cancer, Arnold, p. 7.
Snyder, W. S., and Neufeld, J. (1955). Calculated depth dose curves in tissue for broad beams of fast neutrons, Brit. J. Radiol. **28,** No. 331, 342.
Sola, A. (1960). Flux perturbation by detector foils, Nucleonics **18,** No. 3, 78.
Somerwil, A. (1957). Private communication.
Somerwil, A. (1959). The standard dosimeter of the Rotterdamsch Radiotherapeutisch Instituut, J. Belge de Radiologie **42,** 87–91.
Spencer, L. V., and Fano, U. (1954). Energy spectrum resulting from electron slowing down, Phys. Rev. **93,** 1172.
Spencer, L. V., and Attix, F. H. (1955). A theory of cavity ionization, Radiation Res. **3,** 239.
Starfelt, N., and Koch, H. W. (1956). Differential cross-section measurements of thin-target bremsstrahlung produced by 2.7- to 9.7-Mev electrons, Phys. Rev. **102,** 1598.
Staub, H. (1947). The neutron spectrum of boron bombarded by polonium alphas. MDDC–1490.
Stephens, K. G., and Cooper, W. M. (1960). Calibration of manganese and gold foils for relative neutron flux measurements, Brit. J. Appl. Phys. **11,** 342.

Stephens, K. G., Van der Walt, R., and Williams, G. (1961). Measurements of neutron fluxes and neutron spectra. AEI–Rept. A 1202 (Aldermaston).
Stephenson, S., and Crocker, V. S. (1958). AERE, unpublished. Rept. by Abson . . . l.c.
Sternheimer, R. M. (1952). The density effect for the ionization loss in various materials, Phys. Rev. **88,** 851.
Sternheimer, R. M. (1956). Density effect for the ionization loss in various materials, Phys. Rev. **103,** 511.
Stevens, J., and Richardson, J. F. (1961). Private communication.
Stewart, L. (1955). Neutron spectrum and absolute yield of a plutonium-beryllium source, Phys. Rev. **98,** 740.
Stokes, R. H. (1951). Measurement of electron pairs for the determination of a 65 Mev x-ray spectrum, Phys. Rev. **84,** 991.
Strominger, P., Hollander, J. M., and Seaborg, G. T. (1958). Table of isotopes, Rev. Mod. Phys. **30,** 585.
Sullivan, W. H. (1957). Trilinear chart of nuclides, U.S. Atomic Energy Commission Rept.
Sworski, T. J. (1956). Mechanism for the reduction of ceric ion by thallous ion induced by cobalt-60 gamma radiations, Radiation Res. **4,** 483.
Szilvasi, A. J. D., Geiger, K. W., and Dixon, W. R. (1960). Study of neutrons from a Po-F(α,n) source, J. Nucl. Energy **11,** 131.
Taimuty, S. I., Towle, L. H., and Peterson, D. L. (1959). Ceric dosimetry: Routine use at 10^5–10^7 rads, Nucleonics **17,** No. 8, 103.
Taplin, G. V. (1956). Radiation dosimetry, 1st ed., G. J. Hine and G. L. Brownell, Academic Press, Inc., New York, N.Y.
Tarrant, G. T. P. (1932). Numerical calculation of scattering correction in gamma-ray absorption measurements, Proc. Cambridge Phil. Soc. **28,** 475.
Taylor, L. S. (1931). Absorption measurements of the x-ray general radiation, Radiology **16,** 302.
Teplý, J., and Bednár, J. (1958). Radiation chemistry of aqueous chloroform solution, Proc. 2d Intern. Conf. Peaceful Uses of Atomic Energy, Geneva, 1958, P/2114, **29,** 71.
Thielens, G. (1961). Limitations on the use of ferrous sulfate dosimetry for measuring small γ-radiation doses, p. 325–9 of Selected Topics in Radiation Dosimetry, Vienna, International Atomic Energy Agency.
Thomas, J. K. Private communication.
Thompson, M. W. (1956). Some effects of the self-absorption of neutrons in neutron-detecting foils, J. Nucl. Energy **2,** 286.
Thompson, T. J. (1952). Effect of chemical structure on stopping powers for high-energy protons, Thesis, Univ. Calif., UCRL–1910.
Thoraeus, R. (1932). A study of the ionization method for measuring the intensity and absorption of roentgen rays and of the efficiency of different filters used in therapy, Acta Radiol. Suppl. **15.**
Thoraeus, R. (1936). A new method for calculating combinations of tube-voltage and filtration and some results of its application in roentgen therapy, Acta Radiol. **17,** 579.
Thoraeus, R. (1954). Status of roentgen ray standards in Sweden, and a brief report on the first part of an intercomparison between national roentgen ray standards, Acta Radiol. Suppl. **117,** 33.
Thoraeus, R., Oosterkamp, W. J., Proper, J., Jaeger, R., Rajewsky, B., Bunde, E., Dorneich, M., Lang, D., and Sewkor, A. (1955). Vergleichsmessungen des internationalen röentgen im Bereich von 8 kV bis 170 kV Erzeugungsspannung, Strahlentherapie **98,** 265.
Thoraeus, R. (1956). Monitoring filters in roentgen therapy, Acta Radiol. **45,** 414.
Thoraeus, R. (1958). On the determination of the radiation quality, Symp. Quantities, Units and Measuring Methods of Ionizing Radiation, Rome, Italy.
Thornton, W. T., and Auxier, J. A. (1960). Some X-ray and fast neutron response characteristics of Ag-metaphosphate glass dosimeters, Oak Ridge National Laboratory Rept. ORNL–2912.
Tittle, C. W. (1951). Slow neutron detection by foils, Nucleonics **8,** No. 6, 5; **9,** No. 1, 60.
Tochilin, E., and Alves, R. R. (1958). Neutron spectra from mock-fission sources, Nucleonics **16,** No. 11, 145.
Tochilin, E., and Kohler, G. D. (1958). Neutron beam characteristics from the University of California 60 inch cyclotron, Health Phys. **1,** 332.
Trice, J. B. (1957). APEX–408, U.S. Atomic Energy Commission.
Trout, E. D., Kelley, J. P., and Lucas, A. C. (1960). Determination of half-value layer, Am. J. Roentgenol. Rad. Therapy Nuclear Med. **84,** 729.
Trout, E. D., Kelley, J. P., and Lucas, A. C. (1961). Evaluation of Thoraeus filters, Am. J. Roentgenol. **85,** 933.
Trout, E. D., Kelley, J. P., and Lucas, A. C. (1962). The second half-value layer and the homogeneity coefficient, Am. J. Roentgenol. **87,** 574.
Trumbore, C. N. (1958). The effect of oxygen on ferric ion yields in aqueous solutions containing polonium, J. Am. Chem. Soc. **80,** 1772.
Tuddenham, W. J. (1957). Half-value depth and fall-off ratio as functions of portal area, target skin distance and half-value layer, Radiology **69,** 79.
Tubiana, M., and Dutreix, J. M. High energy radiation dosimetry, Symp. on Quantities, Units and Measuring Methods of Ionizing Radiation—Rome, 1958, Ed. Ulrico Hoephi, p. 149.
Tranter, F. W. (1961). An ion chamber with a wall of air, Symp. on Radiation Dosimetry, IAEA, p. 131, June.
Uthe, P. M. (1957). Attainment of neutron flux-spectra from foil activations. Technical Report 57–3, U.S. Air Force Institute of Technology, Wright-Patterson AFB, Ohio.
Valentine, J. M., and Curran, S. C. (1952). Energy expenditure per ion pair for electrons and α particles, Phil. Mag. **43,** 964.
Valentine, J. M., and Curran, S. C. (1958). Average energy expenditure per ion pair in gases and gas mixtures, Reports on Progress in Physics **21,** 153.
Villforth, J. C., Birkhoff, R. D., and Hubbell, H. H. (1958). Comparison of theoretical and experimental filtered spectra, ORNL–2529.
Wagner, E. B., and Hurst, G. S. (1958). Advances in the standard proportional counter method of fast neutron dosimetry, Rev. Sci. Instr. **29,** 153.
Wagner, E. B., and Hurst, G. S. (1959). Gamma response and energy losses in the absolute fast neutron dosimeter, Health Phys. **2,** 57.
Wagner, E. B., and Hurst, G. S. (1961). A G–M tube γ-ray dosimeter with low neutron sensitivity, Health Phys. **5,** 20.
Wagner, G. (1953). Untersuchungen über den Dosisabfall in Gewebe und den Homogenitätsgrad Berylliumgefensterter Röntgenstrahlungen, Zschr. für Haut-und Geschl. Krkh **15,** 190.
Wagner, G. (1957). Die Bedeutung der characteristischen Eigenstrahlung in der dermatologischen Röntgentherapie, Acta Dermat. venereol. Proc. 11th Intern. Cong. Dermat. **11,** 412.
Walker, R. L. (1946). Absolute calibration of a Ra-Be neutron source, MDDC 414.
Walker, R. L., and McDaniel, B. D. (1948). Gamma-ray spectrometer measurements of fluorine and lithium under proton bombardment, Phys. Rev. **74,** 315.
Walker, W. H., Westcott, C. H., and Alexander, T. K. (1960). Measurement of radiative capture resonance integrals in a thermal reactor spectrum, and the thermal cross section of Pu-240, Can. J. Phys. **38,** 57.
Wang, P. K. S., and Wiener, M. (1949). Spectral analysis of 10 Mev betatron radiation by nuclear emulsion, Phys. Rev. **76,** 1724.
Wang, P. K. S., Raridon, R. J., and Tidwell, M. (1957a). X-ray spectrum from a beryllium window tube: I. Scintillation spectrometry, Brit. J. Radiol. **30,** 70.
Wang, P. K. S., Raridon, R. J., and Crawford, R. C. (1957b). X-ray spectrum from a beryllium window tube: II. Laplace transformation, Brit. J. Radiol. **30,** 153.
Warner, R. M., and Schrader, E. F. (1954). Angle-energy distribution of radiation from high-energy electron accelerators, Rev. Sci. Instr. **25,** 663.

Watson, E. C. (1958). Quoted in J. DePangher's double moderator neutron dosimeter, July 15, 1958 (HW–57293).
Watt, B. E. (1952). Energy spectrum of neutrons from thermal fission of U^{235}, Phys. Rev. **87,** 1037.
Wattenberg, A. (1949). Photo-neutron sources, Natl. Acad. Sci.—Natl. Res. Council, Nuclear Science Series, Preliminary Rept. No. 6.
Weinstock, E. V., and Halpern, J. (1955). Bremsstrahlung spectrum from the internal target of a 22 Mev betatron, Phys. Rev. **100,** 1293.
Weiss, J., and Bernstein, W. (1955). Energy required to produce one ion pair for several gases, Phys. Rev. **98,** 1828.
Weiss, J., and Bernstein, W. (1956). Energy required to produce one ion pair in several noble gases, Phys. Rev. **103,** 1253.
Weiss, J., Allen, A. O., and Schwarz, H. A. (1956). Use of the Fricke sulfate dosimeter for gamma ray doses in the range 4 to 40 kiloroentgen. Proc. 1st Intern. Conf. Peaceful Uses of Atomic Energy, Geneva, 1955, P/155, **14,** 179.
Westcott, C. H. (1960). Effective cross section values for well-moderated thermal reactor spectra, CRRP–960, EANDC(Can)–4.
Westcott, C. H., Walker, W. H., and Alexander, T. K. (1958). Effective cross sections and cadmium ratios for the neutron spectra of thermal reactors, Proc. Conf. Peaceful Uses of Atomic Energy, Geneva, 1955, P/202, **15,** 70.
Wheatley, B. M., Jones, P. C. C., and Sinclair, T. C. (1960). A caesium 137 beam therapy unit: Physical aspects, Brit. J. Radiol. **33,** 251.
White, Grodstein, G. (1957). X-ray attenuation coefficients from 10 kev to 100 Mev., NBS Circ. 583.
Whitmore, B. G., and Baker, W. B. (1950). The energy spectrum of neutrons from a Po-Be source, Phys. Rev. **78,** 799.
Whyte, G. N. (1954). Density effect in gamma-ray measurements, Nucleonics **12,** No. 2, 18–21.
Widder, F., and Huber P. (1958). Druckabhängigkeit der Sättigungsladung von Po-α-Teilchen in CO_2, A-CO_2- und A-CH_4-Mischungen, Helv. Phys. Acta **31,** 601.
Wiesner, L. (1961). The use of polyisobutylene solutions for measuring doses from 10^3 rad up to about 10^{10} rad, p. 361–70 of Selected Topics in Radiation Dosimetry, Vienna, International Atomic Energy Agency.
Wilson, C. W. (1939). Estimation of the "quality" of depth radiations in gamma-ray therapy by means of the ionization produced in chambers with wall materials of different atomic numbers, Brit. J. Radiol. **12,** 231.
Wilson, C. W. (1941). The dependence of the secondary electronic emission produced by gamma radiation upon the direction of the radiation, Proc. Phys. Soc. **53,** 613.
Wilson, C. W., and Perry, B. J. (1951). Secondary electronic emission generated by 1 Mev and 2 Mev X-rays, Brit. J. Radiol. **24,** 293.
Wilson, R. R. (1957). Precision quantameter for high energy x-rays, Nuclear Instr. **1,** 101.
Wolf, G. (1961). Die Absoluteichung von Zerfallsraten mittels der β-γ-Koinzidenzmethode und deren Anwendung zur Messung des thermischen Aktivierungsquerschnitts der Isotope Na^{23}, Sc^{45}, Co^{59} und $Ta^{1\cdot 1}$, Nukleonik **2,** 255.
Worthley, B., Thompson, A. M., and Tooze, M. J. (1957). Precision charge comparison of x-ray dosimeters, Austr. J. Appl. Sci. **8,** 261.
Wyckoff, H. O., Aston, G. H., and Smith, E. E. (1954). A comparison of x-ray standards, Brit. J. Radiol. 27, 325; Acta Radiol. Suppl. **117,** 17.
Wyckoff, H. O., and Attix, F. H. (1957). Design of free-air ionization chambers, NBS Handb. 64.
Wyckoff, H. O. (1960). Measurement of cobalt-60 and cesium-137 gamma rays with a free-air chamber, J. Research NBS **64C** (Eng. Instr.), No. 2, 87 (Apr.-June 1960).
Wyckoff, H. O., Allisy, A., Aston, G. H., Barnard, G. P. Hübner, W., Loftus, T., and Taupin, G. (1963). Intercomparison of National X- and gamma-ray exposure-dose standards, Acta Radiol. **1,** 57.
Wyard, S. J. (1951). Secondary electronic emission produced by cobalt gamma rays, Brit. J. Radiol. **24,** 411.
Yokota, R., Nakajima, S., and Sakai, E. (1961). High sensitivity silver-activated phosphate glass for the simultaneous measurement of thermal neutrons, γ- and/or β-rays, Health Phys. **5,** 219.
Zahn, C. T. (1937). Absorption coefficients for thermal neutrons, Phys. Rev. **52,** 67.
Zanstra, H. (1935). Ein Kurzes Verfahren zur Bestimmung des Sättigungstromes nach der Jaffé'schen Theorie der Kolonnenionisation, Physica **2,** 817.
Zieler, E. (1954). Zur Charakterisierung weicher Röntgenstrahlung durch Halbwertschicht und Homogenitätsgrad, Strahlentherapie **93,** 579.
Zieler, E. (1956). Dosismessungen an Beryllumfenster-Röhren für Spannungen von 10 . . . 100 kV, Strahlentherapie **100,** 595.
Zieler, E. (1957). Der Einfluss des Charaktertischen Röntgenspektrums auf die Qualität weicher Röntgenstrahlen, Strahlentherapie **102,** 88.
Zimmer, K. G. (1938). Dosimetrische und strahlenbiologische Versuche mit schnellen Neutronen I, Strahlentherapie **63,** 517.
Zimmer, K. G. (1956). Vorrichtung zum Nachweis radioaktiver Strahlungen und Verfahren und Vorrichtung zum Herstellen eines dazugehörigen Lichtleiters, German Patent DBP 1.053.108.
Zobel, W. (1961). Experimental determination of flux depression and other corrections for gold foils exposed in water. American Nuclear Society meeting, June 1960, Oak Ridge National Laboratory.

Appendix I

Radiation Quantities and Units*

1. Introduction

There has recently been much discussion of the fundamental concepts and quantities employed in radiation dosimetry. This has arisen partly from the rapid increase in the number of individuals using these concepts in the expanding field of nuclear science and technology, partly because of the need for extending the concepts so that they would be of use at higher photon energies and for particulate as well as for photon radiation, but chiefly because of certain obscurities in the existing formulation of the quantities and units themselves.

The roentgen, for example, was originally defined to provide the best quantitative measure of exposure to medium-energy x radiation which the measuring techniques of that day (1928) permitted. The choice of air as a standard substance was not only convenient but, also appropriate for a physical quantity which was to be correlated with the biological effect of x rays, since the effective atomic number of air is not very different from that of tissue. Thus a given biological response could be reproduced approximately by an equal exposure in roentgens for x-ray energies available at that time. Since 1928 the definition of the roentgen has been changed several times, and this has reflected some feeling of dissatisfaction with the lack of clarity of the concept.

The most serious source of confusion was the failure to define adequately the radiation quantity of which the roentgen was said to be the unit.[1] As a consequence of this omission the roentgen had gradually acquired a double role. The use of this name for the unit had become recognized as a way of specifying not only the magnitude but also the nature of the quantity measured. This practice conflicts with the general usage in physics, which permits, within the same field, the use of a particular unit for all quantities having the same dimensions.

Even before this, the need for accurate dosimetry of neutrons and of charged particles from accelerators or from radionuclides had compelled the International Commission on Radiological Units and Measurements (ICRU) to extend the number of concepts. It was also desired to introduce a new quantity which could be more directly correlated with the local biological and chemical effects of radiation. This quantity, *absorbed dose*, has a generality and simplicity which greatly facilitated its acceptance, and in a very few years it has become widely used in every branch of radiation dosimetry.

The introduction of absorbed dose into the medical and biological field was further assisted by defining a special unit—the *rad*. One rad is approximately equal to the absorbed dose delivered when soft tissue is exposed to 1 roentgen of medium voltage x radiation. Thus in many situations of interest to medical radiology, but not in all, the numbers or roentgens and rads associated with a particular medical or biological effect are approximately equal and experience with the earlier unit could be readily transferred to the new one. Although the *rad* is merely a convenient multiple of the fundamental unit, erg/g, it has already acquired, at least in some circles, the additional connotation that the only quantity which can be measured in rads is absorbed dose. On the other hand, the rad has been used by some authors as a unit for a quantity called by them *first collision dose;* this practice is deprecated by the Commission.

Being aware of the need for preventing the emergence of different interpretations of the same quantity, or the introduction of undesirable, unrelated quantities or units in this or similar fields of measurement, the ICRU set up, during its meeting in Geneva in September 1958, an *Ad Hoc* Committee. The task of this committee was to review the fundamental concepts, quantities, and units which are required in radiation dosimetry and to recommend a system of concepts and a set of definitions which would be, as far as possible, internally consistent and of sufficient generality to cover present requirements and such future requirements as can be foreseen. The committee was instructed to pay more attention to consistency and rigor than to the historical development of the subject and was authorized to reject any existing quantities or units which seemed to hinder a consistent and unified formulation of the concepts.

*Taken from Radiation Quantities and Units, International Commission on Radiological Units and Measurements, Report 10a, National Bureau of Standards Handbook 84 (numbers refer to paragraphs in the original report).

[1] Fränz, H. and Hübner, W. Concepts and Measurement of Dose, Proceedings of Second International Conference on the Peaceful Uses of Atomic Energy, Geneva 1958, P/971 21, 101, United Nations, Geneva (1958).

Bertrand Russell [2] in commenting on the use and abuse of the concept of infinitesimals by mathematicians, remarks: "But mathematicians did not at first pay heed to (these) warnings. They went ahead and developed their science, and it is well that they should have done so. It is a peculiar fact about the genesis and growth of new disciplines that too much rigor too early imposed stifles the imagination and stultifies invention. A certain freedom from the strictures of sustained formality tends to promote the development of a subject in its early stages, even if this means the risk of a certain amount of error. Nonetheless, there comes a time in the development of any field when standards of rigor have to be tightened."

The purpose of the present reexamination of the concepts to be employed in radiation dosimetry was primarily "to tighten standards of rigor." If, in the process, some increased formality is required in the definitions in order to eliminate any foreseeable ambiguities, this must be accepted.

2. General Considerations

The development of the more unified presentations of quantities and units which is here proposed was stimulated and greatly assisted by mathematical models of the dosimetric field which had been proposed by some members of the committee in an effort to clarify the concepts. It appeared, however, that the essential features of the mathematical models had been incorporated into the definitions and hence the need for their exposition in this report largely disappeared. The mathematical approach is published elsewhere.[3]

As far as possible, the definitions of the various fundamental quantities given here conform to a common pattern. Complex quantities are defined in terms of the simpler quantities of which they are comprised.

The passage to a "macroscopic limit" which has to be used in defining point quantities in other fields of physics can be adapted to radiation quantities and a special discussion of this is included in the section headed "limiting procedures."

The general pattern adopted is to give a short definition and to indicate the precise meaning of any special phrase or term used by means of an explanatory note following the definition. There has been no attempt to make the list of quantities which are defined here comprehensive. Rather, the Commission has striven to clarify the fundamental dosimetric quantities and a few others (such as activity) which were specifically referred to it for discussion.

It is recognized that certain terms for which definitions are proposed here are of interest in other fields of science and that they are already variously defined elsewhere. The precise wording of the definition and even the name and symbol given to any such quantity, may at some future date require alteration if discussions with representatives of the other interested groups of scientists should lead to agreement on a common definition or symbol. Although the definitions presented here represent some degree of compromise, they are believed to meet the requirements in the field of radiation dosimetry.

3. Quantities, Units, and Their Names

The Commission is of the opinion that the definition of concepts and quantities is a fundamental matter and that the choice of units is of less importance. Ambiguity can best be avoided if the defined quantity which is being measured is specified. Nevertheless, the special units do exist in this as in many other fields. For example, the hertz is restricted, by established convention, to the measurement of vibrational frequency, and the curie, in the present recommendations, to the measurement of the activity of a quantity of a nuclide. One does not measure activity in hertz nor frequency in curies although these quantities have the same dimensions.

It was necessary to decide whether or not to extend the use of the special dosimetric units to other more recently defined quantities having the same dimensions, to retain the existing restriction on their use to one quantity each, or to abandon the special units altogether. The Commission considers that the addition of further special units in the field of radiation dosimetry is undesirable, but continues to recognize the existing special units. It sees no objection, however, to the expression of any defined quantity in the appropriate units of a coherent physical system. Thus, to express absorbed dose in ergs per gram or joules per kilogram, exposure in coulombs per kilogram or activity in reciprocal seconds, are entirely acceptable alternatives to the use of the special units which, for historical reasons, are usually associated with these quantities.

The ICRU recommends that the use of each special unit be restricted to one quantity as follows:

The rad—solely for absorbed dose
The roentgen—solely for exposure
The curie—solely for activity.

It recommends further that those who prefer to express quantities such as absorbed dose and kerma (see below) in the same units should use units of an internationally agreed coherent system.

Several new names are proposed in the present report. When the absorbed dose concept was adopted in 1953, the Commission recognized the need for a term to distinguish it from the quantity of which the roentgen is the unit. In 1956 the Commission proposed the term *exposure* for this latter quantity. To meet objections by the ICRP, a compromise term, "exposure dose" was agreed upon.[4] While this term has come into some use

[2] Russell, B., Wisdom of the West, p. 280 (Doubleday and Co., Inc., New York, 1959).
[3] Rossi, H. H. and Roesch, W. C., Field Equations in Dosimetry, Radiation Res. **16**, 783 (1962).
[4] For details see ICRU, 1956 Report, NBS Handb. 62, p. 2 (1957).

since then, it has never been considered as completely satisfactory. In the meantime, the basic cause of the ICRP objection has largely disappeared since most legal codes use either the units rad or rem.

Since in this report the whole system of radiological quantities and units has come under critical review, it seemed appropriate to reconsider the 1956 decision. Numerous names were examined as a replacement for exposure dose, but there were serious objections to any which included the word dose. There appeared to be a minimum of objection to the name *exposure* and hence this term has been adopted by the Commission with the hope that the question has been permanently settled. It involves a minimum change from the older name exposure dose. Furthermore, the elimination of the term "dose" accomplishes the long-felt desire of the Commission to retain the term dose for one quantity only—the absorbed dose.

The term *"RBE* dose" has in past publications of the Commission not been included in the list of definitions but was merely presented as a "recognized symbol". In its 1959 report the Commission also expressed misgivings over the utilization of the same term, *"RBE"*, in both radiobiology and radiation protection. It now recommends that the term *RBE* be used in radiobiology only and that another name be used for the linear-energy-transfer-dependent factor by which absorbed doses are to be multiplied to obtain, for purposes of radiation protection, a quantity that expresses, on a common scale for all ionizing radiations, the irradiation incurred by exposed persons. The name recommended for this factor is the *quality factor* (*QF*). Provisions for other factors are also made. Thus a *distribution factor* (*DF*), may be used to express the modification of biological effect due to non-uniform distribution of internally deposited isotopes. The product of absorbed dose and modifying factors is termed the *dose equivalent* (*DE*). As a result of discussions between ICRU and ICRP the following formulation has been agreed upon:

The Dose Equivalent

1. For protection purposes it is useful to define a quantity which will be termed the "dose equivalent" (*DE*).
2. (*DE*) is defined as the product of absorbed dose, *D*, quality factor (*QF*); dose distribution factor (*DF*), and other necessary modifying factors.

$$(DE)=D\ (QF)\ (DF). \ . \ . \ .$$

3. The unit of dose equivalent is the "rem". The dose equivalent is numerically equal to the dose in rads multiplied by the appropriate modifying factors.

Although this statement does not cover a number of theoretical aspects (in particular the physical dimensions of some of the quantities) it fulfills the immediate requirement for an unequivocal specification of a scale that may be used for numerical expression in radiation protection.

Another new name is that for the quantity which represents the kinetic energy transferred to charged particles by the uncharged particles per unit mass of the irradiated medium. This is the same as one of the common interpretations of a concept "first collision dose," that has proved to be of great value in the dosimetry of fast neutrons. The concept is also closely related to the energy equivalent of exposure in an x-ray beam. The name proposed, *kerma*, is based on the initials of *k*inetic *e*nergy *r*eleased in *ma*terial.

Still another new name is the *energy fluence* which is here attached to the quantity in the 1953 ICRU report called *quantity of radiation*. The latter term was dropped in the 1956 ICRU report, but the concept—time integral of intensity—remains a useful one and the proposed term appears to be acceptable in other languages as well as English. A related quantity, *particle fluence*, which is equivalent to the quantity *nvt* used in neutron physics, is included to round out the system of radiation quantities.

The quantity for which the curie is the unit was referred to the committee for a name and definition. Hitherto the curie has been defined as a *quantity of the radioactive nuclide* such that 3.7×10^{10} disintegrations per second occur in it. However, it has never been specified what was meant by quantity of a nuclide, whether it be a number, mass, volume, etc. Meanwhile the custom has grown of identifying the number of curies of a radionuclide with its transformation rate. Because of the vagueness of the original concept, because of the custom of identifying curies with transformation rate and because it appeared not to interfere with any other use of the curie, the Commission recommends that the term *activity* be used for the transformation rate, and that the curie be made its unit. It is recognized that the definition of the curie is of interest to other bodies in addition to the ICRU, but by this report we recommend that steps be taken to redefine it as $3.7\times10^{10}\mathrm{s}^{-1}$, i.e., as a unit of activity and not of quantity of a radioactive nuclide.

It is also recommended that the term *specific gamma-ray constant* be used instead of *specific gamma-ray emission* for the quotient of the exposure rate at a given distance by the activity. The former term focuses attention on the *constancy* of this quotient for a given radio nuclide rather than the *emission* of the source.

4. Detailed Considerations

A. Limiting Procedures

Except in the case of a uniform distribution of sources throughout a large region, radiation fields are in general nonuniform in space. They may also be variable in time. Many of the quantities defined in this report have to be specified as functions of space or time, and in principle they must therefore be determined for sufficiently small regions of space or intervals of time by some limiting procedure. There are conceptual difficulties in taking such limits for quantities which depend upon the discrete interactions between radiations and atoms. Similar difficulties arise with other macroscopic physical quantities such as density or temperature and they must be overcome by means of an appropriate averaging procedure.

To illustrate this procedure we may consider the measurement of the macroscopic quantity "absorbed dose" in a nonuniform radiation field. In measuring this dose the quotient of energy by mass must be taken in an elementary volume in the medium which, on the one hand, is so small that a further reduction in its size would not appreciably change the measured value of the quotient energy by mass and, on the other hand is still large enough to contain many interactions and be traversed by many particles.[5] If it is impossible to find a mass such that both these conditions are met, the dose cannot be established directly in a single measurement. It can only be deduced from multiple measurements that involve extrapolation or averaging procedures. Similar considerations apply to some of the other concepts defined below. The symbol $\triangle$ precedes the symbols for quantities that may be concerned in such averaging procedures.

In the measurement of certain material constants such as stopping power, absorption coefficient, etc., the limiting procedure can be specified more rigorously. Such constants can be determined for a given material with any desired accuracy without difficulties from statistical fluctuations. In these cases the formula quoted in the definitions are presented as differential quotients.

B. Spectral Distributions and Mean Values

In practice many of the quantities defined below to characterize a radiation field and its interaction with matter are used for radiations having a complex energy spectrum. An important general concept in this connection is the *spectral concentration* of one quantity with respect to another. The spectral concentration is the ordinate of the distribution function of the first quantity with respect to the second. The independent quantity need not always be energy or frequency; one can speak of the spectral concentration of flux density with respect to quantum energy or of the absorbed dose with respect to linear energy transfer. The interaction constants (such as μ, S and W) referred to in this report are often mean values taken over the appropriate spectral distributions of the corresponding quantities.

C. Units

For any of the quantities defined below the appropriate unit of an internationally agreed coherent system can be used. In addition certain special units are reserved for special quantities:

the rad for absorbed dose
the roentgen for exposure
the curie for activity.

D. Definitions

(1) *Directly ionizing particles* are charged particles (electrons, protons, α-particles, etc.) having sufficient kinetic energy to produce ionization by collision.

(2) *Indirectly ionizing particles* are uncharged particles (neutrons, photons, etc.) which can liberate directly ionizing particles or can initiate a nuclear transformation.

(3) *Ionizing radiation* is any radiation consisting of directly or indirectly ionizing particles or a mixture of both.

(4) The *energy imparted* by ionizing radiation to the matter in a volume is the difference between the sum of the energies of all the directly and indirectly ionizing particles which have entered the volume and the sum of the energies of all those which have left it, minus the energy equivalent of any increase in rest mass that took place in nuclear or elementary particle reactions within the volume.

NOTES: (a) The above definition is intended to be exactly equivalent to the previous meanings given by the ICRU to "energy retained by matter and made locally available" or "energy which appears as ionization, excitation, or changes of chemical bond energies". The present formulation specifies what energy is to be included without requiring a lengthy, and possibly incomplete, catalog of the different types of energy transfer.

(b) Ultimately, most of the energy imparted will be degraded and appear as heat. Some of it, however, may appear as a change in interatomic bond energies. Moreover, during the degradation process the energy will diffuse and the distribution of heat produced may be different from the distribution of imparted energy. For these reasons the energy imparted cannot always be equated with the heat produced.

(c) The quantity *energy imparted to matter* in a given volume is identical with the quantity often called *integral absorbed dose* in that volume.

[5] In interpreting radiation effects the macroscopic concept of absorbed dose may not be sufficient. Whenever the statistical fluctuations around the mean value are important, additional parameters describing the distribution of absorbed energy on a microscopic scale are necessary.

(5) The *absorbed dose* (D) is the quotient of ΔE_D by Δm, where ΔE_D is the energy imparted by ionizing radiation to the matter in a volume element, Δm is the mass of the matter in that volume element and Δ has the meaning indicated in section 4.A.

$$D=\frac{\Delta E_D}{\Delta m}$$

The special unit of absorbed dose is the *rad*.

$$1 \text{ rad}=100 \text{ erg/g}=\frac{1}{100}\text{ J/kg}$$

NOTE: J is the abbreviation for Joule.

(6) The *absorbed dose rate* is the quotient of ΔD by Δt, where ΔD is the increment in absorbed dose in time Δt and Δ has the meaning indicated in section 4.A.

$$\text{Absorbed dose rate}=\frac{\Delta D}{\Delta t}$$

A special unit of absorbed dose rate is any quotient of the rad by a suitable unit of time (rad/d, rad/min, rad/h, etc.).

(7) The *particle fluence* [6] or *fluence* (Φ) of particles is the quotient of ΔN by Δa, where ΔN is the number of particles which enter a sphere [7] of cross-sectional area Δa and Δ has the meaning indicated in section 4.A.

$$\Phi=\frac{\Delta N}{\Delta a}$$

(8) The *particle flux density* or *flux density* (φ) of particles is the quotient of $\Delta\Phi$ by Δt where $\Delta\Phi$ is the particle fluence in time Δt and Δ has the meaning indicated in section 4.A.

$$\varphi=\frac{\Delta\Phi}{\Delta t}$$

NOTE: This quantity may also be referred to as particle fluence rate.

(9) The *energy fluence* (F) of particles is the quotient of ΔE_F by Δa, where ΔE_F is the sum of the energies, exclusive of rest energies, of all the particles which enter a sphere [8] of cross-sectional area Δa and Δ has the meaning indicated in section 4.A.

$$F=\frac{\Delta E_F}{\Delta a}$$

[6] This quantity is the same as the quantity, nvt, commonly used in neutron physics.

[7] This quantity is sometimes defined with reference to a plane of area Δa, instead of a sphere of cross-sectional area Δa. The plane quantity is less useful for the present purposes and it will not be defined. The two quantities are equal for a unidirectional beam of particles perpendicularly incident upon the plane area.

[8] See footnote 7.

(10) The *energy flux density* or *intensity* (I) is the quotient of ΔF by Δt where ΔF is the energy fluence in the time Δt and Δ has the meaning indicated in section 4.A.

$$I=\frac{\Delta F}{\Delta t}$$

NOTE: This quantity may also be referred to as energy fluence rate.

(11) The *kerma* [9] (K) is the quotient of ΔE_K by Δm, where ΔE_K is the sum of the initial kinetic energies of all the charged particles liberated by indirectly ionizing particles in a volume element of the specified material, Δm is the mass of the matter in that volume element and Δ has the meaning indicated in section 4.A.

$$K=\frac{\Delta E_K}{\Delta m}$$

NOTES: (a) Since ΔE_K is the sum of the initial kinetic energies of the charged particles liberated by the indirectly ionizing particles, it includes not only the kinetic energy these charged particles expend in collisions but also the energy they radiate in bremsstrahlung. The energy of any charged particles is also included when these are produced in secondary processes occurring within the volume element. Thus the energy of Auger electrons is part of ΔE_K.

(b) In actual measurements Δm should be so small that its introduction does not appreciably disturb the radiation field. This is particularly necessary if the medium for which kerma is determined is different from the ambient medium; if the disturbance is appreciable an appropriate correction must be applied.

(c) It may often be convenient to refer to a value of kerma or of kerma rate for a specified material in free space or at a point inside a different material. In such a case the value will be that which would be obtained if a small quantity of the specified material were placed at the point of interest. It is, however, permissible to make a statement such as: "The kerma for air at the point P inside a water phantom is . . ." recognizing that this is a shorthand version of the fuller description given above.

(d) A fundamental physical description of a radiation field is the intensity (energy flux density) at all relevant points. For the purpose of dosimetry, however, it may be convenient to describe the field of indirectly ionizing particles in terms of the kerma rate for a specified material. A suitable material would be air for electromagnetic radiation of moderate energies, tissue for all radiations in medicine or biology, or any relevant material for studies of radiation effects.

[9] Various other methods of specifying a radiation field have been used, e.g., for a neutron source the "first collision dose" in a standard material at a specified point (see Introduction).

Kerma can also be a useful quantity in dosimetry when charged particle equilibrium exists at the position and in the material of interest, and bremsstrahlung losses are negligible. It is then equal to the absorbed dose at that point. In beams of x or gamma rays or neutrons, whose energies are moderately high, transient charged-particle equilibrium can occur; in this condition the kerma is just slightly less than the absorbed dose. At very high energies the difference becomes appreciable. In general, if the range of directly ionizing particles becomes comparable with the mean free path of the indirectly ionizing particles, no equilibrium will exist.

(12) The *kerma rate* is the quotient of ΔK by Δt, where ΔK is the increment in kerma in time Δt and Δ has the meaning indicated in section 4.A.

(13) The *exposure* (X) is the quotient of ΔQ by Δm, where ΔQ is the sum of the electrical charges on all the ions of one sign produced in air when all the electrons (negatrons and positrons), liberated by photons in a volume element of air whose mass is Δm, are completely stopped in air and Δ has the meaning indicated in section 4.A.

$$X=\frac{\Delta Q}{\Delta m}$$

The special unit of exposure is the roentgen (R).

$$1R=2.58\times10^{-4}\ \mathrm{C/kg}^{10}$$

Notes: (a) The words "charges on all the ions of one sign" should be interpreted in the mathematically absolute sense.

(b) The ionization arising from the absorption of bremsstrahlung emitted by the secondary electrons is not to be included in ΔQ. Except for this small difference, significant only at high energies, the exposure as defined above is the ionization equivalent of the kerma in air.

(c) With present techniques it is difficult to measure exposure when the photon energies involved lie above a few Mev or below a few kev.

(d) As in the case of kerma (4D(11), note (c)), it may often be convenient to refer to a value of exposure or of exposure rate in free space or at a point inside a material different from air. In such a case the value will be that which would be determined for a small quantity of air placed at the point of interest. It is, however, permissible to make a statement such as: "The exposure at the point P inside a water phantom is . . . ."

(14) The *exposure rate* is the quotient of ΔX by Δt, where ΔX is the increment in exposure in time Δt and Δ has the meaning indicated in section 4.A,

$$\text{Exposure rate}=\frac{\Delta X}{\Delta t}$$

[10] This unit is numerically identical with the old one defined as 1 e.s.u. of charge per .001293 gram of air. C is the abbreviation for coulomb.

A special unit of exposure rate is any quotient of the roentgen by a suitable unit of time (R/s, R/min, R/h, etc.).

(15) The *mass attenuation coefficient* $\left(\frac{\mu}{\rho}\right)$ of a material for indirectly ionizing particles is the quotient of dN by the product of ρ, N, and dl where N is the number of particles incident normally upon a layer of thickness dl and density ρ, and dN is the number of particles that experience interactions in this layer.

$$\frac{\mu}{\rho}=\frac{1}{\rho N}\frac{dN}{dl}$$

Notes: (a) The term "interactions" refers to processes whereby the energy or direction of the indirectly ionizing particles is altered.

(b) For x or gamma radiations

$$\frac{\mu}{\rho}=\frac{\tau}{\rho}+\frac{\sigma}{\rho}+\frac{\sigma_{\mathrm{coh}}}{\rho}+\frac{\kappa}{\rho}$$

where $\frac{\tau}{\rho}$ is the mass photoelectric attenuation coefficient, $\frac{\sigma}{\rho}$ is the total Compton mass attenuation coefficient, $\frac{\sigma_{\mathrm{coh}}}{\rho}$ is the mass attenuation coefficient for coherent scattering, and $\frac{\kappa}{\rho}$ is the pair-production mass attenuation coefficient.

(16) The *mass energy transfer coefficient* $\left(\frac{\mu_K}{\rho}\right)$ of a material for indirectly ionizing particles is the quotient of dE_K by the product of E, ρ and dl where E is the sum of the energies (excluding rest energies) of the indirectly ionizing particles incident normally upon a layer of thickness dl and density ρ, and dE_K is the sum of the kinetic energies of all the charged particles liberated in this layer.

$$\frac{\mu_K}{\rho}=\frac{1}{E\rho}\frac{dE_K}{dl}$$

Notes: (a) The relation between fluence and kerma may be written as

$$K=F\frac{\mu_K}{\rho}$$

(b) For x or gamma rays of energy $h\nu$

$$\frac{\mu_K}{\rho}=\frac{\tau_a}{\rho}+\frac{\sigma_a}{\rho}+\frac{\kappa_a}{\rho}$$

where

$$\frac{\tau_a}{\rho}=\frac{\tau}{\rho}\left(1-\frac{\delta}{h\nu}\right)$$

($\frac{\tau}{\rho}$=the photoelectric mass attenuation coefficient, δ=average energy emitted as fluorescent radiation per photon absorbed.) and

$$\frac{\sigma_a}{\rho}=\frac{\sigma}{\rho}\frac{E_e}{h\nu}$$

($\frac{\sigma}{\rho}$=total Compton mass attenuation coefficient, E_e=average energy of the Compton electrons per scattered photon.) and

$$\frac{\kappa_a}{\rho}=\frac{\kappa}{\rho}\left(1-\frac{2mc^2}{h\nu}\right)$$

($\frac{\kappa}{\rho}$=mass attenuation coefficient for pair production, mc^2=rest energy of the electron.)

(17) The *mass energy-absorption coefficient* $\left(\frac{\mu_{en}}{\rho}\right)$ of a material for indirectly ionizing particles is $\frac{\mu_K}{\rho}(1-G)$ where G is the proportion of the energy of secondary charged particles that is lost to bremsstrahlung in the material.

Notes: (a) When the material is air, $\frac{\mu_{en}}{\rho}$ is proportional to the quotient of exposure by fluence.

(b) $\frac{\mu_K}{\rho}$ and $\frac{\mu_{en}}{\rho}$ do not differ appreciably unless the kinetic energies of the secondary particles are comparable with or larger than their rest energy.

(18) The *mass stopping power* $\left(\frac{S}{\rho}\right)$ of a material for charged particles is the quotient of dE_s by the product of dl and ρ, where dE_s is the average energy lost by a charged particle of specified energy in traversing a path length dl, and ρ is the density of the medium.

$$\frac{S}{\rho}=\frac{1}{\rho}\frac{dE_s}{dl}$$

Note: dE_s denotes energy lost due to ionization, electronic excitation and radiation. For some purposes it is desirable to consider stopping power with the exclusion of bremsstrahlung losses. In this case $\frac{S}{\rho}$ must be multiplied by an appropriate factor that is less than unity.

(19) The *linear energy transfer* (L) of charged particles in a medium is the quotient of dE_L by dl where dE_L is the average energy locally imparted to the medium by a charged particle of specified energy in traversing a distance of dl.

$$L=\frac{dE_L}{dl}$$

Notes: (a) The term "locally imparted" may refer either to a maximum distance from the track or to a maximum value of discrete energy loss by the particle beyond which losses are no longer considered as local. In either case the limits chosen should be specified.

(b) The concept of linear energy transfer is different from that of stopping power. The former refers to energy imparted within a limited volume, the latter to loss of energy regardless of where this energy is absorbed.

(20) The *average energy* (W) *expended in a gas per ion pair formed* is the quotient of E by N_W, where N_W is the average number of ion pairs formed when a charged particle of initial energy E is completely stopped by the gas.

$$W=\frac{E}{N_W}$$

Notes: (a) The ions arising from the absorption of bremsstrahlung emitted by the charged particles are not to be counted in N_W.

(b) In certain cases it may be necessary to consider the variation in W along the path of the particle, and a differential concept is then required, but is not specifically defined here.

(21) A *nuclide* is a species of atom having specified numbers of neutrons and protons in its nucleus.

(22) The *activity* (A) of a quantity of a radioactive nuclide is the quotient of ΔN by Δt where ΔN is the number of nuclear transformations which occur in this quantity in time Δt and Δ has the meaning indicated in section 4.A.

$$A=\frac{\Delta N}{\Delta t}$$

The special unit of activity is the curie (c).

$$1c=3.7\times10^{10}s^{-1}\text{ (exactly)}$$

Note: In accordance with the former definition of the curie as a unit of quantity of a radioactive nuclide, it was customary and correct to say: "Y curies of P–32 were administered. . . ." It is still permissible to make such statements rather than use the longer form which is now correct: "A quantity of P–32 was administered whose activity was Y curies."

(23) The *specific gamma ray constant* (Γ) of a gamma-emitting nuclide is the quotient of $l^2 \frac{\Delta X}{\Delta t}$ by A, where $\frac{\Delta X}{\Delta t}$ is the exposure rate at a distance l from a point source of this nuclide having an activity A and Δ has the meaning indicated in section 4.A.

$$\Gamma = \frac{l^2 \Delta X}{A \Delta t}$$

Special units of specific gamma ray constant are $Rm^2h^{-1}c^{-1}$ or any convenient multiple of this.

NOTE: It is assumed that the attenuation in the source and along l is negligible. However, in the case of radium the value of Γ is determined for a filter thickness of 0.5 mm of platinum and in this case the special units are $Rm^2h^{-1}g^{-1}$ or any convenient multiple of this.

TABLE 4.1. *Table of quantities and units*

No.	Name	Symbol	Dimensions [a]	Units		
				MKSA	cgs	Special
4	Energy imparted (integral absorbed dose).	------	E	J	erg	g. rad.
5	Absorbed dose	D	EM^{-1}	J kg^{-1}	erg g^{-1}	rad.
6	Absorbed dose rate.	------	$EM^{-1}T^{-1}$	J kg^{-1}s^{-1}	erg g^{-1}s^{-1}	rad s^{-1}, etc.
7	Particle fluence or fluence.	Φ	L^{-2}	m^{-2}	cm^{-2}	
8	Particle flux density.	φ	$L^{-2}T^{-1}$	m^{-2}s^{-1}	cm^{-2}s^{-1}	
9	Energy fluence	F	EL^{-2}	J m^{-2}	erg cm^{-2}	
10	Energy flux density or intensity.	I	$EL^{-2}T^{-1}$	J m^{-2}s^{-1}	erg cm^{-2}s^{-1}	
11	Kerma	K	EM^{-1}	J kg^{-1}	erg g^{-1}	
12	Kerma rate	------	$EM^{-1}T^{-1}$	J kg^{-1}s^{-1}	erg g^{-1}s^{-1}	
13	Exposure	X	QM^{-1}	C kg^{-1}	esu g^{-1}	R (roentgen).
14	Exposure rate	------	$QM^{-1}T^{-1}$	C kg^{-1}s^{-1}	esu g^{-1}s^{-1}	Rs^{-1}, etc.
15	Mass attenuation coefficient.	$\frac{\mu}{\rho}$	L^2M^{-1}	m^{2}kg^{-1}	cm^{2}g^{-1}	
16	Mass energy transfer coefficient.	$\frac{\mu_K}{\rho}$	L^2M^{-1}	m^{2}kg^{-1}	cm^{2}g^{-1}	
17	Mass energy absorption coefficient.	$\frac{\mu_{en}}{\rho}$	L^2M^{-1}	m^{2}kg^{-1}	cm^{2}g^{-1}	
18	Mass stopping power.	$\frac{S}{\rho}$	EL^2M^{-1}	J m^{2}kg^{-1}	erg cm^{2}g^{-1}	
19	Linear energy transfer.	L	EL^{-1}	J m^{-1}	erg cm^{-1}	kev(μm)$^{-1}$.
20	Average energy per ion pair.	W	E	J	erg	ev.
22	Activity	A	T^{-1}	s^{-1}	s^{-1}	c(curie).
23	Specific gamma-ray constant.	Γ	QL^2M^{-1}	Cm^{2}kg^{-1}	esu cm^{2}g^{-1}	Rm^{2}h^{-1}c^{-1}, etc.
	Dose equivalent.	DE				rem

[a] It was desired to present only one set of dimensions for each quantity, a set that would be suitable in both the MKSA and electrostatic-cgs systems. To do this it was necessary to use a dimension Q, for the electrical charge, that is not a fundamental dimension in either system. In the MKSA system (fundamental dimensions M, L, T, I) Q represents the product IT, in the electrostatic-cgs system (M, L, T) it represents $M^{1/2}L^{3/2}T^{-1}$.

U.S. GOVERNMENT PRINTING OFFICE: 1964 O—688-008

Recommendations [a] of International Commission on Radiological Units and Measurements (ICRU)

ICRU Report Number	Reference [b]
1	Discussion on International Units and Standards for X-ray Work Brit. J. Radiol. **23**, 64 (1927)
2	International X-ray Unit of Intensity Brit. J. Radiol. (new series) **1**, 363 (1928)
3	Report of Committee on Standardization of X-ray Measurements Radiology **22**, 289 (1934)
4	Recommendations of the International Committee for Radiological Units Radiology **23**, 580 (1934)
5	Recommendations of the International Committee for Radiological Units Radiology **29**, 634 (1937)
6	Report of International Commission on Radiological Protection and International Commission on Radiological Units National Bureau of Standards Handbook 47, Washington, D.C. (1951)
7	Recommendations of the International Commission for Radiological Units Radiology **62**, 106 (1954)
8	Report of International Commission on Radiological Units and Measurements (ICRU) 1956 National Bureau of Standards Handbook 62, Washington, D.C. (1957)
9	Report of International Commission on Radiological Units and Measurements (ICRU) 1959 National Bureau of Standards Handbook 78, Washington, D.C. (1961)
10a	Radiation Quantities and Units National Bureau of Standards Handbook 84, Washington, D.C. (1962)
10b	Physical Aspects of Irradiation National Bureau of Standards Handbook 85, Washington, D.C. (1964)
10c	Radioactivity National Bureau of Standards Handbook 86, Washington, D.C. (1963)
10d	Clinical Dosimetry National Bureau of Standards Handbook 87, Washington, D.C. (1963)
10e	Radiobiological Dosimetry National Bureau of Standards Handbook 88, Washington, D.C. (1963)
10f	Methods of Evaluating Radiological Equipment and Materials National Bureau of Standards Handbook 89, Washington, D.C. (1963)

[a] Current recommendations are included.
[b] All of these publications are in English and may have been translated in other languages.